Preface

This book is the culmination of about ten years of studying sulfuric acid plants. Its objectives are to introduce readers to sulfuric acid manufacture and to show how acid production may be controlled and optimized.

One of the authors (MJK) operated an acid plant while writing this book. His Ph.D. work also centered on analyzing sulfuric acid manufacture. He is now a sulfuric acid and smelter specialist with Hatch.

The other author (WGD) has been interested in sulfuric acid plants since his 1957 student internship at Cominco's lead/zinc smelter in Trail, British Columbia. Cominco was making sulfuric acid from lead and zinc roaster offgases at that time. It was also making ammonium sulfate fertilizer.

In the book, we consider $SO_2(g)$ to be the raw material for sulfuric acid manufacture. Industrially it comes from:

(a) burning elemental sulfur with air
(b) smelting and roasting metal sulfide minerals
(c) decomposing spent acid from organic catalysis.

These sources are detailed in the book, but our main subject is production of sulfuric acid from $SO_2(g)$. Readers interested in smelting and roasting offgases might enjoy our other books *Extractive Metallurgy of Copper* (2002) and *Flash Smelting* (2003).

The book begins with a 9 chapter description of sulfuric acid manufacture. These chapters introduce the reader to industrial acidmaking and give reasons for each process step. They also present considerable industrial acid plant operating data. We thank our industrial colleagues profusely for so graciously providing this information.

The book follows with a mathematical analysis of sulfuric acid manufacture. It concentrates on catalytic $SO_2(g) + \frac{1}{2}O_2(g) \rightarrow SO_3$ oxidation. It also examines temperature control and production of $H_2SO_4(\ell)$ from $SO_3(g)$.

We have tried to make our analysis completely transparent so that readers can adapt it to their own purposes. We have used this approach quite successfully in our examinations of several metallurgical processes. We hope that we have also succeeded here.

We have used Microsoft Excel for all our calculations. We have found it especially useful for matrix calculations. We also like its Goal Seek, Visual Basic and Chart Wizard features. All the Excel techniques used in this book are detailed in our forthcoming book *Excel for Freshmen*. Please note that, consistent with Excel, we use * for multiply throughout the book.

A note on units - we have used SI-based units throughout. The only controversial choice is the use of K for temperature. We use it because it greatly simplifies thermodynamic calculations. We use bar as our pressure unit for the same reason. Lastly we use Nm^3 as our gas volume unit. It is 1 m^3 of gas at 273 K and 1 atmosphere (1.01325 bar) pressure. 22.4 Nm^3 contain 1 kg-mole of ideal gas.

We were helped enormously by our industrial colleagues during preparation of this book. We thank them all most deeply.

As with all our publications, Margaret Davenport read every word of our typescript. While she may not be an expert on sulfuric acid, she *is* an expert on logic and the English language. We know that if she gives her approval to a typescript, it is ready for the publisher. We also wish to thank George Davenport for his technical assistance and Vijala Kiruvanayagam of Elsevier Science Ltd. for her unflagging support during our preparation of this and other books.

Lastly, we hope that our book *Sulfuric Acid Manufacture* brings us as much joy and insight as Professor Dr von Igelfeld's masterpiece *Portuguese Irregular Verbs*[#] has brought him.

William G. Davenport
Tucson, Arizona

Matthew J. King
Perth, Western Australia

[#] See, for example, *At the Villa of Reduced Circumstances*, Anchor Books, a Division of Random House, Inc., New York (2005), p63.

CHAPTER 1

Overview

Sulfuric acid is a dense clear liquid. It is used for making fertilizers, leaching metallic ores, refining petroleum and for manufacturing a myriad of chemicals and materials. Worldwide, about 180 million tonnes of sulfuric acid are consumed per year (Kitto, 2004).

The raw material for sulfuric acid is SO_2 gas. It is obtained by:

(a) burning elemental sulfur with air

(b) smelting and roasting metal sulfide minerals

(c) decomposing contaminated (spent) sulfuric acid catalyst.

Elemental sulfur is far and away the largest source.

Table 1.1 describes three sulfuric acid plant feed gases. It shows that acid plant SO_2 feed is always mixed with other gases.

Table 1.1. Compositions of acid plant feed gases entering SO_2 oxidation 'converters', 2005. The gases may also contain small amounts of CO_2 or SO_3. The data are from the industrial tables in Chapters 3 through 9.

	Sulfur burning furnace	**Sulfide mineral smelters and roasters**	**Spent acid decomposition furnace**
Gas		*volume %*	
SO_2	11	10	9
O_2	10	11	11
N_2	79	79	76

Sulfuric acid is made from these gases by:

(a) catalytically reacting their SO_2 and O_2 to form $SO_3(g)$

(b) reacting (a)'s product $SO_3(g)$ with the $H_2O(\ell)$ in 98.5 mass% H_2SO_4, 1.5 mass% H_2O sulfuric acid.

Industrially, both processes are carried out rapidly and continuously, Fig. 1.1.

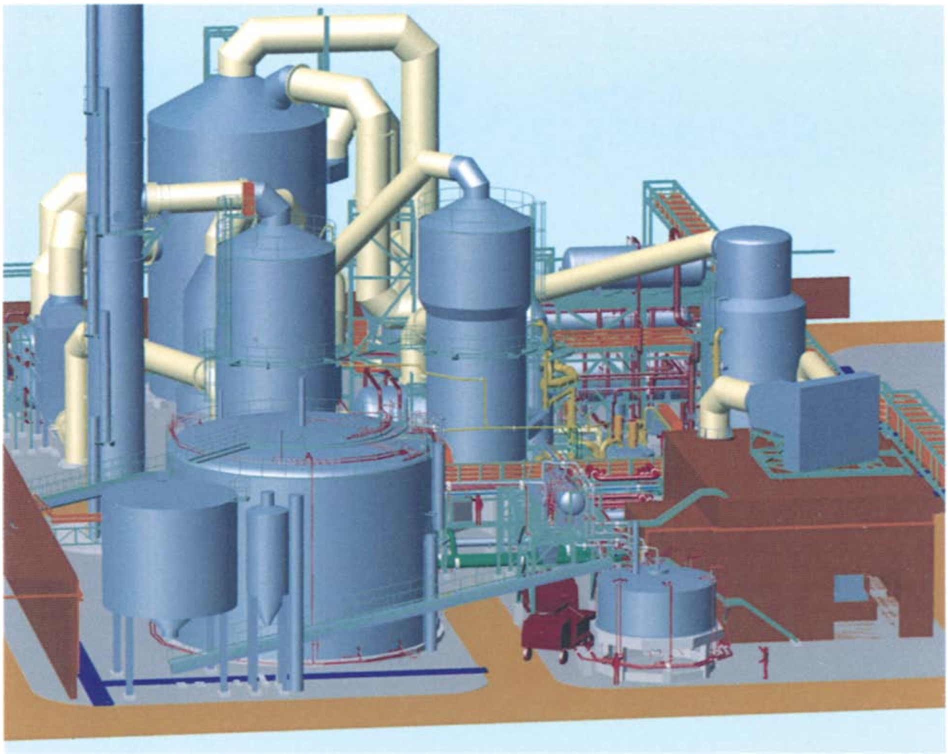

Fig. 1.1. Schematic of sulfur burning sulfuric acid plant, courtesy Outokumpu OYJ www.outokumpu.com The main components are the catalytic $SO_2 + \frac{1}{2}O_2 \rightarrow SO_3$ 'converter' (tall, back), twin H_2SO_4 making ('absorption') towers (middle distance) and large molten sulfur storage tank (front). The combustion air filter and air dehydration ('drying') tower are on the right. The sulfur burning furnace is hidden behind. Catalytic converters are typically 12 m diameter.

1.1 Catalytic Oxidation of SO_2 to SO_3

O_2 does <u>not</u> oxidize SO_2 to SO_3 without a catalyst. All industrial SO_2 oxidation is done by sending SO_2 bearing gas down through 'beds' of catalyst, Fig. 1.2. The reaction is:

$$\underset{\substack{\text{in dry } SO_2,\, O_2,\\ N_2 \text{ feed gas}}}{SO_2(g)} \quad + \quad \underset{\text{in feed gas}}{\frac{1}{2}O_2(g)} \quad \underset{\text{catalyst}}{\xrightarrow{700\text{-}900\text{ K}}} \quad \underset{\substack{\text{in } SO_3,\, SO_2\\ O_2,\, N_2 \text{ gas}}}{SO_3(g)} \qquad (1.1).$$

It is strongly exothermic ($\Delta H° \approx -100$ MJ per kg-mole of SO_3). Its heat of reaction provides considerable energy for operating the acid plant.

Fig. 1.2. Catalyst pieces in a catalytic SO_2 oxidation 'converter'. Converters are ~15 m high and 12 m in diameter. They typically contain four, ½-1 m thick catalyst beds. SO_2-bearing gas descends the bed at ~3000 Nm^3 per minute. Individual pieces of catalyst are shown in Fig. 8.1. They are ~0.01 m in diameter and length.

1.1.1 Catalyst

At its operating temperature, 700-900 K, SO_2 oxidation catalyst consists of a molten film of V, K, Na, (Cs) pyrosulfate salt on a solid porous SiO_2 substrate. The molten film rapidly absorbs $SO_2(g)$ and $O_2(g)$ – and rapidly produces and desorbs $SO_3(g)$, Chapters 7 and 8.

1.1.2 Feed gas drying

Eqn. (1.1) indicates that catalytic oxidation feed gas is always dry[#]. This dryness avoids:

(a) accidental formation of H_2SO_4 by reaction of $H_2O(g)$ with the $SO_3(g)$ product of catalytic SO_2 oxidation

(b) condensation of the H_2SO_4 in cool flues and heat exchangers

(c) corrosion.

The $H_2O(g)$ is removed by cooling/condensation (Chapter 4) and by dehydration with $H_2SO_4(\ell)$, Chapter 6.

[#] A small amount of sulfuric acid is made by wet catalysis. This is discussed in Section 1.9 and Chapter 25.

1.2 H_2SO_4 Production

Catalytic oxidation's $SO_3(g)$ product is made into H_2SO_4 by contacting catalytic oxidation's exit gas with strong sulfuric acid, Fig. 1.3. The reaction is:

$$\begin{array}{ccccc} SO_3(g) & + & H_2O(\ell) & \xrightarrow{\text{350-380 K}} & H_2SO_4(\ell) \\ \text{in } SO_3, SO_2, & & \text{in 98.5\% } H_2SO_4, & & \text{in strengthened} \\ O_2, N_2 \text{ gas} & & 1.5\%\ H_2O & & \text{sulfuric acid} \\ & & \text{sulfuric acid} & & \end{array} \tag{1.2}$$

$$\Delta H^\circ \approx -130 \text{ MJ per kg mole of } SO_3.$$

Reaction (1.2) produces strengthened sulfuric acid because it consumes $H_2O(\ell)$ and makes $H_2SO_4(\ell)$.

$H_2SO_4(\ell)$ is not made by reacting $SO_3(g)$ with water. This is because Reaction (1.2) is so exothermic that the product of the $SO_3(g) + H_2O(\ell) \rightarrow H_2SO_4$ reaction would be hot H_2SO_4 vapor – which is difficult and expensive to condense.

The small amount of $H_2O(\ell)$ and the massive amount of $H_2SO_4(\ell)$ in Reaction (1.2)'s input acid avoids this problem. The small amount of $H_2O(\ell)$ limits the extent of the reaction. The large amount of $H_2SO_4(\ell)$ warms only 25 K while it absorbs Eqn. (1.2)'s heat of reaction.

Fig. 1.3. Top of H_2SO_4-making ('absorption') tower, courtesy Monsanto Enviro-Chem Systems, Inc. www.enviro-chem.com The tower is packed with ceramic saddles. 98.5 mass% H_2SO_4, 1.5 mass% H_2O sulfuric acid is distributed uniformly across this packed bed. Distributor headers and 'downcomer' pipes are shown. The acid flows through slots in the downcomers down across the bed (see buried downcomers below the right distributor). It descends around the saddles while SO_3-rich gas ascends, giving excellent gas-liquid contact. The result is efficient H_2SO_4 production by Reaction (1.2). A tower is ~7 m diameter. Its packed bed is ~4 m deep. About 25 m^3 of acid descends per minute while 3000 Nm^3 of gas ascends per minute.

1.3 Industrial Flowsheet

Fig. 1.4 is a sulfuric acid manufacture flowsheet. It shows:

(a) the three sources of SO_2 for acid manufacture (metallurgical, sulfur burning and spent acid decomposition gas)

(b) acid manufacture from SO_2 by Reactions (1.1) and (1.2).

(b) is the same for all three sources of SO_2. The next three sections describe (a)'s three SO_2 sources.

1.4 Sulfur Burning

About 70% of sulfuric acid is made from elemental sulfur. All the sulfur is obtained as a byproduct from refining natural gas and petroleum.

The sulfur is made into SO_2 acid plant feed by:

melting the sulfur

spraying it into a hot furnace

burning the droplets with dried air.

The reaction is:

$$\underset{}{S(\ell)} + \underset{\text{in air}}{O_2(g)} \xrightarrow{1400\text{ K}} \underset{\substack{\text{in } SO_2,\, O_2,\\ N_2 \text{ gas}}}{SO_2(g)} \qquad (1.3)$$

$\Delta H^\circ \approx$ -300 MJ per kg-mole of $S(\ell)$.

Very little $SO_3(g)$ forms at the 1400 K flame temperature of this reaction, Fig. 7.4. This explains Fig. 1.4's two-step oxidation, i.e.:

(a) burning of sulfur to SO_2

then:

(b) catalytic oxidation of SO_2 to SO_3, 700 K.

The product of sulfur burning is hot, dry SO_2, O_2, N_2 gas. After cooling to ~700 K, it is ready for catalytic SO_2 oxidation and subsequent H_2SO_4-making.

1.5 Metallurgical Offgas

SO_2 in smelting and roasting gas accounts for about 20% of sulfuric acid production. The SO_2 is ready for sulfuric acid manufacture, but the gas is dusty. If left in the gas,

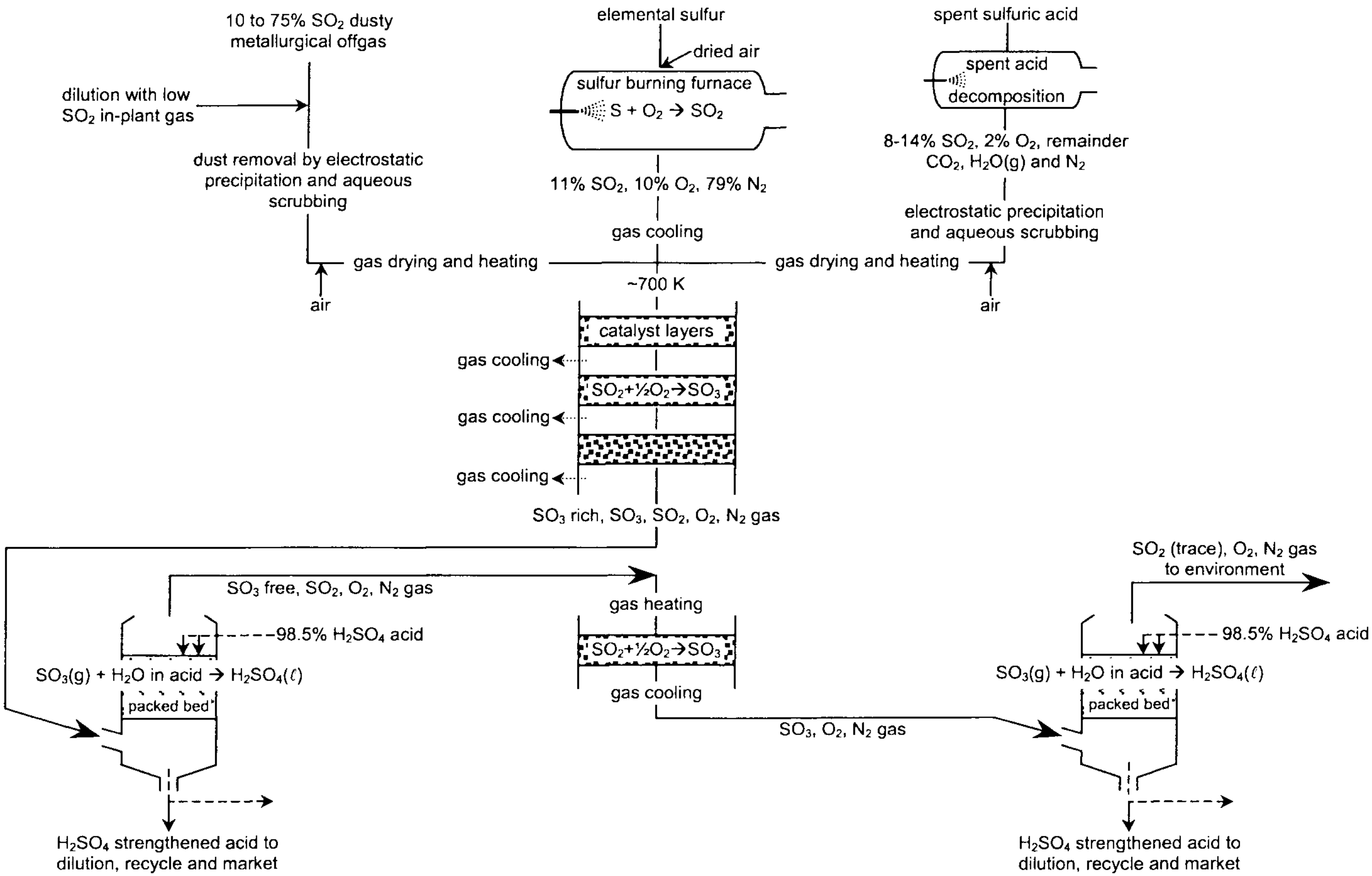

Fig. 1.4. Double contact sulfuric acid manufacture flowsheet. The three main SO_2 sources are at the top. Sulfur burning is by far the biggest source. The acid product leaves from two H_2SO_4 making towers at the bottom. Barren tail gas leaves the final H_2SO_4 making tower, right arrow.

the dust would plug the downstream catalyst layers and block gas flow. It must be removed before the gas goes to catalytic SO_2 oxidation.

It is removed by combinations of:

(a) settling in waste heat boilers

(b) electrostatic precipitation

(c) scrubbing with water (which also removes impurity vapors).

After treatment, the gas contains ~1 milligram of dust per Nm^3 of gas. It is ready for drying, catalytic SO_2 oxidation and H_2SO_4 making.

1.6 Spent Acid Regeneration

A major use of sulfuric acid is as catalyst for petroleum refining and polymer manufacture, Chapter 5. The acid becomes contaminated with water, hydrocarbons and other compounds during this use. It is regenerated by:

(a) spraying the acid into a hot (~1300 K) furnace – where the acid decomposes to SO_2, O_2 and $H_2O(g)$

(b) cleaning and drying the furnace offgas

(c) catalytically oxidizing the offgas's SO_2 to SO_3

(d) making the resulting $SO_3(g)$ into new $H_2SO_4(\ell)$ by contact with strong sulfuric acid, Fig. 1.4.

About 10% of sulfuric acid is made this way. Virtually all is re-used for petroleum refining and polymer manufacture.

1.7 Sulfuric Acid Product

Most industrial acid plants have three flows of sulfuric acid – one gas-dehydration flow and two H_2SO_4-making flows. These flows are connected through automatic control valves to:

(a) maintain proper flows and H_2SO_4 concentrations in the three acid circuits

(b) draw off newly made acid.

Water is added where necessary to give prescribed acid strengths.

Sulfuric acid is sold in grades of 93 to 99 mass% H_2SO_4 according to market demand. The main product in cold climates is ~94% H_2SO_4 because of its low (238 K) freezing point (Gable *et al.*, 1950). A small amount of oleum (H_2SO_4 with dissolved SO_3) is also made and sold (BASF, 2005).

Sulfuric acid is mainly shipped in stainless steel trucks, steel rail tank cars (DuPont, 2003) and double-hulled steel barges and ships (Barge, 1998; Bulk, 2003). Great care is taken to avoid spillage.

1.8 Recent Developments

The three main recent developments in sulfuric acidmaking have been:

(a) improved materials of construction, specifically more corrosion resistant materials (Salehi and Hopp, 2001, 2004; Sulphur, 2004)

(b) improved $SO_2(g) + \frac{1}{2}O_2(g) \rightarrow SO_3(g)$ catalyst, specifically V, Cs, K, Na, S, O, SiO_2 catalyst with low activation temperatures (Hansen, 2004)

(c) improved techniques for recovering the heat from Reactions (1.1), (1.2) and (1.3) (Puricelli *et al.*, 1998).

All of these improve H_2SO_4 and energy recovery.

1.9 Alternative Process

An alternative to the conventional acidmaking described here is *Wet Sulfuric Acidmaking* (Laursen, 2005; Topsoe, 2005; WSA, 2005).

This process:

(a) catalytically oxidizes the SO_2 in $H_2O(g)$, SO_2, O_2, N_2 gas

(b) condenses $H_2SO_4(\ell)$ directly from the gas.

It is described in Chapter 25.

In 2005, it is mainly used for low flow, low% SO_2 gases. It accounts for 1 or 2% of world H_2SO_4 production. Development of a large, rapid-heat-removal condenser will likely widen its use.

1.10 Summary

About 180 million tonnes of sulfuric acid are produced/consumed per year. The acid is used for making fertilizer, leaching metal ores, refining petroleum and for manufacturing a myriad of products.

Sulfuric acid is made from dry SO_2, O_2, N_2 gas. The gas comes from:

burning molten elemental sulfur with dry air, Chapter 3

smelting and roasting metal sulfide minerals, Chapter 4

decomposing contaminated (spent) sulfuric acid catalyst, Chapter 5.

Sulfur burning is far and away the largest source.

The SO_2 in the gas is made into sulfuric acid by:

(a) catalytically oxidizing it to $SO_3(g)$, Chapters 7 and 8

(b) reacting this $SO_3(g)$ with the $H_2O(\ell)$ in 98.5 mass% H_2SO_4, 1.5 mass% H_2O sulfuric acid, Chapter 9.

Suggested Reading

Acid Plants (2005) Acid plants address environmental issues. *Sulfur* **298**, (May-June 2005) 33-38.

Duecker, W.W. and West, J.R. (1966) *The Manufacture of Sulfuric Acid,* Reinhold Publishing Corporation, New York.

Louie, D. (2005) Resources and information sources for the sulphuric acid industry, preprint of paper presented at 29th Annual Clearwater Conference (AIChE), Clearwater, Florida, June 4, 2005. www.aiche-cf.org Also Sulphuric acid on the web www.sulphuric-acid.com

Sulphur 2004 Conference preprints, Barcelona, October 24-27, 2004 (and previous conferences). www.britishsulphur.com

Sander, U.H.F., Fischer, H., Rothe, U., Kola, R. and More, A.I. (1984) *Sulphur, Sulphur Dioxide and Sulphuric Acid*, The British Sulphur Corporation Ltd., London. www.britishsulphur.com

References

Barge (1998) Double skin tank barges www.bollingershipyards.com/barge.htm

BASF (2005) Oleum www.basf.com (Products & Markets, Our products → Sulfur products, Oleum)

Bulk (2003) Acid handling http://bulktransporter.com/mag/transportation_growing_success/

DuPont (2003) Dupont sulfur products, technical data, shipping regulations. www.dupont.com/sulfurproducts/techdata/regulatory.html

Gable, C.M., Betz, H.F. and Maron, S.H. (1950) Phase equilibria of the system sulfur trioxide-water. *Journal of the American Chemical Society*, **72**, 1445 1448. www.acs.org

Hansen, L. (2004) Topsoe's sulphuric acid catalysts VK-series. Paper distributed at Sulphur 2004 conference, Barcelona, October 24-27, 2004. www.haldortopsoe.com

Kitto, M. (2004) The outlook for smelter acid supply and demand. Paper presented at Sulphur 2004 conference, Barcelona, October 25, 2004. www.britishsulphur.com

Laursen, J.K. (2005) Sulfur removal by the WSA process www.haldortopsoe.com

Puricelli, S.M., Grendel, R.W. and Fries, R.M. (1998) Pollution to power, a case study of the Kennecott sulfuric acid plant. In *Sulfide Smelting '98* ed. Asteljoki, J.A. and Stephens, R.L., TMS, Warrendale, PA, 451 462. www.tms.org

Salehi, M. and Hopp, A. (2001) Corrosion protection in sulphuric acid producing plants. Paper presented at Sulphur 2001, Marrakech, October 14-17, 2001. www.steuler.de

Salehi, M. and Hopp, A. (2004) Corrosion protection using polymers in plants handling and producing sulphuric acid. Paper presented at Sulphur 2004 conference, Barcelona, October 27, 2004. www.steuler.de

Sulphur (2004) Sulphuric acid equipment update. *Sulphur* **292** (May-June 2004) 33 42. www.britishsulphur.com

Topsoe (2005) Dusulphurization plants WSA and SNOX www.haldortopsoe.com

WSA (2005) WSA applications in refineries www.haldortopsoe.com

CHAPTER 2

Production and Consumption

Sulfuric acid was first produced around the 10th century AD (Al Hassan and Hill, 1986; Islam, 2004). It was made by (i) decomposing natural hydrated sulfate minerals and (ii) condensing the resulting gas. Example reactions are:

$$CuSO_4{\cdot}5H_2O(s) \xrightarrow{\text{heat}} CuO(s) + SO_3(g) + 5H_2O(g) \qquad (2.1)$$

$$5H_2O(g) \xrightarrow{\text{condensation}} 5H_2O(\ell) \qquad (2.2)$$

$$SO_3(g) + 5H_2O(\ell) \xrightarrow{\text{acidmaking}} H_2SO_4(\ell) + 4H_2O(\ell) \qquad (2.3).$$

The process was carried out in a ceramic retort (inside a furnace) and 'bird-beak' condenser (outside the furnace). Acid composition was adjusted by adding or evaporating water.

The earliest uses for sulfuric and other mineral acids were as solvents for:

(a) separating gold and silver

(b) decorative etching of metals, e.g. Damascus Steel

(Killick, 2005).

Thermal decomposition of sulfates was still being used in the 19th century – to make 90+% H_2SO_4 sulfuric acid. The process entailed (Wikipedia, 2005):

(a) making $Fe_2(SO_4)_3$ by oxidizing pyrite (FeS_2) with air

(b) thermally decomposing the $Fe_2(SO_4)_3$ in a retort to make SO_3 and Fe_2O_3, i.e:

$$Fe_2(SO_4)_3(s) \xrightarrow{750\,K} Fe_2O_3(s) + 3SO_3(g) \qquad (2.4)$$

(c) bubbling the SO_3 through water to make H_2SO_4, i.e:

$$SO_3(g) + H_2O(\ell) \rightarrow H_2SO_4(\ell) \qquad (2.5).$$

The process was slow and costly, but it was the only way to make pure 90+% H_2SO_4 sulfuric acid – until catalytic SO_2 oxidation was invented. Pure, high strength acid was needed for making dyes and other chemicals.

Industrial sulfuric acid production began in the 18th century with the burning of sulfur in the presence of natural niter (KNO_3) and steam. This developed into the lead chamber and tower processes – which used nitrogen oxides to form an aqueous SO_2 oxidation catalyst. The overall acidmaking reaction with this catalyst is:

$$SO_2 + \frac{1}{2}O_2 + H_2O \xrightarrow[\text{NOHSO}_4\text{ catalyst}]{\text{in aqueous solution}} H_2SO_4 \qquad (2.6)$$

(Sander *et al.*, 1984).

The lead chamber and tower processes were used into the 20th century. Unfortunately their H_2SO_4 strength was limited to below about 70 mass% H_2SO_4. Above 70% H_2SO_4, the product acid contained stable nitrosyl hydrogen sulfate which made it unsuitable for many purposes.

The 20th century saw the nitrogen oxide processes gradually but completely replaced by the catalytic SO_2 oxidation/SO_3-sulfuric acid contact process, Chapter 1. This process economically produces sulfuric acid of all H_2SO_4 concentrations. Platinum was the dominant catalyst until the 1930's. V, K, Na, (Cs), S, O, SiO_2 catalyst (Chapters 7 and 8) has dominated since.

World production of sulfuric acid since 1950 is shown in Fig. 2.1. Sources of SO_2 for this production are given in *Table* 2.1.

Table 2.1. Sources of sulfur and SO_2 for producing sulfuric acid (interpreted from Kitto, 2004a and Sander *et al.*, 1984). Virtually all sulfur and SO_2 production is involuntary, i.e. it is the byproduct of other processes.

Source	% of total supply
Elemental sulfur from natural gas purification and petroleum refining, Chapter 3	70
SO_2 from smelting and roasting non-ferrous minerals, Chapter 4	20
SO_2 from decomposing spent petroleum/polymer sulfuric acid catalyst, Chapter 5	10

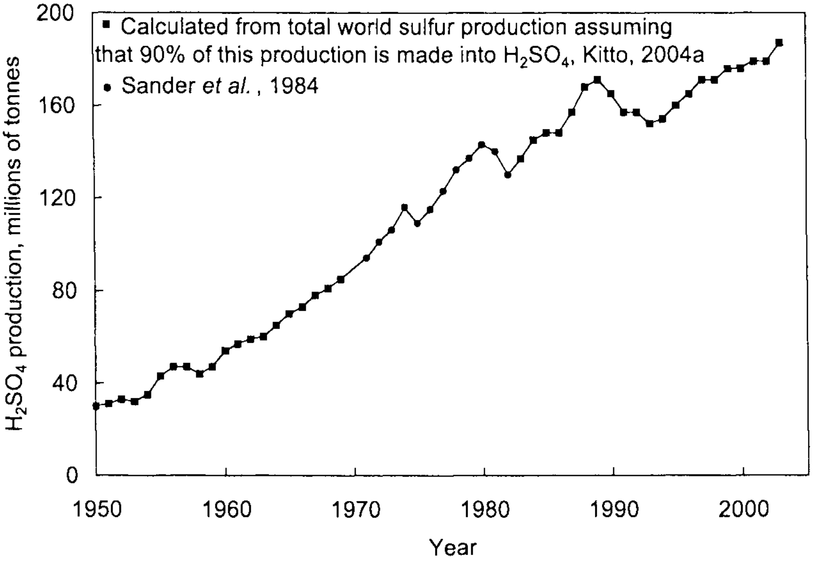

Fig. 2.1. World sulfuric acid production, 1950-2003, in millions of tonnes of contained H_2SO_4. The increase in production with time is notable. It is due to the increased use of phosphate and sulfate fertilizers, virtually all of which are made with sulfuric acid. Data sources:

1950-1969 and 1983-1987, Buckingham and Ober, 2002
1970-1982, Sander *et al.*, 1984, p 412
1988-2003, Kitto, 2004a.

2.1 Uses

Sulfuric acid is mostly used for making phosphate fertilizers, Table 2.2. The most common process is:

(a) production of phosphoric acid by reacting phosphate rock with sulfuric acid, i.e.:

$$\underset{\text{phosphate rock}}{Ca_3(PO_4)_2(s)} + 3H_2SO_4(\ell) + 6H_2O(\ell) \rightarrow \underset{\text{phosphoric acid}}{2H_3PO_4(\ell)} + \underset{\text{gypsum}}{3CaSO_4{\cdot}2H_2O(s)} \qquad (2.7)$$

followed by:

(b) reaction of the phosphoric acid with ammonia to make ammonium phosphates, e.g. $NH_4H_2PO_4$ and $(NH_4)_2H_2PO_4$.

Sulfuric acid is also used extensively as a solvent for ores and as catalyst for petroleum refining and polymer manufacture.

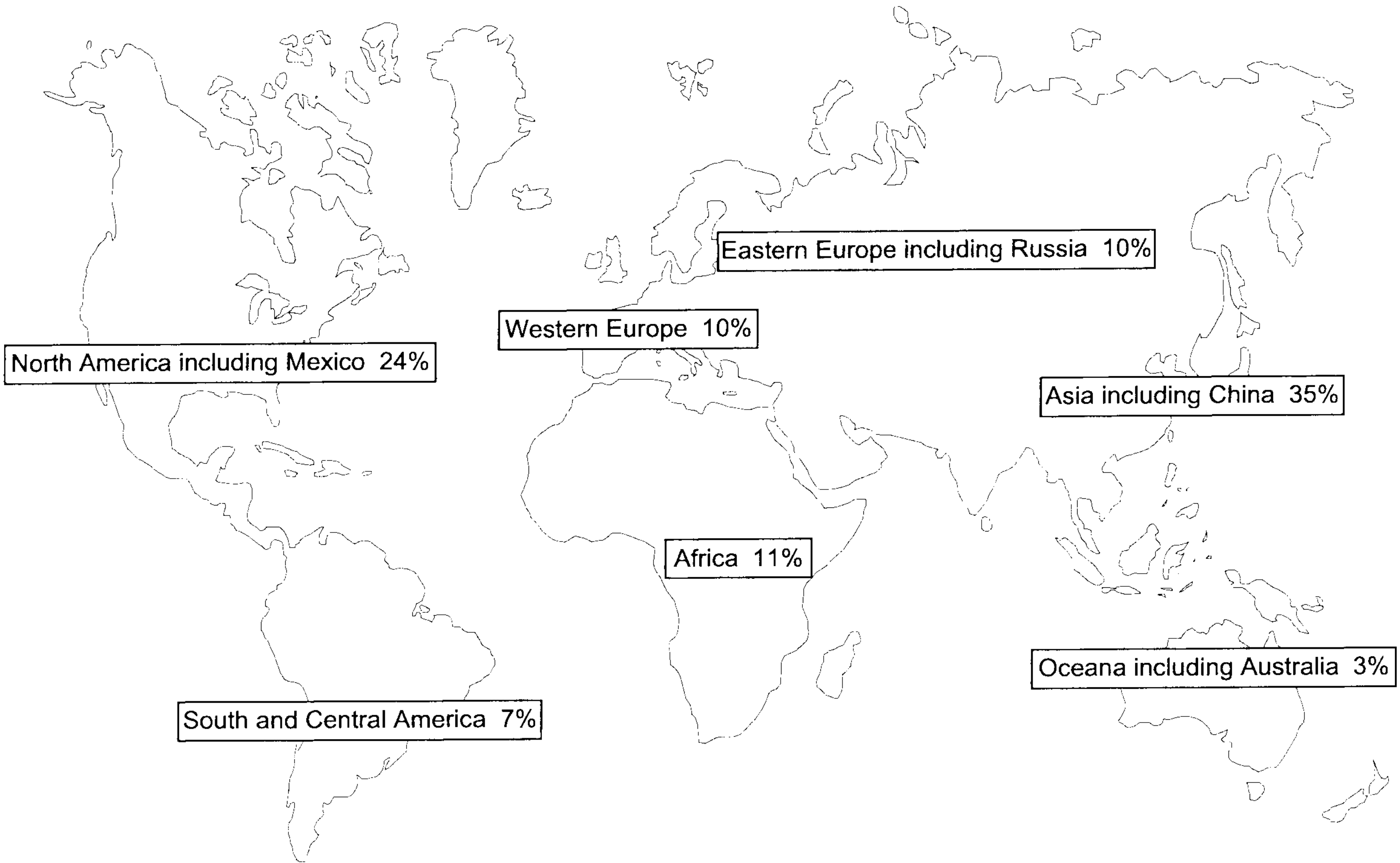

Fig. 2.2. World production of sulfuric acid, percent by region (Sulphur, 2004). Total 2003 world production was 180 million tonnes contained H_2SO_4.

Table 2.2. World uses of sulfuric acid by percentage, 2003. The data are mainly from Kitto, 2004a.

Use	% of total consumption
Phosphoric acid production	48
Single superphosphate fertilizer production	8
Ammonium sulfate fertilizer production	7
Petroleum refining catalyst	5
Copper ore leaching	4
Titanium dioxide pigment production	3
Pulp and paper production	2
Methyl methacrylate catalyst	2
Nickel concentrate leaching	1
Other	20

2.2 Acid Plant Locations and Costs

Sulfuric acid plants are located throughout the industrialized world, Fig. 2.2. Most are located near their product acid's point of use, i.e. near phosphate fertilizer plants, nickel ore leach plants and petroleum refineries. This is because elemental sulfur is cheaper to transport than sulfuric acid. Examples of long distance sulfur shipment are from natural gas purification plants in Alberta, Canada to acid plants near phosphate rock based fertilizer plants in Florida and Australia. A new sulfur-burning sulfuric acid plant (4400 tonnes of acid per day) is costing ~75 million U.S. dollars (Sulfuric 2005).

Smelter acid, on the other hand, must be made from byproduct $SO_2(g)$ *at the smelter* and transported to its point of use. An example of this is production of acid at the Cu-Ni smelters in Sudbury, Canada and rail transport of the product acid to fertilizer plants in Florida. A new metallurgical sulfuric acid plant (3760 tonnes of acid per day) is costing ~59 million U.S. dollars (Sulfuric 2005).

Production of pure sulfuric acid from contaminated 'spent' sulfuric acid catalyst is almost always done near the source of the spent acid – to minimize forward and return acid shipping distance.

2.3 Price

Fig. 2.3 plots sulfuric acid price (actual U.S.$) as function of calendar year. The most notable features of the graph are:

(a) the volatility in price year to year

(b) a slightly downward price trend between 1980 and 2001

(c) the rapid increase in price from 2001 to 2003.

The volatility of year to year price is due to (i) small imbalances between acid demand and supply and (ii) the difficulty of storing large quantities of acid. The large increase in price after 2001 is due to China's increasing demand for fertilizer, hence sulfuric acid.

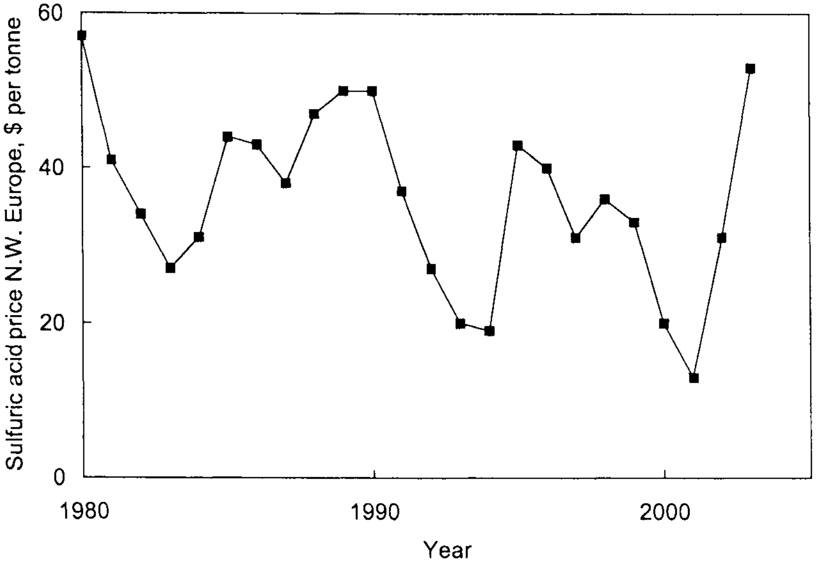

Fig. 2.3. Northwest Europe sulfuric acid price trends, 1980-2003. Actual prices are negotiated between buyer and seller. Data sources:
1980-1982 Sander *et al.*, 1984, p 415
1983-1987 Kitto, 2004b
1988-2003 Kitto 2004c.

2.4 Summary

Worldwide, about 180 million tonnes of sulfuric acid are produced per year. 70% comes from burning elemental sulfur. The remainder comes from SO_2 in smelter, roaster and spent acid regeneration furnace offgases.

By far the largest use of sulfuric acid is in the production of phosphate fertilizers, e.g. ammonium phosphate. Other large uses are as solvent for copper and nickel minerals and as catalyst for petroleum refining and polymer manufacture.

Sulfuric acid price averaged about 33 ± 20 U.S.$ per tonne between 1980 and 2003. It varies widely year to year due to small imbalances between acid demand and supply.

Suggested Reading

Sander, U.H.F., Fischer, H., Rothe, U., Kola, R. and More, A.I. (1984) *Sulphur, Sulphur Dioxide, Sulphuric Acid.* British Sulphur Corporation Ltd., London. www.britishsulphur.com

Kitto, M. (2004) Smelter acid supply and demand. Preprint of paper from Sulphur 2004 conference, Barcelona, October 24-27, 2004; also, The outlook for smelter acid supply and demand. Paper presented at Sulphur 2004 conference, Barcelona, October 25, 2004. www.britishsulphur.com

References

Al Hassan, A.Y. and Hill, D. R. (1986) *Islamic Technology, An Illustrated History*. Cambridge Univ. Press, Cambridge, England. www.uk.cambridge.org

Buckingham, D.A. and Ober, J.A. (2002) Sulfur Statistics (Open File Report 01 006). http://minerals.usgs.gov/minerals/pubs/of01-006/sulfur.html

Islam (2004) Islam in your life – history and culture. The natural sciences Pt. III, pharmacology and chemistry www.masnet.org/history.asp?id=1033

Killick, D. (2005) Personal communication, Department of Materials Science and Engineering, University of Arizona. www.arizona.edu

Kitto, M (2004a) The outlook for smelter acid supply and demand. Paper presented at Sulphur 2004 conference, Barcelona, October 25, 2004. www.britishsulphur.com

Kitto, M (2004b) Personal communication. www.britishsulphur.com

Kitto, M. (2004c) Smelter acid supply and demand. Preprint of paper from Sulphur 2004 conference, Barcelona, October 24-27, 2004. www.britishsulphur.com

Sander, U.H.F., Fischer, H., Rothe, U., Kola, R. and More, A.I. (1984) *Sulphur, Sulphur Dioxide, Sulphuric Acid*. British Sulphur Corporation Ltd., London. www.britishsulphur.com

Sulphur (2004) Sulphuric acid 2001-2003. *Sulphur*, **293** (July-August 2004), p 28.

Sulfuric (2005) Worldwide growth brings boom in acid plant construction. *Sulfuric Acid Today* **11(1)**, (Spring/Summer 2005), p 16. www.H2SO4Today.com

Wikipedia (2005) History of Sulfuric Acid. www.wikipedia.org/wiki/Sulfuric_acid

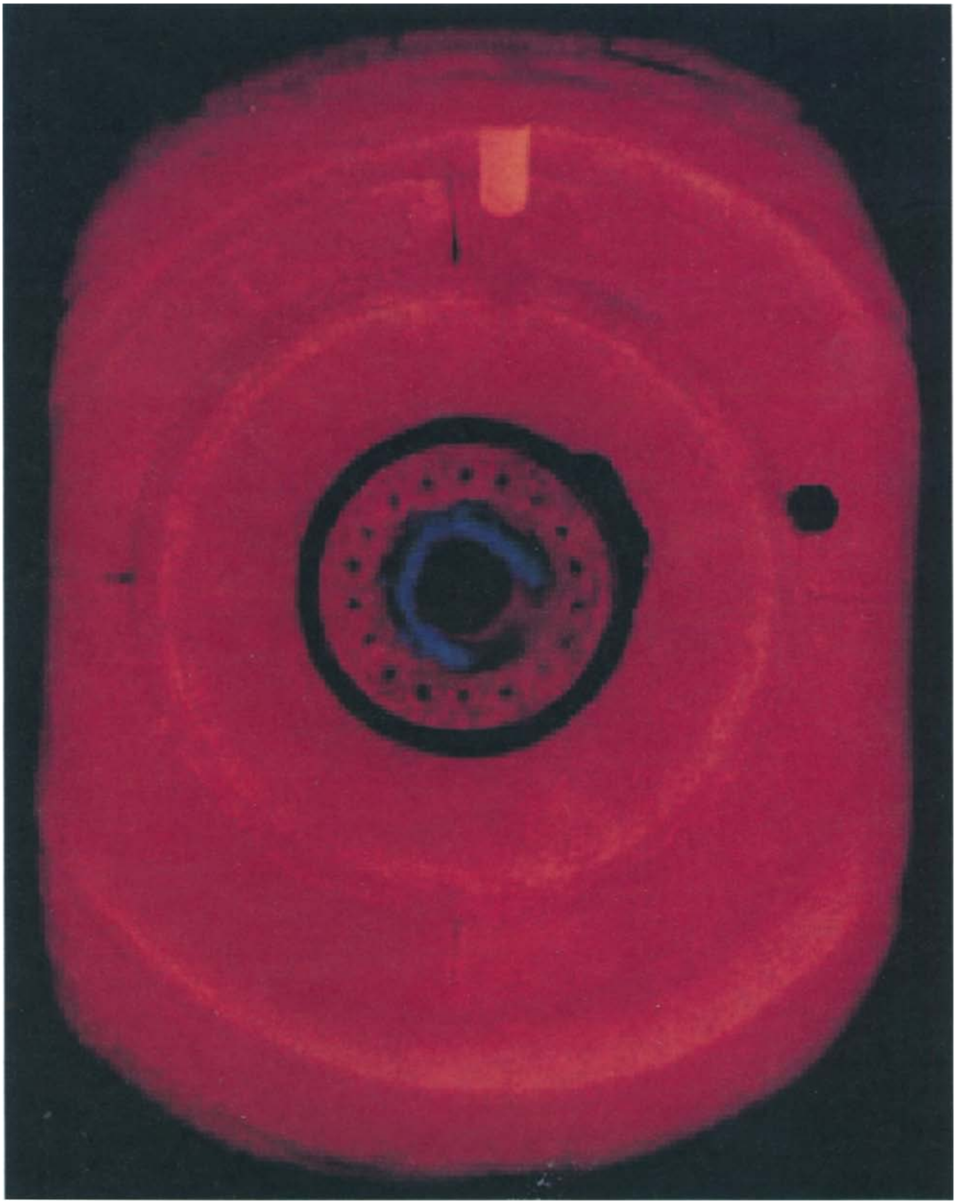

Fig. 3.0. View of spinning cup sulfur burner from inside sulfur burning furnace – burning capacity 870 tonnes of molten sulfur per day. The thermocouple at top and central blue sulfur-rich flame are notable. Photograph courtesy of Outokumpu OYJ. www.outokumpu.com

CHAPTER 3

Sulfur Burning

70% of sulfuric acid is made from elemental sulfur. The elemental sulfur is:

(a) received molten or melted with pressurized steam (sulfur melting point ~390 K)

(b) atomized in a hot (1400 K) furnace

(c) burnt in the furnace with excess dry air to form hot SO_2, O_2, N_2 gas.

Sulfuric acid is then made from step (c)'s gas by:

(d) cooling the gas in a boiler and steam superheater

(e) catalytically reacting its $SO_2(g)$ and $O_2(g)$ to form $SO_3(g)$

(f) contacting step (e)'s product gas with strong sulfuric acid to make H_2SO_4 by the reaction $SO_3(g) + H_2O(\ell)_{\text{in acid}} \rightarrow H_2SO_4(\ell)_{\text{in strengthened acid}}$.

Steps (b) to (f) are continuous.

This chapter describes steps (a) to (d), Fig. 3.1. Steps (e) and (f) are described in Chapters 7, 8 and 9.

3.1 Objectives

The objectives of this chapter are to describe:

(a) the physical and chemical properties of elemental sulfur

(b) transportation of elemental sulfur to the sulfur burning plant

(c) preparation of elemental sulfur for combustion

(d) sulfur burners and sulfur burning furnaces

(e) control of sulfur burning offgas composition, temperature and volume.

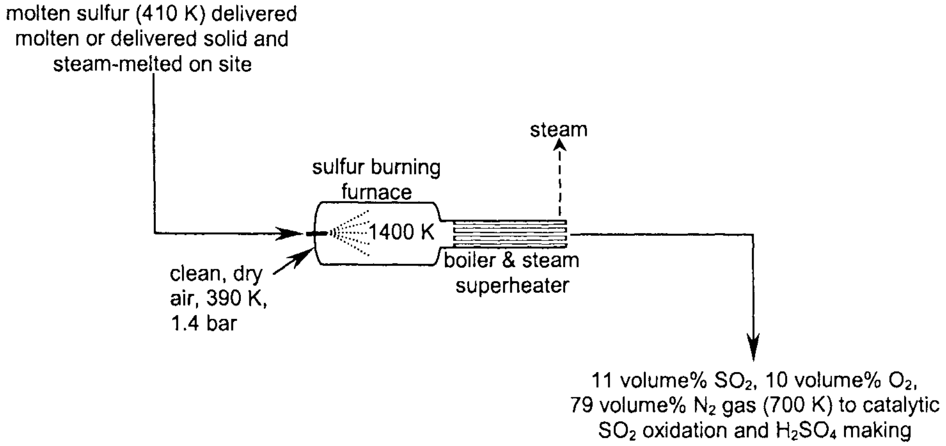

Fig. 3.1. Sulfur burning flowsheet – molten sulfur to clean dry 700 K SO_2, O_2, N_2 gas. The furnace is supplied with excess air to provide the O_2 needed for subsequent catalytic oxidation of SO_2, to SO_3. Table 3.1 gives industrial sulfur burning data.

3.2 Sulfur

The elemental sulfur used for making sulfuric acid is virtually all a byproduct of natural gas and petroleum refining. It contains 99.9+% S. Its main impurity is carbon from natural gas or petroleum.

Its melting point is 388 – 393 K, depending on its crystal structure. It is easily melted with pressurized steam pipes.

3.2.1 Viscosity

The viscosity of molten sulfur is described in Fig. 3.2. Its key features are a viscosity minimum at 430 K and a ten thousand-fold viscosity increase just above 430 K.

Sulfur burners are fed with ~410 K molten sulfur, near the viscosity minimum but safely below the steep viscosity increase. Sulfur temperature is maintained by circulating 420 K steam through sulfur storage tank steam pipes just ahead of sulfur burning. Below ground or insulated above ground storage tanks are used.

Sulfur's huge increase in viscosity just above 430 K is due to a transition from S_8 ring molecules to long interwoven S chain molecules (Dunlavy, 1998).

3.3 Molten Sulfur Delivery

Elemental sulfur is produced molten. It is also burnt molten.

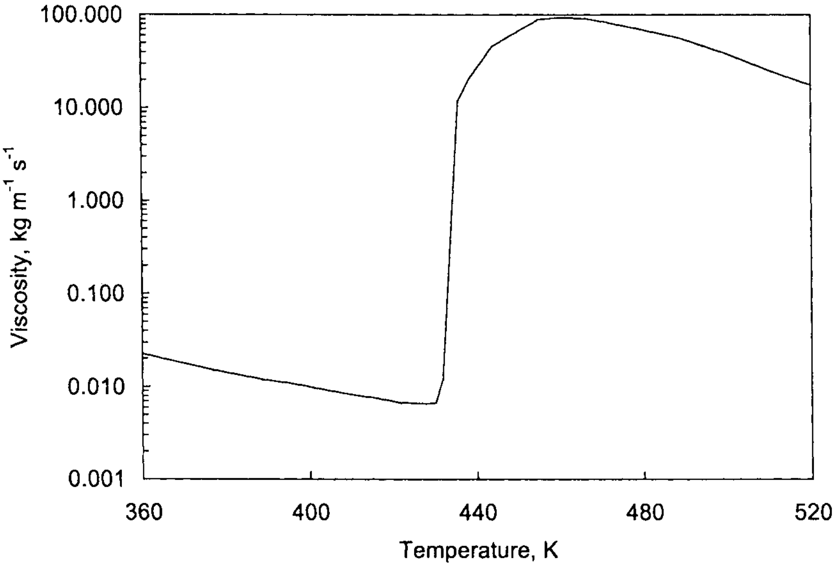

Fig. 3.2. Molten sulfur viscosity as a function of temperature (Tuller, 1954). The viscosity minimum at 430 K and the enormous viscosity increase just above 430 K are notable.

Where possible, therefore, sulfur is transported molten from sulfur *making* to sulfur *burning*. It is mainly shipped in double walled, steam heatable barges and railway tank cars. This gives easy handling at both ends of the journey. Even if the sulfur solidifies during the journey, it is easily melted out with 420 K steam to give a clean, atomizable raw material. Short distance deliveries are sometimes made in single walled tanker trucks.

Sulfur that is shipped this way is ready for burning. Sulfur that is shipped as solidified pellets or flakes picks up dirt during shipping and storage. This sulfur is melted and filtered before being burnt (Sander *et. al.*, 1984, p 174, Sparkler, 2004).

Sulfur is shipped solid when there are several intermediate unloading-loading steps during its journey, e.g. train-ship-train. An example of this is shipment of solid sulfur from interior Canada to interior Australia.

3.3.1 Sulfur pumps and pipes

Molten sulfur has a viscosity (~0.01 kg m^{-1} s^{-1}, 400-420 K, Fig. 3.2) about ten times that of water (~0.001 kg m^{-1} s^{-1}, 293 K). Its density is ~1.8 kg/m^3. It is easily moved in steam jacketed steel pipes (Jondle and Hornbaker, 2004). Steam heated pumps much like that in Fig. 9.2 are used. Molten sulfur is an excellent lubricant at 410 K. Sulfur pump impellers need no additional lubrication.

3.4 Sulfur Atomizers and Sulfur Burning Furnaces

Sulfur burning consists of:

(a) atomizing molten sulfur and spraying the droplets into a hot furnace, Fig. 3.3

(b) blowing clean, dry 390 K air into the furnace.

The tiny droplets and warm air give:

(c) rapid vaporization of sulfur in the hot furnace

(d) rapid and complete oxidation of the sulfur vapor by O_2 in the air.

Representative reactions are:

$$S(\ell) \xrightarrow{\text{boiling point, } 718\text{ K}} S(g) \tag{3.1}$$

$$\underset{}{S(g)} + \underset{\text{in air}}{O_2(g)} \rightarrow \underset{\text{in } SO_2,\, O_2,\, N_2 \text{ gas}}{SO_2(g)} + \text{heat} \tag{3.2}$$

The combined heat of reaction for Reactions (3.1) and (3.2) is ~ -300 MJ per kg-mole of $S(\ell)$.

Fig. 3.3. Burner end of sulfur burning furnace. Atomized molten sulfur droplets are injected into the furnace through steam-cooled lances. Dry combustion air is blown in through the circular openings behind. The sulfur is oxidized to SO_2 by Reactions (3.1) and (3.2). Atomization is done by spiral or right angle flow just inside the burner tip.

3.4.1 Sulfur atomizers

Molten sulfur spraying is done with:

(a) a stationary spray nozzle at the end of a horizontal lance, Fig. 3.3

(b) a spinning cup sulfur atomizer, Fig. 3.0 (Outokumpu, 2005)

In both cases, molten sulfur is pumped into the atomizers by steam jacketed pumps.

The stationary spray nozzle has the advantage of simplicity and no moving parts. The spinning cup atomizer has the advantage of lower input pressure, smaller droplets, more flexible downturn and a shorter furnace.

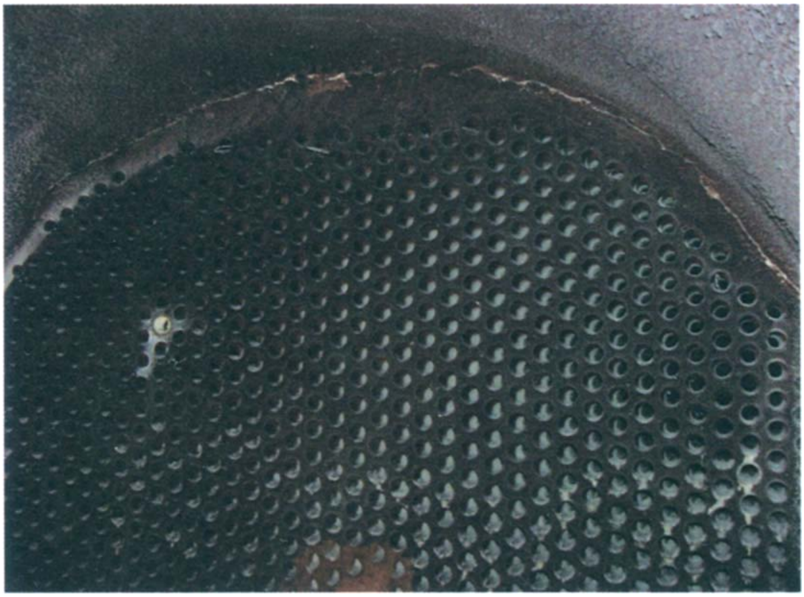

Fig. 3.4. Entrance to fire tube boiler tubes after Fig. 3.3's sulfur burning furnace. 1400 K gas (~11 volume% SO_2, 10 volume% O_2, 79 volume% N_2) leaves the furnace and enters the boiler. It turns 90° in the boiler and flows into the tubes. The tubes are surrounded by water. Heat is transferred from the hot gas to the water – cooling the gas and making (useful) steam. The tubes are typically 0.05 m diameter. Table 3.1 gives industrial furnace data. Sulfur furnace boilers are discussed by Roensch (2005).

3.4.2 Dried air supply

Air for sulfur burning is filtered through fabric and dried. It is then blown into the sulfur burning furnace. It is blown in behind the sulfur spray to maximize droplet-air contact.

The drying is done by contacting the air with strong sulfuric acid, Chapter 6. This removes $H_2O(g)$ down to ~0.05 grams per Nm^3 of air. Drying to this level prevents accidental $H_2SO_4(\ell)$ formation and corrosion after catalytic $SO_3(g)$ production.

Table 3.1. Details of 3

Plant	S1
startup date	
acid production, tonnes H_2SO_4/day	4400
Sulfur	
source	imported pastel
impurities, parts per million by mass	
carbon	
inorganic oxides	
other	
sulfur filtration method	three 35 leaf pressure leach filters, 2 online
Sulfur burning furnace data	
number of furnaces	1
shell length × diameter, m	18.36 × 6.0
refractory types	0.23 m HB fire brick & 0.115 m insulting brick
sulfur burners	
spinning cup or spray guns	spray guns
number of burners per furnace	7
sulfur burning rate, tonnes/hour	60.1
temperatures, K	
dry air into furnace	416
molten sulfur into furnace	405
gas out of furnace	1445
Boiler	
type	fire tube
number	2
length × diameter, m	7.85 × 3.505 (each)
number of tubes	1550 each
tube diameter, m	0.046 ID
tube material	SA-178-A
number of superheaters	2
number of economizers	3
gas temperatures, K	
into boiler	1444
out of economizer	696
steam production, tonnes of steam per tonne of sulfur	3.88
pressure, bar	63.8
temperature, K	554 (753 after super heaters)
Product gas	
flowrate, thousand Nm^3/hour	356
composition, volume%	
SO_3	0.184
SO_2	11.6
O_2	9.06
N_2	79.1

sulfur burning furnace operations.

M1	S2
1974	1965
270	1800
including from molybdenum sulfide roaster gas	
	liquid
	<1000
	<200
none	none
1	1
10.4 × 3.2	18.3 × 5.5 inside shell 0.23 m hard (high T) brick 0.11 m insulating brick
spray gun	spray guns
1	4
2.0 max	24.7
714	363
408	411
870-1260	1362
fire tube	fire tube
1	2
6.4 × 2.2	5 × 3.5; 2.9 × 2.7
600	1860; 1210
0.05	0.05
carbon steel	carbon steel
0	1
0	1
870-1280	1362
810-950	700
	1.64
17	32
	517
50	210
4.7-5.6	8.38
13.6	12.6
	79.02

3.4.3 Main blower

The dried air is blown into the sulfur burning furnace by the acid plant's main blower.

The blower is a steam or electricity driven centrifugal blower (Jacoby, 2004). It blows air into the sulfur burning furnace - and the furnace's offgas through the remainder of the acid plant. 0.3 to 0.5 bar pressure is required.

A 2000 tonnes of H_2SO_4 per day sulfur burning acid plant typically requires a 4000 to 4500 kW main blower.

3.4.4 Furnace

Sulfur burning furnaces are 2 cm thick cylindrical steel shells lined internally with 30 to 40 cm of insulating refractory, Fig. 3.3. Air and atomized molten sulfur enter at one end. Hot SO_2, O_2, N_2 gas departs the other into a boiler and steam superheater (Fig. 3.4). Some furnaces are provided with internal baffles. The baffles create a tortuous path for the sulfur and air, promoting complete sulfur combustion. Complete sulfur combustion is essential to prevent elemental sulfur condensation in downstream equipment.

3.5 Product Gas

Sulfur burning is operated to produce 1400 K gas containing:

~11 volume% SO_2

~10 volume% O_2

79 volume% N_2

This product has enough SO_2 and a high enough O_2/SO_2 ratio for subsequent catalytic $SO_2 + \frac{1}{2}O_2 \rightarrow SO_3$ oxidation. It is also cool enough for its heat to be recovered as steam in a simple fire-tube boiler (Thermal Ceramics, 2005) and steam superheater.

The gas contains only 0.1 or 0.2 volume% SO_3 despite its high O_2 content. This is because the equilibrium constant for $SO_2 + \frac{1}{2}O_2 \rightarrow SO_3$ oxidation is small (0.06) at 1400 K, Fig. 7.3.

3.5.1 Gas destination

Product gas departs the sulfur burning furnace/boiler/superheater into:

(a) a catalytic SO_2 oxidation 'converter'

then to:

(b) $SO_3(g) + H_2O(\ell)_{\text{in sulfuric acid}} \rightarrow H_2SO_4(\ell)_{\text{in strengthened acid}}$ acidmaking.

The boiler and superheater cool the gas to ~700 K, the usual temperature for catalytic SO_2 oxidation. They also produce steam for the acid plant main blower and for making electricity.

3.5.2 Composition and temperature control

The composition and temperature of sulfur burning's product gas are controlled by adjusting the sulfur burning furnace's:

$$\frac{\text{input air}}{\text{input sulfur}}$$

ratio, Figs. 3.5 and 3.6.

As the figures show, raising a furnace's air/sulfur ratio:

(a) increases product gas O_2 concentration, Fig. 3.5

(b) decreases product gas SO_2 concentration, Fig. 3.5

(c) decreases product gas temperature, Fig. 3.6.

These relationships allow simple automatic control of product gas composition and temperature. Note, however, that composition and temperature are not independent variables.

Replacement of some of the sulfur burner's input air with oxygen can be used to give independent temperature control (Miller and Parekh, 2004). Raising the oxygen/air ratio increases offgas temperature because less N_2 has to be heated by the $S(\ell) + O_2 \rightarrow SO_2$ reaction. Lowering the oxygen/air ratio has the opposite effect.

3.5.3 Target gas composition

The Section 3.5 gas (11 volume% SO_2, 10 volume% O_2, 79 volume% N_2) is chosen to give efficient downstream catalytic $SO_2 + \frac{1}{2}O_2 \rightarrow SO_3$ oxidation. A requirement for this is a volume% O_2/volume% SO_2 ratio around one.

In recent years there has been a tendency to increase volume% SO_2 in sulfur burning gas by lowering the input air/sulfur ratio, Fig. 3.5. An increase in SO_2 concentration lowers the volume of gas that must be blown through the acid plant per tonne of product H_2SO_4. It thereby lowers:

(a) blowing energy cost

(b) equipment size requirements, hence capital cost.

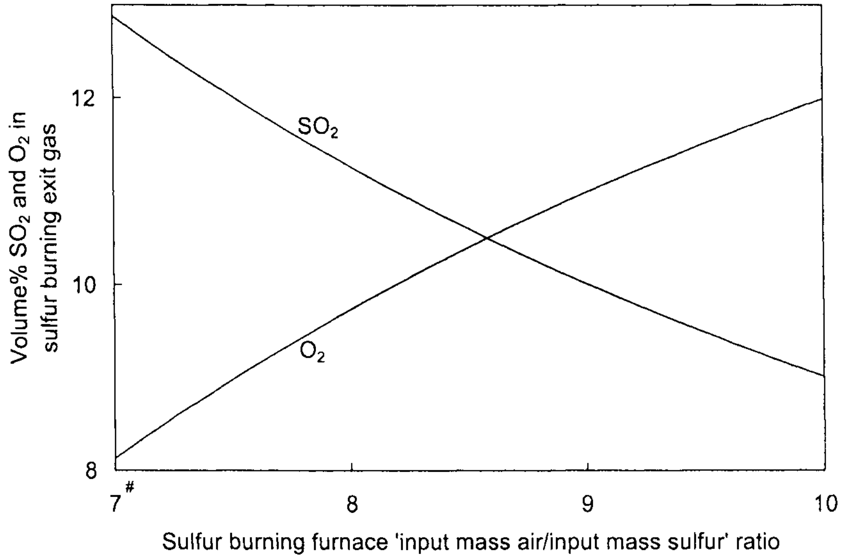

Fig. 3.5. Volume% SO_2 and O_2 in gas produced by burning S with excess dry air (calculated by means of S, O and N molar balances). N_2 concentration is 79 volume% at all ratios, not shown. This is because consumption of one kg-mole of O_2 produces one kg-mole of SO_2. (# For example, 7 kg of input air for every 1 kg of input sulfur.)

Unfortunately, decreasing the input air/input sulfur ratio also decreases the O_2/SO_2 ratio of the gas (Fig. 3.5), potentially lowering catalytic oxidation efficiency.

An alternative way to increase SO_2 concentration (and decrease furnace exit gas volume) is to feed less N_2 to the sulfur burning furnace – by replacing some air with oxygen (Miller and Parekh, 2004).

3.5.4 Target gas temperature

Decreasing sulfur burning's air/sulfur ratio raises product gas temperature, Fig. 3.6. If carried too far (i.e. to raise % SO_2-in-gas), this may damage the sulfur burning furnace or boiler.

11-12 volume% SO_2, 1400 K sulfur burning gas seems optimum.

3.6 Summary

70% of the world's sulfuric acid is made from elemental sulfur. Virtually all of this sulfur is the byproduct of natural gas and petroleum refining.

Elemental sulfur melts at ~390 K. It is easily melted with pressurized steam pipes and pumped molten around the sulfur burning plant.

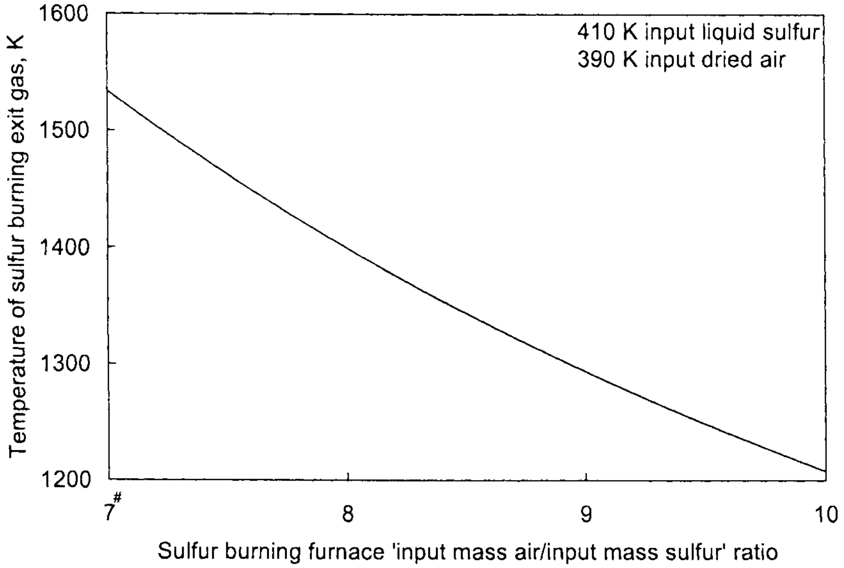

Fig. 3.6. Temperature of offgas from burning sulfur with excess air (calculated by means of S, O, N and enthalpy balances). Offgas temperature is *decreased* by raising input air/input sulfur ratio. This is because (i) excess air in offgas increases with an increasing input air/input sulfur ratio and because (ii) this excess air absorbs sulfur oxidation heat. (# For example, 7 kg of input air for every 1 kg of input sulfur.)

Sulfur burning is the first step in making sulfuric acid from elemental sulfur. It entails:

(a) atomizing molten sulfur in a hot furnace and burning it with excess dried air

(b) cooling the product gas in a boiler and steam superheater.

The product is ~11 volume% SO_2, 10 volume% O_2, 79 volume% N_2 gas (700 K), perfect for subsequent catalytic $SO_2 + \frac{1}{2}O_2 \rightarrow SO_3(g)$ oxidation and H_2SO_4 manufacture.

Sulfur burning's product gas composition and temperature are readily controlled by adjusting the sulfur furnace's input air/input sulfur ratio. Replacement of some of the input air with oxygen gives the process independent O_2/SO_2, temperature and volume control.

References

Dunlavy, D. (1998) An animated view of the polymerization of sulfur. www.molecules.org/experiments/Dunlavy/Dunlavy.html

Jacoby, K. (2004) Main blowers in acid plants. Preprint of paper presented at Sulphur 2004 conference, Barcelona, October 27, 2004, 249 260. www.agkkk.de

Jondle, J. and Hornbaker, D. (2004) Handling molten sulphur in refineries. *Sulfur,* **292**, May-June, 2004, 43 47. www.britishsulphur.com

Miller, D. and Parekh, U. (2004) Upgrading virgin acid plants using oxygen. *Sulfur*, **290**, January-February, 2004, 43 47. www.britishsulphur.com

Outokumpu (2004) *Sulphuric Acid Plants (Sulphur Combustion Section).* Brochure distributed at Sulphur 2004 conference, Barcelona, October 24-27, 2004. www.outokumpu.com

Outokumpu (2005) *Latest Developments in Sulfur Burning Sulfuric Acid Plants.* Brochure distributed at 29th Annual Clearwater Conference (AIChE), Clearwater, Florida, June 3 and 4, 2005 (also presented as paper by Bartlett, C. and Rieder, J., Outokumpu Technology GmbH) www.outokumpu.com

Roensch, L. F. (2005) Steam and boiler water treatment for the modern sulfuric acid plant, paper presented at 29th Annual Clearwater Conference (AIChE), Clearwater, Florida, June 3, 2005 www.chemtreat.com Also, Fahrer, N.D. and Roensch, L.F. (2005) Steam and boiler water treatment technologies for the modern sulfuric acid plant, paper distributed at 29th Annual Clearwater Conference (AIChE), Clearwater, Florida, June 3 and 4, 2005. www.chemtreat.com

Sander, U.H.F., Fischer, H., Rothe, U., Kola, R. and More, A.I. (1984) *Sulphur, Sulphur Dioxide, Sulphuric Acid,* British Sulphur Corporation Ltd., London. www.britishsulphur.com

Sparkler (2004) Vertical Plate Filters. Brochure distributed at Sulphur 2004 meeting, Barcelona, October 24-27, 2004. www.sparkler.nl

Thermal Ceramics (2005) Fire tube boiler.
www.thermalceramics.com/products/firetubeboiler.asp

Tuller, W.N. (1954) *The Sulphur Data Book*, McGraw-Hill, New York, 5 7.
www.mcgraw-hill.com

CHAPTER 4

Metallurgical Offgas Cooling and Cleaning

About 20% of the world's sulfuric acid is made from SO_2 in smelter and roaster offgases. The gases contain 10 to 75 volume% SO_2, Table 4.1. They are hot and dusty. They may also contain impurity vapors, e.g. chlorine and gaseous arsenic compounds.

The SO_2 is suitable for sulfuric acid manufacture, but the gases must be:

(a) cooled

(b) cleaned

(c) diluted with weak SO_2 process gas and/or air

and:

(d) dried

before they go to acidmaking, Fig. 4.1.

This chapter describes gas cooling, cleaning, dilution and $H_2O(g)$ condensation. Final dehydration by contact with strong sulfuric acid is described in Chapter 6.

4.1 Initial and Final SO_2 Concentrations

Continuous smelting and converting gases contain 20-75 volume% SO_2 *as they leave the furnace*. This is too strong for downstream catalytic $SO_2 + \frac{1}{2}O_2 \rightarrow SO_3$ oxidation. The heat of oxidation with this strong gas would overheat the catalyst, Chapters 7 and 8.

For this reason, continuous smelting/converting gas is always diluted with weak process gas (e.g. anode furnace gas) and/or air before it is sent to catalytic SO_2 oxidation.

Table 4.1 shows continuous smelting and converting offgas SO_2 strengths. Tables 7.1 and 7.2 show pre-catalytic oxidation SO_2 strengths.

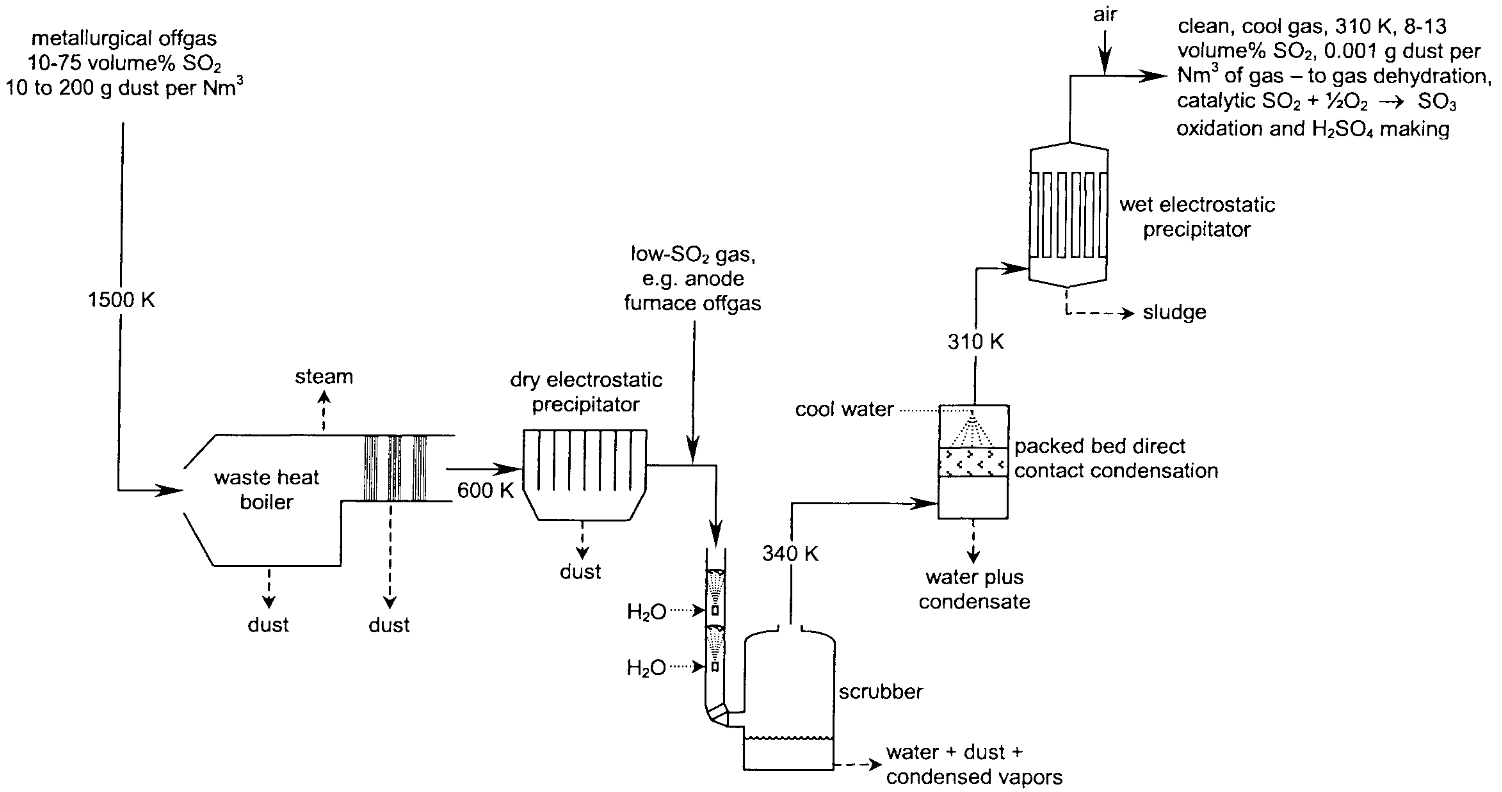

Fig. 4.1. Flowsheet for cooling, diluting and cleaning metallurgical offgas. Gas temperature is lowered from 1500 to 310 K. SO_2 concentration is lowered from 10-75 volume% SO_2 to 8-13 volume% SO_2. Dust plus vapor concentration is lowered from 10-200 g per Nm^3 of gas to 0.001 g per Nm^3 of gas. Efficient gas cleaning minimizes plugging of downstream catalyst and equipment. It also minimizes poisoning of the catalyst. It is the key to efficient, continuous long term metallurgical acid plant operation. Mercury-from-gas removal is described in Section 4.5.3.

Table 4.1. Offgas temperatures and SO_2 and dust concentrations *leaving metallurgical furnaces* (Davenport *et al.*, 2002). The high SO_2 concentrations are due to the use of oxygen enriched air for smelting and continuous converting. The furnace offgases are diluted with weak SO_2 process gases and air to obtain the <13 volume% SO_2 gas required by catalytic SO_2 oxidation. SO_2 gases are also made by gold, lead, molybdenum and pyrite roasting (not shown).

Metallurgical Process	Offgas temperature, K	SO_2 in offgas, volume%	Dust in offgas g per Nm^3
Inco flash smelting	1540-1570	50-75	200-250
Outokumpu flash smelting	1540-1620	30-45	100-250
Outokumpu flash converting	1560	35-40	200
Outokumpu flash direct-to-copper smelting	1590-1670	15-45	200
Mitsubishi smelting	1510-1520	30-35	70
Mitsubishi converting	1500-1520	25-30	100
Submerged-tuyere smelting (Noranda & Teniente)	1470-1510	20-25	15-20
Top-lance smelting (Isasmelt & Ausmelt)	1490-1520	20-25	10
Batch converting (Peirce-Smith & Hoboken)	1470	8-15	3-5
ZnS roasting (fluid bed)	623-673[#]	10[#]	2[#]

[#] After cooling in a waste heat boiler and removing product particulate in a cyclone.

4.2 Initial and Final Dust Concentrations

Metallurgical offgas contains:

10 to 250 grams of dust per Nm^3 of gas

as it leaves the furnace, Table 4.1. If not removed, this dust would quickly plug downstream SO_2 oxidation catalyst. The dust is removed by:

(a) gas cooling and dust settling in a waste heat boiler (occasionally by quenching with water)

(b) dry electrostatic dust precipitation

(c) scrubbing and cooling with water

(d) wet electrostatic 'mist' precipitation.

These steps lower dust-in-gas levels to

~0.001 grams of dust per Nm^3 of gas.

Downstream catalyst beds can be operated continuously for several years with dust at this level.

The next five sections discuss these cooling and dust removal steps.

4.3 Offgas Cooling and Heat Recovery

The first step in treating metallurgical offgas is cooling in preparation for electrostatic dust precipitation. Electrostatic precipitators operate at about 600 K. Above this temperature, their steel structure weakens. Below this temperature, sulfuric acid forms from small amounts of SO_3 and $H_2O(g)$ in the furnace offgas – causing corrosion of the precipitator.

Gas cooling is mostly done in waste heat boilers, Fig. 4.2. These boilers cool the gas and recover its heat in useful form – steam (Abeck, 2003; Peippo *et al*, 1999).

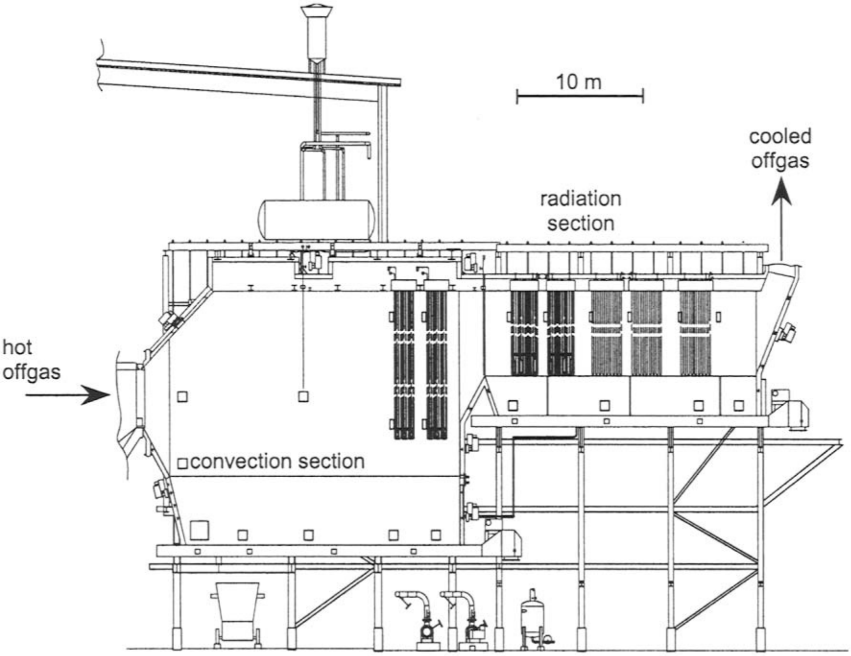

Fig. 4.2. Waste heat boiler for a copper smelting flash furnace (Peippo et al, 1999). Note, left to right: (i) flash furnace gas offtake; (ii) boiler radiation section with water tubes in walls; (iii) suspended water tube baffles in radiation section to evenly distribute gas flow; (iv) convection section with hanging water tubes. Steam from the boiler is used to generate electricity, to power the acid plant's main blower and for general heating and drying.

Most offgas dust falls out in the waste heat boiler. It is collected and recycled to smelting. It falls out due to low gas velocities in the large boiler chambers.

An alternative method of cooling metallurgical offgas is to pass it through sprays of water. Spray cooling avoids investment in waste heat recovery equipment but wastes the heat of the gas. It also generates acidic waste liquid that must be neutralized and treated for solids removal/recycle.

4.4 Electrostatic Collection of Dust

Boiler exit gas is passed through electrostatic precipitators for further dust removal, Figs. 4.3 and 4.4.

The dust particles are caught by:

(a) passing the dusty gas between plate 'dust collection' electrodes and around rod 'corona' electrodes, Fig. 4.3

(b) applying a large electrical potential (~60 000 V) between the plates and rods.

This arrangement causes:

(a) formation of an 'avalanche' of electrons in a corona around the negative rod electrodes (Oglesby and Nichols, 1978)

(b) movement of these electrons towards the positive dust collection plates

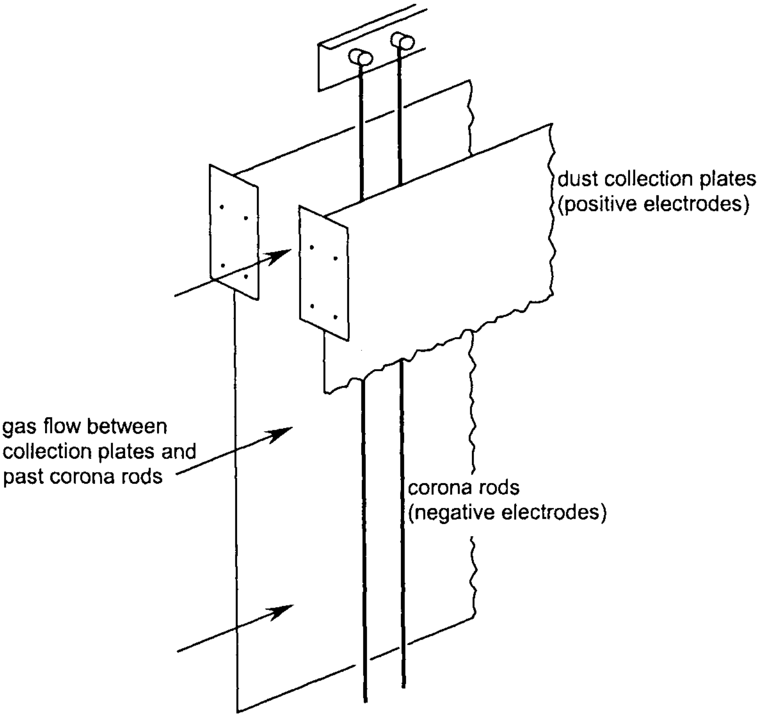

Fig. 4.3. Schematic of dry 'rod and plate' electrostatic precipitator (after Oglesby and Nichols, 1978). The rods have sharp horizontal protrusions (nails) which promote corona formation. Dusty gas flows between the plates and around the rods. A large electrical potential (60 000 V) is applied between the rods and plates. This negatively charges the dust particles – causing them to approach and adhere to the positive collection plates. The dust is gathered by periodically rapping the plates, causing sheets of dust to fall into dust bins below, Fig. 4.4. Table 4.2 gives industrial precipitation data.

Table 4.2. Details of 5 industrial

Operation	M2	M3
startup date	1998	2003
acid plant builder	Korea Zinc Engineering	Outokumpu-Lurgi
acid production, tonnes H_2SO_4 per day	1150 (2 roasters, 2 gas cleaning plants, 1 acid plant)	2200 (nominal)
gas source	zinc sulfide roaster	Noranda smelting furnace, air dilution and water quenching
total gas through precipitators thousand Nm^3 per hour	102	163
number of precipitators	two 3 field precipitators	2 identical
series or parallel	parallel	parallel
Gas composition before precipitation, volume%		
SO_3	0.1	0
SO_2	10.0	11.5
O_2	5.0	13.4
H_2O	10.4	12.6
CO_2		2.1
N_2	remainder	remainder
Precipitator details	each precipitator	each precipitator
height × length × width, m	7.5 × 10.45 × 4.8	19.2 × 20.1 × 8.5
collection plates	11	57
collection plate area, m^2		1134
'corona' electrode type	Variodyn 15 * 2 mm	stiff rods
number	792	756
rod to plate voltage, V	65 000	110 000
rod to plate current, A	0.8	0.5
gas temperature, K		
before precipitation	623-673	653-673
after precipitation	593-643	643-653
Gas composition after precipitation, volume%		
SO_3	0.1	
SO_2	9.5	11
O_2	5.5	14
H_2O	10.0	12
CO_2		2
N_2	remainder	remainder
Dust-in-gas loading, g/Nm^3		
before precipitation	2.0	12
after precipitation	0.2	0.5

dust precipitator plants.

M4	Asarco Hayden	Phelps Dodge Miami
1999	1983	1972 to 1998
Mitsubishi-Lurgi	Monsanto	Lurgi Fleck
2100-2400	1630	2400
Mitsubishi continuous copper smelter	INCO flash furnace and Peirce-Smith converter gas	Isasmelt furnace, Hoboken converters, electric furnace
148	197	230
2 identical	8	1 (3 fields)
parallel	2 parallel sets of 4	
		from Isasmelt
0.48	0	0
15.2	9.0	14.1
10.6	11.4	2
45 g per dry Nm^3	8.4	28.9
3.59		6
remainder	remainder	49
each precipitator	each precipitator	
15.9 × 18.7 × 7.4	6.6 × 5.2 × 4.4	19 × 9.1 × 9.1
57		558
2426		7294
stiff rods	rods	steel ribbons
1134	1408	6480
623	305	616
613	308	610
0.48	0	0
15.2	9.0	14.1
10.6	11.4	2
45 g per dry Nm^3	5.9	28.9
3.59		6
remainder	remainder	49
60		4.8 g per wet Nm^3
0.5		0.2 g per wet Nm^3

(c) negative charging (ionization) of gas molecules outside the corona by collision and combination of electrons with gas molecules

(d) negative charging of dust by collision and attachment of gas ions to dust particles

(e) electrical attraction of negatively charged dust to the positive collection plates

(f) adhesion of the dust to the collection plates by electrical, mechanical and molecular forces.

About 70% of the dust-in-offgas is removed in the waste heat boiler and about 30% in electrostatic precipitators. The small remainder (~1%) is removed by water scrubbing, next section.

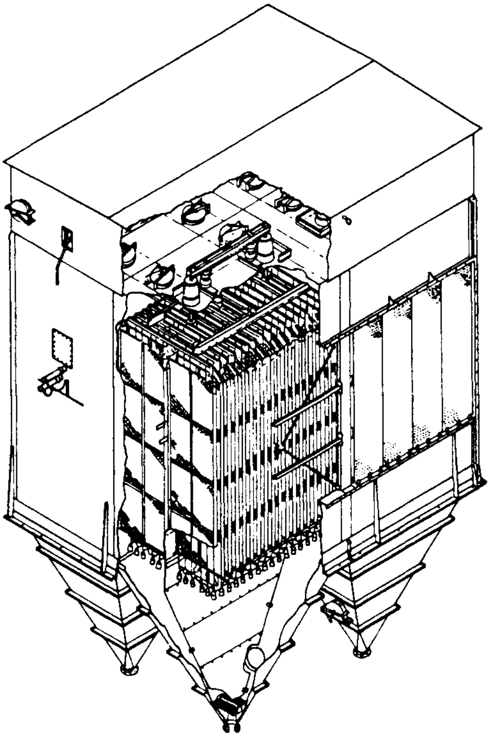

Fig. 4.4. Wire and plate dry electrostatic precipitator, reprinted from Oglesby and Nichols (1978), p 269 by courtesy of Taylor and Francis Group, LLC. The parallel collector plates and bottom dust bins are notable. In this case, wires are hung between the plates – weights for keeping them vertical are just visible. Structural and operating data for a recent precipitator are:

length × width × height, m	8 × 7 × 6
total dust collection plate area, m^2	2200
gas velocity between plates, m per second	0.5
gas residence time in precipitator, s	15
'corona' electrodes	wires and stiff rods
applied rod to plate voltage, V	60 000
rod to plate current, A	0.4

4.5 Water Scrubbing (Table 4.3)

Gas leaves electrostatic precipitators at ~600 K. It still contains 0.1 to 1 g of dust and unwanted vapors per Nm^3 of gas. These are now removed by intimately contacting the gas with water sprays. This contact:

(a) lowers the gas's dust content to ~0.001 g per Nm^3 of gas

(b) condenses and absorbs unwanted vapors, e.g. Cl_2 and gaseous metal compounds.

The result is clean, vapor free gas.

Venturi, radial flow, packed bed and Dynawave®, Fig. 4.5 (Enviro-chem, 2005) scrubbers are used.

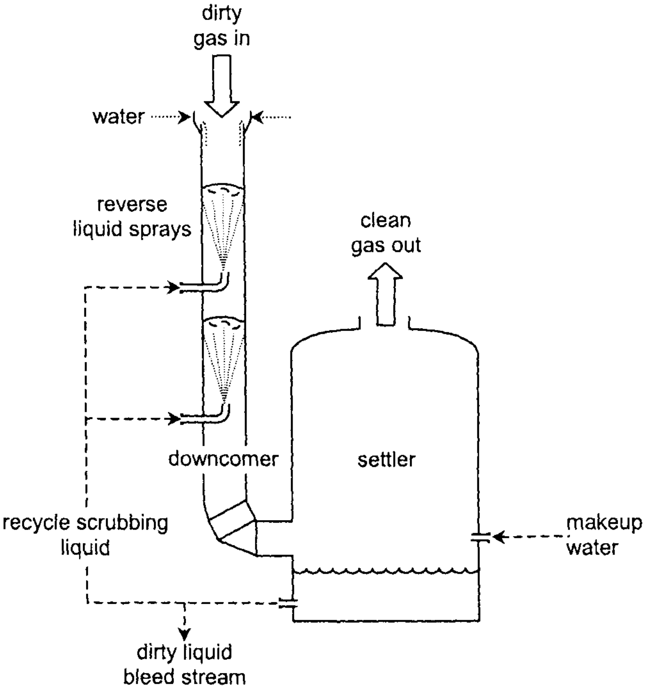

Fig. 4.5. Dynawave® scrubber for removing particulate and soluble impurities from cooled (600 K), partially cleaned furnace offgas (Puricelli *et al.*, 1998; Enviro-chem, 2005). Note the (i) upward sprays in and (ii) the weir atop the 'downcomer'. The sprays clean the gas. The weir continuously overflows water, which wets and cools the downcomer walls. These scrubbers are used for both metallurgical and spent acid regeneration furnace gases. Large scrubber details are:

downcomer diameter:	1 m (Hastelloy G30)
settler diameter:	4 m (Hastelloy G30)
gas flow	1 000 000 Nm^3 per hour
spray flow (total)	8000 m^3 per hour.

The downcomer often enters through the roof of the settler. Multiple sprays at one level, rather than a single spray at two levels, are also used.

Table 4.3. Details of 5 industrial gas

Plant	M2	M3
Scrubber data		
type of scrubber	radial flow, 2 sets	radial flow
number of scrubbers	2	1
height × diameter, m	16 × 2.5	17 × 6
Gas data		
gas source	dry precipitator exit gas	precipitator exit gas
particulate concentration g/Nm^3		
before scrubber	0.2	0.5
after scrubber	0.1	
gas flow through scrubber thousand Nm^3 per hour	50	175
gas temperature, K		
before scrubber	623	643-653
after scrubber	339	339
scrubber liquid flow, m^3/hour	350 × 2 sets	528
liquid temperature, K		
into scrubber	338	339
out of scrubber	338	339
mass% H_2SO_4 in scrubber liquid	1 to 5	1 to 10
Water removal from gas by cooling/condensation		
method	direct cooling/water condensation in packed tower	direct cooling/water condensation in packed tower
number of condensers	2	1
height × diameter, m	15 × 5.2	17 × 6.8
packing or tubes	polypropylene spheres	polypropylene spheres
packing height, m		
liquid flow through condenser		
liquid temperature in, K	310	
gas temperature in, K	339	339
gas temperature out, K	310.5	308
Wet electrostatic precipitation		
number of precipitators	4	6
height × diameter, m	10.7 × 3.7	5.2 × 10.6
number of rods and collection tubes per precipitator	126	248
tube length × diameter, m	4.5 × 0.25	5.7 × 0.25
tube area per precipitator, m^2	445	28
tube material	polypropylene	ceramic
rods	lead, 50 mm diameter	6mm diameter
Gas composition (volume%) after scrubbing, condensing and electrostatic precipitation		
SO_3	0	0.1
SO_2	9.0	11.7
O_2	6.0	14.2
CO_2		1.9
H_2O		76 g per Nm^3 of gas
N_2		remainder
dust concentration g/Nm^3 of gas	0.001	

cleaning and water condensation plants.

M4	Asarco Hayden	Phelps Dodge Miami
Venturi scrubber (VS) + washing tower (WT)	open and packed towers	Venturi scrubbers
1 each	5	2
25×1.2-5.4 (VS); 22×8.2 (WT)	9.1 × 6.1	20 × (2.4 inlet; 1.8 throat; 3 outlet)
dry precipitator exit gas	precipitator exit gas	dry precipitator exit gas
0.5		0.2
148	197	230
673	469	616
337	299	334
580 (VS), 1130 (WT)	132 to 727	950
355 (VS), 340 (WT)	343	
340	363	
10-15	1	
heat exchanger condenser	direct cooling/water condensation in packed tower	Venturi scrubbers, retention coolers & heat exchanger star coolers
3 parallel, 2 series	2	
3.1 × 2.2	9.1 × 6.1	
Pb lined tubes	polypropylene spheres	649 tubes: 0.076 m dia. ×3 m long
	3.7	
337	343	334
320	363	309
3 parallel, 2 series	8	10
13.3 × 6.6		
424	176	129 or 302
5.4 × 0.25	3.7 × 0.25	7.6 × 0.2 or 4.6 × 0.25
60		7200 (total)
PVC	lead	hexagonal PVC
carbon steel, lead lining		
0	0	
14.63	9.0	9.6
11.02	11.4	9.6
3.47	0.9	0.9
101 g per dry Nm^3 of gas	5.9 (volume%)	8.5 (volume%)
remainder	remainder	71.4
		0.009

4.5.1 Gas temperature after scrubbing

Liquid scrubbing removes dust and vapors. It also cools the gas to ~340 K, mainly by evaporating water.

4.5.2 Impure scrubbing liquid

The Fig. 4.5 scrubbing liquid is acidic and impure. Excessive buildup of H_2SO_4 (from $SO_3(g)$ and H_2O) and impurities is avoided by:

(a) continuously bleeding off a small portion of the liquid

(b) replacing the bleed with clean water.

The amount of bleed is controlled to keep the scrubber liquid's acid level to below ~10 mass% H_2SO_4 – to minimize corrosion. The bleed is neutralized and treated for metal recovery (Newman et al., 1999).

4.5.3 Mercury removal

Mercury vapor is not removed from gas by Fig. 4.1 processing. It can, however, be removed (Hultbom, 2003) by:

(a) contacting the gas with an aqueous solution of $HgCl_2$ – forming solid calomel, Hg_2Cl_2

(b) passing the gas through a bed of porous Se impregnated ceramic pieces – forming solid HgSe.

These processes are referred to as the Boliden Norzink Mercury Removal Process (Boliden Norzink, 2004) and the selenium filter process (Selenium Filter, 2004). Combined sequentially, they keep Hg-in-sulfuric acid below 0.25 parts per million.

An alternative is to pass Boliden Norzink exit gas through a column of activated PbS coated pumice (Dowa Process). This precipitates solid HgS and keeps Hg-in-sulfuric acid below 0.05 parts per million (Lossin and Windhager, 1999).

4.6 $H_2O(g)$ Removal from Scrubber Exit Gas (Table 4.3)

Scrubber exit gas is saturated with $H_2O(g)$. This $H_2O(g)$ must be removed prior to catalytic $SO_2 + \frac{1}{2}O_2 \rightarrow SO_3$ oxidation – to avoid accidental downstream $H_2SO_4(\ell)$ formation/corrosion after SO_3 has formed. The $H_2O(g)$ is removed by:

(a) cooling the gas

then:

(b) contacting it with strong sulfuric acid, Chapter 6.

Gas cooling is an inexpensive way to remove most of scrubber exit gas's $H_2O(g)$, Fig. 4.6. It is done by transferring heat to cool water in:

(a) direct contact packed beds

or:

(b) shell and tube heat exchangers.

In a packed bed, the condensing water joins the cool water stream. In a heat exchanger, the condensing water flows down the cool tube walls in a separate stream. In both cases the cooling water is air cooled and recycled to condensation.

The clean, cool, partially dried gas leaves the top of the condenser and passes through electrostatic mist precipitation to final dehydration with strong sulfuric acid, Chapter 6.

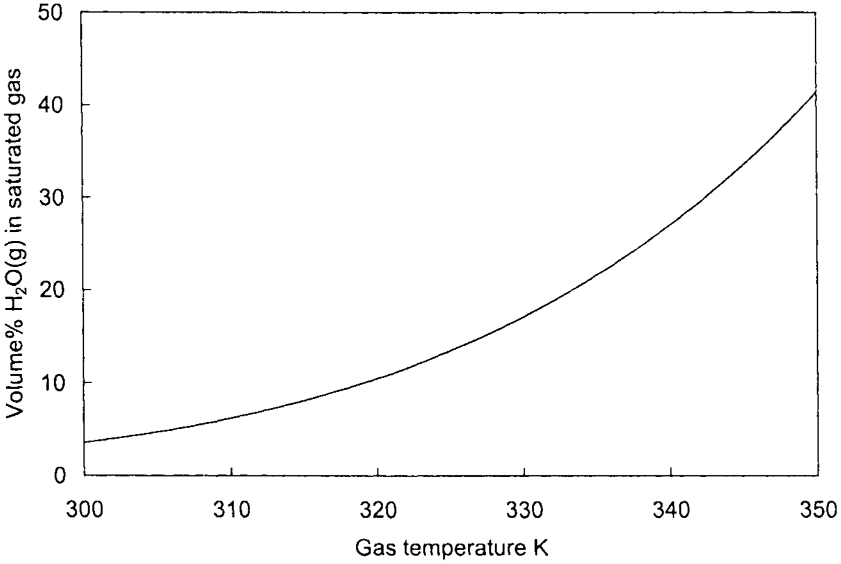

Fig. 4.6. Volume% $H_2O(g)$ in saturated gas as a function of saturation temperature (Perry and Green, 1997). A decrease in gas temperature from 340 K to 310 K is seen to lower volume% $H_2O(g)$-in-gas from ~27 volume% to 6 volume%, equivalent to about 75% $H_2O(g)$ removal.

4.7 Summary

About 20% of the world's sulfuric acid is made from the SO_2 in smelter and roaster offgases. The gases contain 10 to 75 volume% SO_2. Their SO_2 is suitable for making sulfuric acid but the gases must be:

cooled
cleaned of dust and unwanted vapors
diluted with weak SO_2 process gas and/or air
dried

before they are sent to catalytic SO_2 oxidation.

Cooling is usually done in a waste heat boiler – which cools the gas and recovers its heat as steam. Considerable dust also 'falls out' in the waste heat boilers.

Dust and unwanted vapors are removed from the gas by electrostatic precipitation and aqueous scrubbing.

Finally, $H_2O(g)$ is removed by:

gas cooling and water condensation, Section 4.6

then:

dehydration with strong sulfuric acid, Chapter 6.

The gas is now ready for catalytic SO_2 oxidation and subsequent H_2SO_4 making.

Suggested Reading

Friedman, L.J. and Friedman, S.J. (2004a) The wet gas sulphuric acid plant (part 1). *Sulphur*, **292**, May-June 2004, 27 31. www.britishsulphur.com

Friedman, L.J. and Friedman, S.J. (2004b) The wet gas sulphuric acid plant (part 2). *Sulphur*, **293**, July-August 2004, 29 35. www.britishsulphur.com

Ludtke, P. and Muller, H. (2003) Best available acid technology for copper smelters: a state-of-the-art review. In *Copper 03-Cobre 03, Proceedings of the Fifth International Conference, Vol. IV (Book 1) Pyrometallurgy of Copper, the Hermann Schwarze Symposium on Copper Pyrometallurgy, Smelting Operations, Ancillary Operations and Furnace Integrity*, ed. Diaz, C., Kapusta, J. and Newman, C., The Metallurgical Society of the Canadian Institute of Mining, Metallurgy and Petroleum, Montreal, 543 554. www.metsoc.org

References

Abeck, W. (2003) Debottlenecking pyrometallurgical process lines by ultra-modern waste heat boiler upgrades. In *Copper 03-Cobre 03, Proceedings of the Fifth International Conference, Vol. IV (Book 1) Pyrometallurgy of Copper, the Hermann Schwarze Symposium on Copper Pyrometallurgy, Smelting Operations, Ancillary Operations and Furnace Integrity*, ed. Diaz, C., Kapusta, J. and Newman, C., The Metallurgical Society of the Canadian Institute of Mining, Metallurgy and Petroleum, Montreal, 531 541. www.metsoc.org

Boliden Norzink (2004) The Boliden Norzink mercury removal process. Outokumpu Technology AB, Skelleftea, Sweden www.outokumpu.com

Davenport, W.G., King, M., Schlesinger, M. and Biswas, A.K. (2002) *Extractive Metallurgy of Copper, 4th Edition.* Elsevier Science Ltd., Oxford, England, 219. www.elsevier.com

Enviro-chem (2005) Dynawave Reverse Jet Scrubber. www.enviro-chem.com/airpol/common/rjs.html

Hultbom, K.G. (2003) Industrially proven methods for mercury removal from gases. *EPD Congress 2003*, ed. Schlesinger, M., TMS, Warrendale, PA, 147 156 www.tms.org

Lossin, A. and Windhager, H. (1999) Improving the quality of smelter acid: the example of Norddeutsche Affinerie's "premium quality". In Proceedings of Sulphur 99 conference, Calgary, Alberta, October 17-20, 209 220. www.na-ag.com

Newman, C.J., Collins, D.N. and Weddick, A.J. (1999) Recent operation and environmental control in the Kennecott smelter. In *Copper 99-Cobre 99, Proceedings of the Fourth International Conference, Vol. V Smelting Operations and Advances*, ed. George, D.G., Chen, W.J., Mackey, P.J. and Weddick, A.J., TMS, Warrendale, PA, 29 45. www.tms.org

Oglesby, S. and Nichols, G.B. (1978) *Electrostatic Precipitation*, Marcel Dekker Inc., New York. www.dekker.com

Peippo, R., Holopainen, H. and Nokelainen, J. (1999) Copper smelter waste heat boiler technology for the next millennium. In *Copper 99-Cobre 99, Proceedings of the Fourth International Conference, Vol. V Smelting Operations and Advances*, ed. George, D.B., Chen, W.J., Mackey, P.J. and Weddick, A.J., TMS, Warrendale, PA, 71 82. www.tms.org

Perry, R.H. and Green, D.W. (1997) *Perry's Chemical Engineers' Handbook – 7th ed.* McGraw-Hill, New York. www.mcgraw-hill.com

Puricelli, S.M., Grendel, R.W. and Fries, R.M. (1998) Pollution to power, a case study of the Kennecott sulfuric acid plant. In *Sulfide Smelting '98* ed. Asteljoki, J.A. and Stephens, R.L., TMS, Warrendale, PA, 451 462. www.tms.org

Selenium Filter (2004) Mercury removal from gases with selenium filter. Outokumpu Technology AB, Skelleftea, Sweden www.outokumpu.com

CHAPTER 5

Regeneration of Spent Sulfuric Acid

About 10% of sulfuric acid is used as catalyst in petroleum refining and polymer manufacture. The acid is not consumed during these uses, but its effectiveness is diminished by contamination with water, hydrocarbons and other chemicals.

Excessive contamination is prevented by:

(a) bleeding contaminated 'spent' acid from the catalyst circuit

(b) replacing it with new strong (98+ mass% H_2SO_4) acid.

The contaminated 'spent' is made into new strong acid by:

(a) decomposing its $H_2SO_4(\ell)$ to $SO_2(g)$, $O_2(g)$ and $H_2O(g)$ in a hot (1300 K) furnace, Fig. 5.1

(b) cooling the furnace offgas in a heat recovery system

(c) cleaning ash and soot particles from the gas

(d) condensing $H_2O(g)$ from the gas

(e) dehydrating the gas by contact with strong sulfuric acid

(f) oxidizing the gas's SO_2 to SO_3

(g) making $H_2SO_4(\ell)$ by the reaction:

$$SO_3(g) + H_2O(\ell)_{\text{in strong sulfuric acid}} \rightarrow H_2SO_4(\ell)_{\text{in strengthened sulfuric acid}}.$$

The steps are all continuous. This chapter describes steps (a) to (d). Steps (e) to (g) are described in Chapter 6 onwards.

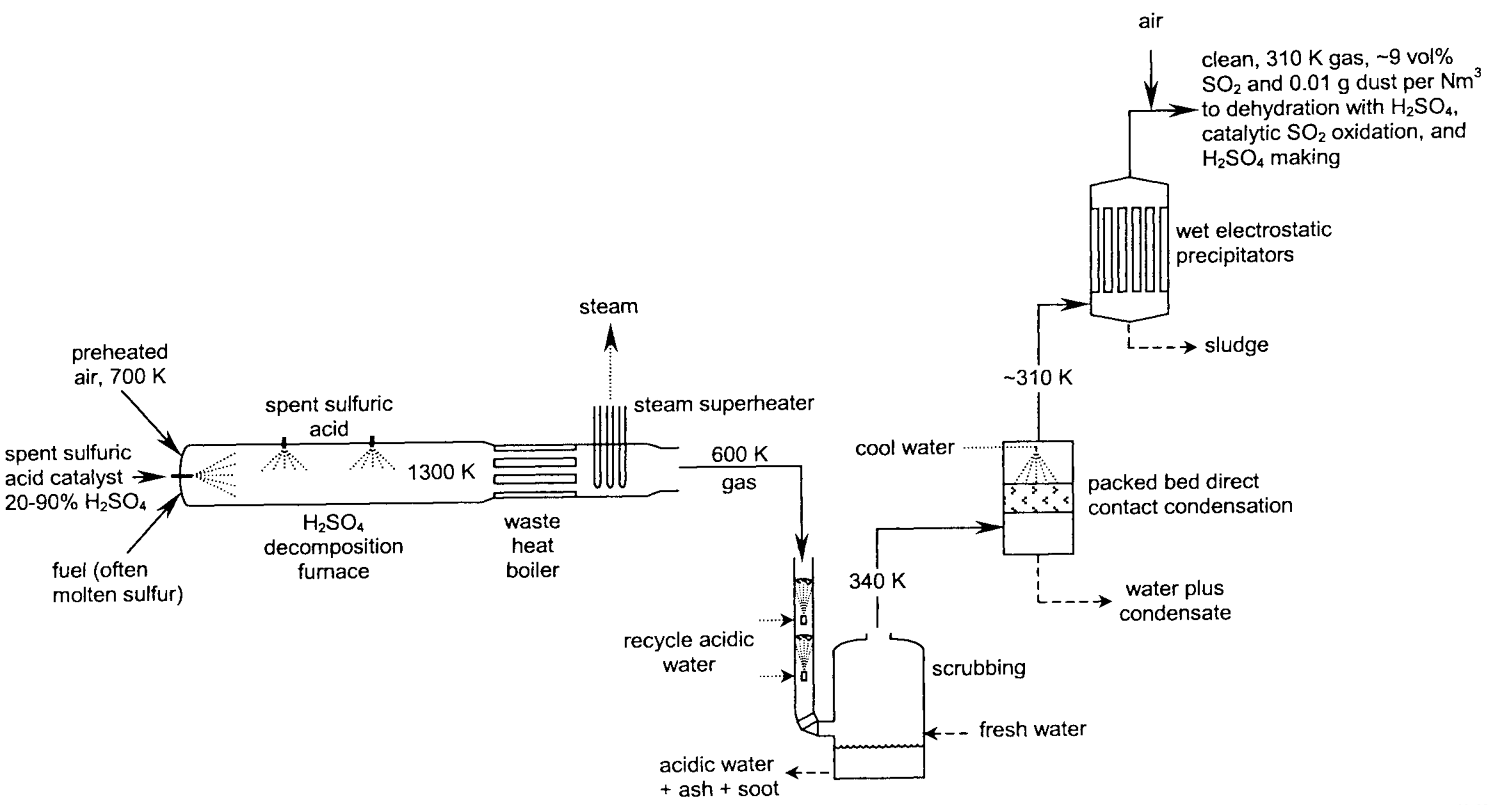

Fig. 5.1. Spent sulfuric acid regeneration flowsheet. $H_2SO_4(\ell)$ in the contaminated spent acid is decomposed to $SO_2(g)$, $O_2(g)$ and $H_2O(g)$ in a mildly oxidizing, 1300 K fuel fired furnace. The furnace offgas (6-14 volume% SO_2, 2 volume% O_2, remainder N_2, H_2O, CO_2) is cooled, cleaned and dried. It is then sent to catalytic $SO_2 + \frac{1}{2}O_2 \rightarrow SO_3$ oxidation and H_2SO_4 making, Eqn. (1.2). Air is added just before dehydration (top right) to provide O_2 for catalytic SO_2 oxidation. Molten sulfur is often burnt as fuel in the decomposition furnace. It provides heat for H_2SO_4 decomposition and SO_2 for additional H_2SO_4 production. Tables 5.2 and 5.3 give details of industrial operations.

5.1 Spent Acid Compositions

Table 5.1 shows the compositions of two spent acids. Both are made into new, strong sulfuric acid as described in Fig. 5.1.

Water rich acids (e.g. methyl methacrylate spent acid) often have part of their water evaporated before they are sent to the H_2SO_4 decomposition furnace (Rohm and Haas, 2003). This decreases:

(a) the amount of liquid that must be treated in the furnace per tonne of new H_2SO_4

(b) the decomposition furnace's fuel requirement per tonne of new H_2SO_4 (because less water has to be heated and evaporated in the furnace).

Table 5.1. Compositions (mass%) of spent sulfuric acids from two chemical processes. Both processes use sulfuric acid as catalyst. The acid becomes contaminated with water, hydrocarbons, and other chemicals during use. It is made into new sulfuric acid as described in Fig. 5.1.

Component	Spent sulfuric acid from	
	petroleum alkylation catalysis	methyl methacrylate catalysis
H_2SO_4, mass%	~90	15
H_2O, mass%	3-5	25
dissolved hydrocarbons, mass%	4-7#	5
ammonium bisulfate, mass%		45###
acetone disulfonic acid, mass%		5###
low fuel value tars, mass%		5
particulate (mainly iron)	<100 parts per million##	

#H/C atomic ratio ~3 ##occasionally higher ###These components are decomposed to CO_2, $H_2O(g)$, N_2 & SO_2.

5.2 Spent Acid Handling

Spent acid is handled very carefully. It is very corrosive. Also, its H_2SO_4 and hydrocarbons may continue to react during storage and transport (Lang, 1998).

The acid is delivered to the spent acid regeneration plant by:

stainless steel pipe (within a chemical complex)

dedicated stainless steel (road) trailers

phenolic lined steel railway cars

double hulled steel barges.

It is stored in isolated corrosion resistant stainless steel tanks. The spent acids from various sources (e.g. alkylation catalyst, jet fuel catalyst) are stored separately. This avoids unanticipated reactions between their different organic components.

5.3 Decomposition

Spent acid is decomposed by spraying fine droplets of the acid into a mildly oxidizing 1300 K furnace, Fig. 5.2. The decomposition reaction is:

$$\underset{\text{in spent acid, 300 K}}{H_2SO_4(\ell)} \rightarrow \underset{\text{in furnace offgas, 1300 K}}{SO_2(g) + \frac{1}{2}O_2(g) + H_2O(g)} \qquad \Delta H^\circ = \sim +380 \text{ MJ/kg-mole } H_2SO_4 \qquad (5.1).$$

Heat for this reaction is mainly provided by burning molten sulfur and other fuels with preheated air (occasionally oxygen-enriched) and the O_2 from Reaction (5.1). A small amount of heat is obtained from oxidizing the spent acid's hydrocarbons. Sulfur burning has the advantages that it increases SO_2 concentration in decomposition furnace offgas and H_2SO_4 production rate.

5.3.1 Other reactions

Other reactions in the decomposition furnace are:

(a) water evaporation, i.e.: $H_2O(\ell) \rightarrow H_2O(g)$ (5.2)

and:

(b) chemical decomposition, e.g. ammonium bisulfate decomposition:

$$4NH_4HSO_4 + O_2 \rightarrow 2N_2 + 10H_2O(g) + 4SO_2 \qquad (5.3)$$

all of which:

(a) require heat

(b) produce $H_2O(g)$.

The heat is provided by burning extra fuel, e.g. molten sulfur or natural gas. The $H_2O(g)$ is removed by condensation (Fig. 5.1) and dehydration (Chapter 6).

5.3.2 Spent acid spraying

Spent acid is sprayed into a decomposition furnace in the form of 500-1000 μm droplets (Dafft and White, 2002). The droplets present a large acid surface to the hot combustion gas, promoting rapid evaporation and decomposition. The droplets are most commonly produced by forcing the acid into the furnace through fine nozzles (Rohm and Haas, 2003; Bete, 2005). Spinning cup atomizers are also used.

The acid is sprayed into the furnace at two to six locations. This multi spray arrangement avoids localized cooling that occurs when all the acid is sprayed in at one location.

Table 5.2. Operating details of 2 industrial spent acid decomposition furnaces.

Plant	SP1	composite
acid production, tonnes H_2SO_4/day	444	
Spent acid	alkylation catalyst	methyl methacrylate catalyst
composition, mass%		
H_2SO_4	88.48	~15
H_2O	4.99	~25
hydrocarbons	6.53	~5
ammonium bisulfate		~45
acetone disulfonic acid		~5
tars		~5
Spent acid decomposition furnace data		
number of furnaces	1	
shell length × diameter, m	15.3 × 4.9	20 x 4
spent acid injection		
spinning cup or spray guns	spray guns	both
number of sprayers per furnace	6	
spent acid input rate, tonnes/hour	24.6	
combustion details		
fuel, e.g. molten sulfur, natural gas	natural gas	molten S and natural gas
rate, MJ per tonne of spent acid	2200	
air rate, kg per tonne of spent acid	1440	
temperatures, K		
air into furnace	678	800
fuel into furnace	ambient	
spent acid into furnace	ambient	ambient
gas out of furnace	1317	1330
Waste heat boiler		
type	fire tube	fire tube
length × diameter, m	5.5 × 2.6	
number of tubes	1000	
tube diameter, m	0.05	
tube material	carbon steel	carbon steel
number of steam superheaters		
gas temperatures, K		
into boiler	1317	1330
out of steam super heater	554	620
steam production,		
tonnes of steam per tonne spent acid		
pressure, bar gage	32	40
temperature, K	511	
Product gas		
flowrate, thousand Nm^3/hour	37	
composition, volume%		
SO_3		
SO_2	14.2	6-8
O_2	2.75	2
H_2O		
CO_2	10.2	

Fig. 5.2. Spent acid decomposition furnace. It is brick lined steel ~4 m diameter and 20 m long. The energy for decomposing $H_2SO_4(\ell)$ into $SO_2(g)$, $O_2(g)$ and $H_2O(g)$ and for evaporating water is provided by burning molten sulfur and natural gas with hot air. Industrial details are given in Table 5.2.

5.4 Decomposition Furnace Product

Decomposition furnace exit gas typically contains:

Component	Concentration, volume%
SO_2	6-14
SO_3	0.1-0.3
O_2	2-3
$H_2O(g)$	25-30
CO_2	10
N_2	50
particulates (mainly ash and soot)	0.1-1 gram per Nm^3

Its H_2O and particulates are removed before it is sent to catalytic SO_2 oxidation. Its O_2 content is increased by adding air just before gas dehydration, Fig. 5.1.

5.5 Optimum Decomposition Furnace Operating Conditions

Decomposition furnaces are operated to efficiently decompose their spent acid into SO_2, O_2 and $H_2O(g)$. Fig. 5.3 suggests optimum conditions for achieving this goal. They are:

furnace temperature:	1250 to 1350 K
O_2 in product gas:	1.5 to 2.5 volume%.

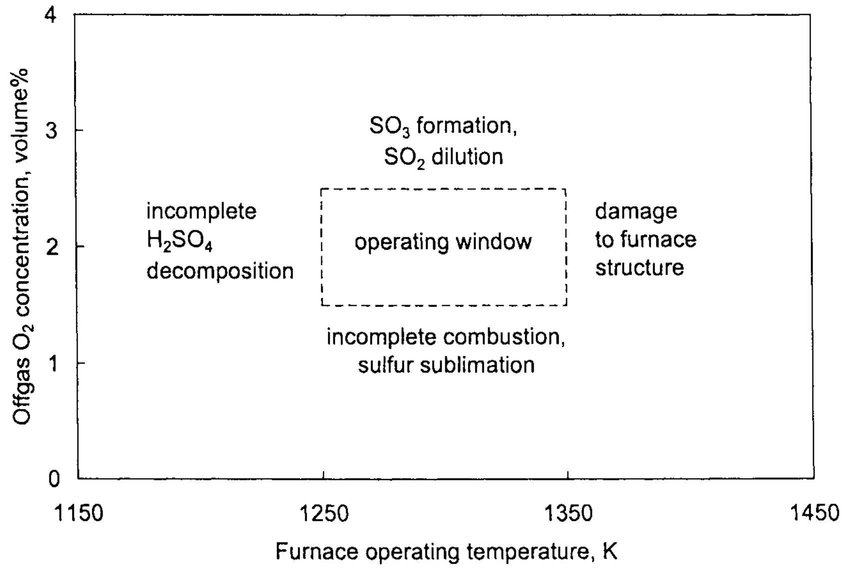

Fig. 5.3. Operating window for spent acid decomposition furnace (Outokumpu, 2004; Monsanto Enviro-Chem, 2005; Lang, 1998). Optimum temperature and O_2-in-furnace-offgas ranges are suggested.

5.5.1 Temperature effects

Decomposition furnace temperatures below ~1250 K give un-decomposed $H_2SO_4(g)$ in the furnace gas. This decreases acid recovery and causes downstream corrosion.

Temperatures above ~1350 K tend to damage the furnace structure.

Furnace temperature is measured with thermocouples. It is controlled to ~ 1300 K by adjusting fuel combustion rate and air preheat temperature. Feed forward control based on scheduled changes in spent acid composition and feed rate is employed to optimize the process (Rohm and Haas, 2003).

5.5.2 O_2 content effects

Low O_2 levels in the decomposition furnace gas give sulfur vapor in the gas. This sulfur sublimes and plugs downstream cooling and cleaning equipment (Monsanto Enviro-Chem, 2005). It is avoided by keeping O_2-in-decomposition furnace gas at 2 to 2.5 volume% (Lang, 1998).

Excessive O_2-in-gas levels, on the other hand, give SO_3 in the product gas. This SO_3 is inadvertently absorbed during gas scrubbing and cooling – which:

(a) decreases acid regeneration efficiency

(b) increases the amount of acidic scrubbing/cooling liquid that must be neutralized and evaporated.

O_2-in-furnace gas concentrations are measured with zirconium oxide sensors (Ametek, 2005; Weiss and Puricelli, 2004). They are controlled by adjusting air input rate.

5.6 Preparation of Offgas for SO_2 Oxidation and H_2SO_4 Making

Decomposition furnace offgas is:

hot (~1300 K)
dusty (~1 g particulate/Nm^3 of gas)
concentrated in $H_2O(g)$ (25+ volume%)
too weak in O_2 for catalytic SO_2 oxidation.

It must, therefore, be:

(a) cooled

(b) treated for dust and $H_2O(g)$ removal

(c) strengthened with O_2, by adding air.

The gas is cooled by:

(a) passing it through a waste heat boiler and steam superheater (or air heater), Fig. 5.1

(b) scrubbing with cool water.

Its dust is removed by aqueous scrubbing and wet electrostatic precipitation.

Its $H_2O(g)$ is removed by condensation with cool water and dehydration with strong sulfuric acid, Chapter 6.

Its O_2 content is raised by adding air just before dehydration.

Industrial details are given in Table 5.3.

5.6.1 Gas composition

After the above treatments, spent acid regeneration gas typically contains:

Component	Concentration entering catalytic SO_2 oxidation volume %
SO_2	8-10
SO_3	0
O_2	10-12
$H_2O(g)$	0
CO_2	6-10
N_2	68-76
particulate	< 0.1 grams per Nm^3 of gas

Table 5.3 Details of spent acid decomposition furnace offgas cleaning and water condensation.

Plant	SP1	composite
Scrubber data		
type of scrubber	spray tower	
number of scrubbers	1	
height × diameter, m	10.6 × 3.96	
Gas data		
gas source	waste heat boiler	waste heat boiler
particulate concentration g/Nm^3		
before scrubber		
after scrubber		
gas flow through scrubber thousand Nm^3/hour	37	
gas temperature, K		
before scrubber	566	600
after scrubber	340	353
scrubber liquid flow, m^3/hour		
liquid temperature, K		
into scrubber	338	
out of scrubber		
mass% H_2SO_4 in scrubber liquid		
Water removal from gas by cooling/condensation		
Method	Karbate heat exchanger	
number of condensers	4	
height × diameter, m	4.88 × 1.1	
liquid flow through tower m^3/hour		
liquid temperature in, K		
gas temperature in, K	377	
gas temperature out, K	312	308
Wet electrostatic precipitation		yes or scrubber
number of precipitators	2	
height × diameter, m	9.2 × 4.8	
number of rods and collection tubes per precipitator	120	
tube diameter, m	round	
tube area per precipitator, m^2	290	
tube material	lead	
rods	star wire	
applied voltage, V	260-360	
wire-to-tube current, milliamps	50-160	
Gas composition (volume%) after scrubbing, condensing and precipitation		
SO_2	9.9	9
SO_3		
O_2	7.9	
H_2O	8.2	
CO_2	8.5	
N_2	60.5	
mist droplets, g/Nm^3 of gas	0.02-0.1	

It is sent to:

(a) catalytic $SO_2 + \frac{1}{2}O_2 \rightarrow SO_3$ oxidation, Chapter 7

(b) H_2SO_4 making from SO_3 by the reaction $SO_3(g) + H_2O_{\text{in strong sulfuric acid}} \rightarrow H_2SO_4(\ell)_{\text{in strengthened sulfuric acid}}$ (Chapter 9).

The new acid is then returned for further catalyst service – or sold.

5.7 Summary

Sulfuric acid is used as catalyst in petroleum refining and other industrial organic processes. The sulfuric acid catalyst is not consumed, but it becomes ineffective as it absorbs water, hydrocarbons and other chemicals over time. Its catalytic properties are maintained by bleeding off some of the contaminated 'spent' acid and replacing the bleed with new strong acid.

The spent acid bleed is recycled and made into new acid by:

(a) decomposing its H_2SO_4 into SO_2, O_2 and $H_2O(g)$ in a hot (1300 K), mildly oxidizing furnace

(b) removing dust and condensing water from the furnace's offgas

(c) adding O_2 (in air)

(d) dehydrating the gas with strong sulfuric acid

(e) catalytically oxidizing the gas's SO_2 to SO_3

(f) making new, strong sulfuric acid from (e)'s SO_3.

Suggested Reading

Rhodia (2002) Rhodia regeneration network offers environmental and economic advantages to California refiners facing MTBE phase-out.
www.us.rhodia.com/news/pr/SulfuricAcid_Ca-4-23-02.htm

Viergutz, M.D. (2004) On-site acid regeneration lowers costs. *Sulphur*, **294**, September-October, 57 59. www.britishsulphur.com

References

Ametek (2005) Model CG1000 Oxygen Analyzer. www.ametekpi.com/products

Bete Fog Nozzle Inc. (2005) Spray Nozzles for Industry, Fire Protection and Pollution Control. www.bete.com

Dafft, C.A. and White, C.R. (2002) United States Patent 6,399,040, *Process for generating recoverable sulfur containing compounds from a spent acid stream*
http://patft.uspto.gov/netahtml/srchnum.htm (Query, 6399040, Search)

Lang, E. (1998) Waste acids used in sulfuric acid regeneration. *Sulfuric Acid Today*, part one, spring/summer 1998, 18; part two fall/winter 1998, 16. www.sulfuricacidtoday.com

Monsanto Enviro-Chem (2005) Spent acid regeneration (SAR).
www.enviro-chem.com/plant-tech/3rdtier/spentaci.html

Outokumpu (2004) *Sulphuric Acid Plants.* Brochure distributed at Sulphur 2004 conference, Barcelona, October 24-27, 2004. www.outokumpu.com

Rhodia (2002) Rhodia regeneration network offers environmental and economic advantages to California refiners facing MTBE phase-out.
www.us.rhodia.com/news/pr/SulfuricAcid_Ca-4-23-02.htm

Rohm and Haas (2003) [Spent] acid plant furnace optimization.
www.oit.doe.gov/showcasetexas/pdfs/tourbooks/tb_rohmhaas.pdf *also*
www.oit.doe.gov/showcasetexas/pdfs/posters/ps_rohmhaas_acidplant.pdf

Weiss, W. and Puricelli, S. (2004) Case histories from the H_2SO_4 industry (Observe cell temperatures of spent acid oxygen analyzers). *Sulfuric Acid Today*, Spring-Summer, 18.
www.sulfuricacidtoday.com

CHAPTER 6

Dehydrating Air and Gases with Strong Sulfuric Acid

Industrial experience has shown that SO_2 bearing gas must be dry before it goes to catalytic:

$$SO_2(g) + \frac{1}{2}O_2(g) \rightarrow SO_3(g) \qquad (1.1)$$

oxidation[#]. Otherwise, Reaction (1.1)'s $SO_3(g)$ will react with the gas's $H_2O(g)$ to form corrosive liquid $H_2SO_4(\ell)$:

(a) in cool flues and heat exchangers during normal operation

and:

(b) in flues, heat exchangers and catalyst during plant shutdowns.

The $H_2SO_4(\ell)$ forms by the reaction:

$$SO_3(g) + H_2O(g) \rightarrow H_2SO_4(\ell) \qquad (6.1).$$

It is avoided by dehydrating:

(a) sulfur combustion air, Fig. 6.1

(b) scrubbed metallurgical offgas

(c) scrubbed spent acid decomposition offgas, Fig. 6.2.

In all three cases the gas is dehydrated by contacting it with strong sulfuric acid.

[#] A small amount of sulfuric acid is made by wet catalysis, Section 1.9.

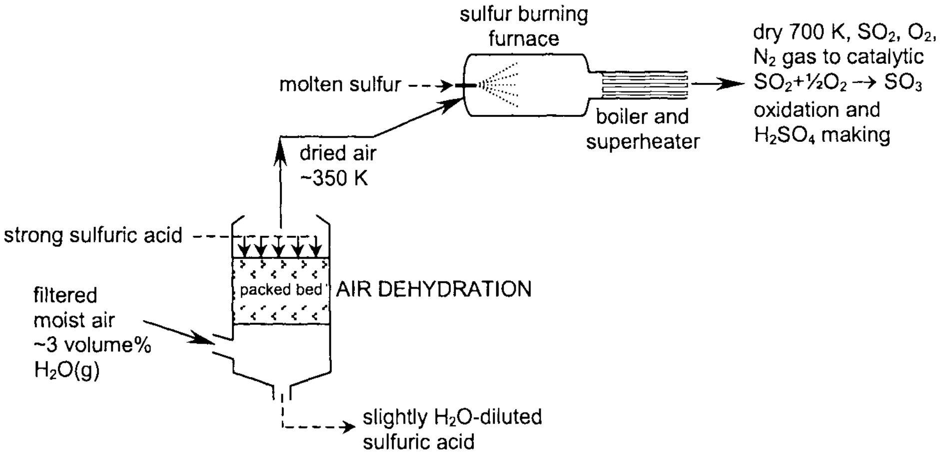

Fig. 6.1. Dehydration of sulfur combustion air in a sulfur burning acid plant. The dried air contains ~50 milligrams of $H_2O(g)$ per Nm^3 of gas.

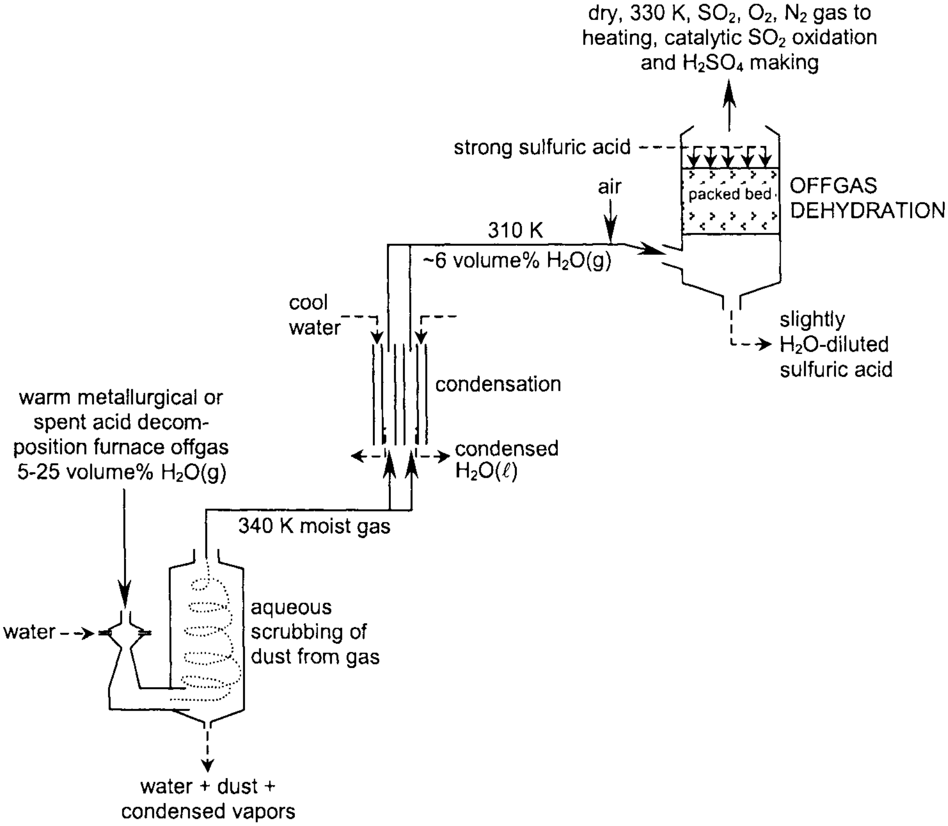

Fig. 6.2. Dehydration of metallurgical and spent acid decomposition furnace offgas. Dehydration is done after (i) $H_2O(g)$ has been condensed by gas cooling and (ii) aqueous mist has been removed by electrostatic precipitation (not shown). The gas leaving dehydration contains ~50 milligrams of $H_2O(g)$ per Nm^3 of gas. The acid plant's main blower is situated immediately after dehydration.

6.1 Objectives

The objectives of this chapter are to describe:

(a) the $H_2O(g)$ contents of pre-dehydration gases

(b) the dehydration process

(c) $H_2O(g)$ contents after dehydration.

6.1.1 $H_2O(g)$ before gas dehydration

The $H_2O(g)$ contents of pre-dehydration acid plant gases are shown in Table 6.1. They range from 2 to 10 volume% $H_2O(g)$.

Table 6.1. $H_2O(g)$ contents of pre-dehydration gases. The $H_2O(g)$ content of air in cool, dry climates is lower than that shown in the table.

Gas	Temperature, K	Volume% $H_2O(g)$ in gas
air for sulfur burning#	305-315	2-4
metallurgical furnace offgas after scrubbing, gas cooling and wet electrostatic mist precipitation	310-315	6-10
spent acid decomposition furnace offgas after scrubbing, gas cooling and wet electrostatic mist precipitation	310-315	6-10

Often filtered through a cloth pad prior to dehydration.

6.2 Dehydration with Strong Sulfuric Acid (Tables 6.3-6.5)

The industrial method of removing $H_2O(g)$ from sulfur burning air and metallurgical/ spent acid offgas is to pass the air or gas upwards through descending strong sulfuric acid, Fig. 6.3. Dehydration is represented by the reaction:

$$\underset{}{H_2O(g)} + \underset{\text{in strong acid}}{H_2SO_4(\ell)} \rightarrow \underset{\text{slightly weakened acid}}{H_2SO_4(\ell) + H_2O(\ell)} \qquad (6.2)$$

for which:

$$\Delta H \approx -80 \text{ MJ per kg-mole } H_2O(g).$$

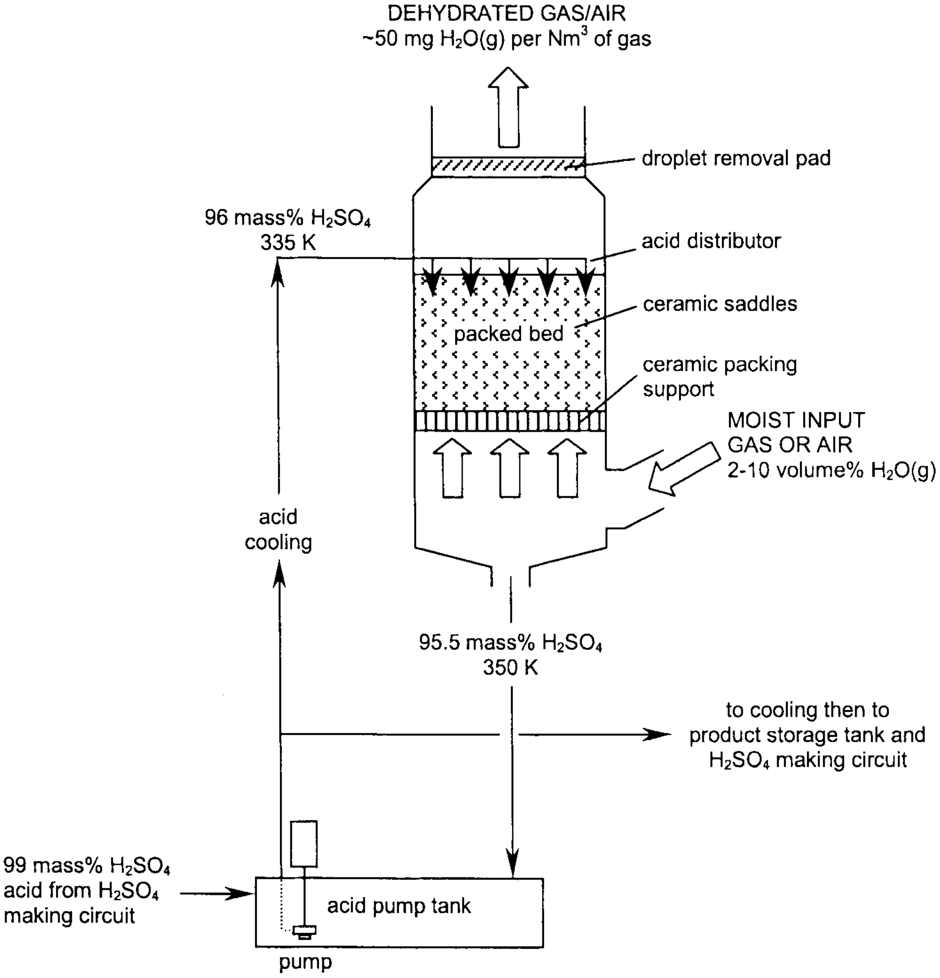

Fig. 6.3. Circuit for dehydrating sulfur burning air and scrubbed metallurgical and spent acid furnace offgas. Sulfuric acid descends around ceramic saddles while moist gas ascends. This creates turbulence, a large gas/acid interfacial area and rapid gas dehydration. At the top, small acid droplets are removed from the exit gas by passing it through a Teflon®/stainless steel mesh pad (Ziebold, 2000). With metallurgical and spent acid gas, the departing acid (right) is stripped of inadvertently absorbed SO_2 before it is sent to product storage or H_2SO_4 making. This is most often done by passing the SO_2 bearing acid down a small packed bed (like that above) while blowing air upwards. The resulting SO_2 bearing air is sent back to the main gas stream just before dehydration. Industrial dehydration data are given in Tables 6.3-6.5.

6.2.1 $H_2O(g)$ concentration after gas dehydration

$H_2O(g)$-in-gas concentrations after dehydration are close to those predicted by equilibrium $H_2O(g)$ pressures over Fig. 6.3's input acid. These pressures are shown in Table 6.2 along with their equivalent volume% $H_2O(g)$ and mg $H_2O(g)$ per Nm^3 of gas.

Table 6.2. Equilibrium $H_2O(g)$ pressures over sulfuric acid at temperatures around those of industrial acid plant gas dehydration (Perry and Green, 1997). The pressures are translated into volume% $H_2O(g)$ in gas and milligrams $H_2O(g)$ per Nm^3 of gas. An industrial dehydration target of ~50 milligrams $H_2O(g)$ per Nm^3 of gas is chosen to avoid downstream corrosion.

Temp K	equilibrium $H_2O(g)$ pressure of feed acid, bar	equivalent volume% $H_2O(g)$ in dehydrated gas	equivalent mg $H_2O(g)$ per Nm^3 of dehydrated gas
93.5 mass% H_2SO_4, 6.5 mass% H_2O sulfuric acid			
320	17.2E-06	16.9E-04	14
330	38.6E-06	38.1E-04	31
340	82.6E-06	81.5E-04	66
350	169 E-06	166 E-04	134
360	329 E-06	324 E-04	261
98.5 mass% H_2SO_4, 1.5 mass% H_2O sulfuric acid			
320	0.9E-06	0.8E-04	1
330	2.0E-06	2.0E-04	2
340	4.5E-06	4.4E-04	4
350	9.5E-06	9.5E-04	8
360	19.7E-06	19.4E-04	16
370	38.5E-06	38.0E-04	31
380	72.0E-06	71.9E-04	58
390	134 E-06	132 E-04	106

The table indicates that its:

50 mg $H_2O(g)$ per Nm^3 of dried gas

target is achievable with:

93.5 mass% H_2SO_4 acid below 340 K

and with:

98.5 mass% H_2SO_4 acid below 380 K.

6.2.2 Choice of dehydration acid strength

Strong acid, ~98.5 mass% H_2SO_4, is an excellent choice for air and gas dehydration. It has a low equilibrium $H_2O(g)$ vapor pressure. It removes $H_2O(g)$ from air/gas very efficiently.

Also it:

(a) is less corrosive than lower strength (e.g. 93 mass% H_2SO_4) acid

(b) minimizes the amount of water that has to be pumped around the dehydration circuit.

It is always used for dehydrating sulfur burning air.

Metallurgical and spent acid regeneration acid plants use 93 to 96 mass% H_2SO_4 acid for dehydrating their gases. The advantage of these low H_2SO_4 acids is that they are easily controlled to their design H_2SO_4 concentrations by:

> making small changes to the rate at which 99% H_2SO_4 acid is pumped over from the H_2SO_4 making circuit, Fig. 6.3.

This is important for smelter gas dehydration towers because their $H_2O(g)$ input rates vary considerably over time – due to inadvertent variations in smelting rates.

Spent acid dehydration $H_2O(g)$ input rates also vary – due to changes in feed acid composition.

H_2SO_4-in-acid concentrations are most commonly determined by speed-of-sound-through-acid measurements (Mesa Labs, 2005).

6.3 Residence Times

The Table 6.3 to 6.5 data indicate that typical industrial tower diameters, packing heights, and residence times are:

tower diameter	7-9 meters
packed bed thickness	2-4 meters
acid residence time in packing	400-700 seconds
gas residence time in packing	2-4 seconds

These conditions are designed to give 50 mg $H_2O(g)$ per Nm^3 of dehydrated gas with low acid droplet entrainment.

6.4 Recent Advances

The main advances in air/gas dehydration have been in the areas of:

(a) materials of construction

(b) ceramic packing and packing supports.

The tendency in dehydration construction and acid distribution materials is towards increased use of strongly corrosion resistant:

stainless steels

ductile iron piping.

Both are simplifying initial construction, decreasing maintenance and extending plant life (Sulphur, 2004).

Table 6.3. Details of two sulfur burning air dehydration plants.

Operation	S1	S2
Dehydration packed tower data		
number of packed towers	1	1
materials of construction	SX stainless steel	brick lined carbon steel
tower height × diameter, m	9.2 × 9.3	4 × 7
packing height, m	2.13	
type of packing	ceramic saddles	ceramic saddles
acid distributor type	trough and downcomers	trough and spouts
materials of construction	SX stainless steel Mondi® ductile iron header pipes	ductile iron
acid mist eliminator type	316 stainless steel mesh pads	Monsanto CS impact
Air		
input filtration method	2 stage dry pads	
input rate thousand Nm^3/hour	361	230
$H_2O(g)$ in air, volume%		
before dehydration	1.37	2.9
after dehydration		<70 mg per Nm^3
temperature, K		
into packed tower	313	305
out of packed tower	347	363
Sulfuric acid used for drying		
acid flowrate, m^3/hour	1349	
composition, mass% H_2SO_4		
into packed tower	98.5	98.5
out of packed tower	98.3	98.3
temperature, K		
into packed tower	347	333
out of packed tower	347	341
outlet acid destination	combination tank	product acid storage tank
Acid plant main blower		
number of blowers	2	1 (before gas dehydration)
power rating, each blower kW	4800 each	4300
steam or electric powered	electric	steam
gas temperature after blower, K	416	363

Table 6.4. Details of 5 copper smelting

Operation	Cumerio (Bulgaria) 1	M3
Dehydration packed tower data		
number of packed towers	1	1
materials of construction	brick lined carbon steel	
tower height × diameter, m	12 × 7.2	11.92 × 8.3 (OD)
packing height, m	3.8	4
type of packing	7.6 & 5.1 cm saddles	5.1 to 7.6 cm saddles
acid distributor type	Lurgi pipes and tubes	Lurgi pipes and tubes
acid mist eliminator type	Alloy 20 – Teflon®	Alloy 20 – Teflon®
Feed gas description#		
gas input rate, thousand Nm^3/hour	160	190
gas composition, volume%		
SO_3	0	0
SO_2	12.11	11.0
O_2	11.51	14.6
CO_2	0.40	1.83
H_2O	5.42	76 g per Nm^3 of gas
N_2	70.56	remainder
gas temperature, K		
into packed tower	313	310
out of packed tower	335	328
Sulfuric acid used for drying		
acid flowrate, m^3/hour	1053	
composition, mass% H_2SO_4		
into packed tower	96	96
out of packed tower	95.43	
temperature, K		
into packed tower	335	328
out of packed tower	354	343
outlet acid destination	H_2SO_4 making	product acid, contact acid, drying tower, stripper
is SO_2 stripped from outlet acid?		yes
Gas composition after drying		
SO_2 (volume%)	11.29	11.0
O_2	13.23	14.6
CO_2	0.38	1.83
H_2O	<0.02	
N_2	75.10	remainder
Acid plant main blower		
number of blowers	1	1
power rating, each blower kW	3950 nominal	6400 (nominal)
steam or electric powered	electric	electric
gas temperature after blower, K	363	392

The feed gases come from wet gas electrostatic precipitation.

gas dehydration plants.

M4	Asarco Hayden	Phelps Dodge Miami
1	1	1
brick lined carbon steel	brick lined steel	steel tower, 316L cone roof, brick lined
20.3 × 8.32 OD	17.8 × 7.6 ID	19.8 × 9.2
6.27	3.7	4.8
5.1 & 7.6 cm saddles	7.6 cm saddles	7.6 & 5.1 cm Intalox® saddles
submerged distributor pipes	ZeCor™	Meehanite® CHS pipe distributor
Teflon®	Teflon® mesh	6.7m dia. 0.15m thick Alloy 20-Teflon® pad
208	200	255
0	0	
11.29	9.0	9.6
13.29	11.4	9.6
2.68	0.9	0.9
85 g per Nm^3 of gas	5.9	8.5
remainder	remainder	71.4
317		313
328		323
910	860	1446
96	93	94.5
		93.9
328	305	
350	322	
	product acid	recy
no	yes with air	
11.0-13.5	9.0	
13.3	12.4	
2.68	1.0	
0	0	
remainder	remainder	
1	2	
4500		
electric	electric	
383	342	

Table 6.5. Details of zinc roaster and spent acid regeneration gas dehydration plants.

Operation	M2	SP1
Dehydration packed tower data		
number of packed towers	1	1
materials of construction	brick lined carbon steel	brick lined steel
tower height × diameter, m	12.6 × 7.2	4 × 7.6
packing height, m	4.3	3.8
type of ceramic packing	ceramic saddles	7.6 cm Intalox®
acid distributor type	pipe distributor, buried	cast iron troughs and spouts
acid mist eliminator type	hanging fiber bed	candle
Feed gas[#]		
gas input rate, thousand Nm^3/hour	101	46
gas composition, volume%		
SO_3	0	
SO_2	10.0	8.5
O_2	5.89	11.6
CO_2	0	5.5
H_2O	68 g per Nm^3 of gas	
N_2	remainder	74.4
gas temperature, K		
into packed tower	311	314
out of packed tower	328	319
Sulfuric acid used for drying		
acid flowrate, m^3/hour	870	384
composition, mass% H_2SO_4		
into packed tower	96	93.5
out of packed tower	96	93.1
temperature, K		
into packed tower	328	319
out of packed tower	347	330
outlet acid destination	absorption tower	
is SO_2 stripped from outlet acid?	no	yes
Gas composition after drying		
SO_2 (volume%)	8.5	
O_2	8.8	
CO_2		
H_2O	0	
N_2	remainder	
Acid plant main blower		
number of blowers	1	1
power rating, each blower kW	3500	1150
steam or electric powered	steam & electric	steam
gas temperature after blower, K	373	349

[#] The feed gases come from wet electrostatic precipitation

The tendency in ceramic packing is towards high surface area, low gas flow resistance perforated saddles. These saddles give rapid dehydration with low resistance to gas flow.

6.5 Summary

SO_2 bearing gas must be dry before it goes to catalytic $SO_2(g) + \frac{1}{2}O_2 \rightarrow SO_3(g)$ oxidation. Otherwise the $SO_3(g)$ made by catalytic oxidation will react with $H_2O(g)$-in-gas to form corrosive liquid sulfuric acid in cool flues and heat exchangers.

This problem is avoided by dehydrating (i) sulfur burning air and (ii) scrubbed metallurgical/spent acid furnace offgas by contacting these gases with strong sulfuric acid. Dehydration is represented by the reaction:

$$H_2O(g) + \underset{\text{in strong acid}}{H_2SO_4(\ell)} \rightarrow \underset{\text{slightly weakened acid}}{H_2SO_4(\ell) + H_2O(\ell)}$$

Industrially, the process is carried out in towers packed with ceramic saddles. Acid descends around the saddles where it meets and reacts with rising $H_2O(g)$ laden gas.

$H_2O(g)$-in-gas is lowered to ~50 mg per Nm^3 of dehydrated gas.

Suggested Reading

Friedman, L.J. and Friedman, S.J. (2004) The wet gas sulphuric acid plant (part 2). *Sulphur*, **293**, July-August 2004, 29 35. www.britishsulphur.com

References

Mesa Labs (2005) Sulfuric acid analyzer application note. www.mesalabs.com/nusonics

Perry, R.H. and Green, D.W. (1997) *Perry's Chemical Engineers' Handbook – 7th Edition*, McGraw-Hill, New York, NY, 2-78 2-79. www.mcgraw-hill.com

Sulphur (2004) Sulphuric acid equipment update. *Sulphur*, **292** (May-June 2004), 33 42. www.britishsulphur.com

Ziebold, S.A. (2000) Demystifying mist eliminator selection. *Chemical Engineering*, **107(5)**, May 2000. www.che.com

CHAPTER 7

Catalytic Oxidation of SO_2 to

Sulfuric acid manufacture from clean, dry, SO_2 bearing

(a) catalytically oxidizing the gas's SO_2 to SO_3, i.e.:

$$\begin{array}{ccccccc} & & & \text{700 K-900 K} & & & \\ SO_2(g) & + & \frac{1}{2}O_2(g) & \rightarrow & SO_3(g) & & \\ \text{in } SO_2, O_2, & & \text{in feed gas} & \text{catalyst} & \text{in } SO_3, SO_2, & & (1.1) \\ N_2 \text{ feed gas} & & \text{or added to} & & O_2, N_2 \text{ gas} & & \\ & & \text{it in air} & & & & \end{array}$$

$\Delta H^\circ \approx -100$ MJ per kg-mole of $SO_3(g)$

(b) making H_2SO_4 from Eqn. (1.1)'s $SO_3(g)$ by reacting it with the $H_2O(\ell)$ in strong sulfuric acid, i.e.:

$$\begin{array}{ccccccc} & & & \text{350 K-380 K} & & & \\ SO_3(g) & + & H_2O(\ell) & \rightarrow & H_2SO_4(\ell) & & \\ \text{in } SO_3, SO_2 & & \text{in } 1.5\%\ H_2O, & & \text{in strengthened} & & (1.2) \\ O_2, N_2 \text{ gas} & & 98.5\%\ H_2SO_4 & & \text{sulfuric acid} & & \\ & & \text{sulfuric acid} & & & & \end{array}$$

$\Delta H^\circ \approx -130$ MJ per kg-mole of $H_2SO_4(\ell)$.

This chapter and Chapter 8 describe catalytic SO_2 oxidation. H_2SO_4 making is described in Chapter 9.

7.1 Objectives

The objectives of this chapter are to:

(a) show how industrial SO_2 oxidation is carried out, Figs. 1.2 and 7.7.

(b) explain why catalyst is necessary for SO_2 oxidation

(c) show how multi catalyst bed processing maximizes $SO_2+\frac{1}{2}O_2 \rightarrow SO_3$ oxidation

(d) describe industrial operating procedures.

7.2 Industrial SO_2 Oxidation

Industrial SO_2 oxidation consists of blowing:

warm (~700 K)
clean
dry

$SO_2 + O_2$ bearing gas down through a 'bed' of warm V, K, Na, Cs, S, O, silica catalyst, Fig. 7.1.

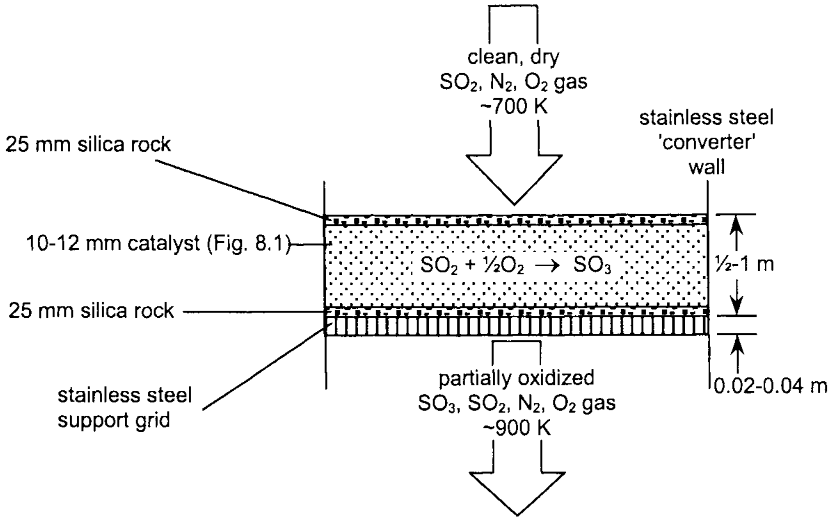

Fig. 7.1. 'Bed' of catalyst pieces for oxidizing SO_2 to SO_3. It is circular, 7 to 17 m diameter. Industrial SO_2 oxidation is done in a 'converter' of 3 to 5 such beds, Figs. 7.6 and 7.7. Downward gas flows are ~25 Nm^3/minute per m^2 of top surface. Active catalyst consists of a molten V, K, Na, Cs, S, O phase supported on a solid porous silica substrate, Chapter 8. A top layer of silica rock holds the catalyst in place. A bottom layer prevents the catalyst from sticking to the stainless steel support grid.

SO_2 oxidation proceeds as the feed gas descends the bed. It:

(a) produces SO_3

(b) consumes SO_2 and O_2

(c) heats the descending gas.

Fig. 7.2 describes these phenomena. It shows that as the gas descends:

(a) SO_2 oxidation proceeds (left graph)

(b) gas and catalyst temperatures increase.

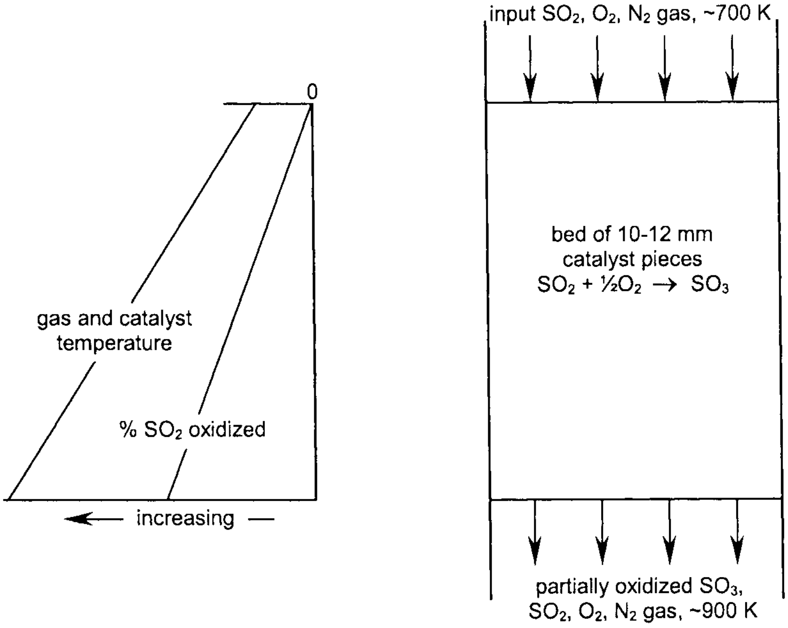

Fig. 7.2. Sketch of SO_2 oxidation in Fig. 7.1 catalyst bed. SO_2 and O_2 in the feed gas react to form SO_3 as the gas descends the catalyst bed. The heat of reaction warms the gas (left graph).

7.2.1 Source of O_2

SO_2 oxidation requires O_2. Sulfur burning furnace offgas already contains O_2, Table 7.1. None needs to be added. Metallurgical and waste acid decomposition furnace offgases often contain little O_2, so some must be added before catalytic SO_2 oxidation. It is added in air or ventilation gas before gas dehydration.

Volume% O_2/volume% SO_2 ratios in industrial catalytic oxidation feed gas are in the range of 1 to 2, Table 7.2. This is 2 to 4 times the stoichiometric $SO_2+\frac{1}{2}O_2 \rightarrow SO_3$ requirement of 0.5 moles O_2 per mole of SO_2. The excess O_2 promotes rapid SO_2 oxidation.

Table 7.1. Compositions of furnace offgases and catalyst bed feed gases. Sulfur burning gases don't change. Metallurgical and waste acid decomposition furnace offgases lose SO_3 and $H_2O(g)$. The SO_3 is removed during water scrubbing. The $H_2O(g)$ is removed during condensation and dehydration.

Gas source and composition, volume%	Sulfur burning furnace	Metallurgical furnaces#	Waste acid decomposition furnace
Offgas leaving furnace			
SO_3	0.2	0-0.5	0.2
SO_2	8-12	8-15	6-14
O_2	9-12	5-15	2-3
CO_2	0	0-5	10
$H_2O(g)$	0	5-30	25-30
N_2	79	50-70	~50

#after electrostatic precipitation, Chapter 4

Acid plant feed gas entering catalytic SO_2 oxidation 'converter'

Prior treatment	usually none, O_2 is occasionally added in dried air	gas cleaning and cooling; O_2 addition in air; dehydration	gas cleaning and cooling; O_2 addition in air; dehydration
SO_3	0.2	0	0
SO_2	8-12	8-13	8-10
O_2	9-12	9-14	10-12
CO_2	0	0-7	6-10
$H_2O(g)$	0	0	0
N_2	79	~75	~70

7.3 Catalyst Necessity

All industrial SO_2 oxidation is done in beds of catalyst. Sander *et al.* (1984) explain the need for catalyst as follows:

"Gas phase oxidation of sulphur dioxide is kinetically inhibited and virtually impossible without a catalyst at any temperature. At ordinary temperatures the reaction is so slow that, in practical terms, it does not occur at all. Increasing the temperature increases the rate of reaction, but simultaneously the position of the equilibrium shifts unfavourably – away from sulphur trioxide and towards sulfur dioxide and oxygen. Without a catalyst, the temperature needed to make the system react at a practical speed is so high that a very poor conversion [i.e. very little SO_3 production] is obtained."

7.3.1 Temperature effect

The temperature effect described in the above statement is confirmed by Fig. 7.3, which shows that the equilibrium constant for SO_2 oxidation, i.e.:

$$K_E = \frac{P^E_{SO_3}}{P^E_{SO_2} * \left(P^E_{O_2}\right)^{\frac{1}{2}}}$$

(P^E = equilibrium partial pressure, bar)

decreases with increasing temperature.

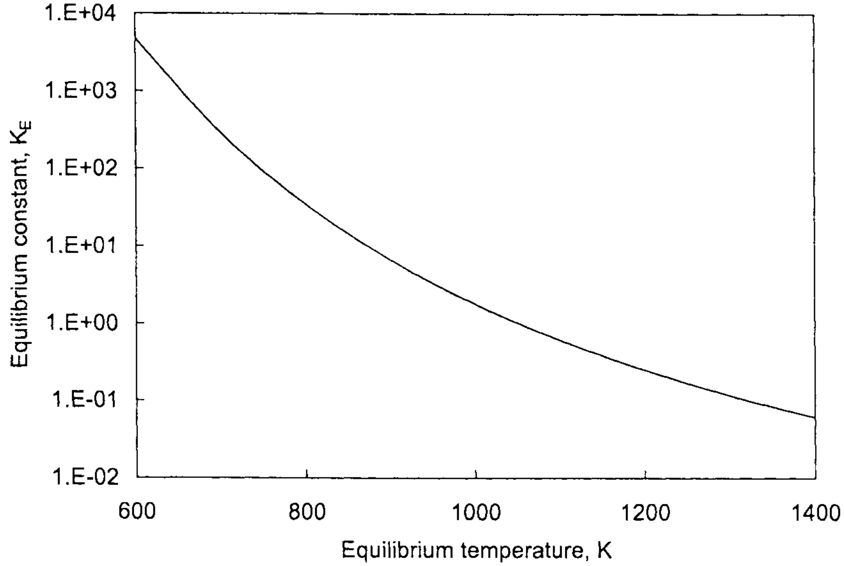

Fig. 7.3. Equilibrium constant for $SO_2 + \frac{1}{2}O_2 \rightarrow SO_3$ oxidation as a function of temperature. It decreases nearly 80 000 times between 600 and 1400 K.

This indicates that:

(a) the equilibrium $\dfrac{P^E_{SO_3}}{P^E_{SO_2} * \left(P^E_{O_2}\right)^{\frac{1}{2}}}$ ratio

and

(b) maximum attainable SO_3 production

both decrease significantly with increasing temperature.

(b) is confirmed by Fig. 7.4 – which shows that maximum attainable SO_2 oxidation decreases from:

nearly 100% at 600 K

to

about 2% at 1400 K.

It can be concluded from this that raising reaction temperature to increase reaction rate *decreases* maximum attainable (equilibrium) SO_3 production.

This problem is overcome by using catalyst which promotes:

rapid SO_2 oxidation

at cool temperatures (~700 K) where:

equilibrium SO_3 production is efficient.

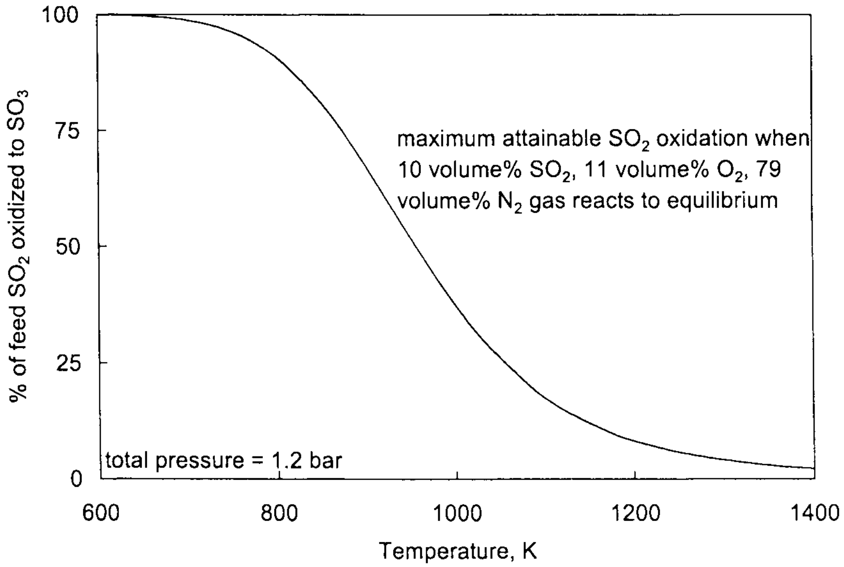

Fig. 7.4. Maximum attainable (equilibrium) SO_2 oxidation as a function of reaction temperature. It decreases markedly with increasing temperature. Calculation and plotting of this curve are described in Chapter 10.

The catalyst is described in Chapter 8. It consists of vanadium oxide; K, Na, Cs pyrosulfates and porous silica substrate. It is in the form of 10-20 mm rings and pellets, Fig. 8.1 (most commonly, 10-12 mm). It begins to speed up SO_2 oxidation at 660-690 K when the vanadium oxide and K, Na, Cs pyrosulfates combine to form a molten layer on the substrate. It becomes fully active at 680-700 K.

Feed gas must enter beds of this catalyst at or above the fully active temperature. Otherwise the gas will cool and solidify (deactivate) the catalyst, preventing SO_2 oxidation.

7.4 SO_2 Oxidation 'Heatup' Path (Chapter 11)

Fig. 7.2 indicates that:

SO_2 oxidation

and

gas temperature

increase as SO_2, O_2, N_2 gas descends an active catalyst bed. Fig. 7.5 quantifies this behavior. It confirms that gas temperature rises as % SO_2 oxidized increases (due to heat from SO_2 oxidation).

Fig. 7.5 also shows that SO_2 oxidation and gas heat up end when the heatup path reaches Fig. 7.4's equilibrium % SO_2 oxidized curve.

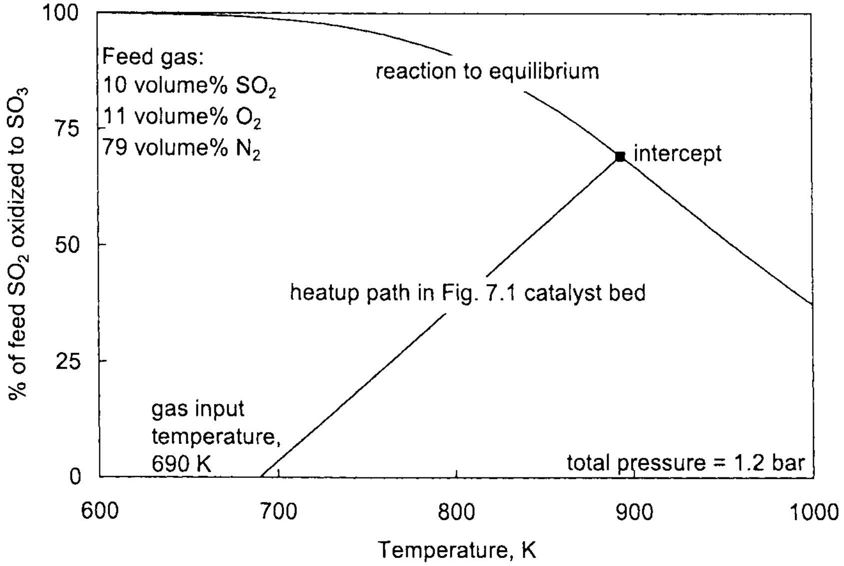

Fig. 7.5. 'Heatup' path for gas descending the Fig. 7.1 catalyst bed. It begins at the feed gas's input temperature and 0% SO_2 oxidized. Its temperature rises as SO_2 oxidizes. Maximum attainable SO_2 oxidation is predicted by the 'heatup' path-equilibrium curve intercept, 69% oxidized at 893 K in this case. This low % SO_2 oxidized confirms that efficient SO_2 oxidation cannot be obtained in a single catalyst bed. Multiple catalyst beds with gas cooling between must be used.

7.5 Industrial Multi Catalyst Bed SO_2 Oxidation (Table 7.2)

Industrial SO_2 oxidation is done in a sequence of 3 to 5 catalyst beds, Figs. 7.6 and 7.7. This section and Fig. 7.8 describe passage of warm feed gas through three catalyst beds with gas cooling between. The sequence is:

Feed gas (10 volume% SO_2, 11 volume% O_2, 79 volume% N_2, 690 K) enters the 1st catalyst bed, Fig. 7.6. It:

(a) descends the 1st catalyst bed where its SO_2 and O_2 react to form SO_3, heating the gas

(b) departs the bed at near-intercept conditions (69% of feed SO_2 oxidized/893 K) into Fig. 7.6's top (1-2) gas cooler where it is cooled to 700 K without composition change

(c) enters and descends the 2nd catalyst bed, reacting to form more SO_3, re-heating the gas

(d) departs the 2nd bed at near-intercept conditions (94% SO_2 oxidized/773 K) into Fig. 7.6's bottom (2-3) gas cooler – where it is cooled to 710 K without composition change

(e) enters and descends the 3rd catalyst bed, forming more SO_3, again re-heating the gas

(f) departs the 3rd catalyst bed at near-intercept conditions (98% SO_2/721 K) and proceeds to cooling and H_2SO_4 making, Chapter 9.

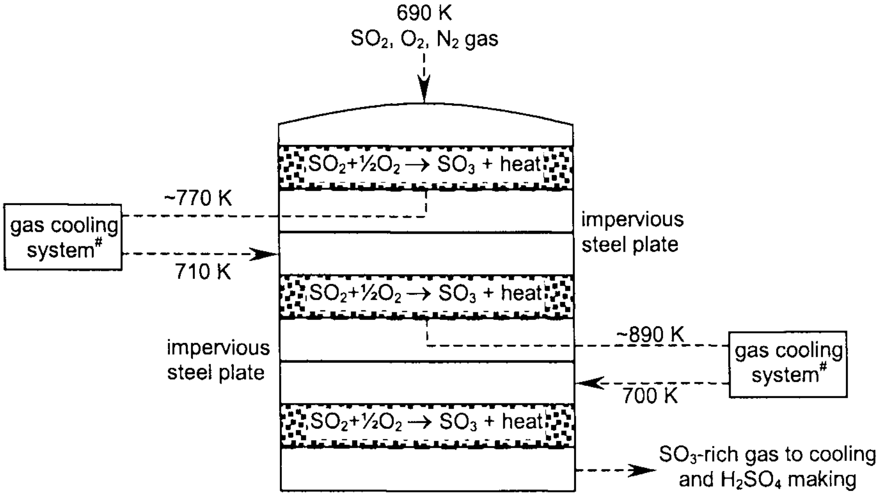

Fig. 7.6. Schematic of SO_2 oxidation 'converter' in which three Fig. 7.1 catalyst beds (with gas cooling between) are used to oxidize ~98% of feed SO_2 to SO_3. Fig. 1.2 shows the inside of an industrial 'converter' – Fig. 7.7, the outside. #Hot gas leaving the catalyst beds is cooled by waste heat boilers, steam superheaters, water heaters, heat exchangers etc.

Fig. 7.7. Photograph of catalyst bed converter, courtesy Outokumpu OYJ www.outokumpu.com Gas inlet and outlet flues are shown. Others are hidden behind. Fig. 7.6's gas coolers are also hidden behind. Converter walls and roofs are designed to be strong enough to withstand their acid plant's main blower 'shutoff ' pressure without damage (Friedman and Friedman, 2004). Catalyst 'tray' supports are also strong enough to withstand the downward force exerted by the descending feed gas (at the converter's operating temperature).

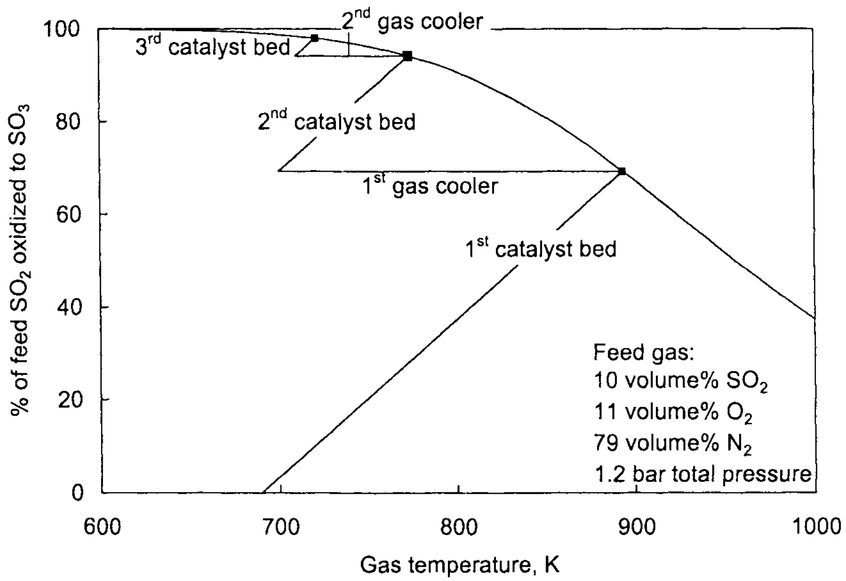

Fig. 7.8. 'Heatup' paths, intercepts and cooldown paths for Fig. 7.6 'converter'. They are described in Section 7.5. Final % SO_2 oxidation after Fig. 7.6's three catalyst beds is ~98%.

7.5.1 Overall multi catalyst bed results

Fig. 7.8 describes the benefits of multi catalyst bed SO_2 oxidation. SO_2 oxidation is increased in each succeeding bed. The figure shows, however, that the incremental amount of SO_2 oxidation diminishes in each successive bed.

Addition of a fourth bed would probably not be worthwhile from the SO_3 production (hence H_2SO_4 production) point of view. It might, however, be worthwhile from the point of view of minimizing SO_2 escape to the environment (because SO_2 passes untouched through subsequent H_2SO_4 making). These factors are detailed in Chapters 12 to 22.

7.5.2 Double contact acidmaking

This chapter describes SO_2 oxidation in 'single contact' acid plants. These plants:

(a) oxidize $SO_2(g)$ to $SO_3(g)$ as described here

then:

(b) make $H_2SO_4(\ell)$ by 'single contact' of the resulting $SO_3(g)$ bearing gas with strong sulfuric acid, Chapter 9.

'Double contact' acidmaking:

(a) oxidizes $SO_2(g)$ to $SO_3(g)$ as described here

(b) makes $H_2SO_4(\ell)$ from the resulting $SO_3(g)$ by contact with strong sulfuric acid

(c) oxidizes the $SO_2(g)$ remaining after (a) and (b) to $SO_3(g)$ in 1 (occasionally 2) catalyst beds

(d) makes H_2SO_4 from the new $SO_3(g)$ by second contact of the gas with strong sulfuric acid.

Its advantage is more efficient SO_2 oxidation and H_2SO_4 production. Its disadvantage is more equipment and more heating and cooling.

(d) is discussed in Chapter 9. (c) is discussed in Chapter 19.

7.6 Industrial Operation (Table 7.2)

7.6.1 Startup

Catalyst must be at its fully active temperature before it is fed with SO_2 bearing feed gas. Otherwise the SO_2 will pass through unreacted. Industrially, the catalyst is heated by passing hot, dry air through the catalyst beds before the SO_2 producing furnace is started (BASF, 2004). The air is heated by heat exchange with hot fossil fuel combustion gas. Metallurgical and spent acid regeneration plants have a dedicated air heater for this purpose. Sulfur burning plants heat the air in their sulfur burning furnace[#].

Once the catalyst beds are hot, the SO_2 production furnace is started and hot, clean, dry SO_2 bearing gas is introduced into the catalytic converter.

Sulfur burning offgas is introduced directly into the hot converter because it leaves the sulfur burning furnace/boiler/superheater at its specified feed gas temperature, ~700 K.

Metallurgical and spent acid decomposition gases are initially passed through their fuel-fired startup heat exchanger because they are cool from gas cleaning/dehydration. Once SO_2 oxidation has begun, this gas heating duty is switched to heat exchange from hot catalyst bed exit gas.

7.6.2 Steady operation

Steady 'converter' operation entails:

(a) feeding constant composition, constant temperature SO_2 bearing gas at a constant rate

---

[#] The furnace is first heated by fossil fuel combustion. Combustion is then stopped and dry air is passed through the furnace into the catalyst beds (repeated several times). Once the catalyst beds are hot enough to avoid $H_2O(g)$ condensation, hot combustion offgas is passed directly through the beds.

(b) continuously monitoring catalyst bed gas input and output temperatures.

7.6.3 Control

The main catalytic converter control objective is maintenance of constant, specified catalyst bed input gas temperatures.

Low input gas temperatures must be avoided because they may cool, solidify and deactivate a bed's catalyst.

High input gas temperatures must be avoided because they:

(a) raise catalyst bed gas output temperature and consequently lower SO_2 oxidation efficiency, Fig. 12.2

(b) raise the gas output temperature above the catalyst degradation temperature, Section 8.3

(c) raise the gas output temperature to the point where it weakens the converter's stainless steel structure.

Catalyst bed input gas temperatures are measured with three thermocouples in the top of each bed. They are controlled by adjusting the amount of gas being bypassed around the catalytic converter's gas cooling devices, Fig. 22.2.

Catalyst bed exit gas temperatures are also measured. They are indicative of each bed's SO_2 oxidation efficiency. First catalyst bed exit gas temperature is especially important. This bed's catalyst may overheat and degrade near the bottom of the bed.

7.6.4 Shutdown

Catalytic $SO_2 \rightarrow SO_3$ oxidation is stopped by:

(a) shutting down the SO_2 production unit, e.g. the sulfur burning furnace

(b) blowing 700 K dehydrated air through the catalyst beds and their gas coolers (BASF, 2004)

(c) gradually cooling the air flow.

Steps (b) and (c) remove SO_2 and SO_3 from all the catalytic oxidation equipment (avoiding corrosion). They also cool equipment and catalyst slowly (avoiding thermal stress and catalyst fragmentation).

An important strategy during short interruptions of SO_2 supply is to keep the catalyst at its chemically active temperature, 680-700 K. This is accomplished by (i) raising the temperature of the catalyst just before a forecast interruption and by (ii) preventing air leakage into the converter.

Table 7.2. Details of before-H_2SO_4 making catalytic

Operation		S1	M2
acid production, tonnes H_2SO_4/day		4400	1150
source of SO_2		sulfur burning	zinc roasting
single or double contact plant		double	double
number of catalyst beds		3 + 1#	3 + 2#
converter height × diameter, m		19.23 × 16.65	15 × 10
construction materials		304 SS; passes 1&2 321 SS; pass 3&4 304 SS	stainless steel
heat recovery system		2 × HRS boilers	economizer for boiler
Input gas data			
flowrate, thousand Nm^3/hour		356	127
temperature, K		696	718
composition, volume%			
SO_3		0.184	0
SO_2		11.6	8.5
O_2		9.06	8.84
CO_2			
N_2		79.1	remainder
Catalyst bed data			
thickness of beds, m			
bed 1		0.78	0.615
bed 2		0.90	0.680
bed 3		1.07	0.750
bed 4			
catalyst type(s)			
bed 1		LP120	12 mm daisy ring VK38
bed 2		LP120	12 mm daisy ring VK38
bed 3		LP110	12 mm daisy ring VK48
bed 4			
catalyst bed temperatures, K			
bed 1	in	696	718
	out	894	847
bed 2	in	713	723
	out	798	790
bed 3	in	718	727
	out	744	748
bed 4	in		
	out		
Product gas to H_2SO_4 making			
SO_3		11.8	8.49
SO_2		0.688	0.38
O_2		3.78	4.88
CO_2			
N_2		83.7	

3 catalyst beds before intermediate H_2SO_4 making, 1 bed after

SO_2 oxidation plants. (SS = stainless steel)

Cumerio 1 (Bulgaria)	Cumerio 2 (Bulgaria)	M5
1940	1500	
copper smelting	copper smelting	lead zinc smelting/roasting
double	double	single
3 + 1#	3 + 1#	4
19.3 x 11.6	22.3 x 12	12.83 x 8.4 ID
stainless steel, gray iron posts and grids	brick lined carbon steel	
none	none	
160	150	85
703	693	698-713
0	0	
11.29	9.5	8.33
13.23	14.9	10.79
0.38	0.3	6.65
75.10	75.3	
0.66	0.70	0.52
0.81	0.60	0.60
0.88	0.80	0.37 combined
		0.37 combined
10 × 4 & 11× 4 mm rings	12 × 6 mm rings	VK38
11 × 4 mm rings	12 × 6 mm rings	VK38
11 × 4 mm rings	12 × 6 mm rings	LP110
		VK38
703	693	698-713
903	868	803-853
723	741	703-723
804	803	763-773
708	708	703-713
737	713	
		713-733
11.47	10.08	8.05
0.51	0.42	0.61
7.37	5.67	7.20
0.32	0.28	6.92
80.33	83.55	

Table 7.2(continued). Details of before-H_2SO_4 making catalytic

Operation		M6	M3
acid production, tonnes H_2SO_4/day		2900	2200 (nominal)
source of SO_2		nickel copper smelting	copper smelting
single or double contact plant		double	single
number of catalyst beds		$3 + 1^{\#}$	4
converter height × diameter, m		17.3 × 12.5	14.515 × 11.75 (OD)
construction materials		304H stainless steel	AISI PT 304H stainless steel
heat recovery system		none	
Input gas data			
flowrate, thousand Nm^3/hour		231 (design)	136
temperature, K		671-703	
composition, volume%			
SO_3			
SO_2		12	11.0
O_2		18.22	14.6
CO_2		2.32	1.83
N_2		remainder	
Catalyst bed data			
thickness of beds, m			
bed 1		0.65	0.67
bed 2		0.78	0.867
bed 3		0.78	0.985
bed 4			1.419
catalyst type(s)		all 12 mm daisy	
bed 1		VK59 and VK38	BASF LP111
bed 2		VK38	BASF LP110
bed 3		LP110 and VK48	BASF LP110
bed 4			BASF LP110
catalyst bed temperatures, K			
bed 1	in	673	
	out	903	897
bed 2	in	709	703
	out	771	853
bed 3	in	713	703
	out	742	764
bed 4	in		683
	out		699
Product gas to H_2SO_4 making			
SO_3		12.20	11.44
SO_2		0.50	0.23
O_2		12	9.61
CO_2			1.94
N_2		remainder	

3 catalyst beds before intermediate H_2SO_4 making, 1 bed after

SO_2 oxidation plants.

M4	Asarco Hayden
2100-2400	1630
continuous copper smelting	copper smelting
double	double
3 + 1[#]	3 + 1[#]
22.1 x 12	16.1 x 14.0
aluminum coated steel	304 stainless
brick lining	steel
none	
188	201
663	672
11.0-13.5	8.5
13.29	12.6
2.68	1.0
remainder	75.0
0.76	0.46
0.85	0.56
1.00	0.56
VK59 and VK 38 layers	LP120/VK38
VK38	LP120/VK38
VK38	LP110/VK48
663	672
873	894
713	700
813	812
693	711
723	727
10.89-13.3	12.1
0.7-1.1	0.6
7.5-8.6	7.1
2.9	1.0
remainder	79.1

Table 7.2(continued). Details of before-H_2SO_4 making catalytic

Operation	Phelps Dodge Miami	M1
acid production, tonnes H_2SO_4/day	2400	270
source of SO_2	copper smelting	MoS_2 roasting & S burning
single or double contact plant	double	double
number of catalyst beds	3 + 1#	2 + 2#
converter height × diameter, m	23.3 × 14.76	9.8 × 6.9
construction materials	all welded stainless steel	carbon steel with cast iron grids
heat recovery system		none
Input gas data		
flowrate, thousand Nm^3/hour	233	50
temperature, K		
composition, volume%		
SO_3	trace	
SO_2	10.5	4.7-5.6
O_2	10.5	13.7
CO_2	1	
N_2	78	
Catalyst bed data		
thickness of beds, m		
bed 1	0.49	0.56
bed 2	0.79	0.48
bed 3	0.84	
bed 4		
catalyst type(s)		
bed 1	13 mm diameter 13 mm long	daisy ring
bed 2	13 mm diameter 13 mm long	daisy ring
bed 3	13 mm diameter 13 mm long	
bed 4		
catalyst bed temperatures, K		
bed 1 in	703	700-727
out	891	805-839
bed 2 in	723	700-727
out	796	708-736
bed 3 in	723	
out	744	
bed 4 in		
out		
Product gas to H_2SO_4 making		
SO_3	10.38	11.8
SO_2	0.66	0.2
O_2	5.85	
CO_2	1.05	
N_2	82.05	

3 catalyst beds before intermediate H_2SO_4 making, 1 bed after

SO$_2$ oxidation plants.

S2	SP1
1800	444
sulfur burning	spent acid regeneration
single	single
4	4
13.7 × 12.8	10.8 × 7.6
carbon steel, gray iron posts and grids	carbon steel & meehanite cast iron superheater
210	51
700	
	0
8.38	8.5
12.6	11.6
	5.5
79.02	72.5
0.51	0.78
0.62	0.86
0.75	0.98
0.92	1.29
daisy ring	10 mm ring
10 mm ring	10 mm ring
10 mm ring	10 mm ring
10 mm ring	10 mm ring
700	705
898	879
705	709
789	800
715	725
733	744
700 (after air dilution)	705
704	
8.18	9.02
0.15	0.19
9.44	7.13
	7.74
82.23	75.92

7.7 Recent Advances (Friedman and Friedman, 2004)

Important recent advances in catalytic SO_2 oxidation have been:

(a) development of low activation temperature, high reaction rate cesium-based catalyst, Chapter 8

(b) adoption of low gas flow resistance daisy ring catalyst pieces, Fig. 8.1

(c) use of strong, corrosion resistant stainless steel in converter construction.

All contribute to efficient, steady, long term $SO_3(g)$ production.

7.8 Summary

Catalytic oxidation of $SO_2(g)$ to $SO_3(g)$ is a key step in sulfuric acid production. It produces the SO_3 required for H_2SO_4 making, Chapter 9.

$SO_2+\frac{1}{2}O_2 \rightarrow SO_3$ oxidation is always done by passing warm SO_2 bearing gas down through horizontal beds of V, K, Na, Cs, S, O, SiO_2 catalyst. The catalyst promotes rapid SO_2 oxidation at temperatures (700-900 K) where SO_2 oxidation is thermodynamically efficient.

Industrially, the oxidation is carried out in a sequence of 3 to 5 catalyst beds with gas cooling between. Removal of heat from the gas between catalyst beds allows it to leave the last bed at a low temperature (~720 K) – where equilibrium $SO_2+\frac{1}{2}O_2 \rightarrow SO_3$ oxidation efficiency is high (98+ percent).

Suggested Reading

Friedman, L.J. and Friedman, S.J. (2004b) The wet gas sulphuric acid plant (part 2). *Sulphur*, **293**, July-August 2004, 29 35. www.britishsulphur.com

Sander, U.H.F., Fischer, H., Rothe, U., Kola, R. and More, A.I. (1984) *Sulphur, Sulphur Dioxide and Sulphuric Acid: An Introduction to their Industrial Chemistry and Technology*. British Sulphur Corp., London, UK. www.britishsulphur.com

References

BASF (2004) BASF catalyst (technical leaflet). www.basf.com

Friedman, L.J. and Friedman, S.J. (2004) The wet gas sulphuric acid plant (part 2). *Sulphur*, **293**, July-August 2004, 29 35. www.britishsulphur.com

Sander, U.H.F., Fischer, H., Rothe, U., Kola, R. and More, A.I. (1984) *Sulphur, Sulphur Dioxide and Sulphuric Acid: An Introduction to their Industrial Chemistry and Technology*. British Sulphur Corp., London, UK, 283. www.britishsulphur.com

CHAPTER 8

SO_2 Oxidation Catalyst and Catalyst Beds

Chapter 7 shows that $SO_2+½O_2 \rightarrow SO_3$ oxidation is a key step in sulfuric acid manufacture. The $SO_3(g)$ is essential for H_2SO_4 making, i.e. for the reaction:

$$\underset{\substack{\text{in } SO_3,\ SO_2\\ O_2,\ N_2 \text{ gas}}}{SO_3(g)} \quad + \quad \underset{\substack{\text{in strong}\\ \text{sulfuric acid}}}{H_2O(\ell)} \quad \rightarrow \quad \underset{\substack{\text{in strengthened}\\ \text{sulfuric acid}}}{H_2SO_4(\ell)} \qquad (1.2).$$

Chapter 7 also shows that V, K, Na, Cs, S, O, SiO_2 catalyst is a key ingredient in ensuring rapid, efficient SO_2 oxidation. Without catalyst, SO_2 oxidation is slow at temperatures where the oxidation is thermodynamically efficient.

This chapter describes SO_2 oxidation catalyst. It does so in terms of:

(a) catalyst physical and chemical characteristics, Fig. 8.1

(b) catalyst reaction mechanisms

(c) choice of catalyst chemical compositions for different industrial tasks, e.g. strong SO_2 gas, weak SO_2 gas

(d) industrial catalyst quantity requirements.

Fig. 8.1. Photograph of catalyst pieces, courtesy Haldor Topsoe A/S www.haldortopsoe.com Rings, daisy (star) rings and pellets are shown. The daisy rings maximize catalyst area and minimize resistance to gas flow. In operation (700-900 K), the catalyst consists of a molten vanadium-alkali metal sulfate/pyrosulfate layer on a porous solid silica substrate. The outside diameter of the largest piece (far left) is 20 mm.

8.1 Catalytic Reactions

Active SO_2 oxidation catalyst consists of molten vanadium-alkali metal pyrosulfate layer on porous solid silica substrate. Catalytic $SO_2+½O_2 \rightarrow SO_3$ oxidation takes place with dissolved V S O ionic complexes by reactions like:

$$(VO)_2O(SO_4)_4^{4-} + O_2(g) \rightarrow (VO)_2O(SO_4)_4O_2^{4-} \quad (8.1)$$

$$(VO)_2O(SO_4)_4O_2^{4-} + SO_2(g) \rightarrow (VO)_2O(SO_4)_4O^{4-} + SO_3(g) \quad (8.2)$$

$$(VO)_2O(SO_4)_4O^{4-} + SO_2(g) \rightarrow (VO)_2O(SO_4)_4SO_3^{4-} \quad (8.3)$$

$$(VO)_2O(SO_4)_4SO_3^{4-} \rightarrow (VO)_2O(SO_4)_4^{4-} + SO_3(g) \quad (8.4)$$

or, overall:

$$2SO_2(g) + O_2(g) \rightarrow 2SO_3(g) \quad (8.5)$$

(Lapina *et al.*, 1999). N_2 and CO_2 don't react during the SO_2 oxidation process.

Reactions (8.1) to (8.4) have smaller activation energies than Reaction (8.5). They give rapid SO_2 oxidation at moderate temperatures.

Rapid reaction between gases and ions requires that the vanadium ion salt be molten (Folkmann *et al.*, 1991; Hatem *et al.*, 2002). Melting at moderate temperatures (~650 K) is obtained by combining high melting point:

vanadium pentoxide (melting point, 943 K)

with low melting point:

potassium (692 K), sodium (675 K), cesium (733 K) pyrosulfates, Fig. 8.2.

The resulting low melting point salt also:

(a) dissolves $SO_2(g)$ and $O_2(g)$

and:

(b) exsolves $SO_3(g)$

as required by Reactions (8.1) through (8.4).

8.1.1 Deactivation and reactivation

Catalyst deactivates when it is cooled below its solidification temperature. This happens when a catalyst bed is fed with cold gas or when the acid plant is shut down.

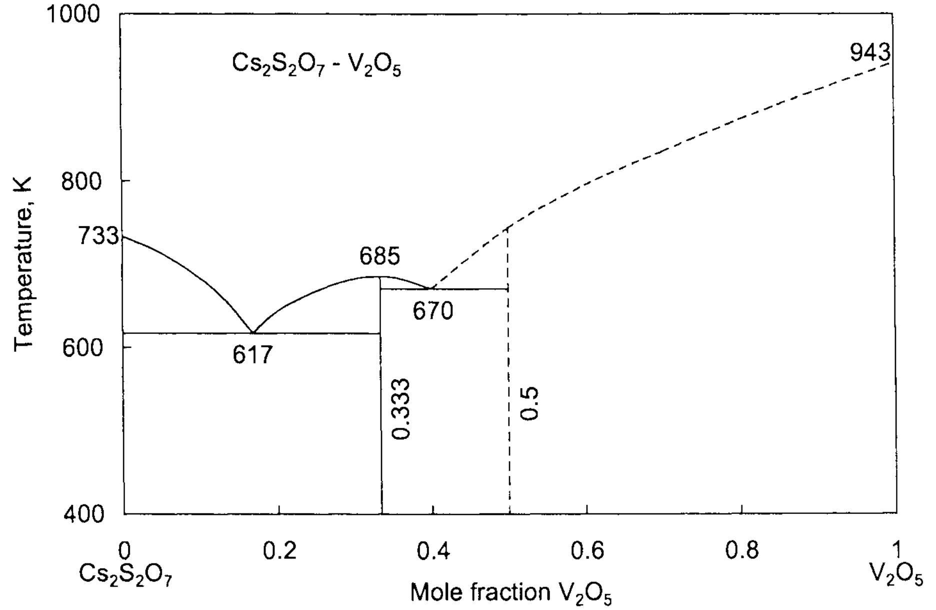

Fig. 8.2. $Cs_2S_2O_7$ -V_2O_5 phase diagram (after Folkmann *et al.*, 1991). The lowest melting point is 617 K, far below V_2O_5's 943 K melting point.

Fortunately, catalyst solidification and melting are reversible so that the catalyst reactivates when it is once again heated and remelted.

8.2 Maximum and Minimum Catalyst Operating Temperatures

Tables 7.2 and 19.3 indicate that industrial catalysts operate between:

~680 K (occasionally lower)

and:

~900 K.

Operating above ~690 K ensures that the catalyst is molten and active.

Operating below ~900 K ensures the presence of Reactions 8.1 to 8.4's active ions in the molten catalyst. Above ~900 K, these active ions transform to inactive vanadates (VO_4^{3-}) causing SO_2 oxidation to cease (Rasmussen, 2001). Also, above 900 K, the molten catalyst and solid substrate tend to irreversibly form a viscous inactive liquid.

8.3 Composition and Manufacture

Compositions and methods of manufacturing commercial catalysts are proprietary. Roughly, however, commercial catalysts contain (mass%):

4 - 9% V_2O_5

15 - 20% potassium sulfate/pyrosulfate (SO_4/S_2O_7)

2 - 5% sodium sulfate/pyrosulfate

5 - 15% cesium sulfate/pyrosulfate (when present)

55 - 70% porous silica substrate.

8.3.1 Manufacture

The catalyst is made by:

(a) mixing vanadium oxide, alkali metal oxides and diatomaceous earth (SiO_2) powders in specified proportions

(b) forming a paste of these components by mixing them with water and inorganic/organic binding additives

(c) extruding the paste into ring- or pellet-shaped rods

(d) chopping the extrudates into rings or pellets

(e) baking the rings and pellets in an SO_2/SO_3 atmosphere to:

remove water
add strength
form alkali metal sulfates and pyrosulfates.

(e)'s SO_2/SO_3 atmosphere is adjusted to give the manufacturer's specified sulfate/pyrosulfate (SO_4/S_2O_7) ratio.

8.3.2 Installation and plant startup

Purchased rings and pellets are carefully shipped in sealed barrels or in 1 m × 1 m × 1 m fiberglass bags. They are carefully loaded onto the acid plant's catalytic converter 'trays'. The catalytic converter is then closed up and SO_2 oxidation is begun as described in Section 7.6.1.

8.3.3 Chemical change and melting

Flow of ~700 K SO_2/SO_3 bearing gas around the loaded catalyst causes it to form a vanadium oxide-alkali metal pyrosulfate melt on the surfaces of the catalyst's porous silica substrate.

It is in this melt that catalytic $SO_2(g) + \frac{1}{2}O_2(g) \rightarrow SO_3(g)$ occurs, Reactions (8.1) through (8.4).

The steady state *in situ* composition of the catalyst melt is affected by the composition of the gas that is passing around the melt. It varies down the catalyst beds.

8.4 Choice of Size and Shape

Catalyst pieces are sold in the form of daisy rings, simple rings and cylindrical pellets, Fig. 8.1.

Daisy rings have the largest surface area and lowest resistance to gas flow. Pellets have the smallest surface area and highest resistance to flow. Simple rings are intermediate.

Industrial data (Table 7.2) suggest that daisy rings and rings are equally favored. Pellets are only used to ensure well distributed gas flow through catalyst beds in low gas velocity converters (Topsoe, 2004).

8.5 Choice of Chemical Composition

Manufacturers choose catalyst chemical composition to give:

(a) a low melting point with a high vanadium ion solubility

(b) strong catalytic activity

(c) a high catalyst degradation temperature.

Low melting point and high V_2O_5 solubility are obtained by choosing a low melting point eutectic mixture of V_2O_5 and K, Na, Cs pyrosulfates.

Strong catalytic activity is provided by vanadium, Eqns. (8.1) to (8.4). Catalytic activity increases with increasing vanadium ion concentration. Cs also contributes to strong catalytic activity (Rasmussen, 2001, p72).

High degradation temperature is favored by low vanadium ion concentration (Rasmussen, 2005). The low V concentration minimizes inert $(VO_4)^{3-}$ formation as temperature rises.

Table 8.1 summarizes these effects.

Table 8.1. Descriptions, advantages and uses of Haldor Topsoe's sulfuric acid catalysts (Hansen, 2004; Topsoe, 2004). Industrial input gas temperatures are somewhat higher than those indicated here, Tables 7.2 and 19.3. Other manufacturers make similar catalysts (BASF, 2004; Monsanto, 2004#).

Catalyst	**VK38**	**VK48**	**VK59**	**VK69**
Characteristic				
alkali metals	K, Na	K, Na	K, **Cs**, Na	K, **Cs**, Na
vanadium ion concentration		high		high
special characteristics			manufactured silica substrate with many uniform, high surface area gas accessible pores	manufactured silica substrate with many uniform, high surface area gas accessible pores
continuous operating temperature range, K	670 - 900	670 - 820	640 - 770	640 - 770
advantage	high temperature stability	strong catalytic activity	low continuous gas input temperature	(i) low continuous gas input temperature (ii) highest catalytic activity
suggested use	all catalyst beds, especially 1st and 2nd	last bed before H_2SO_4 making	(i) ignition layer in any bed (ii) last bed in single contact acid plant	after H_2SO_4 making oxidation

LP120 (high temperature tolerance); LP110 (high vanadium); Cs120 (low gas input temperature); Cs 110, 210 (final catalyst bed).

8.6 Catalyst Bed Thickness and Diameter

Table 7.2 gives measured industrial:

catalyst bed thicknesses, m

catalyst bed (converter) diameters, m

converter input gas rate, Nm^3/hour.

This section discusses these values.

8.6.1 Bed thicknesses

Fig. 8.3 shows industrial catalyst bed thicknesses. Average bed thicknesses are:

1st (feed gas) catalyst bed	0.62 m
2nd catalyst bed	0.72 m
3rd catalyst bed	0.84 m

with a scatter of ±0.2 m each.

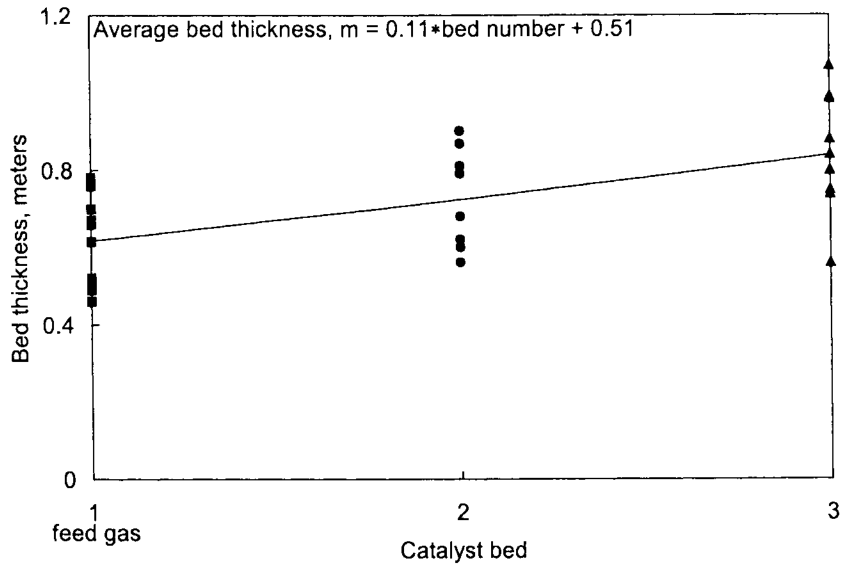

Fig. 8.3. Industrial 1st, 2nd and 3rd catalyst bed thicknesses. They are from Table 7.2. They increase from bed 1 through bed 3.

Bed 2 is thicker than bed 1 to provide a longer gas residence time, Fig. 8.5. This is necessary because bed 2 input gas contains:

less SO_2 and O_2

more SO_3

than bed 1 feed gas. These changes all tend to slow SO_2 oxidation. Bed 2's longer residence time offsets them.

Bed 3 is thicker than bed 2 for the same reason.

8.6.2 Bed diameters

Fig. 8.4 shows industrial catalytic converter (hence catalyst bed) diameters as a function of measured 1st catalyst bed feed gas volumetric flowrates. Bed diameters are between 8 and 16 m. They increase with increasing input gas flowrate. They are quite precisely predicted by the trendline equation on the graph.

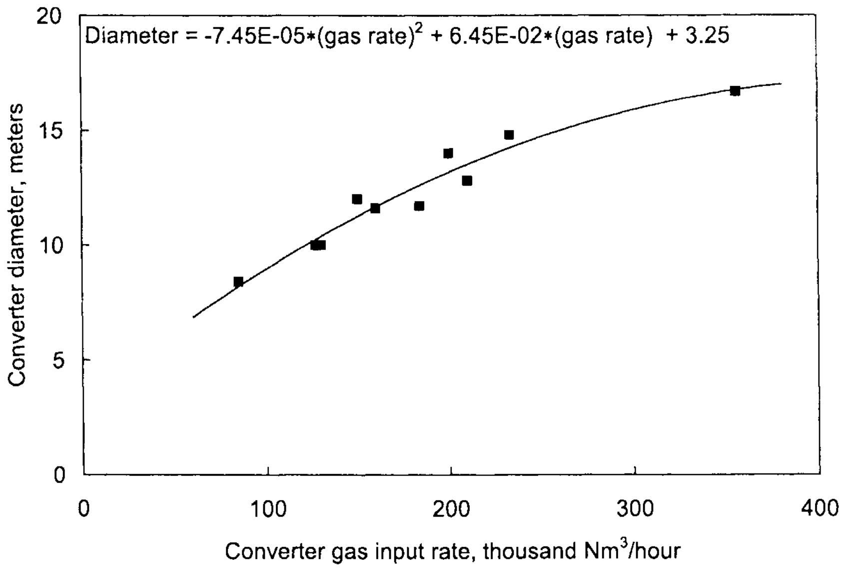

Fig. 8.4. Measured industrial catalytic converter diameter as a function of measured converter gas input rate. Diameter increases with increasing flowrate. This keeps catalyst bed residence times roughly constant, Fig. 8.5.

8.7 Gas Residence Times

Nominal residence times of gas in a converter's catalyst beds are calculated from measured bed thickness, converter diameter and converter gas input rate. The equation is:

$$\text{Nominal gas residence time in catalyst bed, s} = \frac{\text{bed thickness, m}}{\left(\dfrac{\text{converter gas input rate, }\dfrac{\text{Nm}^3}{\text{s}}}{\dfrac{\pi}{4}*(\text{converter diameter, m})^2}\right)}$$

Fig. 8.5 plots values calculated from Table 7.2's measured data. Residence times are seen to be 1½ or 2 seconds, increasing with bed number.

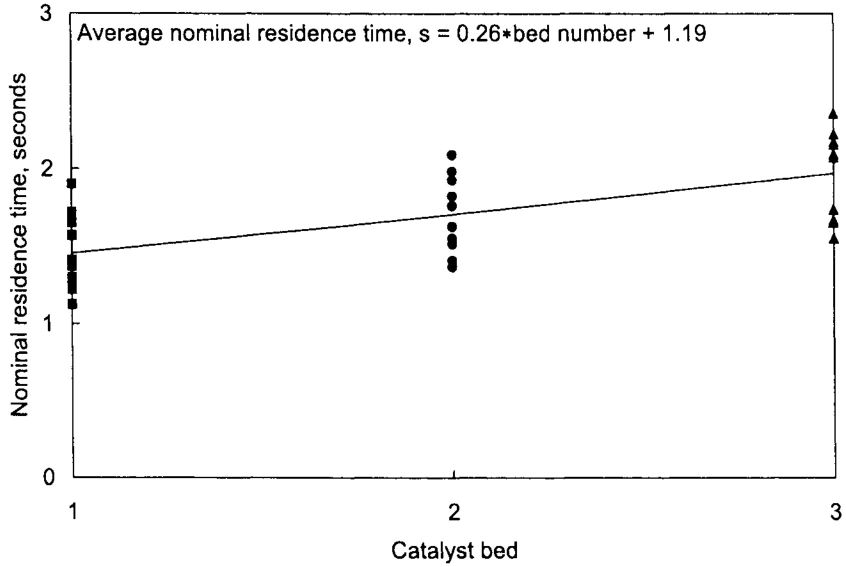

Fig. 8.5. Industrial 1st, 2nd and 3rd catalyst bed gas nominal residence times. They increase with increasing bed number. This is due to the increase in bed thickness with increasing bed number, Fig. 8.3. The points have been calculated from Table 7.2's industrial catalyst bed thicknesses, converter diameters and converter input gas flowrates.

8.8 Catalyst Bed Maintenance

Over time, catalyst beds (especially bed 1) become clogged with dust. This gradually increases the pressure that must be applied to push gas through the beds. Eventually this pressure becomes too high and the dust must be screened out of the catalyst.

Screening entails removing the catalyst from its converter tray, passing it across vibrating screens and loading the screened catalyst back into the tray with a small amount of new catalyst makeup. It is done every year or two, most frequently for the 1st catalyst bed. It is done as quickly as possible to minimize acid production loss.

8.9 Summary

$SO_3(g)$ is a key ingredient in making $H_2SO_4(\ell)$. It is produced rapidly and efficiently by oxidizing $SO_2(g)$ to $SO_3(g)$ in molten V, K, Na, Cs, S, O catalyst, 700-900 K. The molten catalyst is supported on solid, porous silica substrate.

$SO_2(g)$ and $O_2(g)$ dissolve in the molten catalyst. They then react with V, S, O anions to form and exsolve $SO_3(g)$. The reactions are rapid at temperatures (700-900 K) where

$SO_2(g) + ½O_2(g) \rightarrow SO_3(g)$ oxidation is thermodynamically efficient.

The process is carried out industrially in ½ to 1 m thick beds of 10 to 12 mm catalyst rings or pellets, Fig. 8.1. Reaction times are 1½ to 2 seconds.

Suggested Reading

Rasmussen, S.B. (2001) Multidisciplinary Investigation of SO_2 Oxidation Catalyst. Ph.D. Thesis, Technical University of Denmark http://struktur.kemi.dtu.dk/sbr/sbr.pdf

Topsoe (2004) VK series sulphuric acid catalysts for today and for the future, Halder Topsoe A/S brochure, 2004 www.haldortopsoe.com

References

BASF (2004) BASF-Catalyst (technical leaflet). www.basf.com

Folkmann, G.E., Hatem, G., Fehrmann, R., Gaune-Escard, M. and Bjerrum, N.J. (1991) Conductivity, thermal analysis, and phase diagram of the system $Cs_2S_2O_7$-V_2O_5. *Inorganic Chemistry*, **30**, 4057 4061. www.dtu.dk

Hansen, L. (2004) Topsoe Sulphuric Acid Catalysts VK-Series, brochure distributed at Sulphur 2004 conference, Barcelona, October 24-27, 2004. www.haldortopsoe.com

Hatem, G., Eriksen, K.M., Gaune-Escard, M. and Fehrmann, R. (2002) SO_2 oxidation catalyst model systems characterized by thermal methods. *Topics in Catalysis*, **19B (3,4)** 323 331. www.dtu.dk

Lapina, O.B., Bal'zhinimaev, B.S., Boghosian, S., Eriksen, K.M. and Fehrmann, R. (1999) Progress on the mechanistic understanding of SO_2 oxidation catalysts. *Catalysis Today*, **51** 469 479. www.dtu.dk

Monsanto (2004) Sulfuric Acid Catalysts www.enviro-chem/plant-tech/3rdtier/sulfcat.html

Rasmussen, S.B. (2001) Multidisciplinary Investigation of SO_2 Oxidation Catalyst. Ph.D. Thesis, Technical University of Denmark, 64. http://struktur.kemi.dtu.dk/sbr/sbr.pdf

Rasmussen, S.B. (2005) personal communication. sbr@kemi.dtu.dk

Topsoe (2004) VK series sulphuric acid catalysts for today and for the future, Halder Topsoe A/S brochure, 2004 www.haldortopsoe.com

CHAPTER 9

Production of $H_2SO_4(\ell)$ from $SO_3(g)$

The last step in sulfuric acid manufacture is production of liquid H_2SO_4 from SO_3 gas. The H_2SO_4 is produced by reacting:

the SO_3 bearing gas from catalytic SO_2 oxidation

with:

strong sulfuric acid, Fig. 9.1.

The reaction is:

$$\underset{\substack{\text{in } SO_3,\, SO_2\\ O_2,\, N_2 \text{ gas}}}{SO_3(g)} \quad + \quad \underset{\substack{\text{in strong}\\ \text{sulfuric acid}}}{H_2O(\ell)} \quad \xrightarrow{350\text{-}380\text{ K}} \quad \underset{\substack{\text{in strengthened}\\ \text{sulfuric acid}}}{H_2SO_4(\ell)} \qquad (1.2).$$

Industrially the process is carried out by:

(a) trickling 98.5 mass% sulfuric acid down through a packed bed of ceramic 'saddles'

while:

(b) blowing SO_3 bearing gas upward through the descending acid, Figs. 6.3 and 9.1.

The product of the process is ~99 to 99.5 mass% H_2SO_4 sulfuric acid. It is diluted with:

(a) the acid product from air or gas dehydration, Chapter 6

and:

(b) water

to give the acid plant's range of products, mostly 93 to 98 mass% H_2SO_4 acid.

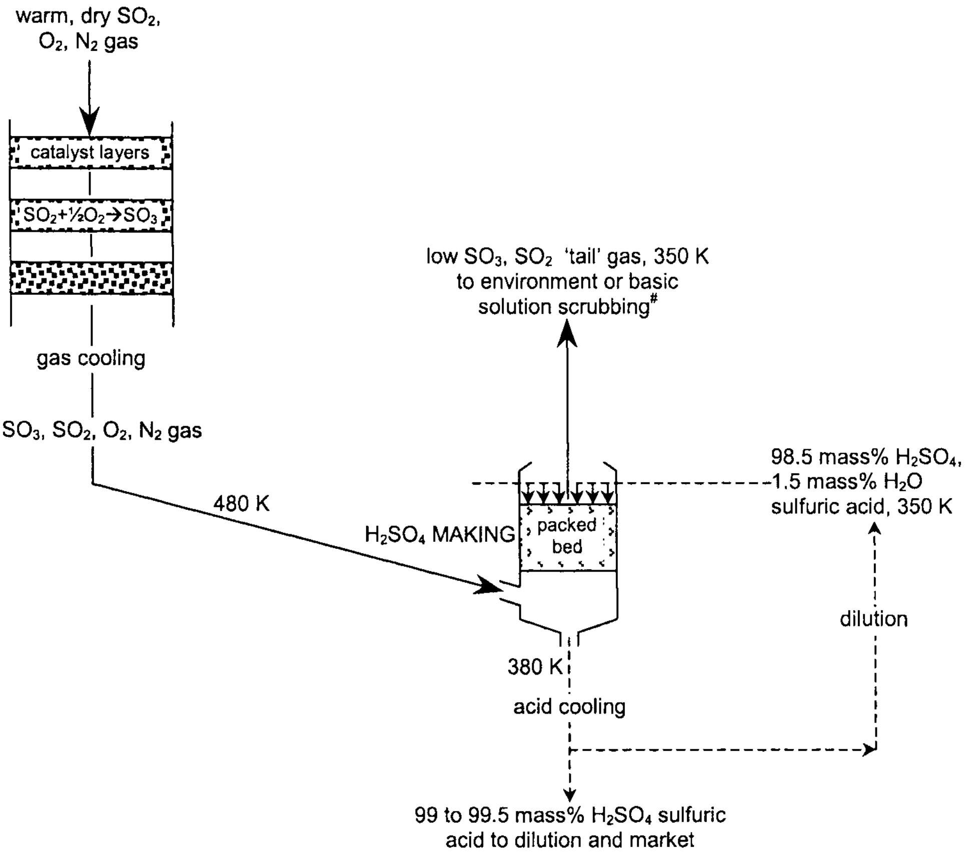

Fig. 9.1. Single contact H_2SO_4 making flowsheet. SO_3 rich gas from catalytic SO_2 oxidation is reacted with strong sulfuric acid, Reaction (1.2). The reaction consumes $H_2O(\ell)$ and makes $H_2SO_4(\ell)$, strengthening the acid. Double contact H_2SO_4 making is described in Fig. 9.6. #A few plants lower the SO_2 content of their 'tail' gas by scrubbing the gas with basic solution (Hay *et al.*, 2003).

9.1 Objectives

The objectives of this chapter are to:

(a) indicate why SO_3 is reacted with strong sulfuric acid rather than water

(b) describe industrial H_2SO_4 making

(c) suggest optimum conditions for efficient H_2SO_4 making.

9.2 Sulfuric Acid Rather than Water

Reaction (1.2) is strongly exothermic. It releases ~130 MJ per kg mole of SO_3. Stoichiometric reaction of 350 K $SO_3(g)$ with 350 K water produces 840 K H_2SO_4 vapor (H$_2$SO$_4$ boiling point ≈ 550 K, Perry and Green, 1997).

Condensation of $H_2SO_4(\ell)$ from this vapor is slow and expensive, so the $SO_3(g)$ water process is never used. Instead, the $SO_3(g)$ is reacted with strong sulfuric acid.

The large amount of H_2SO_4 in the acid reactant absorbs Reaction (1.2)'s heat of reaction while the acid warms only ~30 K, Table 9.3. This ensures that the product acid is liquid and relatively cool.

Pumping acid around the H_2SO_4 making system (Fig. 9.2) requires considerable energy. Nevertheless, reacting $SO_3(g)$ with strong sulfuric acid is the most economic way of producing H_2SO_4.

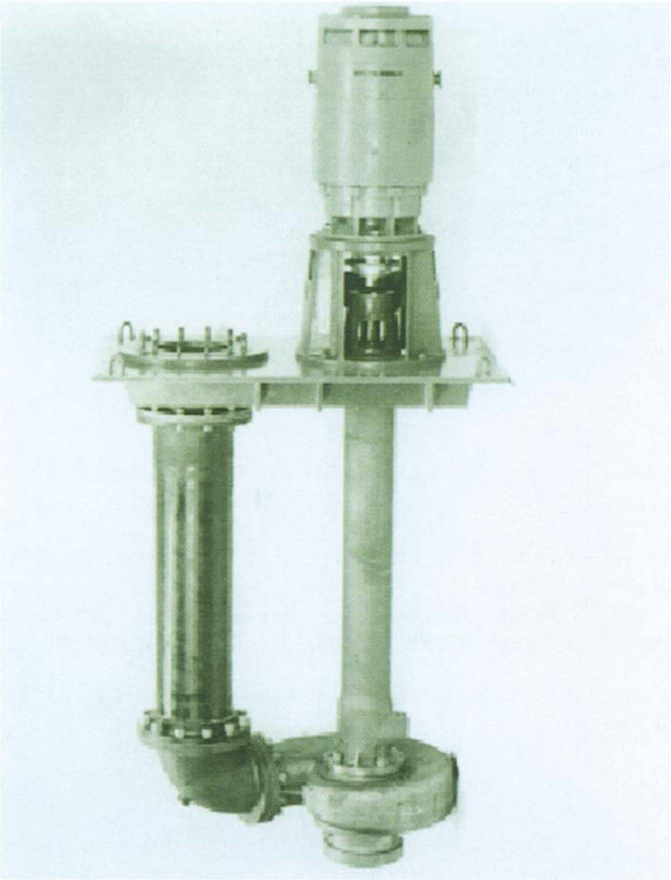

Fig. 9.2. Acid pump, courtesy Lewis Pumps www.lewispumps.com A submerged impeller (right) draws acid in through the bottom mouth and pumps it up the up-leg (left). A pipe extension is bolted to the top of the up-leg to get the acid to its destination. The motor and motor-shaft connection are well above the acid. Details:

design flowrate: 20 m^3 of acid per minute	pumping height: 23 m
pump speed: 1775 RPM	motor: 135 kW
suction mouth diameter: 0.3 m	up-leg diameter: 0.3 m

materials: impeller - Lewmet®; shaft - Alloy 20; suction head and discharge pipe - L14 iron.

9.3 Industrial H_2SO_4 Making (Table 9.3)

Industrial H_2SO_4 making is similar to the air/gas dehydration process described in Chapter 6. In both cases, gas is passed upwards through descending strong sulfuric acid, Figs. 6.3 and 9.1. The difference is that:

air/gas dehydration reacts $H_2O(g)$ with $H_2SO_4(\ell)$ in descending acid, i.e.:

$$H_2O(g) + \underset{\substack{\text{in strong}\\ \text{acid}}}{H_2SO_4(\ell)} \rightarrow \underset{\text{slightly weakened acid}}{H_2SO_4(\ell) + H_2O(\ell)} \qquad (6.2)$$

while:

H_2SO_4 making reacts $SO_3(g)$ with the $H_2O(\ell)$ in descending acid, i.e.:

$$SO_3(g) + \underset{\substack{\text{in strong}\\ \text{sulfuric acid}}}{H_2O(\ell)} \rightarrow \underset{\substack{\text{in slightly}\\ \text{strengthened acid}}}{H_2SO_4(\ell)} \qquad (1.2).$$

Gas dehydration dilutes the input acid while H_2SO_4 making strengthens it. Both reactions are exothermic. Both heat up their circulating acid so that it must be cooled before being recycled or sent to storage.

9.3.1 Residence times

Table 9.3 indicates that typical H_2SO_4 making ('absorption') tower diameters, packing heights, and residence times are:

tower diameter, m	7-9 meters
packing height, m	2-4 meters
gas residence time in packing	2-4 seconds
acid residence time in packing	300-600 seconds.

These residence times give 99+% transformation of $SO_3(g)$ to $H_2SO_4(\ell)$.

9.3.2 Acid mist

Air/gas dehydration (Chapter 6) produces fine spray of 10-250 μm diameter acid droplets. The droplets are removed from the dehydrated gas to prevent downstream corrosion. They are usually captured in a knitted Teflon®/stainless steel pad at the gas exit, Fig. 6.3.

H_2SO_4 making also produces this spray. In addition, $SO_3(g)$ in ascending gas and H_2O vapor from descending acid react to form very fine (<10μm diameter) acid droplets (mist). This mist must also be prevented from leaving in H_2SO_4 making exit gas.

It is most often removed by 'candle' filters suspended near the gas exit, Fig. 9.3 (Brink, 2005; Friedman and Friedman, 2004). These 'candles' remove 99+ % of spray and mist.

Fig. 9.3. Acid mist removal 'candle' filter being installed atop a stainless steel H_2SO_4 making tower. It is one of many. Exiting gas passes inward through the candle fabric and out the top of the candle – then out of the tower. The acid mist is caught in the candle fabric by impact, diffusion and Brownian forces (Brink, 2005; Friedman and Friedman, 2004; Lee and Byszewski, 2005; Ziebold and Azwell, 2005). The large total area of the candles gives a low gas velocity through the fabric, which allows 99+% capture of the mist. The captured mist trickles down the fabric and drips back into the tower or into collection pipes (Outokumpu 2005).

9.4 Choice of Input and Output Acid Compositions

Industrial input and output acid compositions are typically:

input: 98.5 mass% H_2SO_4, 1.5 mass% H_2O

output: 98.8 to 99.6 mass% H_2SO_4, remainder H_2O, Table 9.3.

These compositions are chosen to avoid excessive:

(a) acid mist formation

(b) SO_3(g) and H_2SO_4(g) evolution.

Acid mist formation is minimized by minimizing H_2O vapor pressure. This is done by using high H_2SO_4, low H_2O acid, Fig. 9.4.

SO_3(g) and H_2SO_4(g) evolution is, on the other hand, minimized by using low H_2SO_4 acid, Fig.9.4.

Section 9.4's industrial acid compositions strike a balance between these opposing effects.

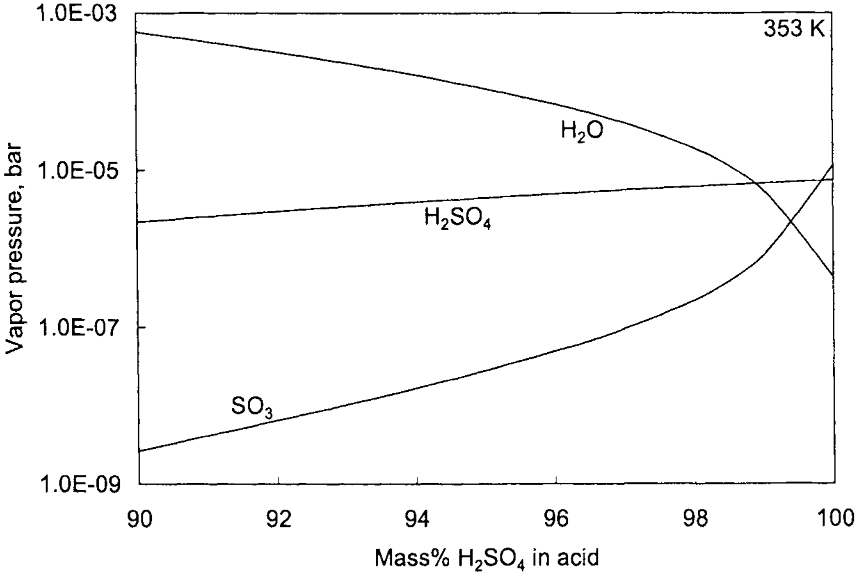

Fig. 9.4. Equilibrium vapor pressures of H_2O, H_2SO_4 and SO_3 over sulfuric acid, 353 K (Perry and Green, 1997). H_2O vapor pressure decreases and H_2SO_4 and SO_3 vapor pressures increase with increasing H_2SO_4-in-acid. All vapor pressures increase with increasing temperature, not shown.

9.5 Acid Temperature

Industrial H_2SO_4 making input and output acid temperatures (Table 9.3) are typically:

input acid temperature = ~350 K
output acid temperature = ~380 K.

They are high enough to give:

rapid H_2SO_4 making, Reaction (1.2)

while avoiding:

excessive $H_2O(g)$, $SO_3(g)$ and $H_2SO_4(g)$ formation
(which increases with increasing acid temperature).

9.5.1 Acid temperature control

Input acid temperature is controlled by indirect water cooling in an acid cooler, Figs. 9.5 and 24.6.

Output acid temperature is controlled by adjusting the H_2SO_4 making tower's:

$$\frac{\text{acid input rate}}{\text{gas input rate}}$$

ratio. Increasing the ratio results in cooler output acid and vice versa.

9.6 Gas Temperatures

Gas enters industrial H_2SO_4 making towers at 450-500 K. This is hot enough to avoid $H_2SO_4(\ell)$ condensation in the flues between catalytic SO_2 oxidation and H_2SO_4 making. It is cool enough to avoid excessive acid mist formation.

Gas leaves H_2SO_4 making near the acid input temperature, 350 K. Corrosive $H_2SO_4(\ell)$ may condense from this gas in cool downstream flues. For this reason, the flues are usually made of stainless steel.

9.7 Operation and Control

9.7.1 Startup and shutdown

H_2SO_4 making is started by:

(a) pumping strong acid around the Fig. 9.1 circuit at its design rate

(b) initiating SO_3 gas production as described in Section 7.6.1

(c) blowing the SO_3 bearing gas into Fig. 9.1's packed bed

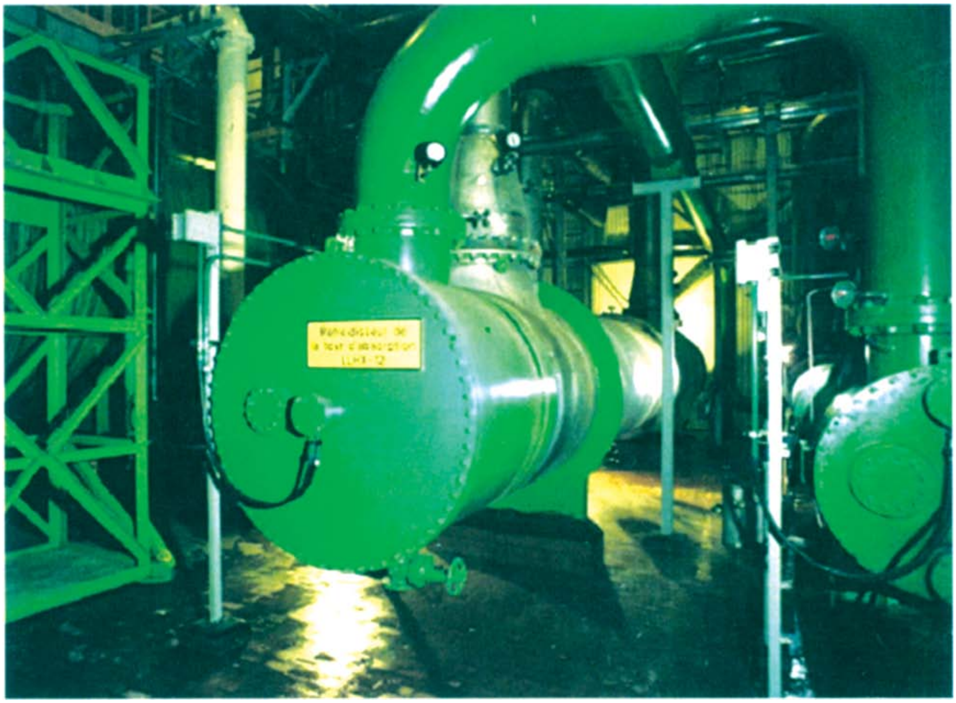

Fig. 9.5. Acid cooler, courtesy Chemetics www.chemetics.com Cool water flows through 1610 internal 2 cm diameter tubes while warm acid flows counter currently (and turbulently) between the tubes. The tubes are 316L stainless steel. They are resistant to water-side corrosion. They are electrochemically passivated against acid-side corrosion by continuously applying an electrical potential between the tubes and several electrically isolated metal rods. Details: shell diameter 1.65 m; shell material: 304L stainless steel; acid flow: 2000 m^3/hour; water flow: 2900 m^3/hour; acid temperature drop: 40 K. (Green pipes = water; metallic pipes = acid.) Fig. 24.6 gives an internal view.

(d) starting acid cooling

(e) adjusting acid and dilution flows to match H_2SO_4 production rate.

It is stopped by:

(a) stopping SO_3 gas production, Section 7.6.4

(b) shutting down (i) acid cooling and (ii) dilution and product acid flows.

Acid circulation through the H_2SO_4 making tower is continued during plant shutdowns. This maintains controlled corrosion conditions in pipes, pumps, coolers and the H_2SO_4 making tower.

9.7.2 Steady Operation and Control

Steady operation of an H_2SO_4 making tower consists of:

(a) steadily producing SO_3 bearing gas at its prescribed rate, composition and temperature, Section 7.6.2

(b) blowing this gas steadily into the Fig. 9.1 H_2SO_4 making tower

(c) steadily circulating strong acid through the tower at its prescribed rate, composition and temperature

(d) adjusting acid circulation rate to give the prescribed output 99 to 99.5 mass% H_2SO_4 acid

(e) cooling the circulating acid and product acid to their prescribed temperatures.

Table 9.1 describes measurements and adjustments that are used to control the process.

Table 9.1. Sensors and adjustments for controlling H_2SO_4 making packed tower. All sensors are placed in ceramic shield tubes to prevent corrosion.

Adjustable parameter	On-line sensor	Method of adjustment
input gas temperature	thermocouple	adjust after-catalytic-oxidation gas cooler bypass valve
input acid composition	'speed of sound through acid' meter (Mesa Labs, 2005)	adjust dilution water input rate
input acid temperature	thermocouple	adjust acid cooler bypass valve
output acid composition	'speed of sound through acid' meter (Mesa Labs, 2005)	adjust H_2SO_4 making tower acid circulation rate at constant gas input rate#
output acid temperature	thermocouple	adjust H_2SO_4 making tower acid circulation rate at constant gas input rate#

Output acid composition and temperature are not independent variables.

9.8 Double Contact H_2SO_4 Making (Tables 19.3, 23.2)

Fig. 9.6 is a flowsheet for double contact H_2SO_4 making. It shows:

(a) catalytic oxidation of most of the feed gas's SO_2 to SO_3 in 3 catalyst beds, Reaction (1.1)

then:

(b) intermediate H_2SO_4 making by contact of step (a)'s SO_3 bearing product gas with strong sulfuric acid, Reaction (1.2)

then:

(c) catalytic oxidation of the SO_2 not oxidized by step (a)

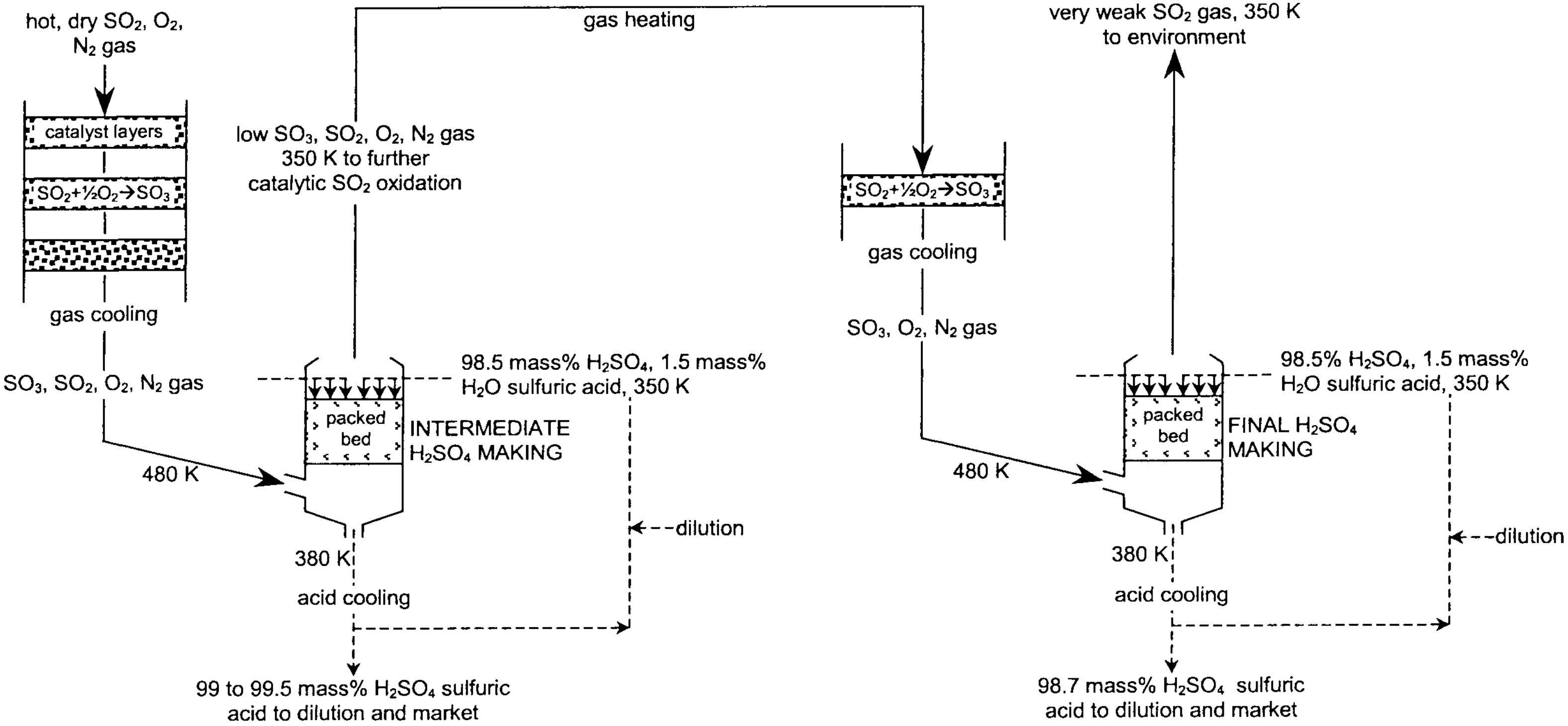

Fig. 9.6. Double contact H_2SO_4 making flowsheet. The two H_2SO_4 making packed towers are notable. The left half of the flowsheet oxidizes most of the SO_2-in-feed-gas and makes the product $SO_3(g)$ into strengthened sulfuric acid. It makes about 95% of the plant's new H_2SO_4. The right half of the flowsheet oxidizes almost all the remaining SO_2 and makes its product $SO_3(g)$ into strengthened sulfuric acid. The final exit gas is very dilute in SO_2. Industrially, all the catalyst beds are in the same 'converter', Fig. 7.7. Table 23.2 gives industrial final H_2SO_4 making data.

then:

(d) final H_2SO_4 making by contacting step (c)'s SO_3 bearing gas with strong sulfuric acid in a second H_2SO_4 making tower.

9.8.1 Double contact advantages

Double contact acidmaking oxidizes its SO_2 more completely to SO_3 than single contact acidmaking. For this reason it:

(a) makes H_2SO_4 more efficiently

(b) emits less SO_2 to the environment.

The more efficient SO_2 oxidation is due not only to Fig. 9.6's extra catalyst bed, but also to the fact that:

> virtually all of the SO_3 produced in the first three catalyst beds
> is removed from the gas in the first H_2SO_4 making tower.

The latter causes $SO_2+\frac{1}{2}O_2 \longrightarrow SO_3$ oxidation to go almost to completion in the after intermediate H_2SO_4 making catalyst bed, Chapter 19.

9.9 Intermediate vs. Final H_2SO_4 Making

Table 9.2 compares intermediate and final H_2SO_4 making. Notably, final contact input gas contains little SO_3 and produces little new H_2SO_4. Also final contact's output acid gains little strength. Otherwise the processes are quite similar.

Table 9.2. Comparison of Fig. 9.6's intermediate and final H_2SO_4 making towers. Note that final contact H_2SO_4 making makes only about 5% of the plant's H_2SO_4.

	H_2SO_4 making tower	
Quantities	**Intermediate contact, Table 9.3**	**Final contact, Table 23.2**
tower diameter, m	7-9	7-9
packed bed height, m	2½-5	2½-6
input gas		
volume% SO_3	8-12	0.4-0.7
temperature, K	440-490	410-460
input acid		
mass% H_2SO_4	98.5	98.5 or slightly less
temperature, K	340-355	330-355
output gas		
temperature, K	340-355	330-355
output acid		
mass% H_2SO_4	0.6% more than input acid	0.1% more than input acid
temperature, K	~30 K more than input acid	~20 K more than input acid
gas input rate, thousand Nm^3/hr	100-250	~10% less than intermediate
acid input rate, m^3/hour	800-1700	500-1100
H_2SO_4 production	~95%	~5%

Table 9.3. Details of packed bed H_2SO_4-from-SO_3 plants. The data are for

Plant	S1 (double contact)	M2 (double contact)
acid production, tonnes H_2SO_4/day	4400	1150
input gas flowrate, thousand Nm^3/hour	336	121
estimated SO_3 utilization efficiency		99.9
Packed bed details		
number of packed beds	2	1
height * diameter, m	23.0 × 9.5	18.5 × 6.5
construction material	310/304 stainless steel	brick lined carbon steel
ceramic packing	7.5 cm saddles	5.1 & 7.6 cm saddles
packing height, m	2.125	4
acid distributor type	trough and downcomer	buried pipe distributor
mist eliminator type	ES mist eliminator candles	hanging fiber bed
exit gas mist concentration, g/Nm^3		
acid flowrate, m^3/hour	1349	762
Temperature data, K		
inlet gas	439	484
outlet gas	344	353
inlet acid	339	353
outlet acid	485	381
acid cooling method	heat recovery system boilers	
Gas composition in, vol.%		
SO_3	11.8	8.49
SO_2	0.688	0.38
O_2	3.78	4.88
CO_2		
N_2	83.7	
Gas composition out, vol.%		
SO_3		
SO_2	0.78	0.42
O_2	4.28	5.34
CO_2		
N_2	94.9	
Acid comp., mass% H_2SO_4		
into tower	98.5	98.5
out of tower	99.6	
Acid plant products, mass% H_2SO_4	98.5	98.5

single contact plants or first (intermediate) contact in double contact plants.

Cumerio 1 (double contact)	Cumerio 2 (double contact)	M5 (single contact)
1940	1500	
160	150	52
99.98	99.98	
1	1	1
19.174 × 7	25.13 × 7	13 × 6.5
brick lined carbon steel	brick lined carbon steel	
7.6 & 5.1 cm saddles	5.1 cm saddles	
3.5	8.5	
Lurgi pipes and tubes	distribution plates	
high efficiency candles	candle type	
1093	950	684
487	473	540
355	343	328
355	343	338
384	373	358
shell and tube	shell and tube	shell and tube
11.47	10.08	8.05
0.51	0.42	0.61
7.37	5.67	7.2
0.32	0.28	6.92
80.33	83.55	
0	0	0.13
0.57	0.45	0.66
8.33	6.31	7.82
0.36	0.31	7.52
90.74	92.93	
		tail gas scrubbed with ammonia
98.5	98.3	
94-98.5	94-98.5	

Table 9.3 (cont.). Details of packed bed H_2SO_4-from-SO_3 plants. The data are for

Plant	M6 (double contact)	M3 (single contact)
acid production, tonnes H_2SO_4/day		2200 (nominal)
input gas flowrate, thousand Nm^3/hour	150-210	184
estimated SO_3 utilization efficiency	96	
Packed bed details		
number of packed beds	1	1
height * diameter, m	23.3 × 6.8	12.2 × 7.8 OD
construction material	brick lined carbon steel	ASTM A 283 Grade C
ceramic packing	saddles & structured packing	5.1-7.6 cm saddles
packing height, m	3.7	4
acid distributor type		Lurgi spray
mist eliminator type	high efficiency candles	suspended candles
exit gas mist concentration, g/Nm^3		0.035
acid flowrate, m^3/hour	1150 top, 517 bottom	3132
Temperature data, K		
inlet gas	505	473
outlet gas	350	335
inlet acid	350	335
outlet acid	383	364
acid cooling method	shell and tube	plate coolers
Gas composition in, vol.%		
SO_3	12.1	11.44
SO_2	0.5	0.23
O_2	12	9.61
CO_2	remainder	1.94
N_2		remainder
Gas composition out, vol.%		
SO_3		<35mg/Nm^3
SO_2	0.56	<0.4
O_2	13.6	10.85
CO_2	remainder	2.18
N_2		
		no tail gas scrubbing
Acid comp., mass% H_2SO_4		
into tower	98.5	
out of tower	99.1	
Acid plant products, mass% H_2SO_4	93, 99, 20% oleum#	97-98

#Liquid H_2SO_4 with dissolved 20 mass% dissolved SO_3, Chapter 19.

single contact plants or first (intermediate) contact in double contact plants.

M4 (double contact)	Asarco Hayden (double contact)
2100-2400	1630
178	192
99.9	99
1	1
20.4 × 7.5 OD	17.8 × 7.0
brick lined carbon steel	brick lined carbon steel
5.1 and 7.6 cm saddles	7.6 cm ceramic saddles
5.66	2.7
submerged distributor pipes	Z core
Alloy 66 + Teflon	energy saver candles
1280	1295
488	470
343	355
343	355
373	
10.9-13.3	12.1
0.7-1.0	0.6
7.5-8.6	7.1
2.9	1.0
remainder	79.1
0.8-1.2	0.69
8.4-9.9	8.0
3.3	1.0
remainder	90.0
98.5	98.5
	98.8
98.5	93/98

Table 9.3 (cont.). Details of packed bed H_2SO_4-from-SO_3 plants. The data are for

Plant	Phelps Dodge (double contact)	M1 (double contact)
acid production, tonnes H_2SO_4/day	2400	270
input gas flowrate, thousand Nm^3/hour	267	46-51
estimated SO_3 utilization efficiency	99.9	99.9
Packed bed details		
number of packed beds	1	1
height * diameter, m	22.3 × 9.5 inside brick	8.5 × 4.0
construction material	brick lined carbon steel	brick lined carbon steel
ceramic packing	5.1 and 7.6 cm saddles	7.6 cm saddles
packing height, m	4.6	4.0
acid distributor type	cast iron header and arms	trough and spouts
mist eliminator type	high efficiency candles	HE candles
exit gas mist concentration, g/Nm^3		
acid flowrate, m^3/hour	1680	227
Temperature data, K		
inlet gas	483	472-494
outlet gas	353	339-366
inlet acid	353	347-358
outlet acid	389	358-375
acid cooling method	acid coolers	shell and tube
Gas composition in, vol.%		
SO_3	10.38	
SO_2	0.66	
O_2	5.85	
CO_2	1.05	
N_2	82.05	
Gas composition out, vol.%		
SO_3	0.03	
SO_2	0.74	
O_2	6.53	
CO_2	1.17	
N_2	91.52	
Acid comp., mass% H_2SO_4		
into tower	98.5	98.5
out of tower	99.23	99.2
Acid plant products, mass% H_2SO_4	94.5	93.5

single contact plants or first (intermediate) contact in double contact plants.

S2 (single contact)	SP1 (single contact)
1800	444
210	
99.9	>99.99
1	1
11 × 7	7.6 × 4
brick lined carbon steel	brick lined carbon steel
5.1-7.6 cm saddles	5.1 cm and 7.6 cm intalox
4	3.8
	cast iron trough and spouts
high efficiency candles	candles
	0.0125 g/Nm^3
505	405
358	356
358	356
389	378
	shell and tube
8.18	9.02
0.15	0.19
9.44	7.13
0	7.74
82.23	75.92
<0.1	
0.17	
10.27	
89.56	
no tail gas scrubbing	no tail gas scrubbing
98.5	98.29
99.1	98.75
93, 98, 99, oleum#	98

#Liquid H_2SO_4 containing dissolved SO_3, Chapter 19.

9.10 Summary

The final step in sulfuric acid manufacture is production of $H_2SO_4(\ell)$ from SO_3 bearing gas.

The H_2SO_4 is made by trickling strong sulfuric acid down between ceramic saddles in a packed bed while blowing SO_3 gas up through the bed.

$SO_3(g)$ in the ascending gas reacts with $H_2O(\ell)$ in the descending acid to produce strengthened sulfuric acid, i.e.:

$$\begin{array}{ccccc} SO_3(g) & + & H_2O(\ell) & \xrightarrow{\text{350-380 K}} & H_2SO_4(\ell) \\ \text{in } SO_3, SO_2 & & \text{in 98.5 mass\%} & & \text{in strengthened} \\ O_2, N_2 \text{ gas} & & H_2SO_4\text{, 1.5 mass\%} & & \text{sulfuric acid} \\ & & H_2O \text{ sulfuric acid} & & \end{array}$$

The strengthened acid is mostly diluted and sold.

Most sulfuric acid plants are double contact plants, Fig. 9.6, Tables 9.3, 19.3 and 23.2. They efficiently oxidize their feed $SO_2(g)$ to $SO_3(g)$ and efficiently make the resulting $SO_3(g)$ into $H_2SO_4(\ell)$. Single contact plants (Fig. 9.1) are simpler and cheaper – but less efficient.

Suggested Reading

Friedman, L.J. and Friedman, S.J. (2004) The wet gas sulphuric acid plant (part 2). *Sulphur*, **293**, July-August 2004, 29 35. www.britishsulphur.com

Guenkel, A. and Orlando, J. (2004) Review of the performance parameters in acid towers. Paper presented at Sulphur 2004 conference, Barcelona, October 27, 2004. www.britishsulphur.com

Sulphur (2004) Sulphuric acid equipment update. *Sulphur*, **292** (May-June 2004), 33 42. www.britishsulphur.com

Ziebold, S.A. (2000) Demystifying mist eliminator selection. *Chemical Engineering*, **107(5)**, May 2000. www.che.com

References

Brink (2005) Air pollution control. www.genuinebrink.com

Chemetics (2004) Acid coolers, sulphuric acid technology. Brochure distributed at Sulphur 2004 conference, Barcelona, October 24-27, 2004. www.chemetics.com Also personal communication, 2005.

Friedman, L.J. and Friedman, S.J. (2004) The wet gas sulphuric acid plant (part 2). *Sulphur*, **293**, July-August 2004, 29 35. www.britishsulphur.com

Hay, S., Porretta, F. and Wiggins, B. (2003) Design and start-up of acid plant tail gas scrubber. In *Copper 03-Cobre 03, Proceedings of the Fifth International Conference, Vol. IV (Book 1) Pyrometallurgy of Copper, the Hermann Schwarze Symposium on Copper Pyrometallurgy, Smelting Operations, Ancillary Operations and Furnace Integrity*, ed. Diaz, C., Kapusta, J. and Newman, C., The Metallurgical Society of the Canadian Institute of Mining, Metallurgy and Petroleum, Montreal, 555 566. www.metsoc.org

Lee, M. and Byszewski, C. (2005) Two new innovations in fiber bed technology from CECO Filters that offer improved efficiency, enhanced performance and longevity, preprint of paper presented at 29th Annual Clearwater Conference (AIChE), Clearwater, Florida, June 4, 2005. www.aiche-cf.org www.cecofilters.com

Lewis Pumps (2005) Lewis Pumps sulfuric acid pumps. www.lewispumps.com Also personal communication.

Mesa Labs (2005) Sulfuric acid analyzer application note. www.mesalabs.com/nusonics

Outokumpu (2005) *Latest Developments in Sulfur Burning Sulfuric Acid Plants*. Brochure distributed at 29th Annual Clearwater Conference (AIChE), Clearwater, Florida, June 3 and 4, 2005 (also presented as paper by Bartlett, C. and Rieder, J., Outokumpu Technology GmbH, June 4, 2005) www.outokumpu.com www.aiche-cf.org

Perry, R.H. and Green, D.W. (1997) *Perry's Chemical Engineers' Handbook – 7th Edition*, McGraw-Hill, New York, NY, 2-78 to 2-79. www.mcgraw-hill.com

Ziebold, S.A. and Azwell, D.E. (2005) New Brink fiberbed technology, preprint of paper presented at 29th Annual Clearwater Conference (AIChE), Clearwater, Florida, June 4, 2005. www.aiche-cf.org www.outokumpu.com

Break

This page marks the end of the descriptive section of our book – and the beginning of the mathematical section.

Most of the mathematical chapters analyze catalytic $SO_2+\frac{1}{2}O_2 \rightarrow SO_3$ oxidation in single and double contact acid plants. The remainder examine temperature control and H_2SO_4 making.

Many of the chapters have problems after their chapter summaries. The problems are not crucial to understanding the concepts in the chapters. They may, however, be useful for learning how our calculations can be extended to control and optimization of industrial acidmaking.

Many of the chapters also refer to appendices, which:

(a) derive equations
(b) provide thermodynamic data
(c) give calculation instructions.

The chapters can be understood without reference to these appendices. The appendices will, however, be useful for readers who wish to derive the book's equations or do its problems.

CHAPTER 10

Oxidation of SO_2 to SO_3 – Equilibrium Curves

Catalytic oxidation of SO_2 to SO_3:

$$SO_2(g) + \tfrac{1}{2}O_2(g) \rightarrow SO_3(g) \qquad (1.1)$$

is a key step in sulfuric acid production. It makes SO_3 for subsequent $H_2SO_4(\ell)$ making.

This chapter describes the equilibrium thermodynamics of Reaction (1.1). Its objectives are to:

(a) determine the maximum extent to which SO_2 in acid plant feed gas can be oxidized in a catalyst bed

(b) describe the factors which affect this maximum, specifically catalyst bed feed gas composition and equilibrium temperature and pressure.

The chapter concludes that maximum industrial SO_2 oxidation is achieved when Reaction (1.1):

(a) proceeds by rapid catalytic oxidation

(b) approaches equilibrium at a low temperature (but warm enough for rapid catalytic oxidation).

This is the basis of all industrial acid plant designs.

10.1 Catalytic oxidation

All industrial SO_2 oxidation is done in contact with V, alkali metal, S, O, SiO_2 catalyst, Chapters 7 and 8.

Fig. 10.1 shows a catalyst bed and describes SO_2 oxidation in it. SO_2 is oxidized by O_2 as feed gas descends through the catalyst bed. This is indicated by an increasing *% SO_2 oxidized* on the left graph.

SO_2, O_2 and SO_3 approach equilibrium as the gas descends the catalyst bed (left graph). *% SO_2 oxidized* at equilibrium is the maximum extent to which the feed SO_2 can be oxidized. As will be seen, this maximum depends on:

(a) equilibrium temperature

(b) equilibrium pressure

(c) feed gas composition, volume% SO_2, O_2, N_2

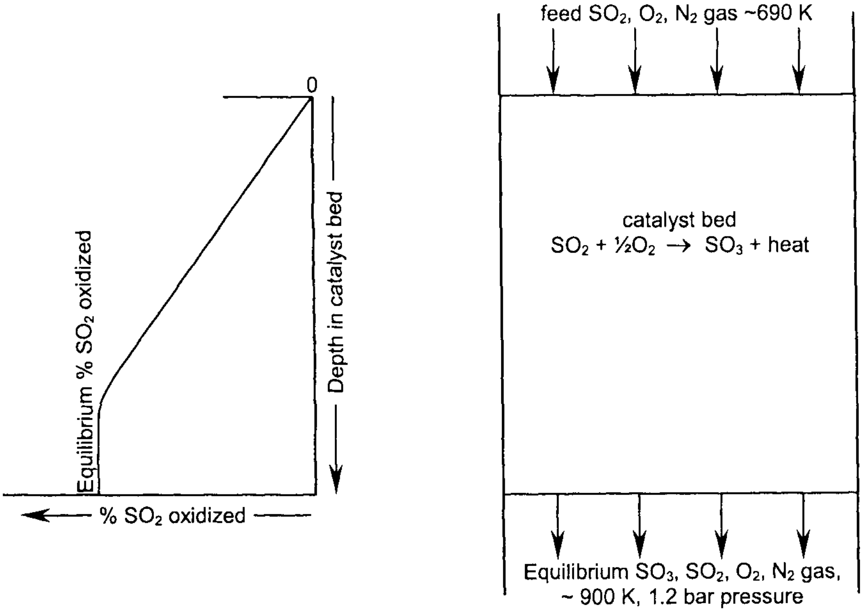

Fig. 10.1. Sketch of SO_2, O_2, N_2 feed gas descending a reactive catalyst bed. It assumes that equilibrium is attained before the gas leaves the bed and that composition and temperature are uniform horizontally at all levels. Rapid catalytic oxidation requires an input gas temperature ~690 K, Table 7.2.

10.1.1 % SO_2 oxidized defined

% SO_2 oxidized anywhere in a catalyst bed is defined as:

$$\% SO_2\ oxidized = \Phi = \frac{\begin{matrix}\text{kg-mole } SO_2 \\ \text{in feed gas}\end{matrix} - \begin{matrix}\text{kg-mole } SO_2 \\ \text{in oxidized gas}\end{matrix}}{\text{kg-mole } SO_2 \text{ in feed gas}} * 100 \tag{10.1}$$

where all the quantities are per kg-mole of feed gas.

A special case of this definition is:

$$\begin{array}{l}\text{Equilibrium}\\ \%\,SO_2\ oxidized\end{array} = \Phi^E = \frac{\begin{array}{c}\text{kg-mole } SO_2\\ \text{in feed gas}\end{array} - \begin{array}{c}\text{kg-mole } SO_2 \text{ in oxidized gas}\\ \text{where equilibrium has been attained}\end{array}}{\text{kg-mole } SO_2 \text{ in feed gas}} * 100 \qquad (10.2).$$

The Eqn. (10.2) definition is used in all our 1st catalyst bed equilibrium curve calculations.

Fig. 10.2 shows a typical equilibrium *% SO_2 oxidized* vs. temperature curve for the Fig. 10.1 catalyst bed. This chapter and Appendix D show how it is prepared.

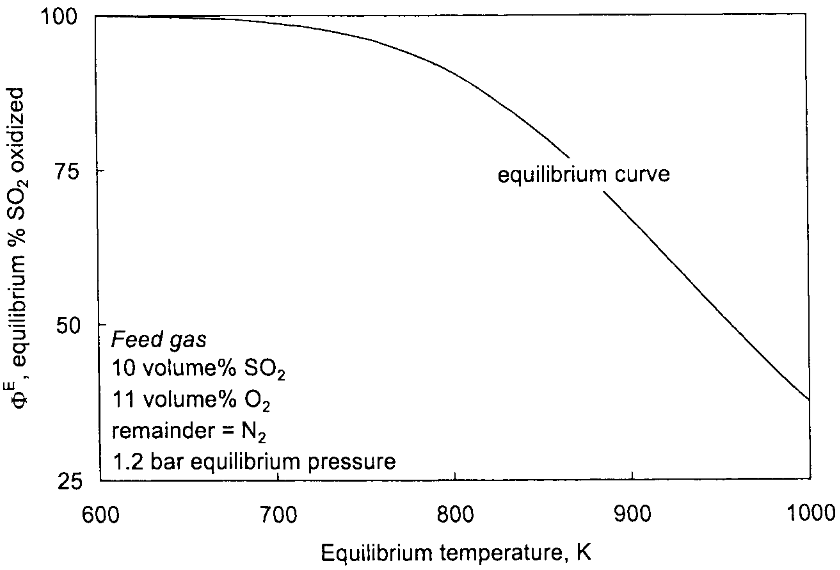

Fig. 10.2. Percentage of SO_2-in-feed-gas that is oxidized when equilibrium is attained in the Fig. 10.1 catalyst bed. The percentage increases with decreasing equilibrium temperature. The curve has been plotted from Eqn. (10.13) as described in Appendix D. It applies only to the specified conditions.

10.2 Equilibrium Equation

Fig. 10.1 indicates that maximum SO_2 oxidation is achieved when Reaction (1.1) comes to equilibrium. The next few sections show how this maximum is predicted.

The equilibrium equation for $SO_2 + ½O_2 \rightarrow SO_3$ oxidation is:

$$K_E = \frac{P^E_{SO_3}}{P^E_{SO_2} * \left(P^E_{O_2}\right)^{\frac{1}{2}}} \qquad (10.3)$$

where:

K_E = equilibrium constant, dependent only on temperature (Gaskell, 1981), $bar^{-\frac{1}{2}}$

$P^E_{SO_2}$, $P^E_{O_2}$, $P^E_{SO_3}$ = equilibrium partial pressures of SO_2, O_2 and SO_3, bar.

$P^E_{SO_2}$, $P^E_{O_2}$ and $P^E_{SO_3}$ in Eqn. (10.3) are related to gas composition by:

$$P^E_{SO_2} = X^E_{SO_2} * P_t \qquad (10.4)$$

$$P^E_{O_2} = X^E_{O_2} * P_t \qquad (10.5)$$

$$P^E_{SO_3} = X^E_{SO_3} * P_t \qquad (10.6)$$

where X^E is equilibrium mole fraction of each gas and P_t is total equilibrium gas pressure. Eqns. (10.4) to (10.6) assume ideal gas behavior (based on the low pressure, ~1 bar, of industrial SO_2 oxidation).

Eqns. (10.3) to (10.6) combine to give:

$$K_E = \frac{X^E_{SO_3}}{X^E_{SO_2} * \left(X^E_{O_2}\right)^{\frac{1}{2}}} * P_t^{-\frac{1}{2}} \qquad (10.7)$$

which indicates that equilibrium SO_2 oxidation (i.e. SO_3 production) increases with increasing K_E and P_t.

10.3 K_E as a Function of Temperature

K_E in Eqn. (10.7) is related to equilibrium temperature by:

$$\ln(K_E) = \frac{-\Delta G^o_T}{(R*T_E)} \qquad (10.8)$$

where ΔG^o_T is the standard free energy change (MJ/kg-mole SO_2) for SO_2 oxidation at equilibrium temperature T_E.

Appendix C gives published ΔG^o_T vs. temperature data. It shows that ΔG^o_T may be related to temperature by:

$$\Delta G^o_T = A*T + B \qquad (10.9)$$

where A and B are empirical constants.

Eqns. (10.8) and (10.9) combine to give:

$$\ln(K_E) = \frac{-(A*T_E + B)}{(R*T_E)} \tag{10.10}$$

where:

K_E = equilibrium constant for Reaction (1.1), bar$^{-\frac{1}{2}}$

A and B = empirical constants for calculating ΔG_T° from T, Eqn. (10.9) and Appendix C

$A = 0.09357$ MJ kg-mole SO_2^{-1} K^{-1}

$B = -98.41$ MJ/kg-mole SO_2

R = gas constant, 0.008314 MJ kg-mole SO_2^{-1} K^{-1}

T_E = equilibrium temperature, K

Eqn. (10.10) rearranges to:

$$R*T_E*\ln(K_E) = -A*T_E - B$$

or:

$$A*T_E + R*\ln(K_E)*T_E = -B$$

or:

$$T_E = \frac{-B}{A + R*\ln(K_E)} \tag{10.11}$$

10.4 K_E in Terms of *% SO_2 Oxidized*

Rewritten in terms of:

(a) Fig. 10.1 feed gas composition

(b) equilibrium *% SO_2 oxidized*, Φ^E

Eqn. 10.7 becomes (Appendix B):

$$K_E = \frac{\Phi^E}{100 - \Phi^E} * \left(\frac{100 - \frac{1}{2} * e * \frac{\Phi^E}{100}}{f - \frac{1}{2} * e * \frac{\Phi^E}{100}} \right)^{\frac{1}{2}} * P_t^{-\frac{1}{2}} \tag{10.12}$$

where:

K_E = equilibrium constant for Reaction (1.1), bar$^{-\frac{1}{2}}$
Φ^E = equilibrium *% SO_2 oxidized*, Section 10.1.1
e = volume% SO_2 in feed gas
f = volume% O_2 in feed gas
} remainder 'inerts', i.e. N_2 and CO_2#
P_t = total equilibrium gas pressure, bar.

#The effect of SO_3 in feed gas is described in Appendix P and Chapter 17.

This equation permits equilibrium *% SO_2 oxidized* (Φ^E) to be calculated from equilibrium constant (K_E), input gas composition and equilibrium pressure. It combines (i) equilibrium thermodynamics and (ii) S and O mass balances. It is derived in Appendix B.

10.5 Equilibrium *% SO_2 Oxidized* as a Function of Temperature

Equilibrium *% SO_2 oxidized* (Φ^E) is related to equilibrium temperature by combining Eqns. (10.11) and (10.12), which gives:

$$T_E = \frac{-B}{A + R * \ln\left(\left(\frac{\Phi^E}{100 - \Phi^E}\right) * \left(\frac{100 - \frac{1}{2} * e * \frac{\Phi^E}{100}}{f - \frac{1}{2} * e * \frac{\Phi^E}{100}}\right)^{\frac{1}{2}} * P_t^{-\frac{1}{2}}\right)} \qquad (10.13)$$

where:

T_E = equilibrium temperature

A and B = empirical constants for calculating ΔG_T° from T, Eqn. 10.9

A = 0.09357; B = -98.41, Appendix C

R = gas constant, 0.008314 MJ kg-mole SO_2^{-1} K^{-1}

Φ^E = equilibrium *% SO_2 oxidized*, Section 10.1.1

e = volume% SO_2 in feed gas

f = volume% O_2 in feed gas

P_t = total equilibrium gas pressure, bar.

Fig. 10.2 plots this equation as described in Appendix D. The figure emphasizes that equilibrium *% SO_2 oxidized* increases with decreasing equilibrium temperature.

10.5.1 Equilibrium pressure effect

Fig. 10.3 shows the effect of equilibrium pressure on equilibrium *% SO_2 oxidized.* Equilibrium *% SO_2 oxidized* increases slightly with increasing equilibrium pressure.

10.5.2 O_2-in-feed-gas effect

Fig. 10.4 shows the effect of volume% O_2 in feed gas on equilibrium *% SO_2 oxidized.*

The curves are for:

(a) constant 10 volume% SO_2-in-feed-gas

(b) 8, 11 and 14 volume% O_2-in-feed-gas

(c) constant equilibrium pressure, P_t = 1.2 bar.

Equilibrium *% SO_2 oxidized* increases slightly with increasing volume% O_2 in feed gas. This is because a high volume% O_2*volume% SO_2 product pushes SO_2 oxidation to the right, Eqn. 10.7.

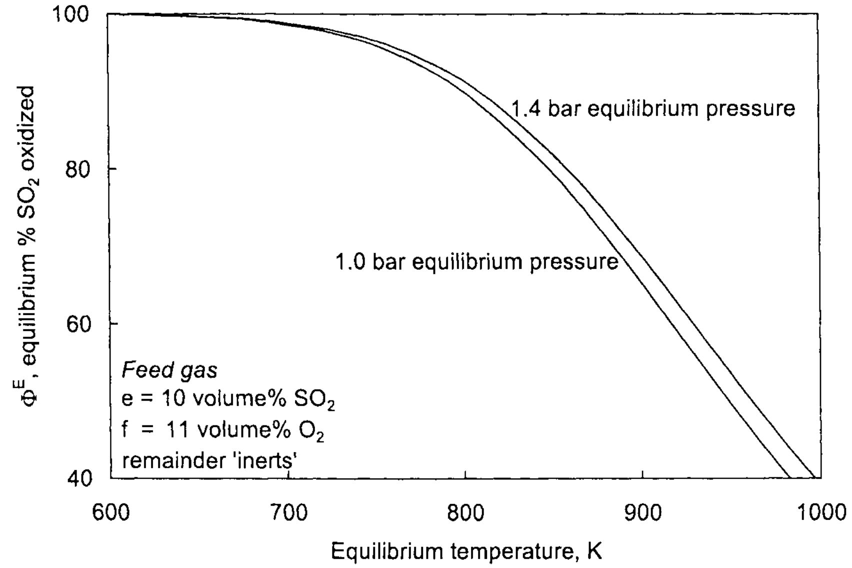

Fig. 10.3. Equilibrium *% SO_2 oxidized* as affected by equilibrium pressure, P_t. Equilibrium *% SO_2 oxidized* is seen to increase slightly with increasing pressure, Eqn. (10.7). Industrial catalyst bed pressures are typically 1 to 1.4 bar.

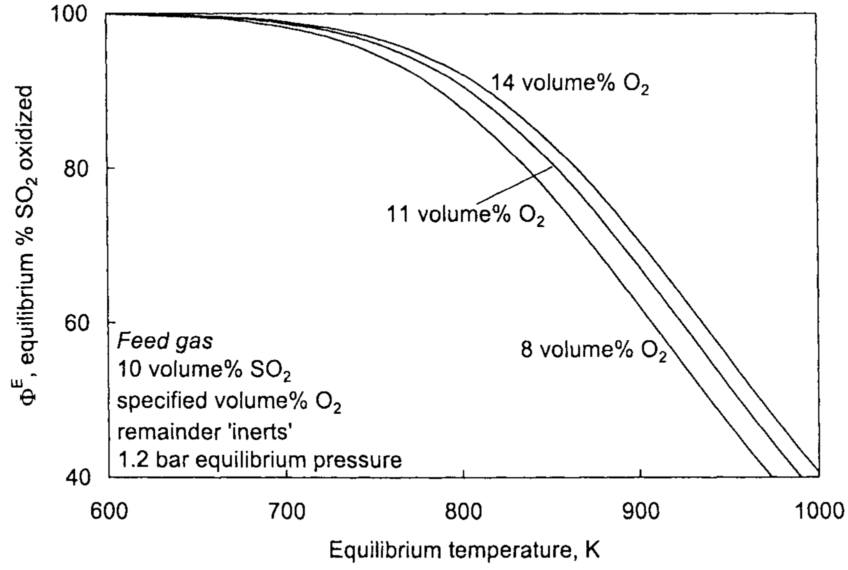

Fig. 10.4. Effect of feed gas O_2 concentration on equilibrium *% SO_2 oxidized.* High O_2 concentration gives high equilibrium *% SO_2 oxidized* and vice versa.

10.5.3 SO_2-in-feed-gas effect

Fig. 10.5 shows the effect of volume% SO_2 in feed gas on equilibrium *% SO_2 oxidized*. The curves are for:

(a) 7, 10 and 13 volume% SO_2-in-feed-gas

(b) constant 1.1 volume% O_2/volume% SO_2 ratio in feed gas

(c) constant equilibrium pressure, P_t = 1.2 bar.

Equilibrium *% SO_2 oxidized* is seen to increase slightly with increasing volume% SO_2 in feed gas. This is because a high volume% O_2*volume% SO_2 product pushes SO_2 oxidation to the right, Eqn. 10.7.

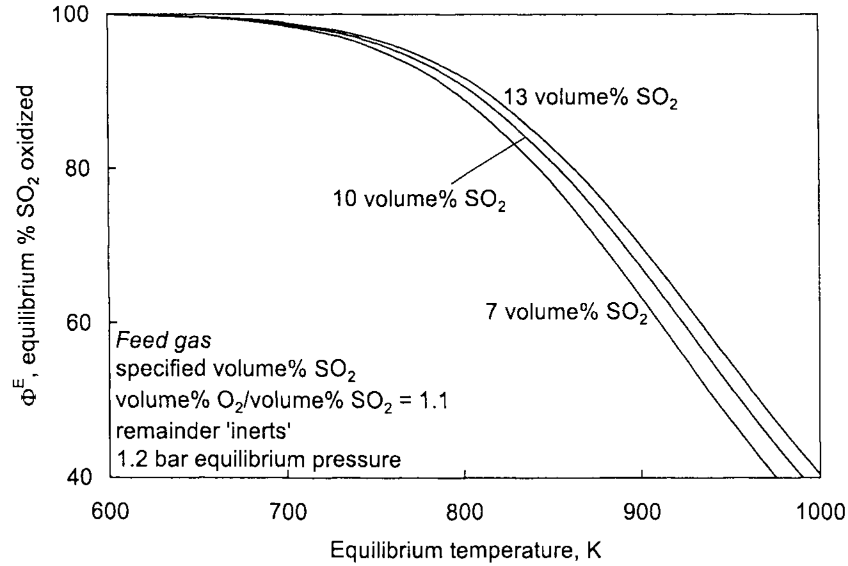

Fig. 10.5. Effect of feed gas SO_2 concentration on equilibrium *% SO_2 oxidized*. High SO_2 concentration gives high *% SO_2 oxidized*.

10.6 Discussion

The curves in Figs. 10.2 to 10.5 combine:

(a) equilibrium thermodynamics

(b) catalyst bed feed gas compositions

(c) S and O balances.

They are not exactly equilibrium curves because their position and shape depend on feed gas composition and equilibrium pressure. Their value is that they show the maximum extent to which SO_2 can be oxidized in a catalyst bed. They provide a visual picture of how catalytic SO_2 oxidation can be optimized.

This value becomes apparent when the equilibrium curves of this chapter are combined with the approach-to-equilibrium heatup paths of Chapters 11 and 12.

10.7 Summary

Catalytic $SO_2(g) + \frac{1}{2}O_2(g) \rightarrow SO_3(g)$ oxidation is a key step in sulfuric acid manufacture. It makes SO_3 for subsequent H_2SO_4 production, Reaction (1.2). Efficient SO_2 oxidation contributes to efficient acid production and small emission of SO_2.

Maximum SO_3 production is attained when SO_2 oxidation comes to equilibrium. Near-attainment of equilibrium is favored by sufficient gas residence time in highly reactive catalyst.

Maximum equilibrium SO_3 production is favored by a cool equilibrium temperature (but warm enough for rapid catalytic oxidation). Temperature exerts a much greater influence on this maximum than pressure or catalyst bed feed gas composition.

Reference

Gaskell, D.R. (1981) *Introduction to Metallurgical Thermodynamics*. McGraw-Hill Book Company, New York, NY, 212 222 and 237 259; K_E independent of pressure 239.
www.mcgraw-hill.com

Problems

10.1 Feed gas containing:

10 volume% SO_2

11 volume% O_2

79 volume% N_2

is fed into the Fig. 10.1 catalyst bed. Its SO_2 reacts with its O_2 to produce SO_3. The SO_2, O_2 and SO_3 come to equilibrium at 1.2 bar total pressure as they leave the catalyst bed.

Chemical analysis of the catalyst bed's exit gas shows that 80% of the feed gas's SO_2 has been oxidized to SO_3.

At what temperature (K) has the feed gas come to equilibrium? Use Eqn. (10.13).

10.2 Re-do Problem 10.1 by means of an Excel calculation. Use Appendix D. Eqn. (10.13) is used for many calculations in this book. Once it is successfully entered into Excel, it is easily copied into future spreadsheets.

10.3 Problem 10.1's feed gas is fed to the Fig. 10.1 catalyst bed at a slightly cooler temperature. It comes to equilibrium at 840 K.

What percentage of the Problem 10.1 feed SO_2 will have been oxidized when equilibrium has been attained at 840 K?

Use the Goal Seek method described in Appendix D, Section D.1. If you wish, check your answer manually by putting your calculated *% SO_2 oxidized* in Eqn (10.13) to back-calculate equilibrium temperature.

10.4 Prepare a table of:

equilibrium *% SO_2 oxidized* vs. equilibrium temperature

points for 12 volume% SO_2, 13.2 volume% O_2, 74.8 volume% N_2 catalyst bed feed gas (1.2 bar equilibrium pressure).

Use the techniques in Appendix D.

Use Excel's Chart Wizard function to plot these points, as in Fig. 10.2.

CHAPTER 11

SO_2 Oxidation Heatup Paths

Chapter 10 describes equilibrium:

$$SO_2(g) + \frac{1}{2}O_2(g) \rightarrow SO_3(g) \qquad (1.1)$$

oxidation in a catalyst bed. It shows that maximum SO_2 oxidation is achieved by:

(a) rapid SO_2 oxidation in active V, alkali metal, S, O, SiO_2 catalyst

(b) a cool equilibrium temperature.

It does not, however, show where a feed gas's equilibrium point lies on its equilibrium curve. That is the task of this chapter and Chapter 12.

11.1 Heatup Paths

This chapter discusses catalytic SO_2 oxidation in terms of heatup paths.

Fig. 11.1 presents one such path. It shows the following.

(a) 10 volume% SO_2, 11 volume% O_2, 79 volume% N_2 is fed to a catalyst bed at 690 K. Zero % of its SO_2 is oxidized at this point.

(b) This gas passes down through the catalyst bed where its $SO_2(g)$ is oxidized by its $O_2(g)$ to give $SO_3(g)$ + heat, Reaction (1.1). The heat from the SO_2 oxidation heats the gas above its 690 K input temperature.

(c) This SO_2 oxidation/temperature rise behavior is described by a heatup path, which is a plot of gas temperature vs % of feed SO_2 oxidized.

(d) Eventually, in a deep catalyst bed, the heatup path will meet Chapter 10's equilibrium curve, at which point no more SO_2 oxidation can take place, Chapter 12.

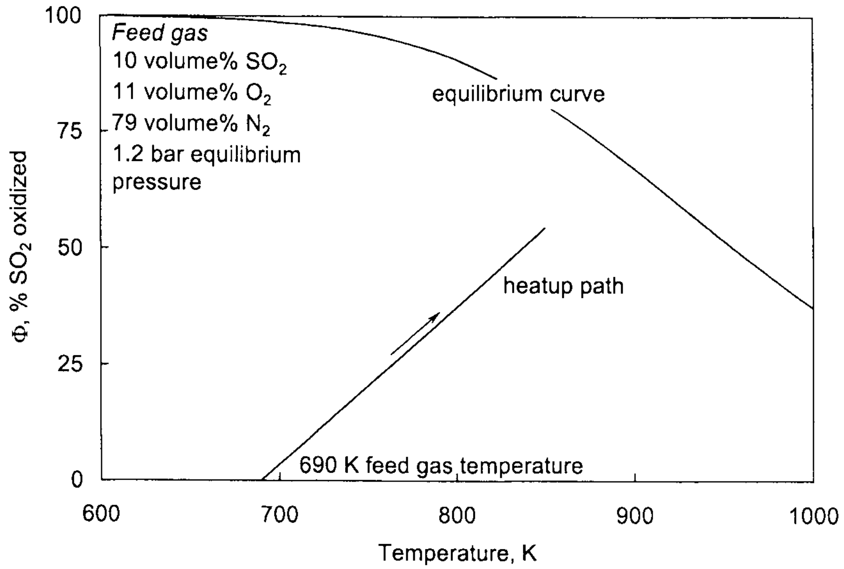

Fig. 11.1. Heatup path for SO_2, O_2, N_2 gas descending a catalyst bed. The SO_2 and O_2 in feed gas react to form SO_3, Eqn. (1.1). The gas is heated by the exothermic heat of reaction. The result is a path with increasing *% SO_2 oxidized* and increasing gas temperature. Notice how the feed gas's heatup path approaches its Chapter 10 equilibrium curve.

11.2 Objectives

The objectives of the chapter are to:

(a) show how *% SO_2 oxidized*/gas temperature heatup paths are prepared

(b) describe the factors affecting heatup path positions and slopes

(c) indicate how heatup paths predict maximum (equilibrium) SO_2 oxidation.

11.3 Preparing a Heatup Path – the First Point

A point on Fig. 11.1's heatup path is determined by:

(a) specifying feed gas composition and temperature, Fig. 11.2

(b) specifying a measured gas temperature part way down the catalyst bed (after some feed SO_2 has been oxidized and some heating has occurred), Fig. 11.2

(c) calculating the extent of SO_2 oxidation which corresponds to this measured temperature.

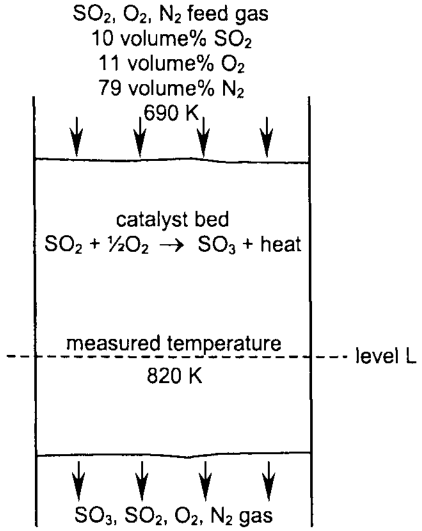

Fig. 11.2. Sketch of catalyst bed showing compositions and temperatures for Section 11.5 example problem.

11.4 Assumptions

Our heatup path calculations assume that there is no transfer of heat between gas and reactor walls or between gas and catalyst. The result is, therefore, an *adiabatic* heatup path.

Specification that there is no heat transfer between gas and reactor walls assumes that the reactor is perfectly insulated.

Specification that there is no transfer of heat between gas and catalyst assumes that the process is proceeding at steady state, i.e. that compositions and temperatures at every position in the catalyst bed are constant with time.

11.5 A Specific Example

The following example problem shows how a heatup path point is determined. The problem is:

> "10 volume% SO_2, 11 volume% O_2, 79 volume% N_2 gas (690 K) is being fed to the Fig. 11.2 catalyst bed.
>
> A thermocouple at level L in the catalyst bed indicates that the gas temperature there is 820 K.
>
> What percent oxidation of Fig. 11.2's feed SO_2 gives 820 K gas in the catalyst bed?"

The following six sections show how this problem is solved.

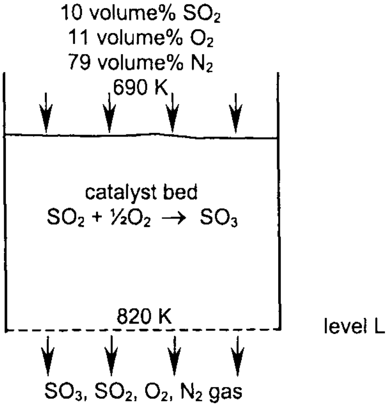

Fig. 11.3. Vertical segment of Fig. 11.2 catalyst bed over which the Section 11.8 and 11.9 mass and enthalpy balances are applied. Compositions and temperatures are assumed to be uniform horizontally at all levels.

11.6 Calculation Strategy

Fig. 11.3 shows the catalyst bed segment from top to level L. Our strategy for solving the Section 11.5 problem is to specify that 1 kg-mole of gas is fed into the top of this segment – and to calculate:

(a) the quantities of SO_2, O_2 and N_2 in this kg-mole of feed gas

(b) the quantities of SO_3, SO_2 and O_2 which correspond to level L's measured 820 K gas temperature

(c) *% SO_2 oxidized* at 820 K, where:

$$\%SO_2\ oxidized = \Phi = \frac{\begin{matrix}\text{kg-mole } SO_2 \\ \text{in feed gas}\end{matrix} - \begin{matrix}\text{kg-mole } SO_2 \text{in oxidized} \\ \text{gas at level L}\end{matrix}}{\text{kg-mole } SO_2 \text{ in feed gas}} * 100 \qquad (10.1).$$

Sulfur, oxygen, nitrogen and enthalpy balances are used. A matrix calculation is employed.

11.7 Input SO_2, O_2 and N_2 Quantities

The calculations of this chapter are all based on feeding 1 kg-mole of dry gas into the acid plant's first catalyst bed. The kg-mole of each component (e.g. SO_2) in this feed gas are calculated by equations like:

$$\text{kg-mole SO}_2\ \textbf{in} = \frac{\text{mole\% SO}_2 \text{ in feed gas}}{100} * 1 \text{ kg-mole of feed gas}$$

or, because mole% = volume% (Appendix E)

$$\text{kg-mole SO}_2\ \textbf{in} = \frac{\text{volume\% SO}_2 \text{ in feed gas}}{100} * 1 \text{ kg-mole of feed gas.}$$

Equations describing input kg-moles for the Section 11.5 problem (10 volume% SO_2, 11 volume% O_2, 79 volume% N_2 feed gas) are, therefore:

$$\text{kg-mole SO}_2\ \textbf{in} = \frac{\text{10 volume\% SO}_2 \text{ in feed gas}}{100} * 1 \text{ kg-mole of feed gas} = 0.10 \qquad (11.1)$$

$$\text{kg-mole O}_2\ \textbf{in} = \frac{\text{11 volume\% O}_2 \text{ in feed gas}}{100} * 1 \text{ kg-mole of feed gas} = 0.11 \qquad (11.2)$$

$$\text{kg-mole N}_2\ \textbf{in} = \frac{\text{79 volume\% N}_2 \text{ in feed gas}}{100} * 1 \text{ kg-mole of feed gas} = 0.79 \qquad (11.3).$$

11.8 Sulfur, Oxygen and Nitrogen Molar Balances

The next step in calculating a heatup path point is to develop steady state molar S, O and N balances for Fig. 11.3's feed and level L gases.

11.8.1 Sulfur balance

The steady state sulfur molar balance for Fig. 11.3 is:

$$\text{kg-mole S } \textbf{in} = \text{kg-mole S } \textbf{out}.$$

Each mole of SO_2 and SO_3 contains 1 mole of S, so this expands to:

$$1*\text{kg-mole SO}_2\ \textbf{in} = 1*\text{kg-mole SO}_3\ \textbf{out} + 1*\text{kg-mole SO}_2\ \textbf{out}$$

or subtracting '1*kg-mole SO_2 **in**' from both sides:

$$0 = -1*\text{kg-mole } SO_2 \textbf{ in} + 1*\text{kg-mole } SO_3 \textbf{ out} + 1*\text{kg-mole } SO_2 \textbf{ out} \qquad (11.4)$$

where **in** means into the top of the Fig. 11.3 segment and **out** means out of the segment at level L.

11.8.2 Oxygen molar balance

The steady state molar oxygen balance for the segment is:

$$\text{kg-mole O } \textbf{in} = \text{kg-mole O } \textbf{out}.$$

Each mole of SO_2 and O_2 contains 2 moles of O while each mole of SO_3 contains 3 moles of O, so this equation expands to:

$$\begin{aligned}2*\text{kg-mole } SO_2 \textbf{ in} + 2*\text{kg-mole } O_2 \textbf{ in} = {} & 3*\text{kg-mole } SO_3 \textbf{ out} + 2*\text{kg-mole } SO_2 \textbf{ out} \\ & + 2*\text{kg-mole } O_2 \textbf{ out}\end{aligned}$$

or, subtracting '2*kg-mole SO_2 **in** + 2*kg-mole O_2 **in**' from both sides:

$$\begin{aligned}0 = {} & -2*\text{kg-mole } SO_2 \textbf{ in} - 2*\text{kg-mole } O_2 \textbf{ in} \\ & + 3*\text{kg-mole } SO_3 \textbf{ out} + 2*\text{kg-mole } SO_2 \textbf{ out} + 2*\text{kg-mole } O_2 \textbf{ out} \qquad (11.5).\end{aligned}$$

11.8.3 Nitrogen molar balance

The segment's steady state molar nitrogen balance is:

$$\text{kg-mole N } \textbf{in} = \text{kg-mole N } \textbf{out}.$$

Each mole of N_2 contains 2 moles of N, so this balance becomes:

$$2*\text{kg-mole } N_2 \textbf{ in} = 2*\text{kg-mole } N_2 \textbf{ out}$$

or, subtracting '2*kg-mole N_2 **in**' from both sides:

$$0 = -2*\text{kg-mole } N_2 \textbf{ in} + 2*\text{kg-mole } N_2 \textbf{ out} \qquad (11.6).$$

11.9 Enthalpy balance

The steady state enthalpy balance for the Fig. 11.3 catalyst bed segment is:

$$\text{enthalpy } \mathbf{in} = \text{enthalpy } \mathbf{out} + \begin{array}{l}\text{conductive, convective}\\ \text{plus radiative heat}\\ \text{loss from the gas}\end{array} \qquad (11.6A).$$

*Enthalpy **in*** for the segment is:

$$\begin{array}{c}\text{kg-mole } SO_2 \ \mathbf{in} * H^{\circ}_{\underset{SO_2}{690}}\\ +\\ \text{kg-mole } O_2 \ \mathbf{in} * H^{\circ}_{\underset{O_2}{690}}\\ +\\ \text{kg-mole } N_2 \ \mathbf{in} * H^{\circ}_{\underset{N_2}{690}}\end{array}$$

where $H^{\circ}_{\underset{SO_2}{690}}$ is the enthalpy of SO_2 (MJ/kg-mole) at the segment's 690 K feed gas temperature (likewise for O_2 and N_2).

Likewise, *enthalpy **out*** for the segment is:

$$\begin{array}{c}\text{kg-mole } SO_3 \ \mathbf{out} * H^{\circ}_{\underset{SO_3}{820}}\\ +\\ \text{kg-mole } SO_2 \ \mathbf{out} * H^{\circ}_{\underset{SO_2}{820}}\\ +\\ \text{kg-mole } O_2 \ \mathbf{out} * H^{\circ}_{\underset{O_2}{820}}\\ +\\ \text{kg-mole } N_2 \ \mathbf{out} * H^{\circ}_{\underset{N_2}{820}}\end{array}$$

where 820 K is the measured gas temperature at level L.

The final term in Eqn. (11.6A) is conductive, convective plus radiative heat loss from the gas. As discussed in section 11.3, it is assumed here to be zero, i.e.:

$$\begin{matrix}\text{conductive, convective}\\ \text{plus radiative heat}\\ \text{loss from gas}\end{matrix} = 0.$$

This assumption is discussed further in Section 18.12.

With these three enthalpy components, the segment's enthalpy balance:

$$\text{enthalpy } \textbf{in} = \text{enthalpy } \textbf{out} + \begin{matrix}\text{conductive, convective}\\ \text{plus radiative heat}\\ \text{loss from the gas}\end{matrix}$$

becomes:

$$\left\{\begin{matrix}\text{kg-mole } SO_2 \textbf{ in} * H^{\circ}_{690\ SO_2}\\ +\\ \text{kg-mole } O_2 \textbf{ in} * H^{\circ}_{690\ O_2}\\ +\\ \text{kg-mole } N_2 \textbf{ in} * H^{\circ}_{690\ N_2}\end{matrix}\right\} = \left\{\begin{matrix}\text{kg-mole } SO_3 \textbf{ out} * H^{\circ}_{820\ SO_3}\\ +\\ \text{kg-mole } SO_2 \textbf{ out} * H^{\circ}_{820\ SO_2}\\ +\\ \text{kg-mole } O_2 \textbf{ out} * H^{\circ}_{820\ O_2}\\ +\\ \text{kg-mole } N_2 \textbf{ out} * H^{\circ}_{820\ N_2}\end{matrix}\right\} + 0$$

(11.6B).

11.9.1 Numerical enthalpy values

690 and 820 K SO_2, O_2, N_2 and SO_3 enthalpies are shown in Table 11.1.

Table 11.1. SO_2, O_2, N_2 and SO_3 enthalpy values (MJ/kg-mole) at 690 and 820 K. They have been calculated with the enthalpy equations in Appendix G.

Compound and temperature	Enthalpy numerical value, MJ per kg-mole
$\underset{SO_2}{H^{o}_{690}}$	-278.7
$\underset{O_2}{H^{o}_{690}}$	12.21
$\underset{N_2}{H^{o}_{690}}$	11.66
$\underset{SO_3}{H^{o}_{820}}$	-362.0
$\underset{SO_2}{H^{o}_{820}}$	-272.0
$\underset{O_2}{H^{o}_{820}}$	16.54
$\underset{N_2}{H^{o}_{820}}$	15.71

With the Table 11.1 enthalpies, the Fig. 11.3 segment enthalpy balance becomes:

$$\left\{\begin{matrix} \text{kg-mole } SO_2 \textbf{ in} * -278.7 \\ + \\ \text{kg-mole } O_2 \textbf{ in} * \quad 12.21 \\ + \\ \text{kg-mole } N_2 \textbf{ in} * \quad 11.66 \end{matrix}\right\} = \left\{\begin{matrix} \text{kg-mole } SO_3 \textbf{ out} * -362.0 \\ + \\ \text{kg-mole } SO_2 \textbf{ out} * -272.0 \\ + \\ \text{kg-mole } O_2 \textbf{ out} * \quad 16.54 \\ + \\ \text{kg-mole } N_2 \textbf{ out} * \quad 15.71 \end{matrix}\right\}$$

or:

$$\begin{aligned} 0 = & - \text{kg-mole } SO_2 \textbf{ in} * -278.7 \\ & - \text{kg-mole } O_2 \textbf{ in} * \quad 12.21 \\ & - \text{kg-mole } N_2 \textbf{ in} * \quad 11.66 \\ & + \text{kg-mole } SO_3 \textbf{ out} * -362.0 \\ & + \text{kg-mole } SO_2 \textbf{ out} * -272.0 \\ & + \text{kg-mole } O_2 \textbf{ out} * \quad 16.54 \\ & + \text{kg-mole } N_2 \textbf{ out} * \quad 15.71 \end{aligned} \qquad (11.7).$$

11.10 Calculating Level L Quantities

The Section 11.5 problem has 7 variables:

kg-mole SO_2 **in**

kg-mole O_2 **in**

kg-mole N_2 **in**

kg-mole SO_3 **out**

kg-mole SO_2 **out**

kg-mole O_2 **out**

kg-mole N_2 **out**.

Sections 11.7-11.9 provide 7 linear equations (11.1-11.7), which must be satisfied by the values of these 7 variables. Each variable has, therefore, a unique value and the question:

> 'What percentage of Fig. 11.3's feed SO_2 has been oxidized to SO_3 when the gas has reached 820 K?'

has a unique solution, next section.

11.11 Matrix Calculation

The above question is answered by:

(a) entering Eqns. (11.1) to (11.7) in matrix form into an Excel worksheet, Table 11.2

(b) solving for the seven variables

(c) calculating *% SO_2 oxidized* in Table 11.2's cell H17.

Matrix calculation instructions are given in Appendix H.

Table 11.2. Excel worksheet and matrix for determining Fig. 11.3's 820 K (level L) gas quantities. '**In**' refers to feed, '**out**' refers to level L. The results are the only quantities that satisfy all the equations in the matrix. Cell H17 contains the equation above and beside it. The matrix has been solved as described in Appendix H. After an initial solving, a change in any matrix cell value causes automatic calculation of a new matrix result.

	A	B	C	D	E	F	G	H	I	J
1	Equation	Description	numerical term	kg-mole SO_2 **in**	kg-mole O_2 **in**	kg-mole N_2 **in**	kg-mole SO_3 **out**	kg-mole SO_2 **out**	kg-mole O_2 **out**	kg-mole N_2 **out**
2	11.1	feed SO_2 kg-mole	0.10	1	0	0	0	0	0	0
3	11.2	feed O_2 kg-mole	0.11	0	1	0	0	0	0	0
4	11.3	feed N_2 kg-mole	0.79	0	0	1	0	0	0	0
5	11.4	S balance	0	-1	0	0	1	1	0	0
6	11.5	O balance	0	-2	-2	0	3	2	2	0
7	11.6	N balance	0	0	0	-2	0	0	0	2
8	11.7	enthalpy balance	0	278.7	-12.21	-11.66	-362.0	-272.0	16.54	15.71
9										
10					690 K, feed#			820 K, level L		
11										
12	Matrix results per kg-mole of feed gas									
13	kg-mole SO_2 **in**	0.1000								
14	kg-mole O_2 **in**	0.1100								
15	kg-mole N_2 **in**	0.7900								
16	kg-mole SO_3 **out**	0.0442			% SO_2 oxidized at level L =	((kg-mole SO_2 **in** - kg-mole SO_2 **out**)/kg-mole SO_2 **in**)*100				(Eqn. 10.1)
17	kg-mole SO_2 **out**	0.0558			=	(B13-B17)/B13*100	=	44.2		
18	kg-mole O_2 **out**	0.0879								
19	kg-mole N_2 **out**	0.7900								

#Notice that cells D8, E8 and F8 contain $-H^{\circ}_{690\,SO_2}$, $-H^{\circ}_{690\,O_2}$ and $-H^{\circ}_{690\,N_2}$ (Section 11.9.1).

Table 11.2 gives the result. It indicates that an 820 K gas temperature is uniquely produced by 44.2% oxidation of Fig. 11.3's feed SO_2.

11.12 Preparing a Heatup Path

The heatup path for the Section 11.5 feed gas is prepared by re-doing the above calculation for many different levels and temperatures in the catalyst bed, Fig. 11.4. Only cells G8 to J8 in Table 11.2 are changed.

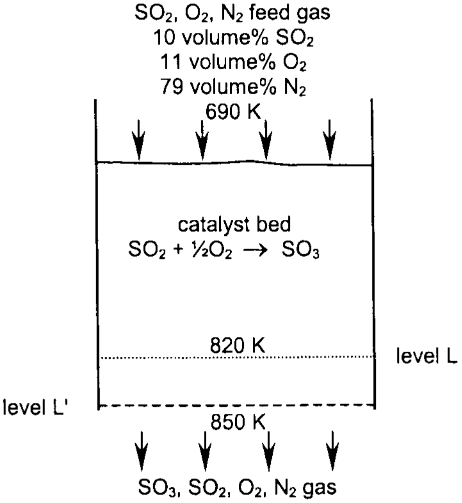

Fig. 11.4. Segment of catalyst bed showing level L' for calculating *% SO_2 oxidized* equivalent to 850 K.

The 850 K gas temperature at level L' is, for example, represented by the enthalpy terms:

Cell	Contents	Numerical value, MJ/kg-mole#
G8	$H^{\circ}_{850\,SO_3}$	-359.9
H8	$H^{\circ}_{850\,SO_2}$	-270.4
I8	$H^{\circ}_{850\,O_2}$	17.54
J8	$H^{\circ}_{850\,N_2}$	16.64

#Calculated with Appendix G's enthalpy equations.

Inserted into Matrix Table 11.2, these values automatically give the result that 850 K gas is produced by 54.4% SO_2 oxidation.

11.12.1 Enthalpy equations in cells

An efficient method of calculating heatup path points is to put enthalpy equations directly into cells D8 - J8 of Table 11.2. This is detailed in Appendix I.

11.12.2 The heatup path

Table 11.3 summarizes *% SO_2 oxidized* vs gas temperature as calculated by the above described method. The points are equivalent to the heatup path in Fig. 11.1. As expected, high gas temperatures are equivalent to extensive $SO_2+½O_2 \rightarrow SO_3$ oxidation and vice versa.

Table 11.3. Heatup path points for 10 volume% SO_2, 11 volume% O_2, 79 volume% N_2, 690 K feed gas. The values are represented graphically in Fig. 11.1.

Temperature, K	Equivalent *% SO_2 oxidized*
690	0
710	6.8
730	13.5
750	20.3
770	27.1
790	33.9
810	40.8
830	47.6
850	54.4

The next two sections describe the effects of:

(a) feed gas composition

and:

(b) feed gas temperature

on heatup paths. The importance of heatup path position and slope is then discussed.

11.13 Feed Gas SO_2 Strength Effect

The effect of feed gas SO_2 strength on heatup path is determined by inserting different values of:

volume% SO_2

volume% O_2

volume% N_2

into Equations (11.1), (11.2) and (11.3). With 13 volume% SO_2, 14.3 volume% O_2 and 72.7 volume% N_2 (for example), the equations become:

$$\text{kg-mole } SO_2 \textbf{ in} = \frac{\begin{array}{l}\text{13 volume\% } SO_2\\ \text{in feed gas}\end{array}}{100} * \text{1 kg-mole of feed gas} = 0.13 \tag{11.1'}$$

$$\text{kg-mole } O_2 \textbf{ in} = \frac{\begin{array}{l}\text{14.3 volume\% } O_2\\ \text{in feed gas}\end{array}}{100} * \text{1 kg-mole of feed gas} = 0.143 \tag{11.2'}$$

$$\text{kg-mole } N_2 \textbf{ in} = \frac{\begin{array}{l}\text{72.7 volume\% } N_2\\ \text{in feed gas}\end{array}}{100} * \text{1 kg-mole of feed gas} = 0.727 \tag{11.3'}$$

These new equations are put into matrix Table 11.2 by placing new values into cells C2 to C4. The new values are:

cell C2	0.13
cell C3	0.143
cell C4	0.727.

With an 820 K measured level L temperature, these values automatically give:

34.7% SO_2 oxidized.

11.13.1 SO_2 strength summary

Fig. 11.5 summarizes the effects of SO_2 feed gas strength on heatup paths. It shows that each *% SO_2 oxidized* gives a larger temperature increase with:

13 volume% SO_2 in feed gas

than with:

7 volume% SO_2 in feed gas.

This is mainly because, per *% SO_2 oxidized*:

more SO_2 is oxidized per kg-mole of strong SO_2
feed gas than per kg-mole of weak SO_2 feed gas,

giving more heat evolution and larger temperature increase.

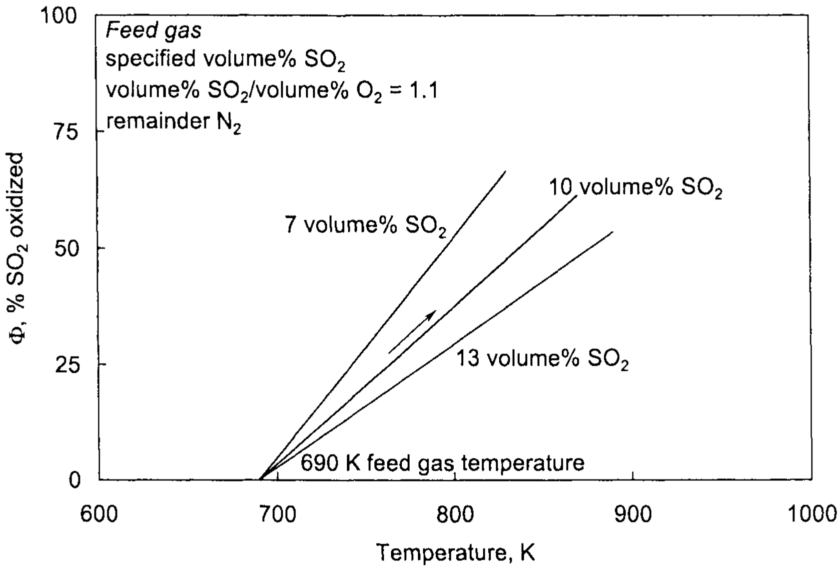

Fig. 11.5. Heatup paths for 7, 10 and 13 volume% SO_2 (volume% O_2/volume% SO_2 = 1.1) feed gas. Per *% SO_2 oxidized*, strong SO_2 gas heats up more than weak SO_2 gas.

11.14 Feed Gas Temperature Effect

The effect of feed gas temperature on heatup path is determined by inserting new enthalpy values into Eqn. (11.7). With 660 K feed gas (for example), enthalpy Eqn. (11.7) becomes:

$$
\begin{aligned}
0 = &\left.\begin{array}{lcr} -\ \text{kg-mole SO}_2\ \textbf{in} & * & -280.2\\ -\ \text{kg-mole O}_2\ \textbf{in} & * & 11.21\\ -\ \text{kg-mole N}_2\ \textbf{in} & * & 10.73\end{array}\right\}660\ \text{K}\\
&\left.\begin{array}{lcr} +\ \text{kg-mole SO}_3\ \textbf{out} & * & -362.0\\ +\ \text{kg-mole SO}_2\ \textbf{out} & * & -272.0\\ +\ \text{kg-mole O}_2\ \textbf{out} & * & 16.54\\ +\ \text{kg-mole N}_2\ \textbf{out} & * & 15.71\end{array}\right\}820\ \text{K}
\end{aligned}
\qquad (11.7')
$$

where:

$$-280.2 = H^{o}_{\substack{660\\ SO_2}}$$

$$11.21 = H^{o}_{\substack{660\\ O_2}}$$

$$10.73 = H^{o}_{\substack{660\\ N_2}}$$

MJ per kg-mole of compound.

These new enthalpy **in** values are put into cells D8, E8 and F8 of matrix Table 11.2 as:

D8	-(-280.2)
E8	-11.21
F8	-10.73

(because of the negative signs on the first three rows of Eqn. 11.7').

A new heatup path is then calculated as described in Section 11.11. The result is a path nearly parallel to the 690 K path ~30 K cooler at all *% SO_2 oxidized* values, Fig. 11.6.

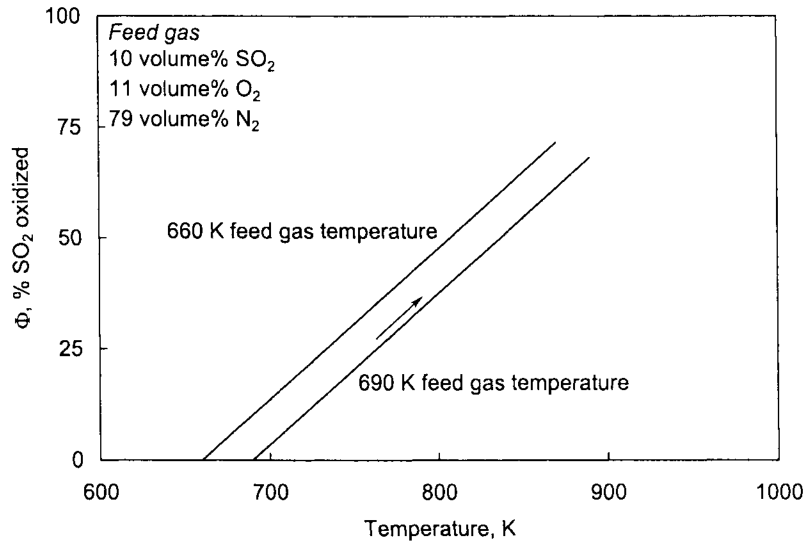

Fig. 11.6. 660 K and 690 K feed gas heatup paths with 10 volume% SO_2, 11 volume% O_2, 79 volume% N_2 feed gas. The two paths are ~30 K apart throughout their length. They are not exactly straight because: $d H^{\circ}_{SO_3}/dT > (d H^{\circ}_{SO_2}/dT + ½ d H^{\circ}_{O_2})/dT$, Appendix G.

11.15 Significance of Heatup Path Position and Slope

Fig. 11.7 superimposes the Fig. 10.2 *% SO_2 oxidized* equilibrium curve on Fig. 11.6. It shows that the:

660 K feed gas heatup path

will reach the equilibrium *% SO_2 oxidized* curve:

at a higher *% SO_2 oxidized* value

than the 690 K feed gas heatup path.

This predicts high SO_2 oxidation efficiency with low feed gas temperature. This prediction is discussed extensively in Chapter 12 onwards.

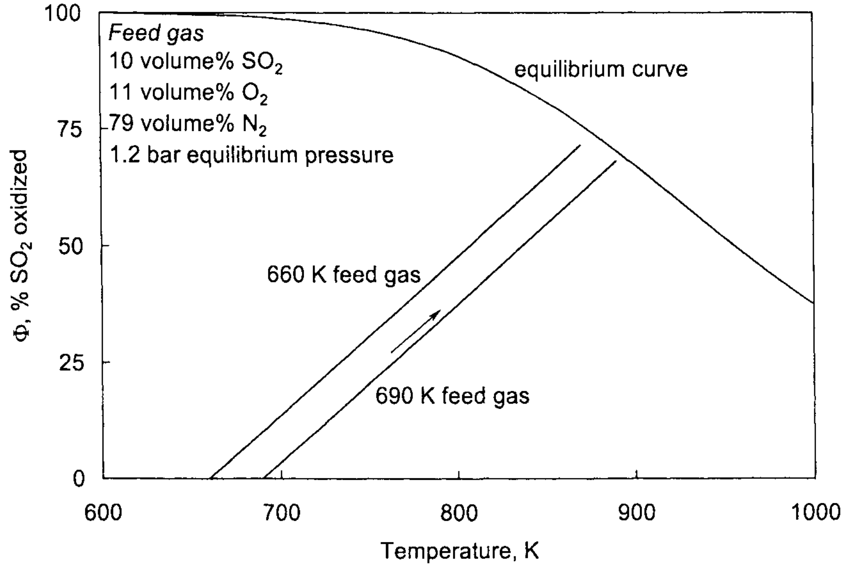

Fig. 11.7. Heatup paths and equilibrium curve for 10 volume% SO_2, 11 volume% O_2, 79 volume% N_2 feed gas. Notably, the 660 K heatup path will reach the equilibrium curve at a higher *% SO_2 oxidized* value than the 690 K heatup path. 660 K is about the lowest feed gas temperature that will keep V, alkali metal, S, O, SiO_2 catalyst active and SO_2 oxidation rapid, Table 8.1.

11.16 Summary

SO_2 oxidizes and gas temperature increases as SO_2, O_2, N_2 gas descends through active V, alkali metal, S, O, SiO_2 catalyst. This behavior is shown by the heatup paths of this chapter.

Chapters 12 onwards combine these heatup paths with Chapter 10's *% SO_2 oxidized* equilibrium curves to show how:

(a) $SO_2 + \frac{1}{2}O_2 \rightarrow SO_3$ oxidation may be maximized

(b) SO_2 emission to the environment may be minimized.

They indicate that cool feed gas (but warm enough for rapid catalytic oxidation) gives efficient SO_2 oxidation and small SO_2 emission.

Problems

11.1 12 volume% SO_2, 13.2 volume% O_2, 74.8 volume% N_2, 690 K gas is fed continuously to the top of a catalyst bed.

A thermocouple is inserted into the catalyst bed part way down the bed. It indicates that the temperature there is 820 K.

What percentage of the input SO_2 has been oxidized at the thermocouple's location?

Use matrix Table 11.2. Only cells C2, C3 and C4 need to be changed (as discussed in Section 11.13).

11.2 Repeat Problem 11.1 with an 850 K thermocouple reading further down the bed. Use your Problem 11.1 matrix with 850 K enthalpy values in cells G8 to J8.

11.3 Repeat Problem 11.2 with 675 K feed gas (and an 850 K thermocouple reading). Use your Problem 11.2 matrix with 675 K enthalpy values in cells D8 to F8.

Remember that these cells contain $-H^\circ$.

11.4 Prepare a heatup path for 12 volume% SO_2, 13.2 volume% O_2, 74.8 volume% N_2, 675 K feed gas – as described in Appendix I. Plot the path with Excel's Chart Wizard function.

CHAPTER 12

Maximum SO_2 Oxidation: Heatup Path-Equilibrium Curve Intercepts

Chapters 10 and 11 discuss oxidation of SO_2 when warm SO_2, O_2, N_2 feed gas descends a catalyst bed. They do so in terms of:

(a) *% SO_2 oxidized*-temperature equilibrium curves, Chapter 10

(b) *% SO_2 oxidized*-temperature heatup paths, Chapter 11.

Together, they indicate that maximum oxidation in a catalyst bed is obtained where a feed gas's:

heatup path

intercepts its:

equilibrium curve, Fig. 11.7.

This chapter:

(a) calculates heatup path-equilibrium curve intercept points

(b) shows how these points are affected by feed gas temperature, feed gas composition and equilibrium pressure

(c) discusses the influence of these points on industrial acid plant practice.

12.1 Initial Specifications

For an intercept calculation to be valid, its heatup path and equilibrium curve must be *for the same feed gas*. Each intercept calculation must, therefore, specify a feed gas composition, volume% SO_2, O_2, N_2 etc.

It must also specify:

(a) feed gas temperature, i.e. the temperature at which the heatup path starts

(b) catalyst bed pressure, i.e. the pressure at which SO_2 oxidation Reaction (1.1) comes to equilibrium.

A calculated intercept is valid only for these specified values.

12.2 *% SO_2 Oxidized*-Temperature Points Near an Intercept

Table 12.1 shows heatup path and equilibrium curve *% SO_2 oxidized*-temperature points near a heatup path-equilibrium curve intercept. They are for:

> 690 K, 10 volume% SO_2, 11 volume% O_2, 79 volume% N_2 feed gas
> and 1.2 bar equilibrium pressure.

Table 12.1 *% SO_2 oxidized*-temperature points near heatup path-equilibrium curve intercept. They have been calculated as described in Appendices I and D. They are plotted in Fig. 12.1. Φ and Φ^E are defined by Eqns. (10.1) and (10.2).

Temperature, K	Heatup path *% SO_2 oxidized*, Φ	Equilibrium *% SO_2 oxidized*, Φ^E
898	70.84	67.85
897	70.49	68.15
896	70.15	68.45
895	69.81	68.75
894	69.47	69.05
893	69.12	69.34
892	68.78	69.64
891	68.44	69.94
890	68.09	70.23

The table shows that at 893 K and below:

> heatup path *% SO_2 oxidized* is less than equilibrium curve *% SO_2 oxidized.*

This indicates that at 893 K and below, $SO_2 + \frac{1}{2}O_2 \rightarrow SO_3$ oxidation can proceed further up the heatup path towards equilibrium, Fig. 12.1.

At 894 K and above, however, heatup path *% SO_2 oxidized* is greater than equilibrium *% SO_2 oxidized.* This is, of course, impossible because equilibrium *% SO_2 oxidized* cannot be exceeded up a heatup path.

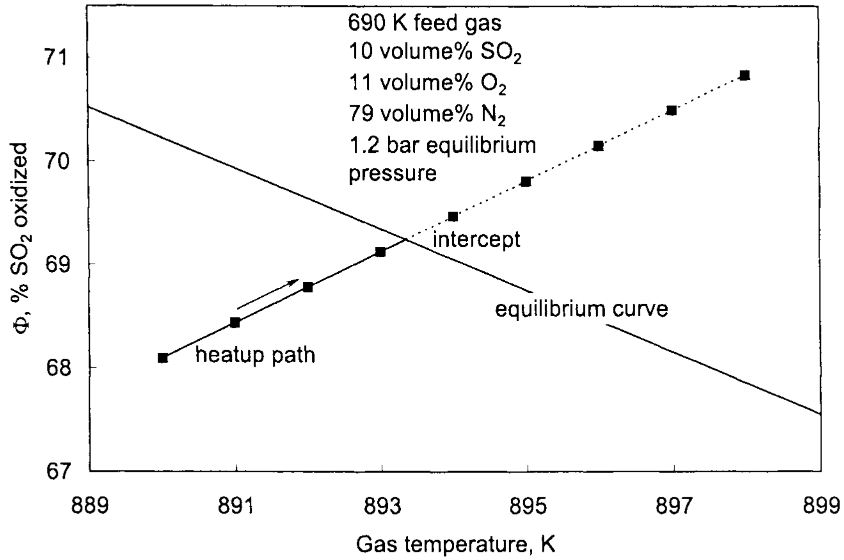

Fig. 12.1. Plot of Table 12.1 heatup path points and equilibrium curve, expanded from Fig. 11.7. Below the equilibrium curve, SO_2 is being oxidized, gas temperature is increasing and equilibrium is being approached up the heatup path. Maximum (equilibrium) oxidation is attained where the heatup path meets the equilibrium curve.

Maximum (equilibrium) *% SO_2 oxidized* occurs, therefore, between 893 K and 894 K. Interpolation shows that it occurs at:

893.3 K

69.2 *% SO_2 oxidized.*

This is confirmed by the Excel Goal Seek calculation in Appendix Table J.2.

The Table J.2 Goal Seek calculation also shows that the intercept gas contains:

0.0692 kg-mole SO_3
0.0308 kg-mole SO_2
0.0754 kg-mole O_2
0.7900 kg-mole N_2

per kg-mole of feed gas. These quantities are used in Chapter 14 and 15's 2nd catalyst bed heatup path and intercept calculations.

12.3 Discussion

The above calculations assume that:

(a) the acid plant's 1st catalyst bed is thick enough

and its:

(b) catalytic SO_2 oxidation is rapid enough

for equilibrium to be attained.

Industrial 1st catalyst beds are ½ to 1 m thick, Fig. 8.3. This thickness gives near equilibrium oxidation under the (i) warm and (ii) strong $SO_2 + O_2$ conditions in the 1st catalyst bed. More catalyst could be added but this isn't often necessary. Non-attainment of equilibrium is discussed further in Section 18.12.

12.4 Effect of Feed Gas Temperature on Intercept

Fig. 12.2 shows the effect of *feed gas temperature* on intercept temperature and *% SO_2 oxidized*. It indicates that cool feed gas gives:

(a) a low intercept temperature

(b) a high intercept (equilibrium) *% SO_2 oxidized*.

The high intercept *% SO_2 oxidized* gives efficient SO_3 and H_2SO_4 production. It also minimizes SO_2 emission.

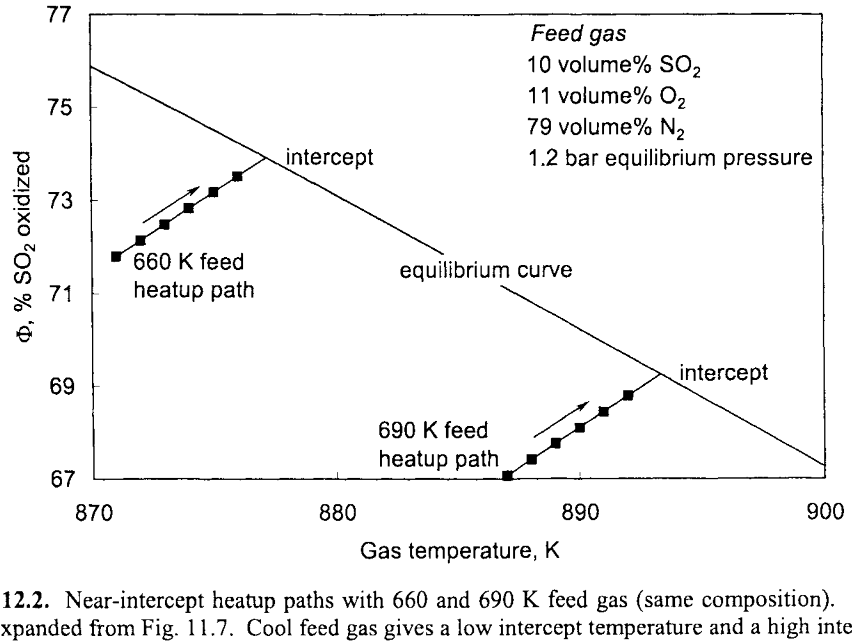

Fig. 12.2. Near-intercept heatup paths with 660 and 690 K feed gas (same composition). They are expanded from Fig. 11.7. Cool feed gas gives a low intercept temperature and a high intercept *% SO_2 oxidized*. 660 K is about the lowest temperature at which V, alkali metal, S, O, SiO_2 catalyst is fully active, Table 8.1.

12.5 Inadequate *% SO_2 Oxidized* in 1st Catalyst Bed

$SO_2 + ½O_2 \longrightarrow SO_3$ oxidation efficiency in a 1st catalyst bed is always below ~ 80%. This is totally inadequate for efficient, low SO_2 emission H_2SO_4 production.

This limitation is overcome industrially by passing 1st catalyst bed exit gas through two or more **gas cooling/catalytic oxidation steps** – bringing SO_2 oxidation efficiency up to 98+ %.

Multi-catalyst bed processing is discussed in Chapter 13 onwards.

12.6 Effect of Feed Gas SO_2 Strength on Intercept

Fig. 12.3 shows the effect of feed gas SO_2 strength on intercept temperature and *% SO_2 oxidized*. Increased SO_2 strength is seen to:

(a) increase intercept temperature

(b) decrease intercept *% SO_2 oxidized*.

The industrial impact of these effects is discussed in Section 12.10.

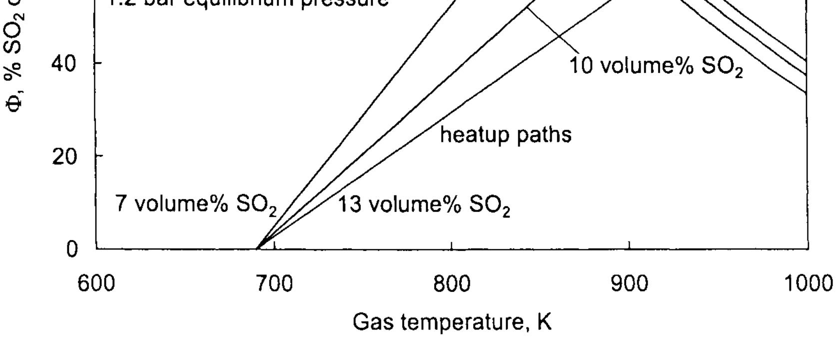

Fig. 12.3. Heatup paths, equilibrium curves and intercepts for 7, 10, and 13 volume% SO_2 feed gas. Volume% O_2/volume% SO_2 ratio = 1.1. Intercept temperature increases with increasing SO_2 strength. Intercept *% SO_2 oxidized* decreases with increasing SO_2 strength. The intercepts have been calculated as described in Appendix J.

12.7 Minor Influence – Equilibrium Gas Pressure

Industrial catalyst bed gas pressure varies slightly between acid plants depending on altitude. It also tends to increase slightly over time as catalyst beds become clogged with dust and catalyst fragments.

These pressure differences have no effect on heatup paths, Fig. 12.4 – and little effect on equilibrium curves and intercepts. Intercept temperature and *% SO_2 oxidized* both increase slightly with increasing pressure.

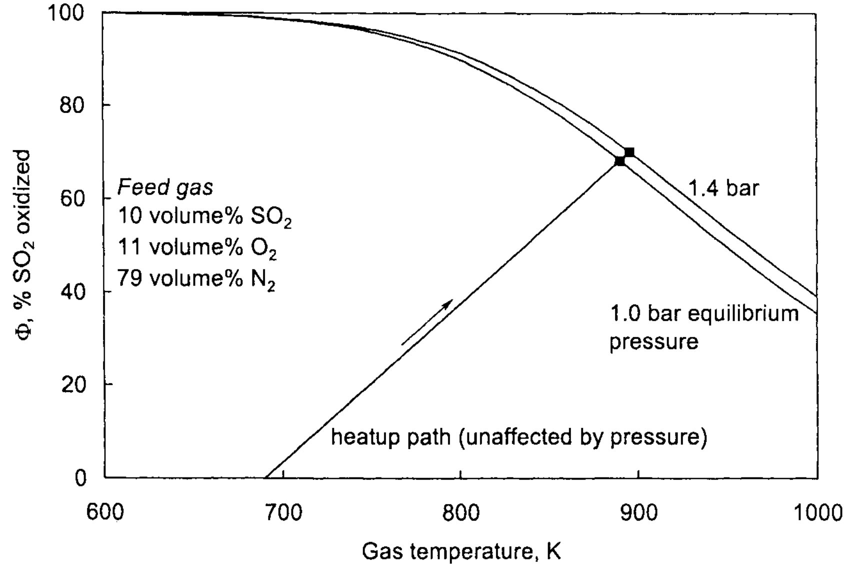

Fig. 12.4. Effect of pressure on equilibrium curves and heatup path-equilibrium curve intercepts. Equilibrium curves and intercepts are affected by pressure. Heatup paths are not. Intercept temperature and *% SO_2 oxidized* both increase slightly with increasing pressure. The intercepts have been calculated as described in Appendix J.

12.8 Minor Influence – O_2 Strength in Feed Gas

Industrial 1st catalyst bed feed gas typically contains O_2 and SO_2 in the ratio:

$$\text{volume\% } O_2/\text{volume\% } SO_2 \approx 1 \text{ to } 2, \text{ Table 7.2.}$$

This is 2 to 4 times the $SO_2 + \frac{1}{2}O_2 \longrightarrow SO_3$ stoichiometric $O_2/SO_2 = 0.5$ requirement. It gives rapid oxidation.

Fig. 12.5 shows that O_2 strength has a negligible effect on heatup paths and a small effect on equilibrium curves and intercepts. Intercept temperature and *% SO_2 oxidized* both increase slightly with increasing O_2 strength.

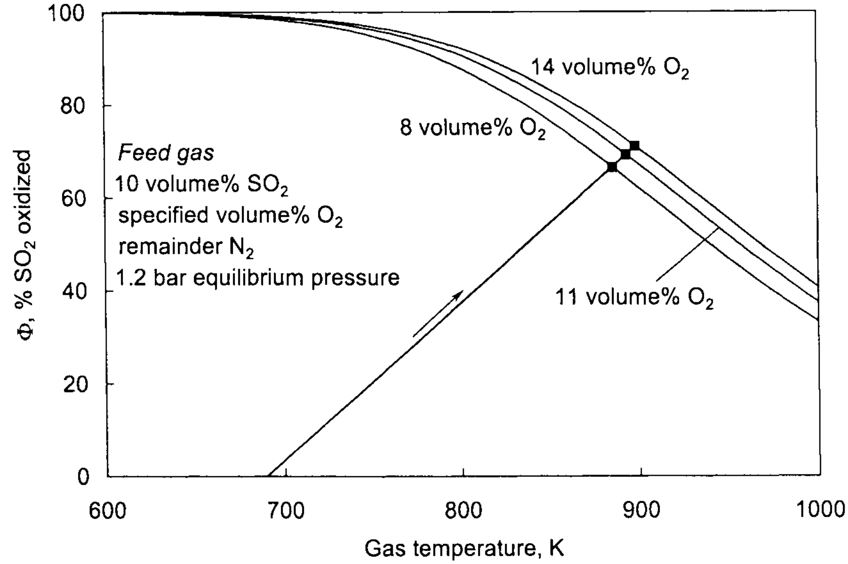

Fig. 12.5. Effect of feed gas O_2 strength on constant SO_2 strength heatup paths, equilibrium curves and intercepts. Intercept temperature and *% SO_2 oxidized* increase slightly with increasing O_2-in-feed-gas. Heatup path is barely affected by O_2 strength – 3 paths are superimposed on this graph. The effect is small because:

(a) O_2 and N_2 substitute for each other at constant SO_2 strength
(b) the heat capacities of O_2 and N_2 are almost the same, Appendix G.

12.9 Minor Influence – CO_2 in Feed Gas[#]

Metallurgical and spent acid regeneration gases contain CO_2 from fossil fuel and spent acid impurities. CO_2 concentrations in 1st catalyst bed feed gas are typically:

metallurgical	0 to 7 volume% CO_2
acid regeneration	6 to 10 volume% CO_2.

CO_2 has no effect on $SO_2 + \frac{1}{2}O_2 \longrightarrow SO_3$ equilibrium curves, Appendix F. It does, however, have a small effect on heatup paths and intercepts, Fig. 12.6.

Intercept temperature decreases slightly with increasing CO_2-in-feed-gas. Intercept *% SO_2 oxidized* increases slightly.

[#] Effects of SO_3 in feed gas are described in Chapter 17 and Appendices P and Q.

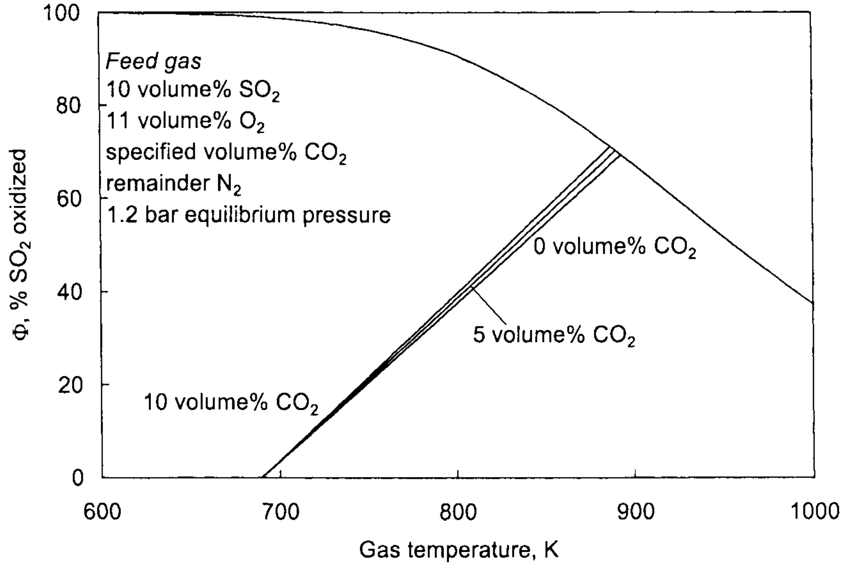

Fig. 12.6. Effect of CO_2 on intercept temperature and *% SO_2 oxidized.* Heatup path slope increases slightly with increasing CO_2 in gas – because CO_2 heat capacity is greater than N_2 heat capacity, Appendix G. This decreases intercept temperature and increases *% SO_2 oxidized.* CO_2 calculations are described in Chapter 17.

12.10 Catalyst Degradation, SO_2 Strength, Feed Gas Temperature

V, alkali metal, S, O, SiO_2 catalyst begins to degrade when continuously operated above ~900 K, Table 8.1. This can be a problem with high SO_2 strength feed gas.

Fig. 12.7 shows, for example, that the intercept temperature with:

12 volume% SO_2, 690 K feed gas

is 915 K, which may cause catalyst degradation.

Fig. 12.7 also shows, however, that this problem can be overcome by feeding the gas at 660 K. This explains industrial use of low gas input temperature cesium-enhanced catalyst in 1st catalyst beds, Table 8.1. This catalyst can be fed with ~660 K gas without falling below its de-activation temperature.

12.10.1 Two catalyst layers

A number of acid plants use two layers of catalyst in their 1st catalyst beds:

(a) V, Cs, K, Na, S, O, SiO_2 catalyst at the gas input surface for SO_2 oxidation with cool feed gas

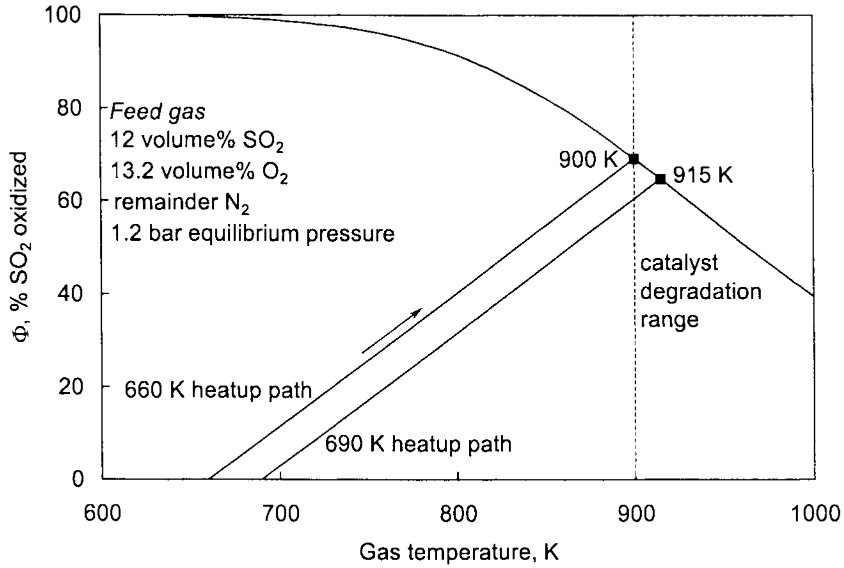

Fig. 12.7. Equilibrium curves, heatup paths and intercepts for 12 volume% SO_2 feed gas. 690 K feed gas gives a 915 K intercept temperature, in the catalyst degradation range. 660 K feed gas gives a 900 K intercept temperature, avoiding degradation.

(b) V, K, Na, S, O, SiO_2 catalyst at the gas exit surface to prevent high temperature catalyst degradation.

About 1/3 of the bed is Cs enhanced catalyst; 2/3 is K, Na catalyst.

12.11 Maximum Feed Gas SO_2 Strength

Fig. 12.8 shows that 13 volume% SO_2 gas gives an intercept temperature of ~910 K even when fed at 660 K. This may cause catalyst degradation.

Gases stronger than 13 volume% SO_2 will always give intercept temperatures in the catalyst degradation range. They must be diluted with air before they are catalytically oxidized.

Dilution is not a problem, but it requires more equipment and gas blowing power.

12.12 Exit Gas Composition ≡ Intercept Gas Composition

This chapter assumes that equilibrium is attained in an acid plant's 1st catalyst bed, i.e. that a feed gas's heatup path always intercepts its equilibrium curve.

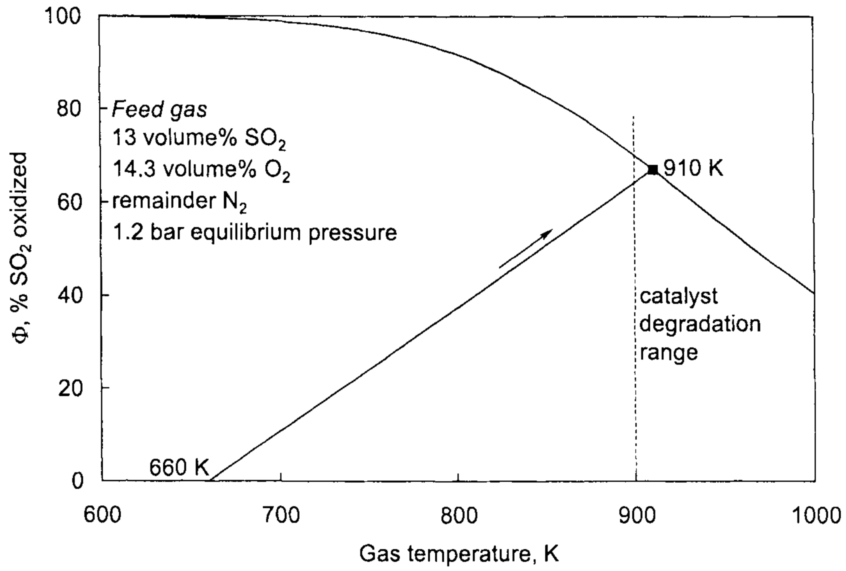

Fig. 12.8. Heatup path, equilibrium curve and intercept for 660 K, 13 volume% SO_2 feed gas. With 13 volume% SO_2 and higher, catalyst degradation is likely even with 660 K feed gas. 660 K is about the lowest temperature at which V, alkali metal, S, O, SiO_2 catalyst is fully active.

We now add the specification that there is no oxidation or reduction once equilibrium is attained, i.e. that:

catalyst bed exit gas composition

is the same as:

catalyst bed intercept gas composition, Fig. 12.9.

This exit gas composition ≡ intercept gas assumption is important because it links catalyst beds in multi-bed SO_2 oxidation calculations, Chapter 14 onwards.

12.13 Summary

Catalyst bed $SO_2 + ½O_2 \longrightarrow SO_3$ oxidation is represented by heatup paths and equilibrium curves. Maximum SO_2 oxidation occurs where a feed gas's heatup path intercepts its equilibrium curve.

High intercept *% SO_2 oxidized* values are equivalent to efficient SO_3 production. They give efficient H_2SO_4 production and low SO_2 emission. They are obtained by using cool feed gas – but warm enough (>660 K) for rapid catalytic oxidation.

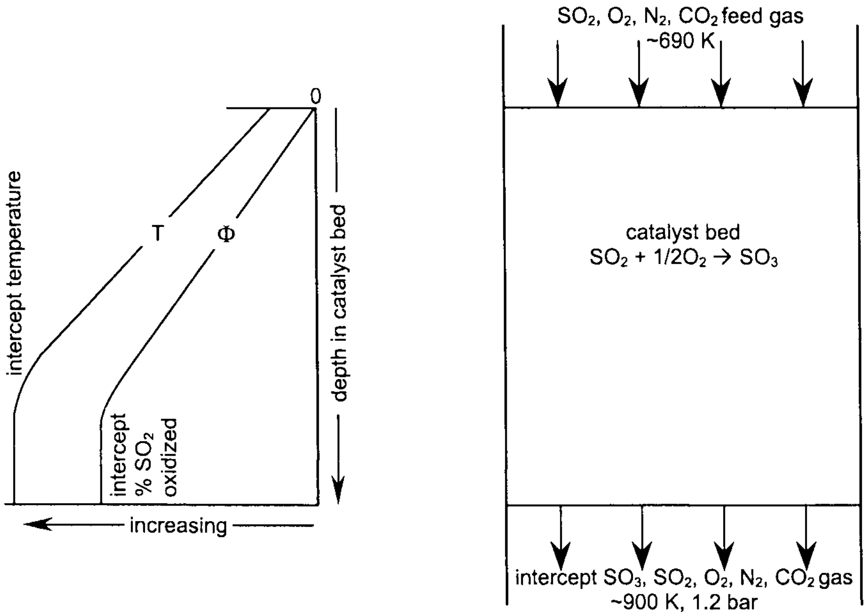

Fig. 12.9. Sketch of catalyst bed indicating that exit gas composition and temperature ≡ intercept gas composition and temperature. It assumes that there is no transfer of heat from gas to surroundings, Section 11.3. So once equilibrium is attained, temperature remains constant and the gas remains at its intercept composition. This is discussed further in Section 18.12.

Strong SO_2 feed gas gives high intercept temperatures. Above about 12 volume% SO_2, intercept temperatures begin to exceed V, alkali metal, S, O, SiO_2 catalyst's 900 K degradation temperature.

Gas stronger than ~13 volume% SO_2 must be diluted with air before catalytic oxidation. This is not a problem, but it increases cost.

Problems

12.1 In Problem 10.4, you prepared an equilibrium curve for 12 volume% SO_2, 13.2 volume% O_2, 74.8 volume% N_2 gas (1.2 bar equilibrium pressure).

In Problem 11.4 you prepared a heatup path for the same gas (fed into the catalyst bed at 675 K).

Now determine the *%SO$_2$ oxidized* - temperature point at which the Problem 11.4 heatup path intercepts the Problem 10.4 equilibrium curve.

Use the technique described in Table 12.1 as follows.

(a) You can see from Fig. 12.7 that the intercept temperature will be ~908 K. This suggests that you should calculate your equilibrium curve and heatup path points at ~904, 905............911 K.

(b) Use the technique you used in Problem 10.3 to calculate your equilibrium curve points. This gives integer temperatures and simplifies interpolation, Table 12.1.

(c) Use the technique you used in Problem 11.4 to calculate the heatup path points.

12.2 Plot your Problem 12.1 points as in Fig. 12.1. Use Excel's Chart Wizard.

12.3 Repeat Problem 12.1 using the technique described in Appendix J. Familiarity with this technique is essential for later multi-catalyst bed calculations.

Include in your answer:

(a) intercept temperature and *% SO_2 oxidized*

(b) kg-mole SO_3, SO_2, O_2 and N_2 in intercept gas, per kg-mole of 1st catalyst bed feed gas.

The problem in Chapter 13 requires the answer to (a).

The problems in Chapters 14 and 15 require the answer to (b).

CHAPTER 13

Cooling 1st Catalyst Bed Exit Gas

Chapter 12 shows that a 1st catalyst bed oxidizes less than 80% of its input SO_2. It also indicates that this SO_2 oxidation efficiency is increased to 98+% by passing 1st catalyst bed exit gas through a series of gas cooling/catalytic oxidation steps.

This chapter describes gas cooling between 1st and 2nd catalyst beds, Fig. 13.1. It sets the stage for Chapter 14's examination of 2nd catalyst bed SO_2 oxidation.

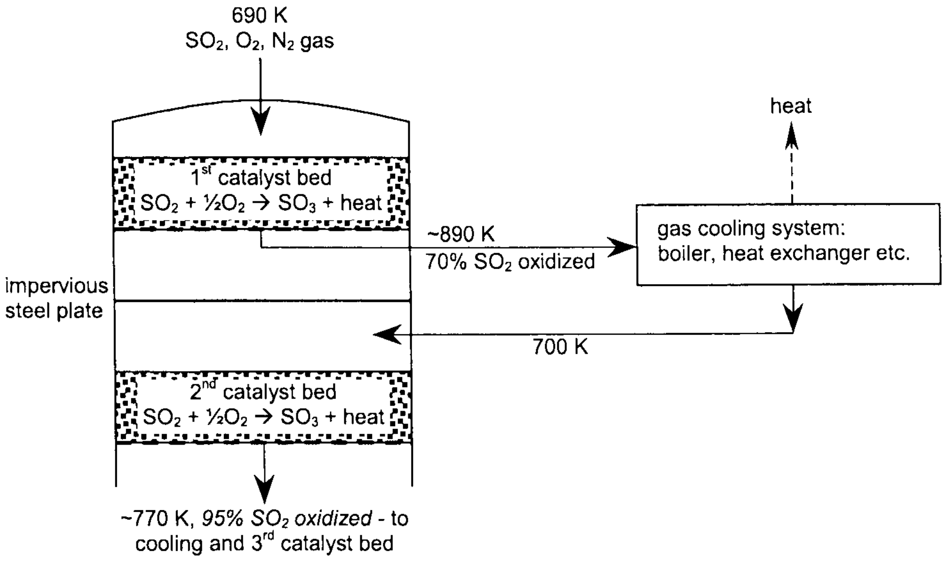

Fig. 13.1. Schematic of 1st and 2nd catalyst beds with gas cooling between. The cooling system cools 1st catalyst bed exit gas in preparation for more catalytic SO_2 oxidation in a 2nd catalyst bed. Industrial catalyst bed arrangements are discussed in Chapters 7 and 8. Gas cooling is discussed in Chapter 21.

The objectives of this chapter are to:

(a) show how gas cooling is represented on *% SO_2 oxidized*/temperature graphs

(b) indicate how gas cooling makes more SO_2 oxidation possible.

13.1 1st Catalyst Bed Summary

Fig. 13.2 summarizes 1st catalyst bed SO_2 oxidation. It is for:

10 volume% SO_2
11 volume% O_2
79 volume% N_2
690 K

feed gas and 1.2 bar bed pressure.

It confirms that intercept temperature and *% SO_2 oxidized* under these conditions are:

893.3 K
69.2 *% SO_2 oxidized.*

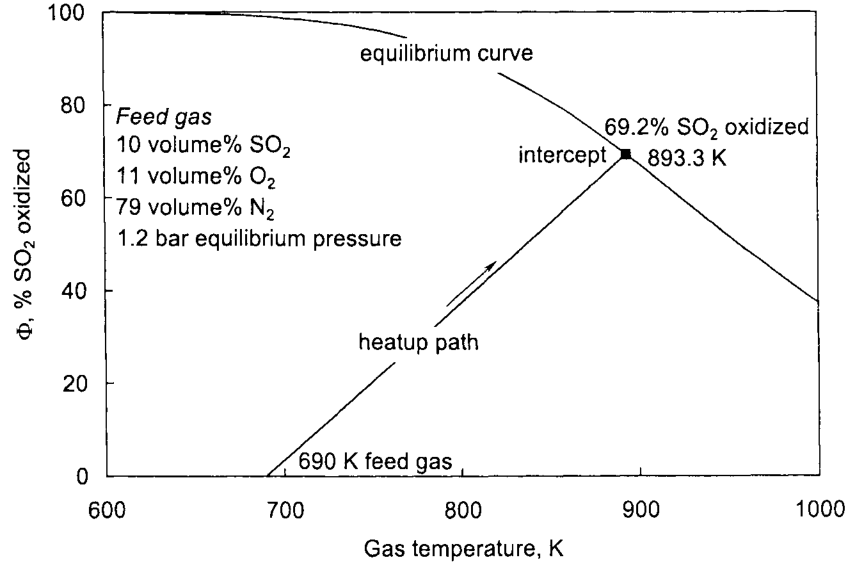

Fig. 13.2. 1st catalyst bed heatup path, equilibrium curve and intercept point, from Fig. 12.1. The 1st catalyst bed's exit gas is its intercept gas, Section 12.12. It is cooled and fed to a 2nd catalyst bed for more SO_2 oxidation.

13.1.1 Inefficient SO_2 oxidation explained

Fig. 13.2's SO_2 oxidation efficiency is less than 70%. This low efficiency arises because:

(a) feed gas enters the 1st catalyst bed at 690 K, warm enough for rapid catalytic oxidation

(b) heat from $SO_2 + \frac{1}{2}O_2 \longrightarrow SO_3$ oxidation raises gas temperature even further

(c) the resulting heatup path reaches the equilibrium curve at a high temperature where equilibrium SO_2 oxidation is inefficient.

13.2 Cooldown Path

This section adds a cooldown path to Fig. 13.2. It does so by preparing a data table which specifies that:

(a) a 1st catalyst bed's exit gas is its intercept gas, Section 12.12

(b) exit gas composition doesn't change during gas cooling – because the cooling equipment doesn't contain catalyst

(c) the cooldown target temperature is 700 K.

These specifications give the following two cooldown path points. They are plotted in Fig. 13.3 with a straight cooldown path between.

Description	**gas temperature, K**	***% SO_2 oxidized***
1st catalyst bed exit gas ≡ 1st catalyst bed intercept gas	893.3 (Fig. 13.2)	69.2 (Fig. 13.2)
Cooldown target temperature ≡ specified 2nd catalyst bed gas input temperature	700	69.2 (unchanged during catalyst free cooling)

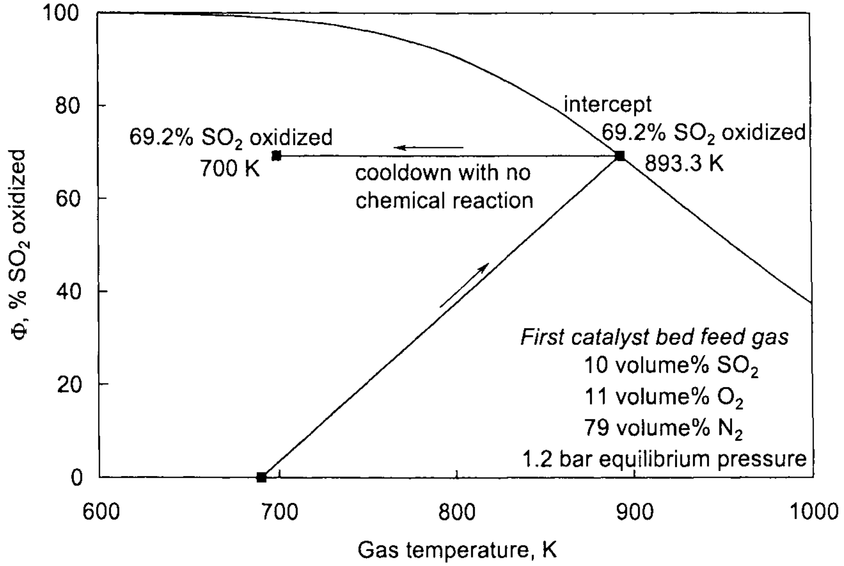

Fig. 13.3. Cooldown path added to Fig. 13.2. It is a horizontal line at the 1st catalyst bed intercept *% SO_2 oxidized* level – between the 1st catalyst bed intercept temperature and the specified 2nd catalyst bed gas input temperature. Gas composition and *% SO_2 oxidized* don't change in the gas cooling equipment.

13.2.1 2nd catalyst bed gas input temperature

SO_2 and O_2 concentrations in 2nd catalyst bed input gas are lower than in 1st catalyst bed feed gas, Section 12.2. SO_3 concentration is higher. Both of these tend to slow SO_2 oxidation in the 2nd catalyst bed.

This slowing effect is offset industrially by using slightly warmer input gas in the 2nd catalyst bed, Fig. 13.1. ~700 K is quite common, Table 7.2.

13.2.2 Industrial gas cooling (Chapter 21)

Catalyst bed exit gas is cooled by:

(a) making steam from water in a boiler

(b) superheating this steam

(c) heating water for the boiler in an economizer

(d) transferring heat to another gas in a gas-to-gas heat exchanger.

The steam is mainly used to make electricity.

The transferred heat is usually used to heat 1st catalyst bed feed gas to its specified input temperature (in metallurgical and waste acid regeneration plants).

13.3 Gas Composition Below Equilibrium Curve

Fig. 13.3 shows that gas cooling without composition change:

> moves *% SO_2 oxidized* from its 893.3 K position on the equilibrium curve

to:

> a position below the equilibrium curve, i.e. to a position where more SO_2 oxidation is possible.

It prepares the gas for more SO_2 oxidation.

13.4 Summary

A 1st catalyst bed oxidizes less than 80% of its feed SO_2 to SO_3. This percentage is increased by passing its exit gas through a series of gas cooling/catalytic oxidation steps.

Gas cooling between catalyst beds is done in water-to-steam boilers, superheaters, economizers and gas-to-gas heat exchangers. Gas composition doesn't change in these cooling devices because they don't contain catalyst.

Gas cooling between 1st and 2nd catalyst beds is represented graphically by a horizontal line at:

> the 1st catalyst bed intercept *% SO_2 oxidized* level

between:

(a) the 1st catalyst bed intercept temperature

and:

(b) the specified 2nd catalyst bed gas input temperature.

Problem

13.1 Prepare a graph like Fig. 13.3 for:

> 675 K, 12 volume% SO_2, 13.2 volume% O_2,
> 74.8 volume% N_2 1st catalyst bed feed gas.

Assume that this gas:

(a) attains equilibrium (1.2 bar) in a 1st catalyst bed at Problem 12.3's intercept temperature and *% SO_2 oxidized*

(b) is cooled to 685 K without any reaction in preparation for input to a 2nd catalyst bed.

Hints:

(a) You calculated the equilibrium curve for this gas in Problem 10.4.

(b) You calculated most of this gas's 1st catalyst bed heatup path in Problem 11.4. Now add your Problem 12.3 intercept point to the heatup path. This will join it to the equilibrium curve.

(c) Add a cooldown path to 685 K as described in Section 13.2.

CHAPTER 14

2^{nd} Catalyst Bed Heatup Path

Chapter 12 indicates that a 1st catalyst bed oxidizes less than 80% of its feed gas's SO_2. Most of the remaining SO_2 is oxidized to SO_3 in a sequence of gas cooling/catalytic oxidation steps. The oxidant is unused O_2 in 1st catalyst bed exit gas. The reaction is:

$$SO_2(g) + \frac{1}{2}O_2(g) \rightarrow SO_3(g)$$

This chapter examines oxidation of the SO_2 in cooled 1st catalyst bed exit gas – in a 2nd catalyst bed.

14.1 Objectives

The objectives of the chapter are to:

(a) define *% SO_2 oxidized* as it applies to a 2nd catalyst bed

(b) prepare a 2nd catalyst bed heatup path – starting with cooled 1st catalyst bed exit gas

(c) show how 2nd catalyst bed oxidation increases overall SO_2 oxidation efficiency.

14.2 *% SO_2 Oxidized* Re-defined

Chapter 10 defines catalyst bed *% SO_2 oxidized* anywhere in a 1st catalyst bed as:

$$\%\,SO_2\ oxidized = \Phi = \frac{\underset{\text{in feed gas}}{\text{kg-mole } SO_2} - \underset{\text{in oxidized gas}}{\text{kg-mole } SO_2}}{\text{kg-mole } SO_2 \text{ in feed gas}} * 100 \tag{10.1}$$

where all quantities are per kg-mole of 1st catalyst bed feed gas.

This chapter expands that definition to cover all acid plant catalyst beds. The expanded definition is:

$$\%\,SO_2\ oxidized = \Phi = \frac{\begin{matrix}\text{kg-mole } SO_2 \text{ in 1st} \\ \text{catalyst bed feed gas}\end{matrix} - \begin{matrix}\text{kg-mole } SO_2 \text{in any cat-} \\ \text{alyst bed's oxidized gas}\end{matrix}}{\text{kg-mole } SO_2 \text{ in 1st catalyst bed feed gas}} * 100 \tag{14.1}$$

where all quantities are per kg-mole of 1st catalyst bed feed gas.

This definition is used throughout the rest of this book.

14.3 2nd Catalyst Bed Heatup Path

Fig. 14.3 shows a 2nd catalyst bed heatup path. It is similar to a 1st catalyst bed heatup path but it starts at Fig. 13.3's:

(a) 1st catalyst bed intercept *% SO_2 oxidized*

(b) specified 2nd catalyst bed input gas temperature.

14.3.1 A heatup path point

2nd catalyst bed heatup path points are calculated much like 1st catalyst bed heatup points. The steps are:

(a) 2nd catalyst bed input temperature and input gas kg-mole are specified

(b) a gas temperature partway down the 2nd bed (after some SO_2 oxidation has occurred) is specified

(c) *% SO_2 oxidized* equivalent to (b)'s gas temperature is calculated.

Figs. 14.1 and 14.2 are used.

14.3.2 2nd catalyst bed difference

A significant difference between 2nd catalyst bed input gas and 1st catalyst bed feed gas is that:

2nd catalyst bed input gas always contains SO_3 as well as SO_2, O_2 and N_2.

This adds:

(a) a new variable (kg-mole SO_3 **in**) and an equivalent:

(b) new equation (SO_3 input quantity)

to our calculations, Table 14.2.

It also alters our heatup path S, O and enthalpy balances, Sections 14.6 and 14.7.

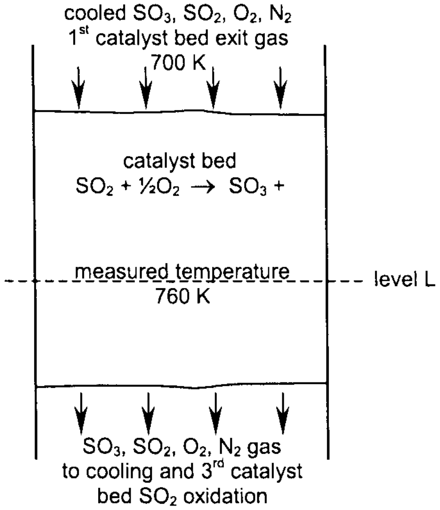

Fig. 14.1. Sketch of 2nd catalyst bed showing a temperature measured part way down the bed. Compositions and temperatures are assumed to be uniform horizontally at all levels.

14.4 A Specific Heatup Path Question

The problem solved in this chapter is:

> "Fig. 13.3's cooled 1st catalyst bed exit gas is fed to a 2nd catalyst bed, Fig. 14.1.
>
> A thermocouple at level L in the bed indicates that the temperature there is 760 K.
>
> What percentage of 1st catalyst bed feed SO_2 has been oxidized to SO_3 where the 2nd catalyst bed gas is 760 K?"

Fig. 14.2 defines the problem and specifies 2nd catalyst bed gas input temperature and input SO_3, SO_2, O_2 and N_2 kg-mole.

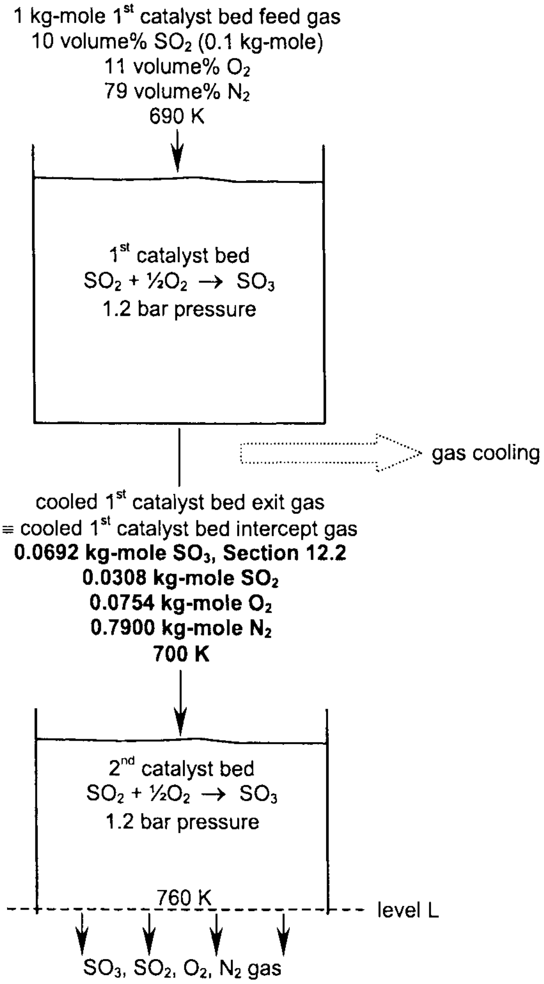

Fig. 14.2. Sketch defining Section 14.4's 2nd catalyst bed heatup path problem.

14.5 2nd Catalyst Bed Input Gas Quantities

2nd catalyst bed input gas quantities are specified to be:

1st catalyst bed <u>intercept</u> gas quantities.

This specification is based on the assumptions that:

(a) equilibrium is attained in the 1st catalyst bed, Fig. 12.1
(b) 1st catalyst bed exit gas composition ≡ 1st catalyst bed intercept (equilibrium) gas composition, Section 12.12

(c) 2nd catalyst bed input gas composition ≡ 1st catalyst bed exit gas composition, Section 13.2.

These assumptions link the two catalyst beds.

14.5.1 Input SO_3, SO_2, O_2 and N_2 equations

Fig. 14.2's 2nd catalyst bed input gas quantities are represented by the equations:

$$\text{kg-mole } SO_3 \textbf{ in} = 0.0692 \tag{14.2}$$

$$\text{kg-mole } SO_2 \textbf{ in} = 0.0308 \tag{14.3}$$

$$\text{kg-mole } O_2 \textbf{ in} = 0.0754 \tag{14.4}$$

$$\text{kg-mole } N_2 \textbf{ in} = 0.7900 \tag{14.5}$$

where the numerical values are those in Fig. 14.2.

These equations will, of course, be different for different 2nd catalyst bed input gases.

14.6 S, O and N Molar Balances

SO_3 in 2nd catalyst bed input gas alters molar balance Eqns. (11.4) to (11.6) as follows.

(a) Sulfur balance Eqn. (11.4) becomes:

$$0 = \underline{-\text{kg-mole } SO_3 \textbf{ in}} - \text{kg-mole } SO_2 \textbf{ in} + \text{kg-mole } SO_3 \textbf{ out} + \text{kg-mole } SO_2 \textbf{ out} \tag{14.6}$$

where **in** means into the top of Fig. 14.2's 2nd catalyst bed segment and **out** means out of the segment at level L.

(b) Oxygen balance Eqn. (11.5) becomes:

$$0 = \underline{-3*\text{kg-mole } SO_3 \textbf{ in}} - 2*\text{kg-mole } SO_2 \textbf{ in} - 2*\text{kg-mole } O_2 \textbf{ in}$$
$$+ 3*\text{kg-mole } SO_3 \textbf{ out} + 2*\text{kg-mole } SO_2 \textbf{ out} + 2*\text{kg-mole } O_2 \textbf{ out} \tag{14.7}$$

(c) Nitrogen balance Eqn. (11.6) is unchanged:

$$0 = -2*\text{kg-mole } N_2 \textbf{ in} + 2*\text{kg-mole } N_2 \textbf{ out} \tag{14.8}$$

14.7 Enthalpy Balance

SO_3 in 2nd catalyst bed feed gas changes Section 11.9's enthalpy balance to:

$$\begin{aligned}
0 \quad = \quad & \underline{-\text{kg-mole } SO_3 \textbf{ in}} * H^{\circ}_{\substack{700\\SO_3}} \\
& -\text{kg-mole } SO_2 \textbf{ in} * H^{\circ}_{\substack{700\\SO_2}} \\
& -\text{kg-mole } \ O_2 \textbf{ in} * H^{\circ}_{\substack{700\\O_2}} \\
& -\text{kg-mole } \ N_2 \textbf{ in} * H^{\circ}_{\substack{700\\N_2}} \\
& +\text{kg-mole } SO_3 \textbf{ out} * H^{\circ}_{\substack{760\\SO_3}} \\
& +\text{kg-mole } SO_2 \textbf{ out} * H^{\circ}_{\substack{760\\SO_2}} \\
& +\text{kg-mole } \ O_2 \textbf{ out} * H^{\circ}_{\substack{760\\O_2}} \\
& +\text{kg-mole } \ N_2 \textbf{ out} * H^{\circ}_{\substack{760\\N_2}} \qquad (14.8A)
\end{aligned}$$

where 700 K and 760 K are Fig. 14.2's 2nd catalyst bed input and level L temperatures. With the enthalpy values in Table 14.1, this enthalpy balance is:

$$\begin{aligned}
0 \quad = \quad & -\text{kg-mole } SO_3 \textbf{ in} * (-370.6) \\
& -\text{kg-mole } SO_2 \textbf{ in} * (-278.2) \\
& -\text{kg-mole } \ O_2 \textbf{ in} * 12.54 \\
& -\text{kg-mole } \ N_2 \textbf{ in} * 11.97 \\
& +\text{kg-mole } SO_3 \textbf{ out} * (-366.3) \\
& +\text{kg-mole } SO_2 \textbf{ out} * (-275.1) \\
& +\text{kg-mole } \ O_2 \textbf{ out} * 14.54 \\
& +\text{kg-mole } \ N_2 \textbf{ out} * 13.84 \qquad (14.9).
\end{aligned}$$

Table 14.1. 700 K and 760 K enthalpies for Section 14.4 problem. They have been calculated with the enthalpy equations in Appendix G.

Compound and temperature	enthalpy numerical value, MJ/kg-mole
$\underset{SO_3}{H^{\circ}_{700}}$	-370.6
$\underset{SO_2}{H^{\circ}_{700}}$	-278.2
$\underset{O_2}{H^{\circ}_{700}}$	12.54
$\underset{N_2}{H^{\circ}_{700}}$	11.97
$\underset{SO_3}{H^{\circ}_{760}}$	-366.3
$\underset{SO_2}{H^{\circ}_{760}}$	-275.1
$\underset{O_2}{H^{\circ}_{760}}$	14.54
$\underset{N_2}{H^{\circ}_{760}}$	13.84

14.8 Calculating 760 K (level L) Quantities

The Section 14.4 problem has 8 variables:

kg-mole SO_3 **in**

kg-mole SO_2 **in**

kg-mole O_2 **in**

kg-mole N_2 **in**

kg-mole SO_3 **out**

kg-mole SO_2 **out**

kg-mole O_2 **out**

kg-mole N_2 **out**

It also has 8 linear equations (14.2 to 14.9) which must be satisfied by the values of the above 8 variables. Each variable has, therefore, a unique value and the question:

> "What percentage of 1st catalyst bed feed SO_2 has been oxidized to SO_3 where the 2nd catalyst bed input gas has reached 760 K?"

has a unique answer.

14.9 Matrix Calculation and Result

The answer is obtained by:

(a) entering Eqns. (14.2) to (14.9) in matrix form into an Excel worksheet, Table 14.2

(b) solving for the 8 variables

(c) entering 1st catalyst bed feed kg-mole SO_2 in cell D2 (0.1 kg-mole from Fig. 14.2)

(d) calculating *% SO_2 oxidized* in cell H25 by Eqn. (14.1).

The results are shown in Table 14.2. They indicate that a 2nd bed temperature increase from 700 K to 760 K is equivalent to raising *% SO_2 oxidized* from 69.2% after the 1st catalyst bed to 89.7% at level L in the 2nd catalyst bed.

14.10 Preparing a Heatup Path

The 2nd catalyst bed heatup path is prepared by re-doing Section 14.9's calculation for many different temperatures in the bed. Only cells H15 to K15 are changed (most easily with enthalpy equations in cells, Appendix K). The results are tabulated in Table 14.3 and plotted in Fig. 14.3.

Table 14.3. Heatup path points for Fig. 14.2's 2nd catalyst bed. The points are shown graphically in Fig. 14.3. They have been calculated using matrix Table 14.2 with enthalpy equations in cells H15-K15, Appendix K. An increase in gas temperature from 700 K to 760 K in the 2nd catalyst bed is seen to be equivalent to an increase in *% SO_2 oxidized* from 69.2% to 89.7%.

Gas temperature, K	Equivalent *% SO_2 oxidized*
700	69.2
710	72.6
720	76.0
730	79.4
740	82.8
750	86.3
760	89.7

Table 14.2. Worksheet for calculating *% SO_2 oxidized* value equivalent to 760 K gas in a 2nd catalyst bed#. The 2nd bed input gas temperature and SO_3, SO_2, O_2 and N_2 quantities are from Fig. 14.2. The 1st catalyst bed feed kg-mole SO_2 (cell D2) is 0.1, also from Fig. 14.2. It is required for Eqn. (14.1) as shown. An increase in gas temperature from 700 to 760 K is seen to be equivalent to an increase from 69.2% *SO_2 oxidized* after the 1st catalyst bed to 89.7% *SO_2 oxidized* at level L in the 2nd catalyst bed. The matrix has been solved as described in Appendix H.

	A	B	C	D	E	F	G	H	I	J	K
1	**All calculations are based on 1 kg-mole of 1st catalyst bed feed gas.**										
2	kg-mole SO_2 in 1 kg-mole of 1st catalyst bed feed gas			0.1							
3											
4											
5											
6	**2nd catalyst bed matrix**										
7	Equation	description	numerical term	kg-mole SO_3 **in**	kg-mole SO_2 **in**	kg-mole O_2 **in**	kg-mole N_2 **in**	kg-mole SO_3 **out**	kg-mole SO_2 **out**	kg-mole O_2 **out**	kg-mole N_2 **out**
8	14.2	input SO_3 kg-mole	0.0692	1	0	0	0	0	0	0	0
9	14.3	input SO_2 kg-mole	0.0308	0	1	0	0	0	0	0	0
10	14.4	input O_2 kg-mole	0.0754	0	0	1	0	0	0	0	0
11	14.5	input N_2 kg-mole	0.7900	0	0	0	1	0	0	0	0
12	14.6	S balance	0	-1	-1	0	0	1	1	0	0
13	14.7	O balance	0	-3	-2	-2	0	3	2	2	0
14	14.8	N balance	0	0	0	0	-2	0	0	0	2
15	14.9	enthalpy balance	0	370.6	278.2	-12.54	-11.97	-366.3	-275.1	14.54	13.84
16											
17					700 K input				760 K, level L		
18											
19	Matrix results per kg-mole of 1st catalyst bed feed gas										
20	kg-mole SO_3 **in**	0.0692									
21	kg-mole SO_2 **in**	0.0308									
22	kg-mole O_2 **in**	0.0754			% SO_2 oxidized	kg-mole SO_2 in 1st		kg-mole SO_2 at level L			
23	kg-mole N_2 **in**	0.7900			at level L in	=	catalyst bed feed gas - in 2nd catalyst bed		* 100	(14.1)	
24	kg-mole SO_3 **out**	0.0897			2nd catalyst bed		kg-mole SO_2 in 1st catalyst bed feed gas				
25	kg-mole SO_2 **out**	0.0103				=(D2-B25)/D2*100 =		89.7	% SO_2 oxidized		
26	kg-mole O_2 **out**	0.0652									
27	kg-mole N_2 **out**	0.7900									

#Cells D15 to G15 contain $-H^{\circ}_{700}$ values, Section 14.7. Cells H15 to K15 contain $+H^{\circ}_{760}$ values.

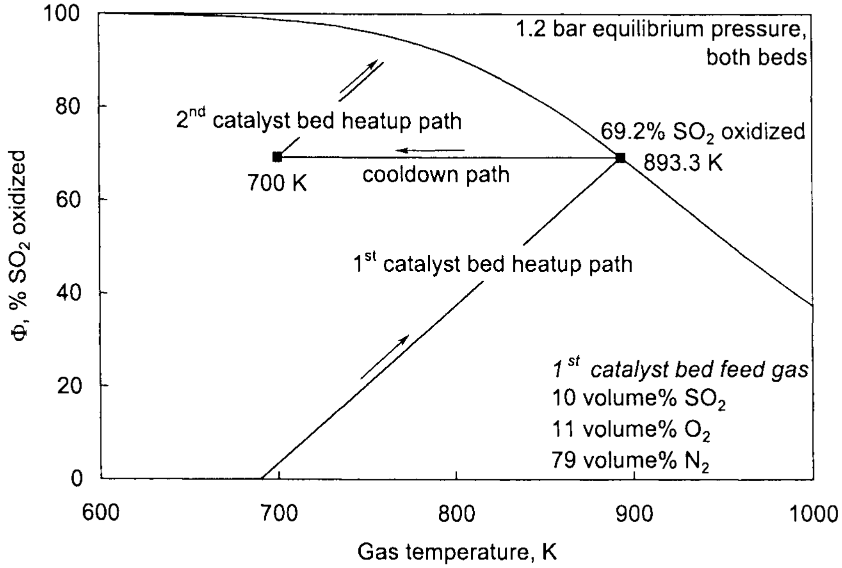

Fig. 14.3. Fig. 13.3 with the addition of Table 14.3's heatup path (upper left). The heatup path starts at 1st catalyst bed intercept *% SO_2 oxidized* and 2nd catalyst bed gas input temperature.

14.11 Discussion

Table 14.3 and Fig. 14.3 show that:

(a) cooling of 1st catalyst bed exit gas

and

(b) passing of this cooled gas through a 2nd catalyst bed

increases SO_2 oxidation efficiency from ~70% to ~90%.

This explains the success of industrial multi-catalyst bed SO_2 oxidation.

14.12 Summary

Cooling 1st catalyst bed exit gas to 700 K and passing the cooled gas through a 2nd catalyst bed raises SO_2 oxidation efficiency from ~70% to ~90%, Fig. 14.3.

The next chapter shows that attainment of equilibrium in the 2nd catalyst bed increases SO_2 oxidation efficiency even further – to almost 95%

Problem

14.1 Prepare a graph like Fig. 14.3 for the following.

(a) 12 volume% SO_2, 13.2 volume% O_2, 74.8 volume% N_2 1st catalyst bed feed gas.

(b) This gas enters the 1st catalyst bed at 675 K and reacts to equilibrium (1.2 bar) at the gas's heatup path-equilibrium curve intercept.

(c) The intercept gas exits the catalyst bed and is cooled to 685 K with no chemical reaction during cooling.

(d) The cooled exit gas is fed into a 2nd catalyst bed where SO_2 oxidation (by O_2 in the gas) and gas warming occur.

Hints:

(a) Your answer to Problem 13.1 already contains most of the required graph.

(b) Calculate the 2nd catalyst bed heatup path as described in Sections 14.4 to 14.10. Use 770 K as your top temperature. The 2nd bed's input gas quantities are those in your Problem 12.3(b) answer.

(c) Prepare a matrix like Table K.1 for this purpose. Note the new input SO_3 column and row. Note also the changed S, O and enthalpy balance equations.

(d) Remember that the 2nd catalyst bed input gas temperature is 685 K. Your input enthalpies must be for that temperature.

(e) Note that cell D2 must contain 0.12. This is because 1 kg-mole of 12 volume% SO_2 1st catalyst bed feed gas contains 0.12 kg-mole of SO_2. This value is needed for Eqn. (14.1)'s *% SO_2 oxidized* calculation.

CHAPTER 15

Maximum SO_2 Oxidation in a 2^{nd} Catalyst Bed

Chapter 14 describes 2^{nd} catalyst bed heatup paths. This chapter describes 2^{nd} catalyst bed:

equilibrium curves

and:

heatup path-equilibrium curve intercepts.

The objectives of the chapter are to:

(a) show that equilibrium curve Eqn. (10.13) applies to 2^{nd} catalyst beds as well as to 1^{st} catalyst beds

(b) determine a 2^{nd} catalyst bed heatup path-equilibrium curve intercept

(c) quantify two bed SO_2 oxidation efficiency.

15.1 2^{nd} Catalyst Bed Equilibrium Curve Equation

Fig. 14.3's 1^{st} catalyst bed equilibrium curve is described by Equation (10.13), i.e.:

$$T_E = \frac{-B}{A + R * \ln\left(\left(\frac{\Phi^E}{100 - \Phi^E}\right) * \left(\frac{100 - \frac{1}{2} * e * \frac{\Phi^E}{100}}{f - \frac{1}{2} * e * \frac{\Phi^E}{100}}\right)^{\frac{1}{2}} * P_t^{-\frac{1}{2}}\right)} \qquad (10.13)$$

where:

T_E = equilibrium temperature

A and B = empirical constants relating ΔG_T° for $SO_2(g) + \frac{1}{2}O_2(g) \rightarrow SO_3(g)$ oxidation to temperature, Eqn. (10.9) and Appendix C

A = 0.09357 MJ kg-mole SO_2^{-1} K^{-1}
B = -98.41 MJ/kg-mole SO_2

R = gas constant, 0.008314 MJ kg-mole SO_2^{-1} K^{-1}

Φ^E = 1st catalyst bed equilibrium *% SO_2 oxidized*, Eqn. (10.2)

e = volume% SO_2 in 1st catalyst bed feed gas, 10% in Fig. 14.3

f = volume% O_2 in 1st catalyst bed feed gas, 11% in Fig. 14.3

P_t = 1st catalyst bed pressure, 1.2 bar in Fig. 14.3.

Re-written with the above numerical e, f and P_t values, Eqn. (10.13) becomes:

$$T_E = \frac{-B}{A + R * \ln\left(\left(\frac{\Phi^E}{100 - \Phi^E}\right) * \left(\frac{100 - \frac{1}{2}\mathbf{*10*}\frac{\Phi^E}{100}}{\mathbf{11} - \frac{1}{2}\mathbf{*10*}\frac{\Phi^E}{100}}\right)^{\frac{1}{2}} \mathbf{* 1.2}^{-\frac{1}{2}}\right)} \quad (15.1).$$

So far, this equation has been shown to apply to Fig. 14.3's 1st catalyst bed. This section indicates that it also applies to Fig. 14.3's 2nd catalyst bed – with, however, a slightly different definition of equilibrium *% SO_2 oxidized.*

The new, more general, definition of equilibrium *% SO_2 oxidized* is:

Equilibrium *%SO_2 oxidized* = Φ^E

$$= \frac{\begin{matrix}\text{kg-mole } SO_2 \text{ in } 1^{st} \\ \text{catalyst bed feed gas}\end{matrix} - \begin{matrix}\text{kg-mole } SO_2 \text{ in oxidized gas in any catalyst} \\ \text{bed where equilibrium has been attained}\end{matrix}}{\text{kg-mole } SO_2 \text{ in } 1^{st} \text{ catalyst bed feed gas}} * 100 \quad (15.2)$$

where all quantities are per kg-mole of 1st catalyst bed feed gas.

15.1.1 Proof of 2nd catalyst bed applicability

All equations used in deriving Eqn. (15.1) for Fig. 14.2's 1st catalyst bed also apply to Fig. 14.2's 2nd catalyst bed, Appendix L. So Eqn. (15.1) is also applicable to both beds.

In fact, equilibrium Eqn. (15.1) applies to all before-H_2SO_4-making catalyst beds where:

(a) the feed to the 1st catalyst bed contains 10 volume% SO_2, 11 volume% O_2 and 79 volume% N_2

(b) bed pressure is 1.2 bar pressure.

Industrial bed pressures are discussed in Section 18.7.

15.2 2nd Catalyst Bed Intercept Calculation

Table 15.1 presents:

heatup path

and

equilibrium curve

% SO_2 oxidized/temperature points near Fig. 14.3's expected 2nd catalyst bed intercept point.

The points are for the conditions in Fig. 14.2, i.e.:

(a) 690 K, 10 volume% SO_2, 11 volume% O_2, 79 volume% N_2 1st catalyst bed feed gas

(b) attainment of intercept (equilibrium) conditions in the 1st catalyst bed at 1.2 bar pressure

(c) assumption that 1st catalyst bed exit gas ≡ 1st catalyst bed intercept gas, Section 12.12

(d) cooldown of 1st catalyst bed exit gas to 700 K with no change in gas composition

(e) feeding of this cooled gas to the 2nd catalyst bed

(f) 1.2 bar pressure in the 2nd catalyst bed.

Table 15.1. 2nd catalyst bed *% SO_2 oxidized*/temperature points near heatup path-equilibrium curve intercept. They have been calculated as described in Appendices K and D.

Temperature, K	Heatup path *% SO_2 oxidized*, Φ	Equilibrium *% SO_2 oxidized*, Φ^E from Eqn. (15.1)
777	95.49	93.78
776	95.15	93.89
775	94.81	94.00
774	94.47	94.11
773	94.12	94.21
772	93.78	94.32
771	93.44	94.42
770	93.10	94.53

15.2.1 Intercept

Table 15.1 shows that at 773 K and below:

heatup path *% SO_2 oxidized* is below equilibrium *% SO_2 oxidized.*

This indicates that $SO_2 + \frac{1}{2}O_2 \rightarrow SO_3$ oxidation can proceed further up the heatup path towards equilibrium.

At 774 K and above, however:

heatup path *% SO_2 oxidized* is greater than equilibrium *% SO_2 oxidized*

which is impossible because equilibrium *% SO_2 oxidized* cannot be exceeded up a heatup path.

Interpolation suggests that Table 15.1's heatup path intercepts its equilibrium curve at:

773.2 K
94.2 % SO_2 oxidized, Fig. 15.1.

This is confirmed by a Goal Seek calculation in Table M.2.

15.2.2 Intercept gas composition

Intercept gas quantities are needed for Chapter 16's 3rd catalyst bed calculations. They are obtained from the intercept results in Table M.2. They are:

0.0942 kg-mole SO_3

0.0058 kg-mole SO_2

0.0629 kg-mole O_2

0.7900 kg-mole N_2

per kg-mole of 1st catalyst bed feed gas.

15.3 Two Bed SO_2 Oxidation Efficiency

Fig. 15.1 extends Fig. 14.3's 2nd catalyst bed heatup path to the Section 15.2.1 intercept.

It shows that:

(a) cooling Fig. 14.2's 1st catalyst bed exit gas to 700 K

(b) passing the cooled gas through a 2nd catalyst bed

increases SO_2 oxidation efficiency from:

69.2% after the 1st catalyst bed

to:

94.2% after the 2nd catalyst bed.

This confirms the efficacy of multi-bed catalytic oxidation with gas cooling between beds.

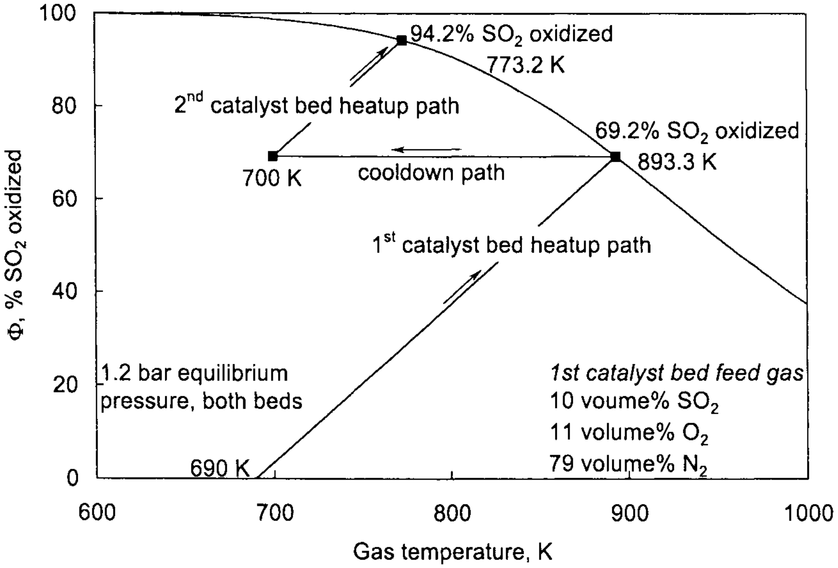

Fig. 15.1. SO_2 oxidation efficiency in two catalyst beds with gas cooling between beds. The 1st bed oxidizes 69.2% of 1st catalyst bed feed SO_2 – the 2nd bed an additional 25%. Note that the equilibrium curve is exactly the same for both catalyst beds, Section 15.1.1.

15.4 Summary

Cooling 1st catalyst bed exit gas and passing the cooled gas through a 2nd catalyst bed increases SO_2 oxidation efficiency from:

~70% to ~95%.

SO_2 oxidation efficiency can be increased even further by:

(a) cooling the 2nd catalyst bed exit gas

(b) passing the cooled gas through a 3rd catalyst bed, next chapter.

Problems

15.1 Prepare a graph like Fig. 15.1 for the following.

(a) 12 volume% SO_2, 13.2 volume% O_2, 74.8 volume% N_2 1st catalyst bed feed gas

(b) This gas enters the 1st catalyst bed at 675 K and reacts to equilibrium (1.2 bar) at the gas's heatup path-equilibrium curve intercept.

(c) The intercept gas exits the catalyst bed and is cooled to 685 K with no chemical reaction during cooling.

(d) The cooled gas is fed into a 2nd catalyst bed where SO_2 oxidation (by O_2 in the gas) and gas warming occur.

(e) The gas in (d) reacts until its heatup path intercepts its equilibrium curve.

Hints:

(a) Your answer to Problem 14.1 already contains most of the required graph. You only need to calculate the intercept point.

(b) The equilibrium equation for catalyst bed 2 is the same as for catalyst bed 1 because no gas has been added or removed between beds and because 1st and 2nd bed equilibrium pressures are the same (1.2 bar).

(c) Calculate the 2nd catalyst bed intercept point as described in Appendix M. Make sure that you use 685 K for the 2nd catalyst bed gas input temperature.

(d) The 2nd catalyst bed gas input quantities are those in your Problem 12.3(b) answer.

(e) Add your intercept point to Problem 14.1's heatup path and re-plot the path. This completes your graph.

15.2 Tabulate Problem 15.1's intercept kg-mole SO_3, SO_2, O_2 and N_2. They are needed for Problem 16.1.

CHAPTER 16

3rd Catalyst Bed SO_2 Oxidation

Simplest industrial sulfuric acidmaking consists of:

> SO_2 oxidation in three catalyst beds with gas cooling between beds

then:

> H_2SO_4 making by contact of cooled 3rd catalyst bed exit gas with strong sulfuric acid, Fig. 16.1.

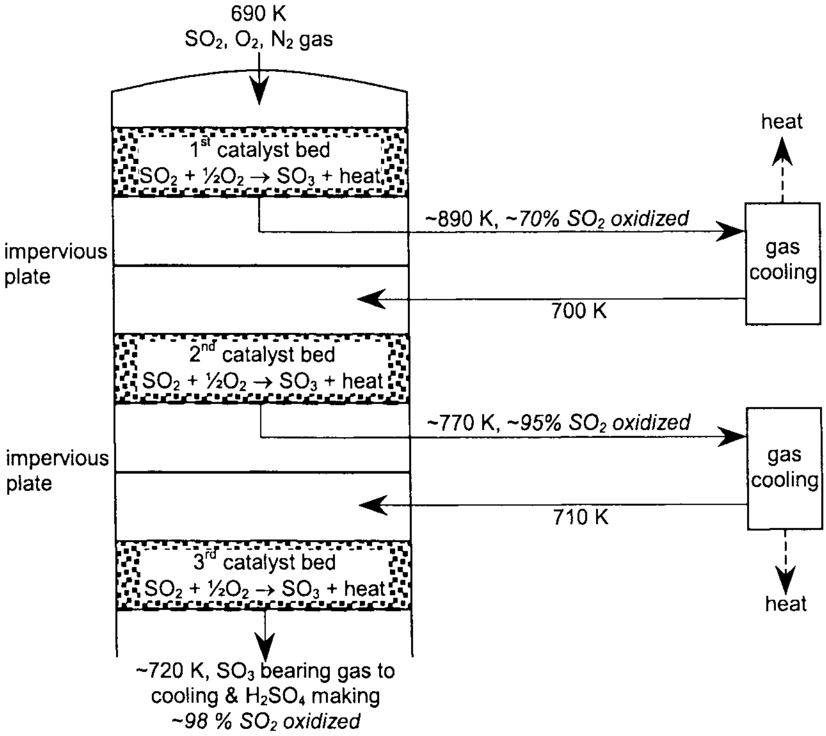

Fig. 16.1. Schematic of single contact, 3 catalyst bed sulfuric acid plant. It is a single contact plant because it has only one H_2SO_4 making step. Note gas cooling between catalyst beds. It permits additional SO_2 oxidation in the next catalyst bed.

The SO_2 oxidation reaction is:

$$\underbrace{SO_2(g) \quad + \quad \tfrac{1}{2}O_2(g)}_{\text{in catalyst bed input gas}} \quad \xrightarrow[700\text{-}900\ K]{\text{catalyst}} \quad SO_3(g)$$

The H_2SO_4 making reaction is:

$$\underset{\substack{\text{in cooled 3rd catalyst}\\ \text{bed exit gas}}}{SO_3(g)} \quad + \quad \underset{\substack{\text{in strong}\\ \text{sulfuric acid}}}{H_2O(\ell)} \quad \xrightarrow{350\text{-}380\ K} \quad \underset{\substack{\text{in strengthened}\\ \text{sulfuric acid}}}{H_2SO_4(\ell)}$$

This chapter describes cooling of 2nd catalyst bed exit gas and oxidation of the cooled gas's SO_2 in a 3rd catalyst bed. Its objectives are to:

(a) prepare a 2-3 cooldown path

(b) prepare a 3rd catalyst bed heatup path

(c) calculate a 3rd bed heatup path-equilibrium curve intercept.

Specifications for the calculations are shown in Fig. 16.2. Calculation results are summarized in Figs. 16.3 and 16.4.

16.1 2-3 Cooldown Path

This chapter's 2-3 cooldown path is prepared like Fig. 13.3's 1-2 cooldown path. It is a horizontal line at:

94.2% *SO_2 oxidized* (2nd catalyst bed intercept *% SO_2 oxidized)*

between:

773.2 K (2nd catalyst bed intercept temperature)

and:

710 K (specified 3rd catalyst bed input gas temperature).

It is shown in Figs. 16.3 and 16.4.

16.2 Heatup Path

This chapter's 3rd catalyst bed heatup path is calculated much like Chapter 14's 2nd catalyst bed heatup path. Differences are:

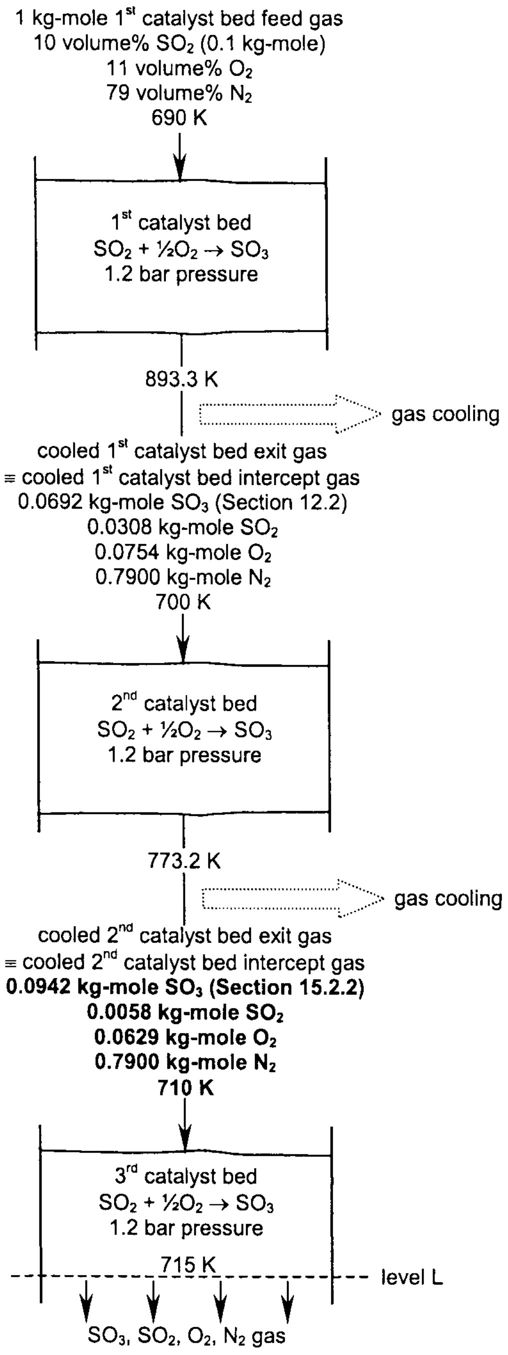

Fig. 16.2. Specifications for (i) 2-3 cooldown and (ii) 3rd catalyst bed heatup path and intercept calculations. The 1st and 2nd catalyst bed exit gas quantities are equivalent to:

69.2% SO_2 oxidized after the 1st catalyst bed

94.2% SO_2 oxidized after the 2nd catalyst bed, Fig. 15.1.

(a) the input gas temperature is 710 K rather than 700 K

(b) the input gas quantities are different, Fig. 16.2.

The latter are represented by the equations:

$$\text{kg-mole } SO_3 \textbf{ in} = 0.0942 \tag{16.1}$$

$$\text{kg-mole } SO_2 \textbf{ in} = 0.0058 \tag{16.2}$$

$$\text{kg-mole } O_2 \textbf{ in} = 0.0629 \tag{16.3}$$

$$\text{kg-mole } N_2 \textbf{ in} = 0.7900 \tag{16.4}.$$

Appendix N shows a 3rd catalyst bed heatup path matrix with these equations. It also shows several heatup path points. Figs. 16.3 and 16.4 show the entire heatup path.

16.3 Heatup Path-Equilibrium Curve Intercept

Appendix O describes a 3rd catalyst bed intercept calculation – with the Fig. 16.2 specifications. The 3rd bed intercept with these specifications is:

721.1 K

98.0 *% SO_2 oxidized.*

Its gas quantities are:

0.098 kg-mole SO_3
0.002 kg-mole SO_2
0.061 kg-mole O_2
0.790 kg-mole N_2

per kg-mole of 1st catalyst bed feed gas. These quantities go forward to the next acidmaking step – almost always to H_2SO_4 making but occasionally to a 4th catalyst bed.

16.4 Graphical Representation

Figs. 16.3 and 16.4 describe 3-bed SO_2 oxidation with Fig. 16.2's specifications. They indicate that the percentages of SO_2 oxidized in each bed are:

69.2% in the 1st catalyst bed
25.0% in the 2nd catalyst bed
3.8% in the 3rd catalyst bed

for a total of 98.0%

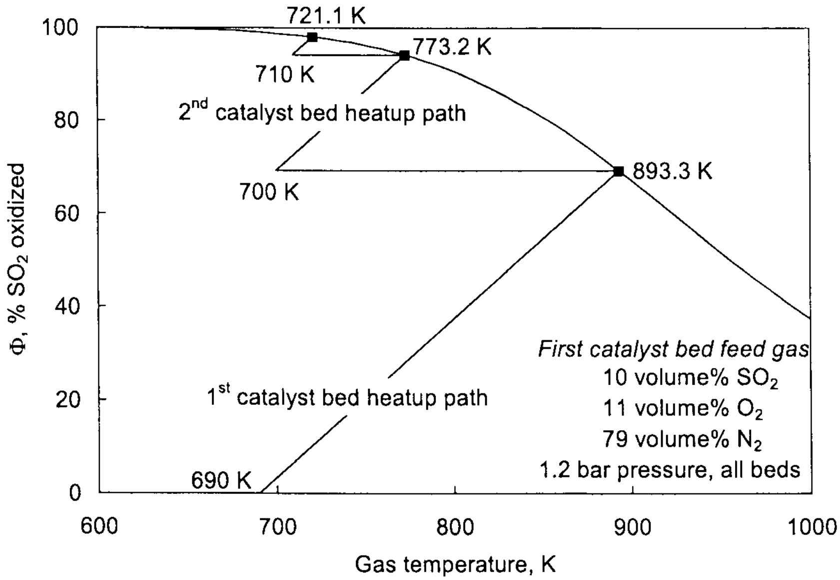

Fig. 16.3. 3 catalyst bed SO_2 oxidation with gas cooling between beds. The equilibrium curve is the same for all beds (Section 15.1.1) because:

- (a) no component gas (e.g. SO_3) is selectively removed from the Fig. 16.2 gas stream (Appendix L)
- (b) no air is added to the Fig. 16.2 gas stream
- (c) all beds are at the same pressure.

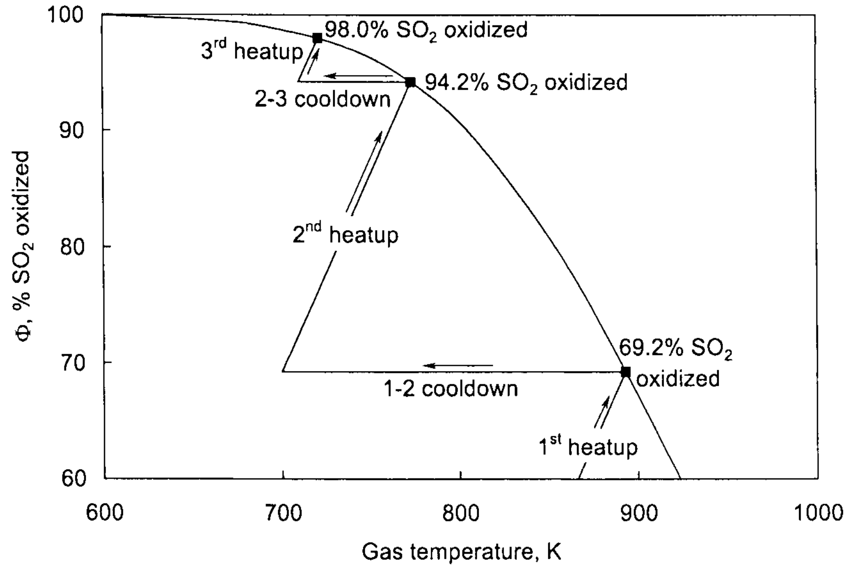

Fig. 16.4. Blowup of top portion of Fig. 16.3. Overall SO_2 oxidation efficiency increases with each bed but the gain diminishes.

16.5 Summary

2nd and 3rd catalyst bed heatup path and intercept calculations are very similar.

Their differences are:

(a) different SO_3, SO_2, O_2 and N_2 input quantities

(b) different gas input temperatures.

3 catalyst bed SO_2 oxidation efficiency is about ~98%. Beds 1, 2 and 3 contribute ~69%, 25% and 4%.

Chapter 17 examines the effects of SO_3 and CO_2 in feed gas on these catalytic oxidation efficiencies.

Problems

16.1 Prepare a graph like Fig. 16.3 for:

(a) 12 volume% SO_2, 13.2 volume% O_2, 74.8 volume% N_2 1st catalyst bed feed gas

(b) the following gas input temperatures

1st catalyst bed	675 K
2nd catalyst bed	685 K
3rd catalyst bed	695 K.

(c) 1.2 bar gas pressure in all beds.

(d) attainment of intercept *% SO_2 oxidized* in all beds.

Hints:

(a) Your answer to Problem 15.1 contains most of the required graph. You only need to prepare:

  (i) a 2-3 cooldown path

  (ii) a 3rd catalyst bed heatup path

  (iii) a 3rd catalyst bed intercept point (which you can join to the heatup path).

(b) The 3rd catalyst bed's input gas quantities are those in your Problem 15.2 answer.

16.2 Tabulate the intercept kg-mole of SO_3, SO_2, O_2 and N_2 equivalent to Prob. 16.1's 3rd catalyst bed intercept point (all per kg-mole of 1st catalyst bed feed gas).

CHAPTER 17

SO_3 and CO_2 in Feed Gas

Industrial **sulfur-burning exit gas** contains ~0.2 volume% SO_3 when it reaches an acid plant's 1st catalyst bed, Chapter 3. The SO_3 slightly affects catalyst bed:

equilibrium curves
heatup paths
heatup path-equilibrium curve intercepts.

Industrial **metallurgical and waste acid regeneration gases** don't contain SO_3 when they reach an acid plant's 1st catalyst bed. SO_3 is water scrubbed from these gases during gas cooling and cleaning, Chapters 4 and 5. They do, however, contain up to 8 volume% CO_2 when they reach the acid plant's 1st catalyst bed. The CO_2 comes from fossil fuel and waste acid hydrocarbons. The CO_2 slightly affects:

heatup paths
heatup path-equilibrium curve intercepts.

This chapter describes 1st catalyst bed calculations with SO_3 and CO_2 in feed gas. Its objectives are to show how:

(a) feed gas SO_3 and CO_2 are included in our 1st catalyst bed equilibrium curve, heatup path and intercept calculations

(b) these gases affect 1st catalyst bed SO_2 oxidation efficiency.

The effects are shown to be quite small.

17.1 SO_3

17.1.1 SO_3 effect on equilibrium curve equation

SO_3-in-feed-gas changes $SO_2 + \frac{1}{2}O_2 \rightarrow SO_3$ equilibrium curve Eqn. (10.13) to:

$$T_E = \frac{-B}{A + R * \ln\left(\left(\frac{d + e*\frac{\Phi^E}{100}}{e*\left(1 - \frac{\Phi^E}{100}\right)}\right) * \left(\frac{100 - \frac{1}{2}*e*\frac{\Phi^E}{100}}{f - \frac{1}{2}*e*\frac{\Phi^E}{100}}\right)^{\frac{1}{2}} * P_t^{-\frac{1}{2}}\right)} \quad (17.1).$$

where:

T_E = equilibrium temperature, K

A and B = empirical constants for calculating ΔG_T° $SO_2(g) + \frac{1}{2}O_2(g) \rightarrow SO_3(g)$ from temperature, Eqn. (10.9) and Appendix C

$A = 0.09357$ MJ kg-mole $SO_2^{-1}K^{-1}$

$B = -98.41$ MJ/kg-mole SO_2

R = gas constant, 0.008314 MJ kg-mole $SO_2^{-1}K^{-1}$

$$\left.\begin{array}{l} d = \text{volume\% } SO_3 \text{ in 1st catalyst bed feed gas} \\ e = \text{volume\% } SO_2 \quad '' \quad '' \\ f = \text{volume\% } O_2 \quad '' \quad '' \end{array}\right\} \text{remainder } N_2 \text{ and } CO_2$$

Φ^E = equilibrium *% SO_2 oxidized*, Section 15.1

P_t = total gas pressure, bar.

Eqn. (17.1) is developed in Appendix P. Notice that a zero value of 'd' reduces it to Eqn. (10.13).

17.1.2 Effect of SO_3 on heatup path matrix

SO_3-in-feed-gas changes Chapter 11's heatup path matrix by introducing a new input variable:

kg-mole SO_3 **in**

and a new SO_3 input equation:

$$\text{kg-mole } SO_3 \textbf{ in} = \frac{\text{mole\% } SO_3 \text{ in feed gas}}{100}$$

which, for 0.2 volume% SO_3, is:

$$\text{kg-mole } SO_3 \textbf{ in} = \frac{0.2\% \; SO_3}{100} = 0.002 \quad (17.2)$$

per kg-mole of 1st catalyst bed feed gas.

17.1.3 SO_2 input equation changed by SO_3

Assuming a 0.2 volume% SO_3, 9.8 volume% SO_2, 11 volume% O_2, 79 volume% N_2 feed gas, 0.2% SO_3 changes SO_2 input Equation (11.7) to:

$$\text{kg-mole } SO_2\ \textbf{in} \;=\; \underline{9.8\%\ SO_2} \;=\; 0.098 \qquad (17.3).$$

17.1.4 Balances changed by SO_3

SO_3-in-feed-gas changes 1st catalyst bed:

(a) S balance Eqn. (11.4) to:

$$0 = \underline{-\text{kg-mole } SO_3\ \textbf{in}} - \text{kg-mole } SO_2\ \textbf{in} + \text{kg-mole } SO_3\ \textbf{out} + \text{kg-mole } SO_2\ \textbf{out} \qquad (14.6)$$

(b) O balance Eqn. (11.5) to:

$$\begin{aligned} 0 = {} & \underline{-\,3*\text{kg-mole } SO_3\ \textbf{in}} - 2*\text{kg-mole } SO_2\ \textbf{in} - 2*\text{kg-mole } O_2\ \textbf{in} \\ & + 3*\text{kg-mole } SO_3\ \textbf{out} + 2*\text{kg-mole } SO_2\ \textbf{out} + 2*\text{kg-mole } O_2\ \textbf{out} \end{aligned} \qquad (14.7)$$

(c) enthalpy balance Eqn. (11.6B) to:

$$\begin{aligned} 0 \;=\; & \underline{-\,\text{kg-mole } SO_3\ \textbf{in}\ *}\ \underset{SO_3}{H^{\circ}_{T\,\text{feed}}} \\ & -\,\text{kg-mole } SO_2\ \textbf{in}\ *\ \underset{SO_2}{H^{\circ}_{T\,\text{feed}}} \\ & -\,\text{kg-mole } O_2\ \textbf{in}\ *\ \underset{O_2}{H^{\circ}_{T\,\text{feed}}} \\ & -\,\text{kg-mole } N_2\ \textbf{in}\ *\ \underset{N_2}{H^{\circ}_{T\,\text{feed}}} \\ & +\text{kg-mole } SO_3\ \textbf{out}\ *\ \underset{SO_3}{H^{\circ}_{T\,\text{bed}}} \\ & +\text{kg-mole } SO_2\ \textbf{out}\ *\ \underset{SO_2}{H^{\circ}_{T\,\text{bed}}} \\ & +\text{kg-mole } O_2\ \textbf{out}\ *\ \underset{O_2}{H^{\circ}_{T\,\text{bed}}} \\ & +\text{kg-mole } N_2\ \textbf{out}\ *\ \underset{N_2}{H^{\circ}_{T\,\text{bed}}} \end{aligned} \qquad (14.8A)$$

where:

$H^{\circ}_{T\,\text{feed}}$ = enthalpy at the 1st catalyst bed feed gas temperature

$H^{\circ}_{T\,\text{bed}}$ = enthalpy at a temperature part way down the catalyst bed.

The result of the Section 17.1.2-17.1.4 changes is heatup path matrix Table 17.1.

Table 17.1. 1st catalyst bed heatup path worksheet with 0.2 volume% SO_3 and 9.8 volume% SO_2 in feed gas#. It is similar to Table 14.2's 2nd catalyst bed worksheet. Cells D15 to G15 contain $-H^{\circ}_{690K}$ values. Cells H15 to K15 contain H°_{820K} values. All are calculated with Appendix G's enthalpy equations. 820 K part way down the catalyst bed is shown to be equivalent to oxidation of 45.2% of the feed gas's SO_2.

	A	B	C	D	E	F	G	H	I	J	K
1	**All calculations are based on 1 kg-mole of 1st catalyst bed feed gas.**										
2	volume% SO_2 in 1st catalyst bed feed gas =			9.8							
3	kg-mole SO_2 in 1 kg-mole of 1st catalyst bed feed gas = volume% SO_2/100% =					0.098	=D2/100	(11.1)			
4											
5											
6	**1st catalyst bed matrix**										
7	Equation	description	numerical term	kg-mole SO_3 **in**	kg-mole SO_2 **in**	kg-mole O_2 **in**	kg-mole N_2 **in**	kg-mole SO_3 **out**	kg-mole SO_2 **out**	kg-mole O_2 **out**	kg-mole N_2 **out**
8	17.2	input SO_3 kg-mole	0.0020	1	0	0	0	0	0	0	0
9	17.3	input SO_2 kg-mole	0.0980	0	1	0	0	0	0	0	0
10	11.2	input O_2 kg-mole	0.1100	0	0	1	0	0	0	0	0
11	11.3	input N_2 kg-mole	0.7900	0	0	0	1	0	0	0	0
12	14.6	S balance	0	-1	-1	0	0	1	1	0	0
13	14.7	O balance	0	-3	-2	-2	0	3	2	2	0
14	14.8	N balance	0	0	0	0	-2	0	0	0	2
15		enthalpy balance	0	371.3	278.7	-12.21	-11.66	-362.0	-272.0	16.54	15.71
16											
17					690 K feed				820 K part way down bed		
18											
19	Matrix results per kg-mole of 1st catalyst bed feed gas										
20	kg-mole SO_3 **in**	0.0020									
21	kg-mole SO_2 **in**	0.0980									
22	kg-mole O_2 **in**	0.1100									
23	kg-mole N_2 **in**	0.7900									
24	kg-mole SO_3 **out**	0.0463		% SO_2 oxidized equivalent to 820 K =		(kg-mole SO_2 **in** - kg-mole SO_2 **out**)/kg-mole SO_2 **in***100				(Eqn. 10.1)	
25	kg-mole SO_2 **out**	0.0537			=	(F3-B25)/F3*100	=	45.2	% SO_2 oxidized		
26	kg-mole O_2 **out**	0.0879									
27	kg-mole N_2 **out**	0.7900									

#Feed gas: 0.2 volume% SO_3, 9.8 volume% SO_2, 11 volume% O_2, 79 volume% N_2; 690 K.

17.1.5 Effect of SO_3 on heatup path-equilibrium curve intercepts

Appendix Q shows how:

new equilibrium Eqn. (17.1)

and:

new matrix Table 17.1

are combined to calculate an SO_3-in-feed gas heatup path-equilibrium curve intercept.

The results are given in the next section.

17.2 SO_3 Effects

Table 17.2 shows 1st catalyst bed intercept temperature-*% SO_2 oxidized* points with and without 0.2 volume% SO_3 in feed gas. The presence of 0.2% SO_3 is shown to have little effect on intercept *% SO_2 oxidized.*

Table 17.2. Comparison of 1st catalyst bed intercept temperature and *% SO_2 oxidized* values with 0 and 0.2 volume% SO_3 in feed gas. Intercept *% SO_2 oxidized* is slightly smaller with SO_3 than without SO_3. This is because the pre-existing SO_3 prevents $SO_2+\frac{1}{2}O_2 \rightarrow SO_3$ oxidation from going quite as far to the right.

	0.0 volume% SO_3 9.8 volume% SO_2 metallurgical or spent acid regeneration feed gas#	0.2 volume% SO_3 9.8 volume% SO_2 sulfur-burning feed gas#
	temperature, K; *% SO_2 oxidized*	
1st catalyst bed		
feed	690; *0*	690; *0*
intercept	891.4; *69.9*	890.3; *69.7*

#11 volume% O_2, remainder N_2; 1.2 bar

17.3 CO_2

CO_2-in-feed-gas affects catalyst bed heatup paths and intercepts (but not equilibrium curves, Appendix F). The remainder of this chapter indicates how CO_2-in-feed-gas affects:

(a) the Table 17.1 heatup path matrix

(b) 1st catalyst bed intercepts.

It considers 10 volume% CO_2 in feed gas (plus 0 volume% SO_3, 10 volume% SO_2, 11 volume% O_2, 69 volume% N_2).

17.3.1 CO_2 effect on heatup path matrix

CO_2 in feed gas introduces two new variables into the Table 17.1 heatup path matrix:

$$\text{kg-mole } CO_2\ \textbf{in}$$

$$\text{kg-mole } CO_2\ \textbf{out}.$$

Of course, their numerical values are the same because CO_2 doesn't react during SO_2 oxidation or H_2SO_4 making.

It also provides two new equations:

(a) a CO_2 input quantity equation:

$$\text{kg-mole } CO_2\ \textbf{in} = \frac{\begin{matrix}\text{mole\% } CO_2\\ \text{in feed gas}\end{matrix}}{100}$$

or, with 10 volume% CO_2 in feed gas:

$$\text{kg-mole } CO_2\ \textbf{in} = \frac{\begin{matrix}\text{10\% } CO_2\\ \text{in feed gas}\end{matrix}}{100} = 0.1 \qquad (17.4)$$

(b) a carbon balance equation:

$$\text{kg-mole C } \textbf{in} = \text{kg-mole C } \textbf{out}.$$

or:

$$1*\text{kg-mole } CO_2\ \textbf{in} = 1*\text{kg-mole } CO_2\ \textbf{out}$$

or:

$$0 = -1*\text{kg-mole } CO_2\ \textbf{in} + 1*\text{kg-mole } CO_2\ \textbf{out} \qquad (17.5).$$

Changed equations

CO_2-in-feed-gas also changes:

(a) oxygen balance Eqn. (14.7) to:

$$0 = -3*\text{kg-mole } SO_3\ \textbf{in} - 2*\text{kg-mole } SO_2\ \textbf{in} - 2*\text{kg-mole } O_2\ \textbf{in} - \underline{2*\text{kg-mole } CO_2\ \textbf{in}}$$
$$+ 3*\text{kg-mole } SO_3\ \textbf{out} + 2*\text{kg-mole } SO_2\ \textbf{out} + 2*\text{kg-mole } O_2\ \textbf{out} + \underline{2*\text{kg-mole } CO_2\ \textbf{out}}$$

(17.6)

(b) enthalpy balance Eqn. (14.8A) to:

$$\begin{aligned}
0 = &- \text{kg-mole } SO_3 \textbf{ in} * H^\circ_{T\,feed\,SO_3} \\
&- \text{kg-mole } SO_2 \textbf{ in} * H^\circ_{T\,feed\,SO_2} \\
&- \text{kg-mole } O_2 \textbf{ in} * H^\circ_{T\,feed\,O_2} \\
&- \text{kg-mole } N_2 \textbf{ in} * H^\circ_{T\,feed\,N_2} \\
&- \text{kg-mole } CO_2 \textbf{ in} * H^\circ_{T\,feed\,CO_2} \\
&+ \text{kg-mole } SO_3 \textbf{ out} * H^\circ_{T\,bed\,SO_3} \\
&+ \text{kg-mole } SO_2 \textbf{ out} * H^\circ_{T\,bed\,SO_2} \\
&+ \text{kg-mole } O_2 \textbf{ out} * H^\circ_{T\,bed\,O_2} \\
&+ \text{kg-mole } N_2 \textbf{ out} * H^\circ_{T\,bed\,N_2} \\
&+ \text{kg-mole } CO_2 \textbf{ out} * H^\circ_{T\,bed\,CO_2}
\end{aligned} \qquad (17.7)$$

where:

$H^\circ_{T\,feed}$ = enthalpy at the 1st catalyst bed feed gas temperature

$H^\circ_{T\,bed}$ = enthalpy at a temperature part way down the catalyst bed.

(c) nitrogen input quantity equation Eqn. (11.3) to:

$$\text{kg-mole } N_2 \textbf{ in} = \frac{\text{volume\% } N_2 \text{ in feed gas}}{100} = \frac{69 \text{ volume\% } N_2 \text{ in feed gas}}{100} = 0.69 \qquad (17.8)$$

because the feed gas contains 69 volume% N_2 rather than the 79 volume% N_2 in matrix Table 17.1.

All of these changes are summarized in heatup path matrix Table 17.3.

Table 17.3. 1st catalyst bed heatup path matrix with SO_3 and CO_2 in feed gas#. Cells D15 to H15 contain $-H^\circ_{690K}$ values. Cells I15 to M15 contain H°_{820K} values. All are calculated with Appendix G's enthalpy equations. 820 K part way down the catalyst bed is shown to be equivalent to oxidation of 46.7% of the feed gas's SO_2.

	A	B	C	D	E	F	G	H	I	J	K	L	M
1	**All calculations are based on 1 kg-mole of 1st catalyst bed feed gas.**												
2	volume% SO_2 in 1st catalyst bed feed gas =			10									
3	kg-mole SO_2 in 1 kg-mole of 1st catalyst bed feed gas = volume% SO_2/100% =					0.1	=D2/100	(11.1)					
4													
5	Equation	description	numerical term	kg-mole SO_3 **in**	kg-mole SO_2 **in**	kg-mole O_2 **in**	kg-mole N_2 **in**	kg-mole CO_2 **in**	kg-mole SO_3 **out**	kg-mole SO_2 **out**	kg-mole O_2 **out**	kg-mole N_2 **out**	kg-mole CO_2 **out**
6		feed SO_3 kg-mole	0	1	0	0	0	0	0	0	0	0	0
7	11.1	feed SO_2 kg-mole	0.10	0	1	0	0	0	0	0	0	0	0
8	11.2	feed O_2 kg-mole	0.11	0	0	1	0	0	0	0	0	0	0
9	17.8	feed N_2 kg-mole	0.69	0	0	0	1	0	0	0	0	0	0
10	17.4	feed CO_2 kg-mole	0.10	0	0	0	0	1	0	0	0	0	0
11	14.6	S balance	0	-1	-1	0	0	0	1	1	0	0	0
12	17.6	O balance	0	-3	-2	-2	0	-2	3	2	2	0	2
13	14.8	N balance	0	0	0	0	-2	0	0	0	0	2	0
14	17.5	C balance	0	0	0	0	0	-1	0	0	0	0	1
15		enthalpy balance	0	371.3	278.7	-12.21	-11.66	376.2	-362.0	-272.0	16.54	15.71	-369.7
16													
17						690 K feed#				820 K part way down catalyst bed			
18	Matrix results per kg-mole of 1st catalyst bed feed gas												
19	kg-mole SO_3 **in**	0.0000											
20	kg-mole SO_2 **in**	0.1000											
21	kg-mole O_2 **in**	0.1100											
22	kg-mole N_2 **in**	0.6900											
23	kg-mole CO_2 **in**	0.1000											
24	kg-mole SO_3 **out**	0.0467	% SO_2 oxidized equivalent to 820 K =			(kg-mole SO_2 **in** - kg-mole SO_2 **out**)/kg-mole SO_2 **in***100				(Eqn. 10.1)			
25	kg-mole SO_2 **out**	0.0533			=	(F3-B25)/F3*100		46.7	% SO_2 oxidized				
26	kg-mole O_2 **out**	0.0866											
27	kg-mole N_2 **out**	0.6900											
28	kg-mole CO_2 **out**	0.1000											

Feed gas: 0 volume% SO_3, 10 volume% SO_2, 11 volume% O_2, 69 volume% N_2, 10 volume% CO_2; 690 K

17.4 CO_2 Effects

Fig. 17.1 shows the effect of CO_2 on a 1st catalyst bed heatup path and intercept. CO_2 has no effect on equilibrium curves, Appendix F.

The heatup path is slightly steeper with CO_2. This is because:

(a) CO_2 replaces N_2 in Fig. 17.1

(b) CO_2 heat capacity > N_2 heat capacity, Appendix G.

The overall result is a slightly:

lower temperature

higher *% SO_2 oxidized*

intercept, Fig. 17.1.

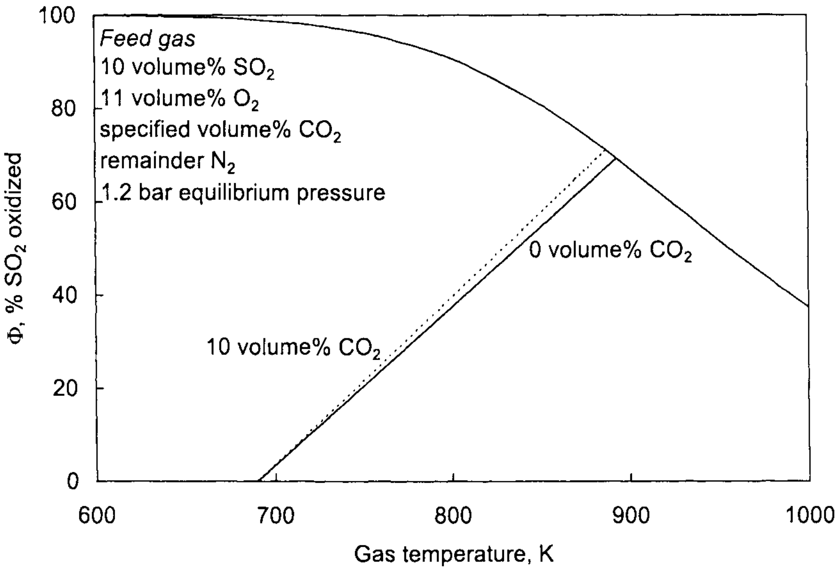

Fig. 17.1. Effect of CO_2-in-feed-gas on 1st catalyst bed heatup path and heatup path-equilibrium curve intercept. CO_2 increases heatup path slope and slightly increases intercept (equilibrium) *% SO_2 oxidized*, Section 17.4. Appendix Table R.1 describes the 10 volume% CO_2 intercept calculation.

17.5 Summary

Feed gas SO_3 and CO_2 are readily included in our catalyst bed calculations. SO_3 and CO_2 affect catalyst bed:

heatup paths

heatup-path/equilibrium curve intercepts.

SO_3 also affects $SO_2 + \frac{1}{2}O_2 \rightarrow SO_3$ equilibrium curves.

All the effects are quite small.

Problems

17.1 A sulfur burning 1st catalyst bed feed gas contains:

0.2 volume% SO_3
10.8 " SO_2
9.9 " O_2
79.1 " N_2

It enters a 1st catalyst bed at 695 K and 1.2 bar bed pressure.

Calculate:

(a) the percentage of the input SO_2 that will be oxidized when the gas's 1st catalyst bed intercept is attained

(b) the total kg-mole of SO_3 in the 1st catalyst bed's exit gas under these conditions (per kg-mole of 1st catalyst bed feed gas).

Use the technique described in Appendix Q.

17.2 A spent acid regeneration 1st catalyst bed feed gas contains:

10.5 volume% SO_2
10.5 " O_2
9.0 " CO_2
70.0 " N_2

It enters the 1st catalyst bed at 705 K. The bed is at 1.2 bar pressure.

Calculate the percentage of this gas's SO_2 that will be oxidized to SO_3 when the 1st catalyst bed intercept is attained. Use the technique described in Appendix R.

Compare this result to that of a:

10.5 volume% SO_2
10.5 " O_2
79.0 " N_2

1st catalyst bed feed gas under the same conditions.

CHAPTER 18

3 Catalyst Bed Acid Plant

Chapters 10 through 17 do separate 1st, 2nd and 3rd catalyst bed calculations. This chapter joins these calculations. Its objectives are to:

(a) combine Chapter 12 to 17's 1st, 2nd and 3rd catalyst bed intercept calculations in one Excel worksheet

(b) calculate 1st, 2nd and 3rd catalyst bed intercept SO_2 oxidation efficiencies for various feed gas compositions, gas input temperatures and bed pressures

(c) use (b)'s calculations to show how 3 catalyst bed SO_2 oxidation can be maximized.

18.1 Calculation Specifications

Chapter 12 through 17's intercept calculations are combined by specifying:

1. a 1st catalyst bed feed gas composition
2. 1st, 2nd and 3rd catalyst bed input gas temperatures
3. 1st, 2nd and 3rd catalyst bed equilibrium pressures
4. that equilibrium is attained in each catalyst bed
5. that a catalyst bed's exit gas composition is its intercept (equilibrium) gas composition
6. that gas composition doesn't change during gas cooldown.

Specifications 4 to 6 link the 1st, 2nd and 3rd catalyst bed calculations.

18.2 Example Calculation

Table 18.1 gives numerical specifications for an example 3 catalyst bed calculation. The calculation itself is described in Appendix S. The objective of the calculation is to determine intercept *% SO_2 oxidized* and temperature values for each of the 3 catalyst beds.

Table 18.1. Numerical specifications for Section 18.3 and 18.4 three catalyst bed calculations.

Description	Value
1st catalyst bed:	
feed gas composition	
volume% SO_3	0
volume% SO_2	10
volume% O_2	11
volume% N_2	79
volume% CO_2	0
feed gas temperature, K	690
bed pressure, bar	1.2
kg-mole SO_2 per kg-mole of feed gas	calculated
2nd catalyst bed	
input gas temperature, K	700
bed pressure, bar	1.2
3rd catalyst bed	
input gas temperature, K	710
bed pressure, bar	1.2

18.3 Calculation Results

The results of a 3 catalyst bed calculation with the above specifications are given in Table 18.2. They are plotted in Figs. 18.1 and 18.2. They show that 98% of 1st catalyst bed feed SO_2 is oxidized to SO_3 after 3 catalyst beds.

Table 18.2. Results of 3 catalyst bed calculation with Table 18.1 specifications. They are calculated in Appendix S. They are plotted in Fig. 18.1.

Description	Intercept temperature, K	Intercept % SO_2 oxidized
1st catalyst bed		
feed	690	0
intercept	893.3	69.2
2nd catalyst bed		
input	700	69.2
intercept	773.1#	94.2
3rd catalyst bed		
input	710	94.2
intercept	721.0#	98.0

These temperatures are 0.1 K lower than those calculated in Sections 15.2 and 16.3. The differences are due to different roundings.

18.4 3 Catalyst Bed Graphs

Fig. 18.1 shows Table 18.2's results as temperature *% SO_2 oxidized* points. Fig. 18.2 shows the results as:

(a) an equilibrium curve with 1.2 bar pressure in all beds

(b) heatup and cooldown paths.

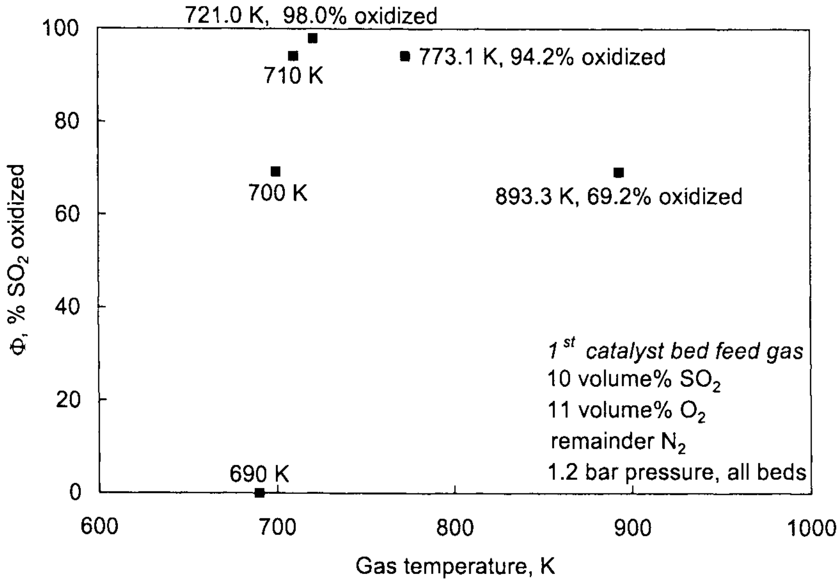

Fig. 18.1. Plot of Table 18.2 catalyst bed input and intercept points. The intercepts are the same as those in Sections 12.2, 15.2.1 and 16.4.

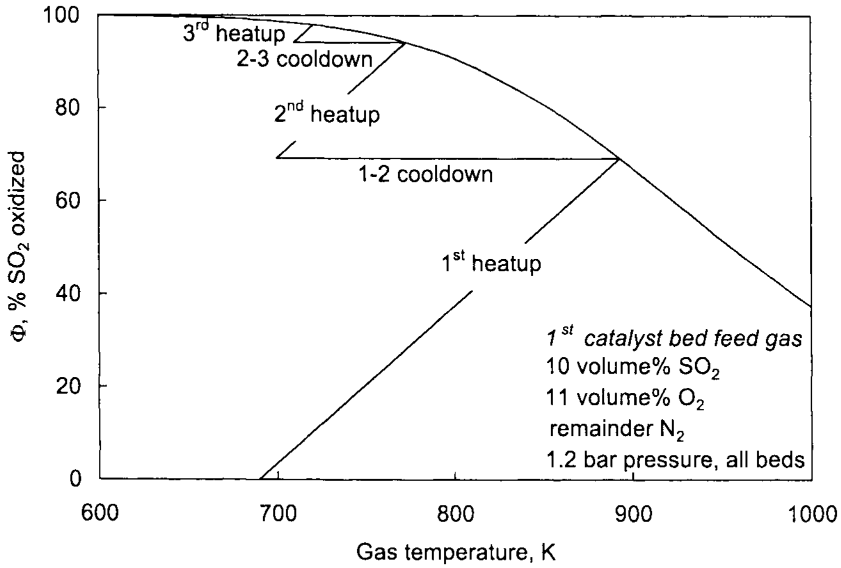

Fig. 18.2. Equilibrium curve and straight lines between Fig. 18.1's calculated points. The straight line heatup paths closely approximate the 'real' heatup paths in Chapters 11 through 17.

18.4.1 Straight heatup paths

Previous chapters indicate that heatup paths are slightly curved, Fig. 11.6. This and subsequent chapters represent heatup paths as straight lines between:

input and intercept points, Figs. 18.1 and 18.2.

This:

(a) simplifies graphing
(b) closely represents the previous chapters' 'real' heatup paths
(c) has no effect on intercept calculations, Fig. 18.1.

18.4.2 SO_2 oxidation efficiency

The following sections describe the effects of six industrial variables on 3-bed SO_2 oxidation efficiency. *Except where gas input temperature is variable, input gas temperature is 690 K, all beds.*

18.5 Minor Effect - SO_3 in Feed Gas

Industrial sulfur burning gas contains ~0.2 volume% SO_3 when it reaches an acid plant's 1st catalyst bed, Chapter 3. This SO_3 slightly affects:

equilibrium curves
heatup paths
equilibrium curve-heatup path intercepts,

Chapter 17 and Appendix P.

18.5.1 Effect of SO_3 on intercept % SO_2 oxidized

0.2 volume% SO_3 in acid plant feed gas has little effect on intercept *% SO_2 oxidized*, Table 18.3. The effect is noticeable after 1 and 2 beds – but not after 3 beds.

Nevertheless, feed SO_3 is included in our calculations, whenever specified.

18.6 Minor Effect – CO_2 in Feed Gas

Metallurgical and waste acid regeneration gases contain up to 8 volume% CO_2 – from fuels and waste acid hydrocarbons. This CO_2 has no effect on $SO_2 + \frac{1}{2}O_2 \longrightarrow SO_3$ equilibrium curves but it does affect:

heatup path slope
intercept temperature and *% SO_2 oxidized.*

The effect is quite small, especially after 3 beds, Fig. 18.3.

Table 18.3. Comparison of intercept *% SO_2 oxidized* values for feed gas containing 0 and 0.2 volume% SO_3. The difference after 3 beds is very small. The 1st catalyst bed feed gas contains 9.8 volume% SO_2, 11 volume% O_2, the specified amount of SO_3, remainder N_2. Gas pressure is 1.2 bar in all beds. Gas input temperature is 690 K, all beds.

	0.0 volume% SO_3 9.8 volume% SO_2 metallurgical or acid-regeneration feed gas	**0.2 volume% SO_3 9.8 volume% SO_2 sulfur-burning feed gas**
	% SO_2 oxidized	
1st catalyst bed		
feed	0	0
intercept	69.9	69.7
2nd catalyst bed		
input	69.9	69.7
intercept	95.2	95.1
3rd catalyst bed		
input	95.2	95.1
intercept	98.76	98.72

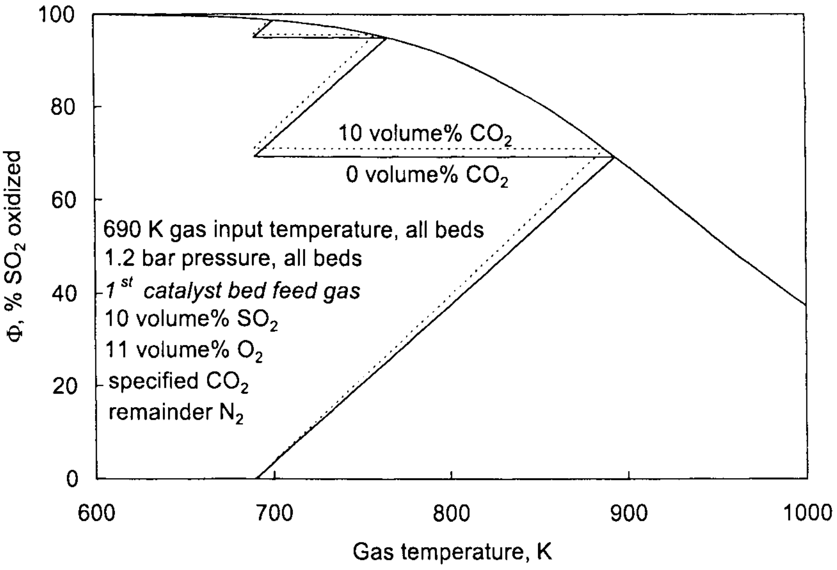

Fig. 18.3. Heatup paths and intercepts for 0 and 10 volume% CO_2 1st catalyst bed feed gas. CO_2 heatup paths are steeper than non CO_2 heatup paths because CO_2 heat capacity > N_2 heat capacity, Appendix G. The steeper paths give higher intercept *% SO_2 oxidized* values in each catalyst bed.

18.7 Minor Effect – Bed Pressure

Industrial catalyst bed pressures are typically 1.1 to 1.4 bar. They are highest in 1st catalyst beds and lowest in last beds – due to dissipation of mechanical energy as gas passes through the beds.

The effect of bed pressure on intercept *% SO_2 oxidized* is shown in Fig. 18.4. It is small, especially after 3 catalyst beds.

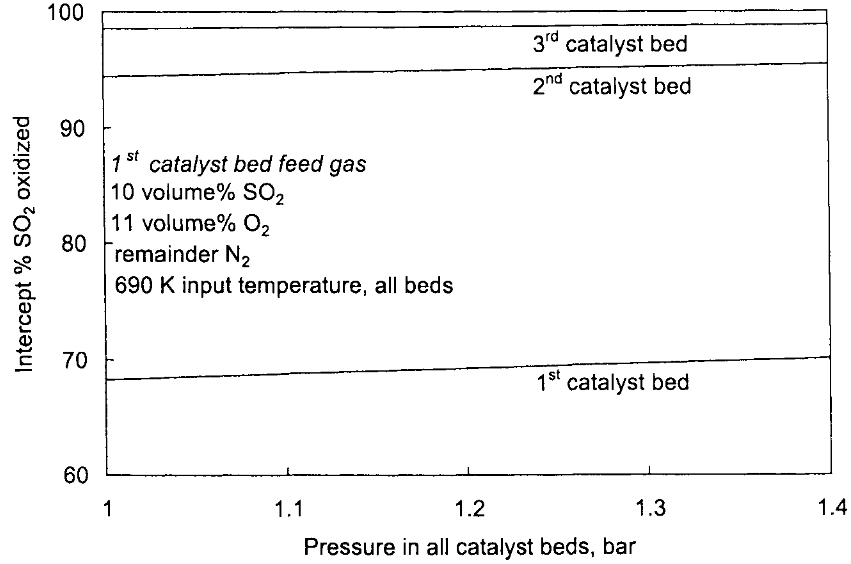

Fig. 18.4. Effect of gas pressure on intercept SO_2 oxidation efficiency. The lines show that *% SO_2 oxidized* increases with increasing pressure, all beds. After 3 catalyst beds the effect is small.

18.7.1 Validity of constant pressure specification

Figs. 18.1 through 18.4 specify the same pressure in all 3 catalyst beds. This specification is not necessary – the Appendix S worksheet can specify individual bed pressures. It is, however, convenient for graphing.

Fig. 18.5 compares intercept *% SO_2 oxidized* results for:

(a) 1.2 bar pressure in all beds

(b) 1.3, 1.2 and 1.1 bar pressure in beds 1, 2 and 3.

The difference between the results is tiny, especially after 3 beds.

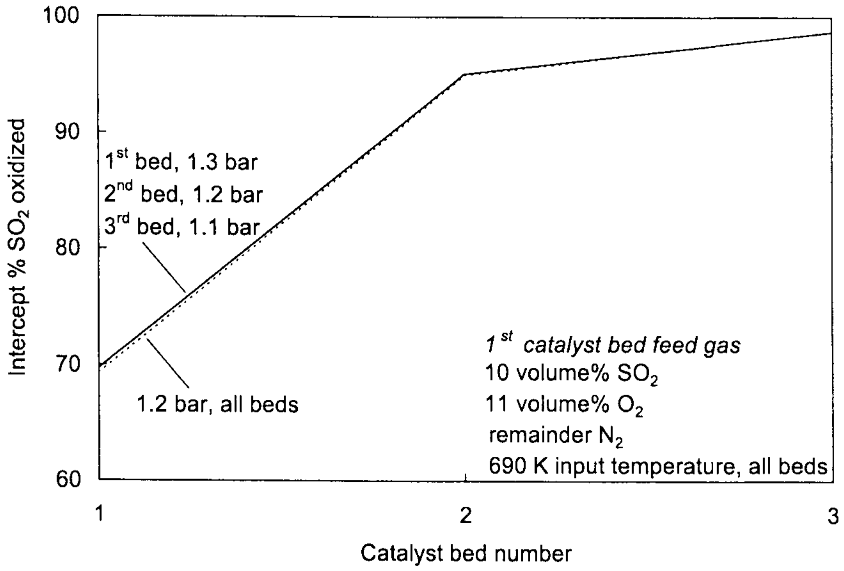

Fig. 18.5. Comparison of intercept SO_2 oxidation efficiency with (i) 1.2 bar pressure in all beds and (ii) 1.3, 1.2 and 1.1 bar pressure in beds 1, 2 and 3. After 3 beds, the predicted efficiencies are virtually identical.

18.8 Minor Effect – SO_2 Strength in Feed Gas

SO_2 strength in industrial catalytic oxidation feed gas varies from ~8 volume% to ~12 volume%, Table 7.2. The strength depends mainly on the preceding SO_2 production process.

Fig. 18.6 describes the effect of SO_2 concentration on intercept SO_2 oxidation efficiency. It indicates that:

(a) 1st and 2nd bed SO_2 oxidation efficiency decreases significantly with increasing volume% SO_2 in feed gas

(b) 3rd bed SO_2 oxidation efficiency is only slightly affected by feed SO_2 concentration.

Industrial plants could send higher SO_2 strength gas to their acid plant – by enriching their combustion air with oxygen (Miller and Parekh, 2004). This strong SO_2 would:

(a) give a large production of sulfuric acid per Nm^3 of gas passed through the acid plant

(b) only slightly lower SO_2 oxidation efficiency.

It would, however, tend to give catalyst overheating and degradation in the 1st catalyst bed, Section 12.11. For this reason, 12 volume% SO_2 is about the maximum strength used in industrial acid plants.

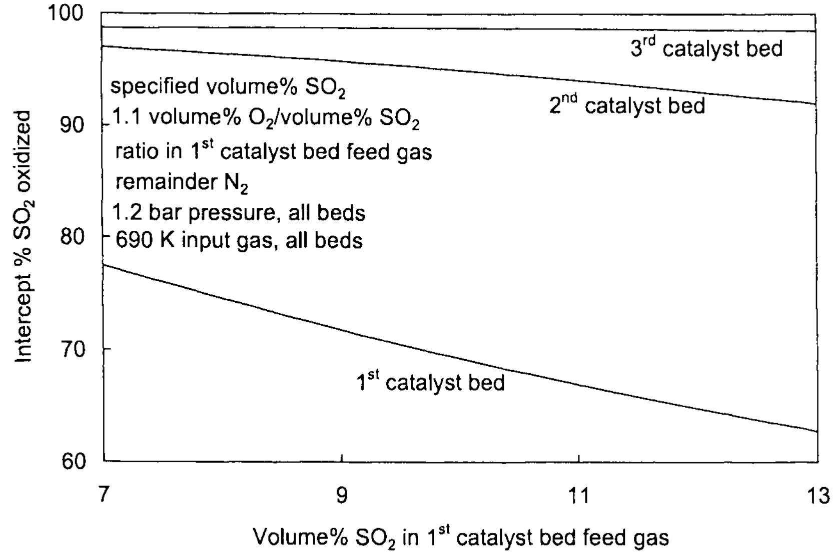

Fig. 18.6. Effect of 1st catalyst bed feed gas SO_2 strength on intercept SO_2 oxidation efficiency. The effect is significant after beds 1 and 2 but not after bed 3. The lower SO_2 oxidation efficiency with higher SO_2 strength is explained in Section 11.13.1 and Fig. 12.3.

18.9. Minor Effect – O_2 Strength in Feed Gas

Fig. 18.7 shows the effect of feed gas O_2 strength on intercept SO_2 oxidation efficiency.

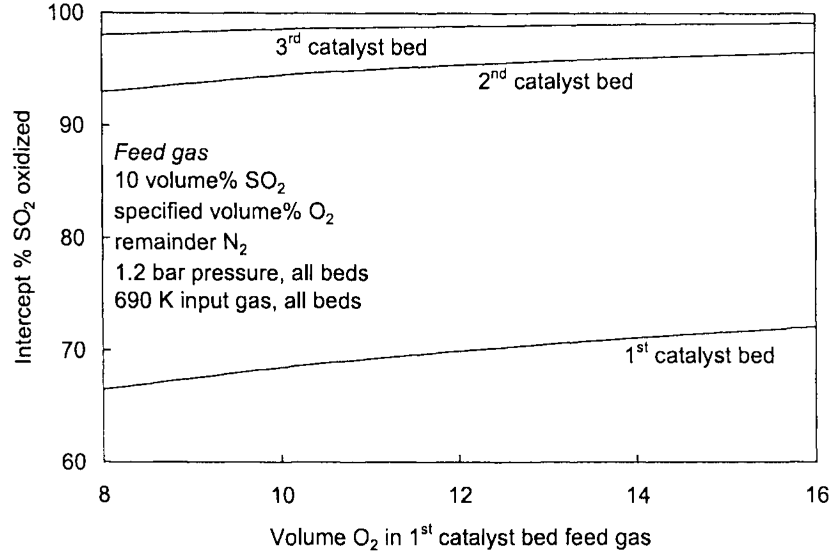

Fig. 18.7. Effect of volume% O_2 in feed gas on intercept SO_2 oxidation efficiency. *% SO_2 oxidized* increases with increasing O_2 strength – but the effect is small, especially after 3 catalyst beds.

% SO_2 oxidized increases with increasing O_2 strength. However, the effect is quite small, especially after 3 catalyst beds.

8 to 16 volume% O_2 in Fig. 18.8 are equivalent to volume% O_2/volume% SO_2 ratios of:

0.8 and 1.6.

These are typical industrial O_2/SO_2 ratios, Table 7.2.

18.10 Summary of Minor Effects

Sections 18.5 through 18.9 indicate that:

volume% SO_3 in feed gas
" CO_2 "
" SO_2 "
" O_2 "
catalyst bed pressure

have little effect on 3 bed catalytic SO_2 oxidation efficiency. Also, these variables are often not readily adjusted – because they are either:

(a) the result of their preceding SO_2 production process

or:

(b) the consequence of atmospheric pressure and the pressure required to move gas through catalyst beds and other equipment.

In fact, the only truly adjustable parameters in industrial SO_2 oxidation are catalyst bed input gas temperatures, next section.

18.11 Major Effect – Catalyst Bed Input Gas Temperatures

Catalyst bed input gas temperatures are readily adjusted by heating and cooling the gas in boilers, economizers, heat exchangers etc. Industrial input temperatures vary from ~660 K to 720 K, Table 7.2.

Figs. 18.8 and 18.9 show how catalyst bed input gas temperature affects intercept SO_2 oxidation efficiency. Efficiency increases significantly with decreasing input gas temperature.

This is because:

(a) low gas input temperatures give low intercept temperatures, Fig. 18.8.

(b) low intercept temperatures give high SO_2 oxidation efficiencies.

This result suggests that industrial catalyst bed input gases should always be as cool as possible – consistent with steady, well controlled, long term catalyst bed operation.

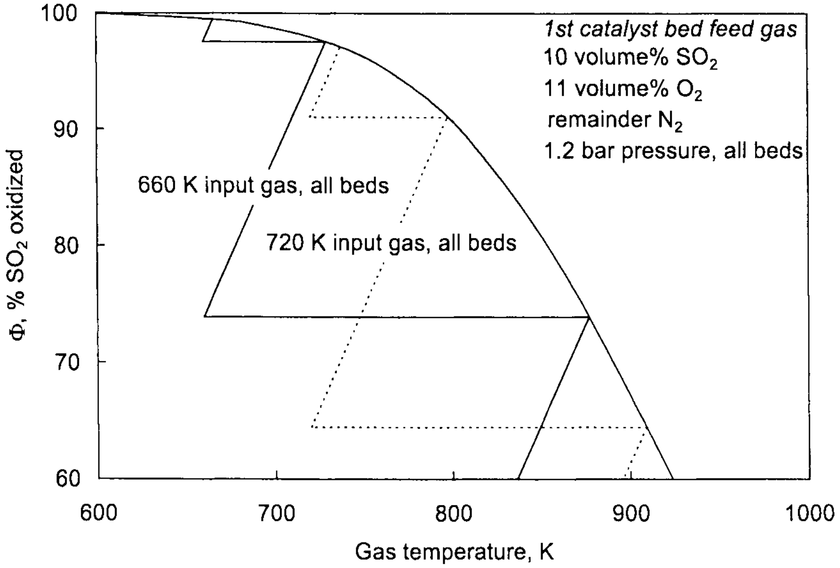

Fig. 18.8. Three catalyst bed oxidation with 660 and 720 K input gas, all beds. 660 K input gas gives significantly more SO_2 oxidation. Notice that two catalyst beds with 660 K input gas give more SO_2 oxidation than three catalyst beds with 720 K input gas. The graph is the top portion of a graph like Fig. 18.3.

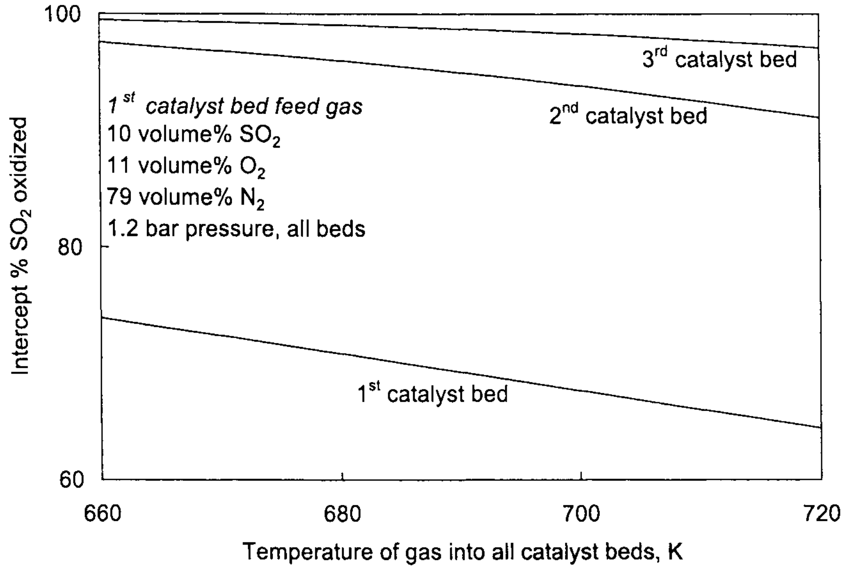

Fig. 18.9. Intercept *% SO_2 oxidized* values as a function of catalyst bed gas input temperature. SO_2 oxidation efficiency is seen to increase with decreasing input gas temperature.

18.12 Discussion of Book's Assumptions

This book makes three assumptions:

(a) that all processes are proceeding under steady state conditions, i.e. that temperatures and compositions are not changing with time anywhere in the system

(b) that there are no conductive, convective plus radiative heat losses from the system's catalyst beds

(c) that intercept (equilibrium) SO_2 oxidation is achieved in all catalyst beds.

This section discusses these three assumptions.

18.12.1 Steady state assumption

Sulfur burning acid plants operate steadily almost all the time. The main significance of this is that temperature is constant at every point in the plant's catalyst beds. It means that none of the gas's heat is being used to heat catalyst.

Metallurgical and spent acid regeneration plants are not quite so steady, but the steady state assumption is still reasonable.

18.12.2 No heat loss assumption

The assumption of no conductive, convective plus radiative heat loss from catalytic SO_2 oxidation converters is not perfectly correct. There is always some heat loss. Nevertheless:

(a) gas-in-catalyst bed residence times are short (~2 seconds per bed, Fig. 8.4)

(b) catalyst converters are well insulated

so that heat loss per kg-mole of gas is probably quite small.

Fig. 18.10 demonstrates the effect that heat loss would have on our SO_2 oxidation calculations.

18.12.3 Intercept attainment assumption

It is not easy to know how close industrial catalytic SO_2 oxidation comes to equilibrium. Our opinion is that it comes quite close, especially if the beds are run somewhat above their catalyst activation temperature. The effect of non-attainment is demonstrated in Fig. 18.10.

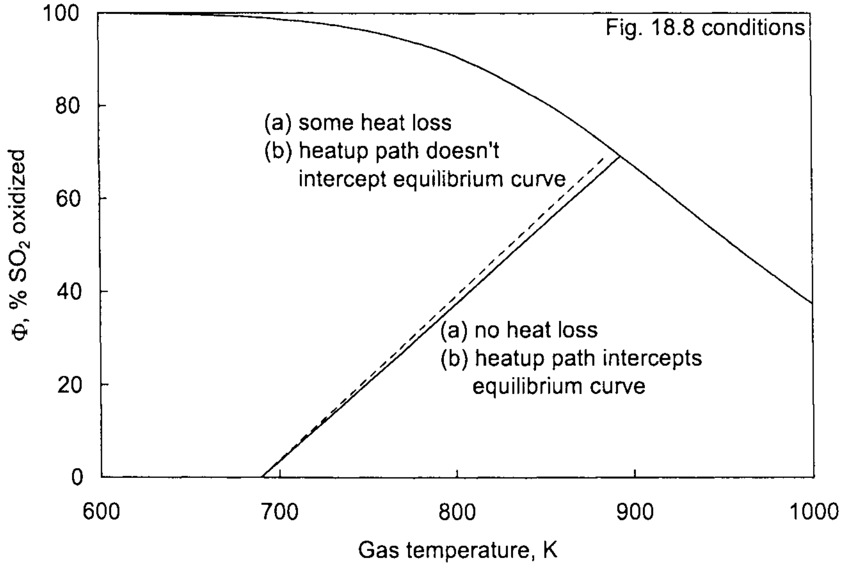

Fig. 18.10. Effect of:

conductive, convective plus radiative heat loss
non-attainment of equilibrium

on a 1st catalyst bed's final % SO_2 oxidized. The two effects are seen to offset each other. (The heat loss heatup path is steeper because less heat is available to warm the gas.)

18.13 Summary

This chapter combines Chapter 12 to 17's intercept calculations in a single worksheet. It then shows how:

SO_3 concentration in feed gas
CO_2 " "
SO_2 " "
O_2 " "
catalyst bed pressure
catalyst bed input gas temperature

affect intercept (equilibrium) catalytic SO_2 oxidation efficiency.

Only input gas temperature has a significant effect. Cool input gas (but warm enough for rapid SO_2 oxidation) gives highly efficient SO_2 oxidation. Warmer input gas gives less efficient oxidation.

Reference

Miller, D. and Parekh, U. (2004) Upgrading virgin acid plants using oxygen. *Sulfur*, **290**, January-February, 2004, 43-47. www.britishsulphur.com

CHAPTER 19

After-H_2SO_4-Making SO_2 Oxidation

Many acid plants:

(a) catalytically oxidize most of their input SO_2 to SO_3 in 3 (occasionally 2 or 4) catalyst beds, Fig. 19.1

then:

(b) make $H_2SO_4(\ell)$ from the resulting $SO_3(g)$

then:

(c) catalytically oxidize the SO_2 remaining in step (b)'s exit gas – in 1 (occasionally 2) additional catalyst beds

then:

(d) make $H_2SO_4(\ell)$ from (c)'s new SO_3.

The process is called double contact acidmaking because gas and sulfuric acid are contacted twice, steps (b) and (d).

The (a) and (c) reaction is:

$$\underset{\text{in feed gas}}{SO_2(g)} + \frac{1}{2}O_2(g) \xrightarrow[\text{catalyst}]{700\text{-}900\text{ K}} SO_3(g) \qquad (1.1).$$

The (b) and (d) reaction is:

$$\underset{\substack{\text{in Eqn.(1.1)}\\ \text{product gas}}}{SO_3(g)} + \underset{\substack{\text{in strong}\\ \text{sulfuric acid}}}{H_2O(\ell)} \xrightarrow{350\text{-}380\text{ K}} \underset{\substack{\text{in strengthened}\\ \text{sulfuric acid}}}{H_2SO_4(\ell)} \qquad (1.2).$$

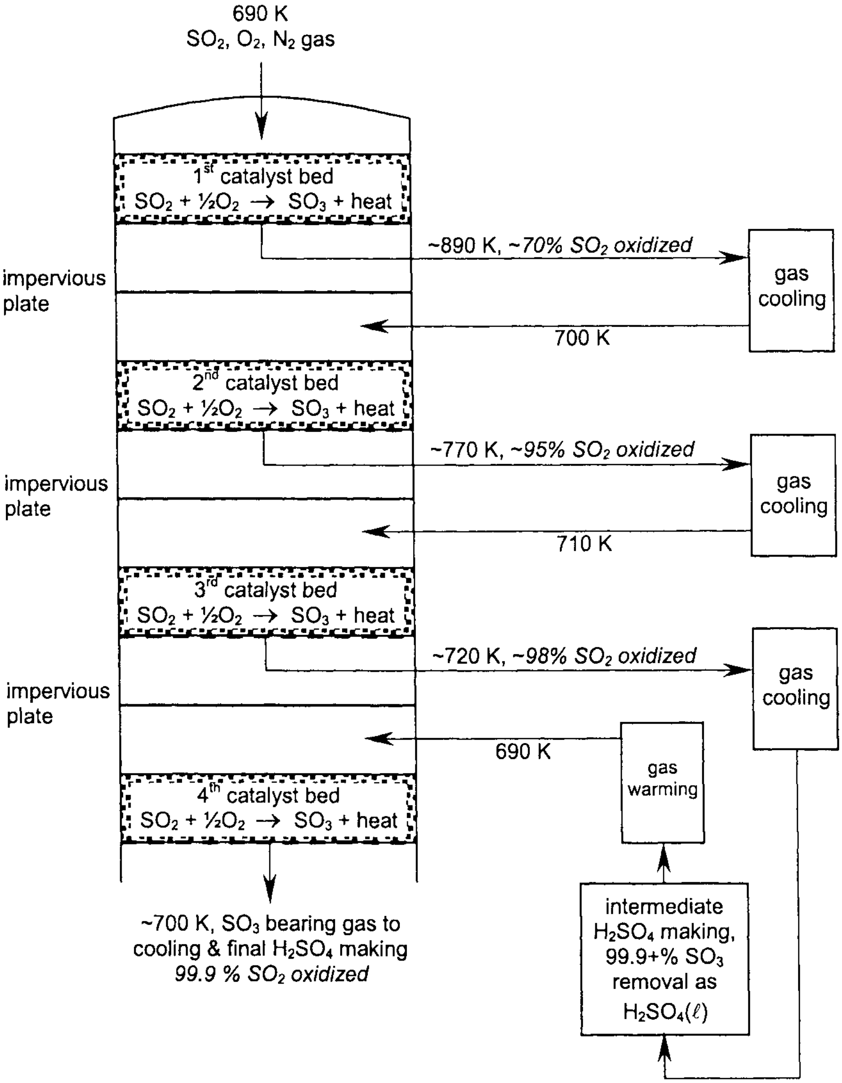

Fig. 19.1. Schematic of 3-1 double contact sulfuric acid plant. The plant consists of:

3 catalyst beds before intermediate H_2SO_4 making
intermediate H_2SO_4 making, Eqn. (1.2)
1 catalyst bed after intermediate H_2SO_4 making#
final H_2SO_4 making (not shown).

The increase in *% SO_2 oxidized* after each bed is notable. Other industrial versions of double contact acid plants are:

2 catalyst beds before H_2SO_4 making, 2 beds after
4 catalyst beds before H_2SO_4 making, 1 bed after, Chapter 20.

#See Table 19.3 (end of this chapter) for industrial after H_2SO_4 making catalyst bed data.

19.1 Double Contact Advantage

Double contact acidmaking always gives more efficient $SO_2 + ½O_2 \rightarrow SO_3$ oxidation than single contact acidmaking. This leads to:

(a) more efficient SO_3 (hence H_2SO_4) production

(b) less SO_2 emission to the environment or a smaller SO_2-from-gas scrubbing plant.

The reason for double contact's high SO_2 oxidation efficiency is given in Figs. 19.6 and 19.7.

19.2 Objectives

The objectives of this chapter are to:

(a) show how after-intermediate-H_2SO_4-making SO_2 oxidation:
equilibrium curves
heatup paths
heatup path-equilibrium curve intercepts
are calculated

and to:

(b) calculate the SO_2 oxidation efficiency of Fig. 19.1's 3-1 double contact acid plant

(c) compare (b)'s SO_2 oxidation efficiency with that of a 4 catalyst bed single contact acid plant

(d) identify the extra costs of double contact acidmaking.

19.3 After-H_2SO_4-Making Calculations

The starting point for this chapter's calculations is the product gas from a specific:

3 catalyst bed + intermediate H_2SO_4 making

sequence, Fig. 19.2.

The exit gas from the 3 catalyst beds is specified to be that in Section 16.4. It contains:

0.098 kg-mole SO_3 (Fig. 19.2)

0.002 kg-mole SO_2

0.061 kg-mole O_2

0.790 kg-mole N_2

per kg-mole of 1st catalyst bed feed gas.

This gas goes to intermediate H_2SO_4 making where 100% of its SO_3 is specified as being removed as $H_2SO_4(\ell)$. The gas departing this step contains:

0.000 kg-mole SO_3 (Fig. 19.2)

0.002 kg-mole SO_2

0.061 kg-mole O_2

0.790 kg-mole N_2
0.853 total kg-mole

per kg-mole of 1st catalyst bed feed gas. It is sent to further catalytic SO_2 oxidation in Fig. 19.2's 4th catalyst bed.

Appendix U examines the case where less than 100% of H_2SO_4 making's input SO_3 is made into H_2SO_4.

19.4 Equilibrium Curve Calculation

This chapter treats after-H_2SO_4-making SO_2 oxidation as a completely new problem. This is necessary because selective SO_3 removal from gas during $H_2SO_4(\ell)$ making invalidates Appendix B's before-H_2SO_4-making equations.

The after intermediate H_2SO_4 making equilibrium curve equation is:

$$T_E = \frac{-B}{A + R * \ln\left(\left(\frac{\Phi^{E\ after}}{100 - \Phi^{E\ after}} \right) * \left(\frac{100 - \frac{1}{2} * e' * \frac{\Phi^{E\ after}}{100}}{f' - \frac{1}{2} * e' * \frac{\Phi^{E\ after}}{100}} \right)^{\frac{1}{2}} * P_t^{-\frac{1}{2}} \right)} \qquad (19.1)$$

where T_E, A, B, R and P_t are the same as in Eqn (10.13), Section 15.1,

and where:

e' and f' are volume% SO_2 and O_2 in 1st after-intermediate-H_2SO_4-making catalyst bed input gas

$\Phi^{E\ after}$ = equilibrium percentage of after-H_2SO_4-making input SO_2 that is oxidized in an after-H_2SO_4-making catalyst bed.

Eqn. (19.1) is similar to before-H_2SO_4-making equilibrium Eqn. (10.13), Section 15.1. It is derived the same way.

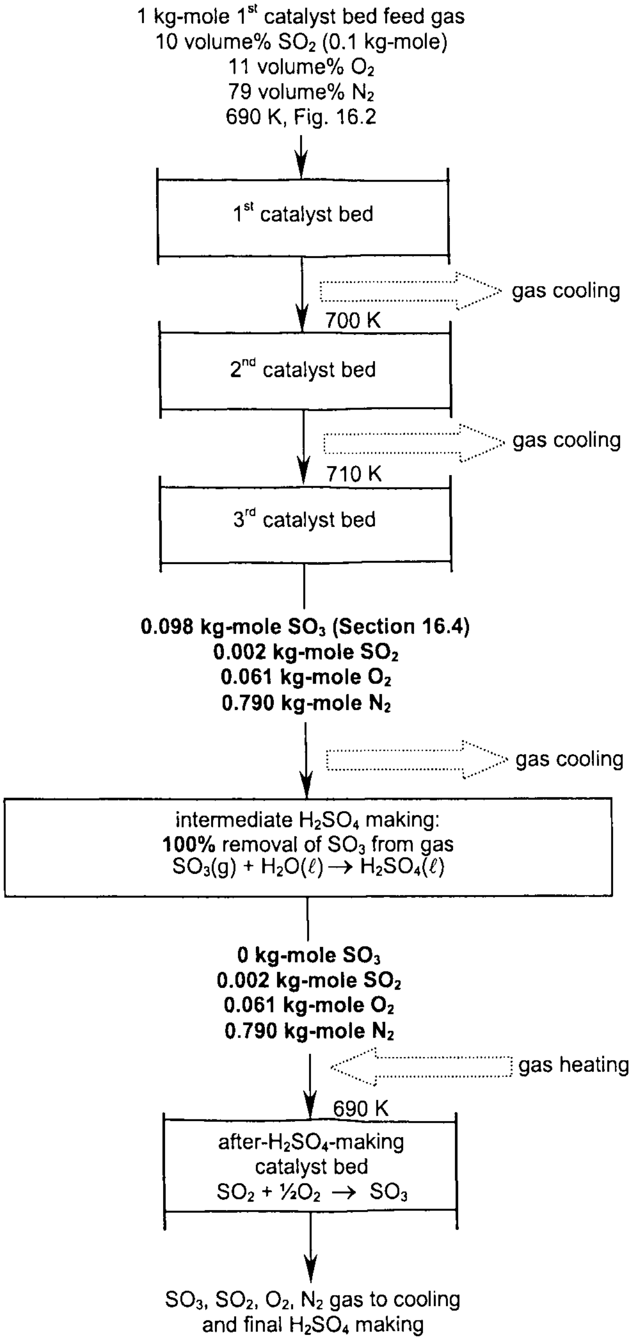

Fig. 19.2. Double contact acidmaking flowsheet with numerical values used in this chapter's calculations. The plant consists of 3 catalyst beds followed by intermediate H_2SO_4 making and a 4th catalyst bed. The gas from the last catalyst bed goes to cooling and final H_2SO_4 making (not shown). All kg-mole values are per kg-mole of 1st catalyst bed feed gas. Gas pressure = 1.2 bar, all beds.

19.4.1 e' and f '

e' and f ' are volume% SO_2 and O_2 in <u>1st after-H_2SO_4-making catalyst bed</u> input gas. They are calculated from Fig. 19.2's intermediate H_2SO_4 making exit gas quantities, as follows:

$$e' = \text{volume\% } SO_2 = \text{mole\% } SO_2 = \frac{\text{kg-mole } SO_2}{\text{total kg-mole}} * 100\%$$

$$= \frac{0.002}{0.853} * 100\% = 0.234\%$$

and:

$$f' = \text{volume\% } O_2 = \text{mole\% } O_2 = \frac{\text{kg-mole } O_2}{\text{total kg-mole}} * 100\%$$

$$= \frac{0.061}{0.853} * 100\% = 7.15\%$$

19.4.2 After-H_2SO_4-making % SO_2 oxidized defined

After-intermediate-H_2SO_4-making *% SO_2 oxidized* is defined as:

$$\begin{array}{l}\textit{\%SO}_2\textit{ oxidized}\text{ in}\\ \textbf{after}\text{-}H_2SO_4\text{-making}\\ \text{catalyst beds}\end{array} = \Phi^{after} = \frac{\begin{array}{l}\text{kg-mole } SO_2 \text{ in 1}^{st}\\ \textbf{after}\text{-}H_2SO_4\text{-making}\\ \text{catalyst bed input gas}\end{array} - \begin{array}{l}\text{kg-mole } SO_2 \text{ in any}\\ \textbf{after}\text{-}H_2SO_4\text{-making}\\ \text{catalyst bed's oxidized gas}\end{array}}{\begin{array}{l}\text{kg-mole } SO_2 \text{ in } \textbf{1}^{st}\ \textbf{after}\text{-}H_2SO_4\\ \text{-making catalyst bed input gas}\end{array}} * 100 \qquad (19.2)$$

(all quantities per kg-mole of 1st before-H_2SO_4-making catalyst bed feed gas).

When equilibrium is attained in an after-H_2SO_4-making catalyst bed, Φ^{after} becomes:

$$\begin{array}{l}\textit{Equilibrium \%SO}_2\\ \textit{oxidized}\text{ in }\textbf{after}\text{-}H_2SO_4\\ \text{-making catalyst beds}\end{array} = \Phi^{E\ after} =$$

$$\frac{\begin{array}{l}\text{kg-mole } SO_2 \text{ in 1}^{st}\\ \text{after-}H_2SO_4\text{-making}\\ \text{catalyst bed input gas}\end{array} - \begin{array}{l}\text{kg-mole } SO_2 \text{ in oxidized gas in any}\\ \text{after-}H_2SO_4\text{-making catalyst bed}\\ \text{where equilibrium has been attained}\end{array}}{\text{kg-mole } SO_2 \text{ in } \textbf{1}^{st}\ \textbf{after}\text{-}H_2SO_4\text{-making catalyst bed input gas}} * 100 \qquad (19.3).$$

19.4.3 Preparation of equilibrium curve

After-intermediate-H_2SO_4-making equilibrium curves are prepared from Eqn. (19.1) as described in Appendix D. e', f' and P_t are specified and equilibrium temperatures are calculated for a series of $\Phi^{E\ after}$ values (or vice versa). Fig. 19.3 shows the after-H_2SO_4-making equilibrium curve with this chapter's specifications.

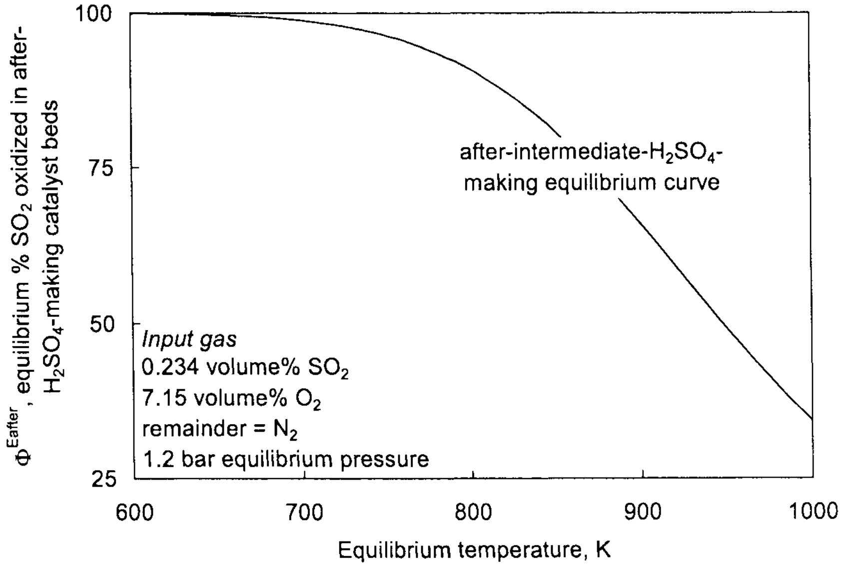

Fig. 19.3. Equilibrium curve for after-H_2SO_4-making catalyst beds. It is quite similar to Chapter 10.1's before-H_2SO_4-making curves. Input gas composition and equilibrium pressure specifications are shown. The curve is only valid for these specifications. $\Phi^{E\ after}$ is defined by Eqn. (19.3).

19.5 Heatup Path Calculation

After-intermediate-H_2SO_4-making heatup paths are calculated exactly as before-H_2SO_4-making heatup paths, Chapter 11 and Appendix I. Table 19.1 shows the matrix for this chapter's after-H_2SO_4-making input gas. Fig. 19.4 shows an equivalent partial heatup path.

19.6 Heatup Path Equilibrium Curve Intercept Calculation

Maximum SO_2 oxidation in a catalyst bed is obtained where its:

heatup path

intercepts its:

equilibrium curve.

Table 19.1. Heatup path matrix for after-intermediate-H_2SO_4-making catalyst bed. The 1st three rows represent the equations:

$$n_{SO_2}\ \mathbf{in} = 0.002 \text{ kg-mole, Fig. 19.2} \qquad (19.4)$$

$$n_{O_2}\ \mathbf{in} = 0.061 \text{ kg-mole} \qquad (19.5)$$

$$n_{N_2}\ \mathbf{in} = 0.790 \text{ kg-mole.} \qquad (19.6)$$

All values are per kg-mole of 1st before-H_2SO_4 making catalyst bed feed gas. The matrix shows that a 695 K gas temperature is equivalent to oxidation of 69.3% of the after-H_2SO_4-making catalyst bed's input SO_2. Cells D8 to F8 contain -H° values, Eqn. (11.7). Cells G8 to J8 contain H° values.

	A	B	C	D	E	F	G	H	I	J
1	Equation	Description	numerical term	kg-mole SO_2 **in**	kg-mole O_2 **in**	kg-mole N_2 **in**	kg-mole SO_3 **out**	kg-mole SO_2 **out**	kg-mole O_2 **out**	kg-mole N_2 **out**
2	19.4	input SO_2 kg-mole	0.0020	1	0	0	0	0	0	0
3	19.5	input O_2 kg-mole	0.0610	0	1	0	0	0	0	0
4	19.6	input N_2 kg-mole	0.7900	0	0	1	0	0	0	0
5	11.4	S balance	0	-1	0	0	1	1	0	0
6	11.5	O balance	0	-2	-2	0	3	2	2	0
7	11.6	N balance	0	0	0	-2	0	0	0	2
8		enthalpy balance	0	278.7	-12.21	-11.66	-370.9	-278.4	12.37	11.82
9										
10					690 K, input			695 K		
11										
12	Matrix results per kg-mole of 1st before-H_2SO_4-making feed gas									
13	kg-mole SO_2 **in**	0.0020								
14	kg-mole O_2 **in**	0.0610								
15	kg-mole N_2 **in**	0.7900								
16	kg-mole SO_3 **out**	0.0014			% SO_2 oxidized = Φ^{after} =	(kg-mole SO_2 **in** - kg-mole SO_2 **out**)/kg-mole SO_2 **in***100				(Eqn. 19.2)
17	kg-mole SO_2 **out**	0.0006			=	(B13-B17)/B13*100	=	69.3	%	
18	kg-mole O_2 **out**	0.0603								
19	kg-mole N_2 **out**	0.7900								

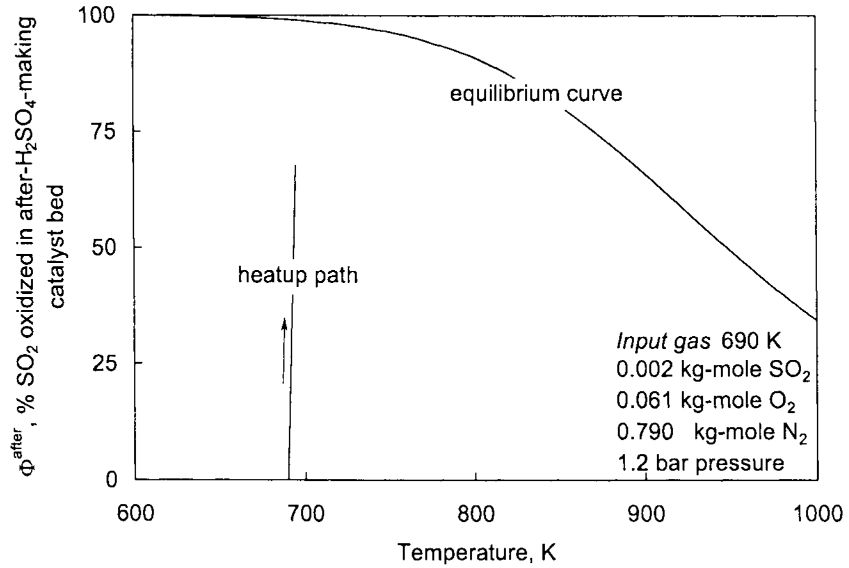

Fig. 19.4. Equilibrium curve and partial heatup path for after-intermediate-H_2SO_4-making catalyst bed. The heatup path has been calculated with matrix Table 19.1 as in Appendix I. The steepness of the heatup path is due to the small amount of SO_2 'fuel' in the input gas. The equilibrium curve and heatup path are only valid for the specified inputs. The SO_2 and O_2 inputs are equivalent to 0.234 volume% SO_2 and 7.15 volume% O_2.

This chapter's after-H_2SO_4-making SO_2 oxidation intercept is shown in Table 19.2 and Figs. 19.5/19.6. It occurs at 697.3 K with 98.9% of the after-H_2SO_4-making catalyst bed input SO_2 oxidized to SO_3.

Table 19.2. After-intermediate-H_2SO_4-making *% SO_2 oxidized*-temperature points near heatup path-equilibrium curve intercept#. The intercept temperature is shown to be between 697.30 and 697.31 K. The points are calculated as described in Appendices D and I. They are plotted in Fig. 19.5.

Temperature, K	Heatup path *% SO_2 oxidized*, Φ^{after}	Equilibrium *% SO_2 oxidized*, $\Phi^{E\ after}$
697.26		98.886
697.27	98.354	98.886
697.28	98.490	98.885
697.29	98.635	98.885
697.30	98.760	98.885
697.31	98.896	98.885
697.32	99.031	98.884
697.33	99.166	98.884
697.34	99.302	98.884
697.35		98.884

#Input gas: 690 K; 0.002 kg-mole SO_2, 0.061 kg-mole O_2, 0.790 kg-mole N_2 (0.234 volume% SO_2, 7.15 volume% O_2); 1.2 bar equilibrium pressure.

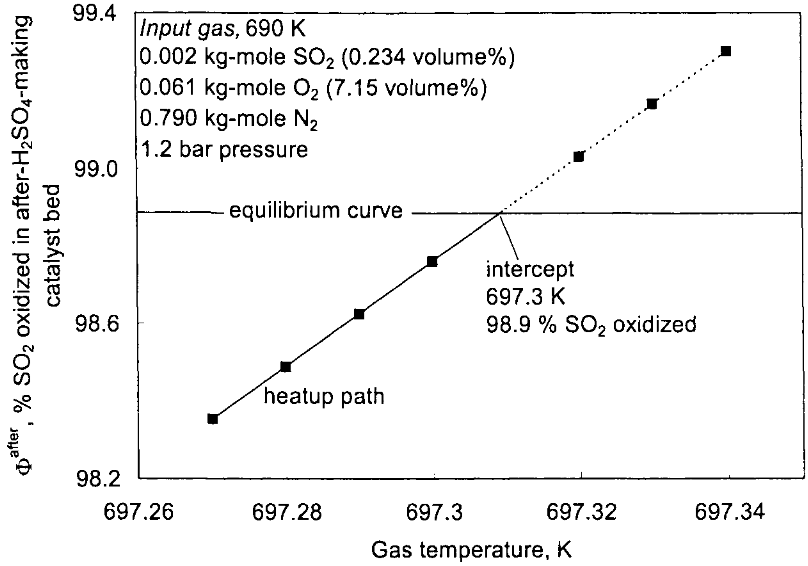

Fig. 19.5. Equilibrium curve, heatup path and heatup path-equilibrium curve intercept for after-intermediate-H_2SO_4-making catalyst bed. Attainment of equilibrium in the catalyst bed gives 98.9% oxidation of the bed's input SO_2. The lines apply only to the graph's specified inputs and bed pressure. This graph is a blowup of Fig. 19.6. Its intercept is confirmed by a Goal Seek calculation in Appendix T. The SO_2 and O_2 inputs are equivalent to 0.234 volume% SO_2 and 7.15 volume% O_2.

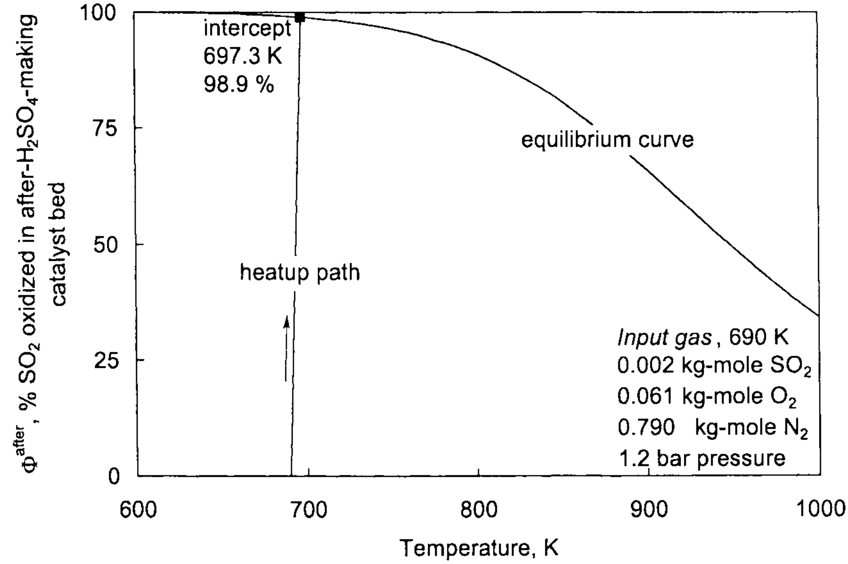

Fig. 19.6. Overall view of after-intermediate-H_2SO_4-making SO_2 oxidation. The high intercept *% SO_2 oxidized* is notable. It is due to the low intercept temperature. The SO_2 and O_2 inputs are equivalent to 0.234 volume% SO_2 and 7.15 volume% O_2.

This 98.9% efficiency is equivalent to:

0.001978 kg-mole SO_3

0.000022 kg-mole SO_2

0.060011 kg-mole O_2

0.790000 kg-mole N_2

in after-H_2SO_4-making catalyst bed exit gas, Appendix T.

19.7 Overall SO_2 Oxidation Efficiency

So far, this chapter has examined after-intermediate-H_2SO_4-making SO_2 oxidation efficiency. However, Section 19.6 also provides the information needed to calculate total % SO_2 oxidized after SO_2 oxidation in all of Fig. 19.2's catalyst beds. The values are:

from Fig. 19.2: **kg-mole SO_2 in 1st catalyst bed feed gas** **= 0.1**

from Section 19.6: **kg-mole SO_2 in after-intermediate-H_2SO_4-making catalyst bed exit gas** **= 0.000022**

(both per kg-mole of 1st catalyst bed feed gas).

Total SO_2 oxidation efficiency is calculated by the equation:

$$\text{total } \%\, SO_2 \text{ oxidized} = \Phi^{\text{total}} = \frac{\begin{matrix}\text{kg-mole } SO_2 \text{ in } 1^{\text{st}} \\ \text{catalyst bed feed gas}\end{matrix} - \begin{matrix}\text{kg-mole } SO_2 \text{ in last} \\ \text{catalyst bed exit gas}\end{matrix}}{\text{kg-mole } SO_2 \text{ in } 1^{\text{st}} \text{ catalyst bed feed gas}} * 100 \tag{19.7}$$

where all quantities are per kg-mole of 1st catalyst bed feed gas.

The above numerical values give:

$$\textbf{Total } \%SO_2 \textbf{ oxidized after 3 before-}H_2SO_4\textbf{-making beds and 1 after-}H_2SO_4\textbf{-making catalyst bed} = \frac{(0.1 - 0.000022)}{0.1} * 100\% = 99.98\%$$

This is somewhat above industrial total SO_2 oxidation (99.5-99.9%: Hansen, 2004), but it confirms the high SO_2 oxidation and H_2SO_4 making efficiencies of double contact acid plants.

19.7.1 Effect of incomplete SO_3-from-gas removal during intermediate H_2SO_4 making

Chapter 9 indicates that SO_3-from-gas removal during H_2SO_4 making may be 99.9% rather than 100%. This would mean that 0.1% of Fig. 19.2's H_2SO_4 making input SO_3 (0.0001 kg-mole) would get through to after-H_2SO_4-making SO_2 oxidation.

Appendix U examines this situation. It shows that this small amount of SO_3 has little effect on double contact's overall SO_2 oxidation efficiency.

19.8 Double/Single Contact Comparison

Section 19.7 shows that 3 - 1 double contact acidmaking has oxidized:

99.98% of its feed gas SO_2 to SO_3

after all its catalyst beds. Fig. 19.7, on the other hand, shows that 4 bed single contact acidmaking has oxidized only:

98.9% of its feed gas SO_2 to SO_3.

This confirms double contact's SO_2 oxidation advantage.

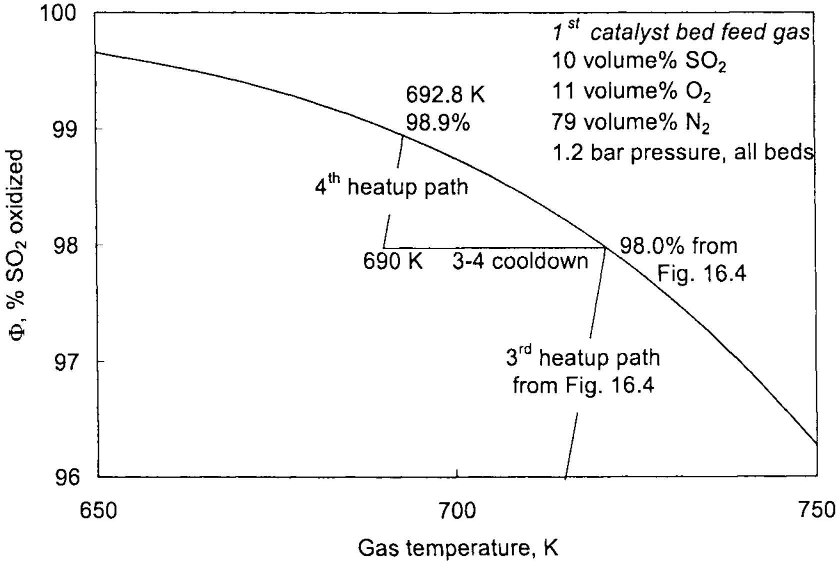

Fig. 19.7. 4 catalyst bed single contact acid plant. The 3rd catalyst bed heatup path and intercept are the same as in Figs. 16.3 and 16.4. The 4th bed is new, Table S.4. Note that:

(a) the 4th bed oxidizes less than half of the 3rd bed exit SO_2, while:

(b) Fig. 19.6's after-H_2SO_4-making bed oxidizes 98.9% of the 3rd bed exit SO_2, Section 19.6. This explains the greater efficiency of double contact acidmaking.

19.8.1 Double contact's extra costs

Double contact acidmaking is more efficient than single contact acidmaking. However, this extra efficiency comes with extra costs. They are for:

(a) a second H_2SO_4 making system with its associated acid handling equipment

(b) 2 additional heat exchangers (1 for cooling before-intermediate-H_2SO_4-making gas and 1 for heating after-intermediate-H_2SO_4-making gas)

(c) additional energy for moving gas and acid through the second H_2SO_4 making system.

Widespread industrial adoption of double contact acidmaking indicates, however, that the high efficiency of the process more than offsets these extra costs.

19.9 Summary

Many sulfuric acid plants:

(a) oxidize most of their feed SO_2 to SO_3 in 3 (occasionally 2 or 4) catalyst beds

(b) make $H_2SO_4(\ell)$ from (a)'s product $SO_3(g)$, Eqn. (1.2)

(c) oxidize the SO_2 remaining in (b)'s exit gas to SO_3 - in 1 (occasionally 2) after-H_2SO_4-making catalyst beds

(d) make $H_2SO_4(\ell)$ from (c)'s new $SO_3(g)$.

This is called double contact acidmaking because it contacts gas and acid twice, steps (b) and (d). The advantage of double contact acidmaking is that it makes SO_3 and $H_2SO_4(\ell)$ more efficiently than single contact acidmaking.

The calculations of this chapter confirm this high efficiency.

Table 19.3 (after this chapter's problems) gives industrial after-H_2SO_4-making catalyst bed operating data.

References

Hansen, L. (2004) Topsoe Sulphuric Acid Catalysts VK-Series, paper distributed at Sulphur 2004 conference, Barcelona, October 24-27, 2004. Also - VK series sulphuric acid catalysts for today and for the future, Halder Topsoe A/S brochure, 2004 www.haldortopsoe.com

Problems

19.1 Calculate Fig. 19.2's overall SO_2 oxidation efficiency when:

Table 19.3. Details of after-intermediate H_2SO_4-making catalytic SO_2 oxidation plants.

Operation		S1	M2
number of catalyst beds		3 + 1#	3 + 2#
converter height × diameter, m		19.23 × 16.65	10.4 × 9.4
construction materials		304 stainless steel	carbon steel insulation brick
heat recovery system			none
Input gas data			
flowrate, thousand Nm^3/hour		297	102
temperature, K		693	685
composition, volume%			
SO_3		0.005	
SO_2		0.780	0.42
O_2		4.29	5.34
CO_2		0	
N_2		94.9	
Catalyst bed data			
thickness of beds, m			
bed 4		1.34	0.64
bed 5			0.78
catalyst type(s)			
bed 4		LP110	12 mm daisy ring, VK38
bed 5			9 mm daisy ring, VK69
catalyst bed temperatures, K			
bed 4	in	693	687
	out	716	704
bed 5	in		698
	out		698
Product gas to H_2SO_4 making			
SO_3		0.745	0.42
SO_2		0.04	0.01
O_2		3.94	5.14
CO_2		0	
N_2		95.3	
Design % SO_2 oxidation after all catalyst beds		99.7	99.9

Catalyst beds before intermediate H_2SO_4 making + beds after intermediate H_2SO_4 making.

Their equivalent before-intermediate-H_2SO_4-making details are given in Table 7.2.

Cumerio 1 (Bulgaria)	Cumerio 2 (Bulgaria)	M6
$3 + 1^{\#}$	$3 + 1^{\#}$	$3 + 1^{\#}$
19.3 × 11.6	22.3 × 12	17.3 × 12.5
304 stainless steel, gray iron posts and grids	brick lined carbon steel	304H stainless steel
	none	none
160	150	191
683	688	694
0	0	
0.57	0.45	0.56
8.33	6.31	13.6
0.36	0.31	
90.74	92.93	
1.28	1.00	0.78
11 × 4 mm ring	12 × 6 mm ring	12 mm daisy
		VK48 + LP110
683	688	694
701	693	714
0.56	0.45	0.51
0.01	0.014	0.05
8.06	6.12	13.4
0.36	0.31	
91.01	93.11	
99.70	99.80	99.7

Table 19.3 (cont.) Details of after-intermediate H_2SO_4-making catalytic SO_2 oxidation plants.

Operation	M4	Asarco Hayden
number of catalyst beds	3 + 1#	3 + 1#
converter height × diameter, m	22.1 × 12	16.9 × 7.0
construction materials	carbon steel, aluminum coating, brick lining	brick lined steel
heat recovery system	none	
Input gas data		
flowrate, thousand Nm^3/hour	188	192
temperature, K	663	666
composition, volume%		
SO_3	0	0
SO_2	0.8-1.2	0.69
O_2	8.4-9.9	8.0
CO_2	3.3	1.0
N_2	remainder	90.0
Catalyst bed data		
thickness of beds, m		
bed 4	1.28	0.71
bed 5		
catalyst type(s)		
bed 4	VK69	LP110/VK48
bed 5		
catalyst bed temperatures, K		
bed 4 in	663	666
out	683	700
bed 5 in		
out		
Product gas to H_2SO_4 making		
SO_3	1.1	0.6
SO_2	0.025	0.05
O_2	8.7	7.77
CO_2	3.3	1.2
N_2	remainder	90.9
Design % SO_2 oxidation after all catalyst beds		

#Catalyst beds before intermediate H_2SO_4 making + beds after intermediate H_2SO_4 making.

Their equivalent before-intermediate-H_2SO_4-making details are given in Table 7.2.

Phelps Dodge Miami	M1
3 + 1[#]	2 + 2[#]
23.3 × 14.76	9.8 × 6.9
all welded stainless steel	carbon steel, cast iron grids
	mild steel division plates
	none
199	50
703	
0.3	
0.6	0.21
6.4	12.2
1.2	
91.5	
1.24	0.33
	0.33
0.28 m of VK69 (top)	daisy ring, V_2O_5
0.96 m of VK38/48 mix	
	daisy ring, V_2O_5
703	700-727
720	708-736
	700-714
	700-716
0.9	
0.03	0.008
6.2	12.2
1.2	
91.7	
	99.8

(a) its 1st catalyst bed feed gas contains:

12.0 volume%	SO_2
13.2	O_2
74.8	N_2

(b) its catalyst bed input gas temperatures are:

1st catalyst bed	675 K
2nd	685 K
3rd	695 K
4th	695 K.

(c) its catalyst bed pressures are all 1.2 bar

(d) 100% of the $SO_3(g)$ in Fig. 19.2's 3rd catalyst bed exit reacts to form $H_2SO_4(\ell)$ during intermediate H_2SO_4 making.

Hints:

(a) The composition of Fig. 19.2's intermediate H_2SO_4 making input gas under the above conditions is given in your answer to Prob. 16.2. It is:

0.1183	kg-mole	SO_3
0.0017	"	SO_2
0.0728	"	O_2
0.7480	"	N_2.

(b) All the above SO_3 is removed from this gas during intermediate H_2SO_4 making.

19.2 Calculate the equivalent SO_2 oxidation efficiency with 4 catalyst beds but no intermediate H_2SO_4 making. Use the technique described in Appendix S with all of Prob. 19.1's temperatures and pressures.

CHAPTER 20

Optimum Double Contact Acidmaking

Chapter 19 examines after-H_2SO_4-making catalytic SO_2 oxidation. It shows how after-H_2SO_4-making catalyst bed:

equilibrium curves
heatup paths
heatup path-equilibrium curve intercepts

are calculated. It also shows how:

total SO_2 oxidation after SO_2 oxidation in all before and after intermediate-H_2SO_4-making catalyst beds

is calculated.

This chapter uses the latter calculation to analyze double-contact acidmaking. Its objectives are to:

(a) compare the SO_2 oxidation efficiencies of different double-contact catalyst bed arrangements, e.g.:

3 beds before intermediate H_2SO_4 making, 1 bed after
2 " " 2 beds after

(b) show which bed arrangement gives maximum SO_2 oxidation efficiency

(c) indicate the catalyst bed where low activation temperature (Cs) catalyst will most enhance total oxidation efficiency.

The calculations are based on the following specifications and Eqn. 19.7.

Table 20.1. Specifications for this chapter's calculations.

Specification	Value
1st catalyst bed feed gas	10 volume% SO_2 11 volume% O_2 79 volume% N_2
Input gas temperature, all beds	**690 K**
Bed pressure, all beds	1.2 bar
Intercept specification	equilibrium is achieved in all beds
SO_3-from-gas removal during H_2SO_4 making	100%

20.1 Total *% SO_2 Oxidized* After All Catalyst Beds

All of this chapter's efficiency comparisons are based on total *% SO_2 oxidized* after all catalyst beds, defined as:

$$\text{total } \% \, SO_2 \text{ oxidized} = \Phi_{total} = \frac{\begin{array}{c}\text{kg-mole } SO_2 \text{ in } 1^{st} \\ \text{catalyst bed feed gas}\end{array} - \begin{array}{c}\text{kg-mole } SO_2 \text{ in last} \\ \text{catalyst bed exit gas}\end{array}}{\begin{array}{c}\text{kg-mole } SO_2 \text{ in } 1^{st} \\ \text{catalyst bed feed gas}\end{array}} * 100 \qquad (19.7)$$

(all quantities per kg-mole of 1st catalyst bed feed gas).

20.2 Four Catalyst Beds

Most industrial acid plants have 4 catalyst beds. The arrangements of these beds in order of decreasing industrial use are:

3 catalyst beds before intermediate H_2SO_4 making; 1 catalyst bed after
2 " " " 2 "
4 " " " 0 " .

Fig. 20.1 compares the total SO_2 oxidation efficiencies of these arrangements. The theoretical 1 - 3 arrangement is also shown.

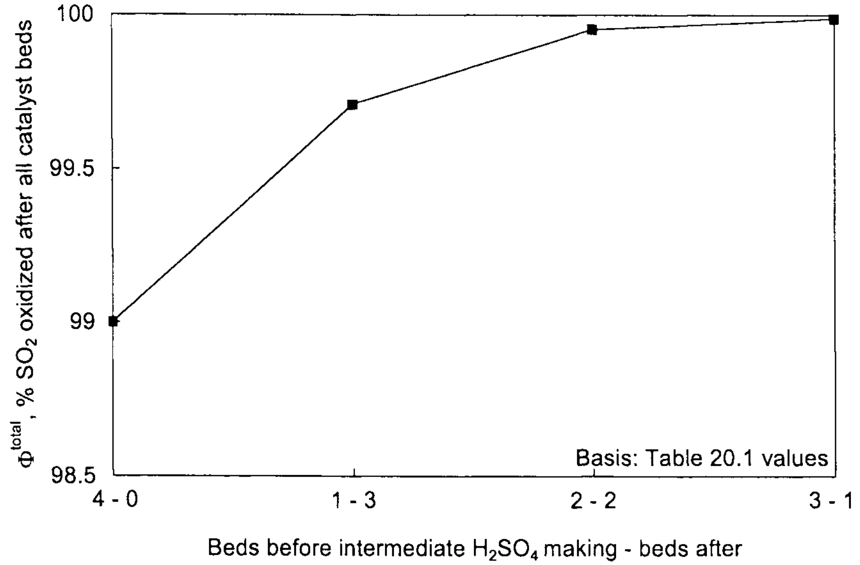

Fig. 20.1. Total SO_2 oxidation efficiencies of 4 four-catalyst-bed arrangements. The 3 - 1 bed arrangement is seen to be the most efficient.

The figure indicates that:

(a) double contact acidmaking is always more efficient than single contact acidmaking.

(b) the 3 - 1 bed arrangement gives maximum SO_2 oxidation.

These results explain the widespread industrial use of the 3 - 1 process.

20.3 Improved Efficiency with 5 Catalyst Beds

Fig. 20.2 shows the efficiencies of 5 five-catalyst-bed SO_2 oxidation systems. It confirms that:

(a) double contact acid plants are always more efficient than single contact plants

(b) the single after-intermediate-H_2SO_4-making bed arrangement is the most efficient.

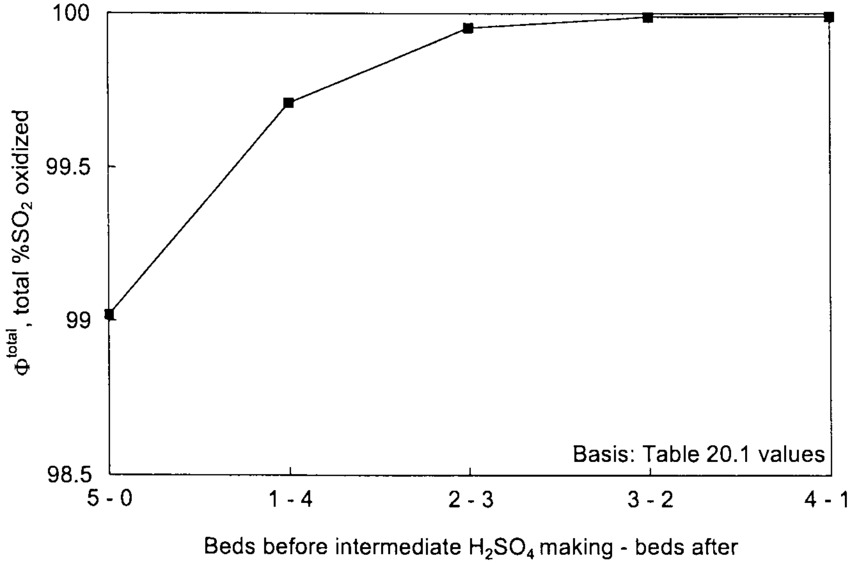

Fig. 20.2. SO_2 oxidation efficiency of 5 five-catalyst bed arrangements. The 4 - 1 arrangement is the most efficient. It is, however, only slightly more efficient that the 3 - 2 arrangement.

20.3.1 Benefit from each additional bed

Figs. 20.1 and 20.2 indicate that the single after-intermediate-H_2SO_4-making bed arrangement gives maximum SO_2 oxidation efficiency. Fig 20.3 examines this further by comparing SO_2 oxidation efficiency with 1 to 4 beds before H_2SO_4 making - 1 bed after. As expected, overall efficiency with this arrangement increases with each additional before-H_2SO_4-making bed.

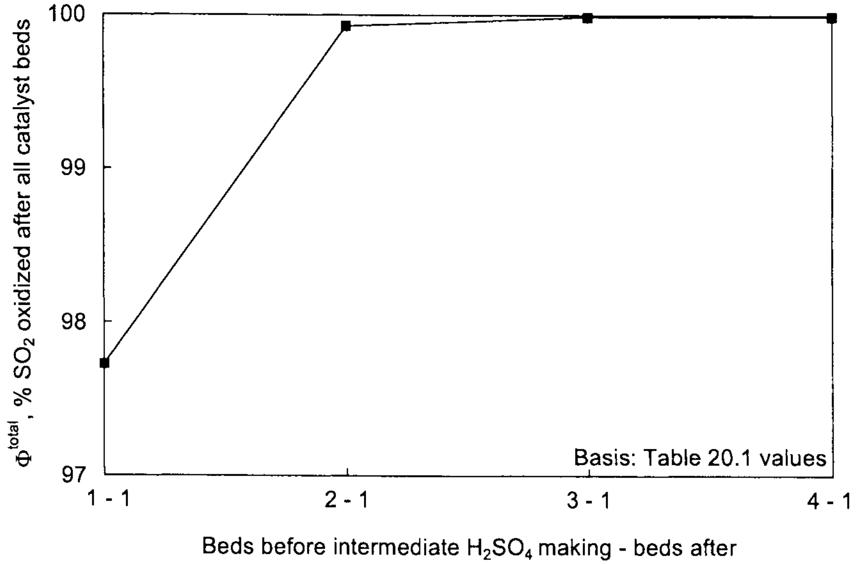

Fig. 20.3. SO_2 oxidation efficiency of acid plants with 1 catalyst bed after intermediate H_2SO_4 making. Oxidation efficiency increases with increasing number of before-intermediate-H_2SO_4-making beds. However, the difference between 3 - 1 and 4 - 1 plants is very small.

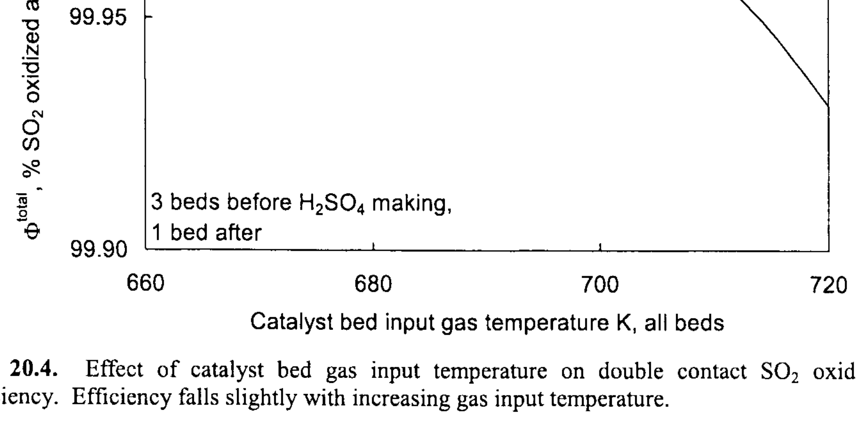

Fig. 20.4. Effect of catalyst bed gas input temperature on double contact SO_2 oxidation efficiency. Efficiency falls slightly with increasing gas input temperature.

20.4 Input Gas Temperature Effect

Fig 20.4 shows the effect of gas input temperature on:

3 - 1 acid plant SO_2 oxidation efficiency.

It indicates that total *% SO_2 oxidized*:

(a) is always high

(b) increases with decreasing input gas temperature.

20.5 Best Bed for Cs Catalyst

Cs-enhanced catalyst is useful in permitting cool input gas – because it deactivates at a relatively cool temperature, Chapter 8.

However, Cs catalyst is costly, so many acid plants use it in only 1 catalyst bed. Fig. 20.5 indicates that the best location for the Cs catalyst bed is after H_2SO_4 making – where it gives maximum total SO_2 oxidation.

Prevention of catalyst overheating may, however, lead it to be used in the 1st catalyst bed (Fig. 12.7) – even though this is not the best SO_2 oxidation efficiency location.

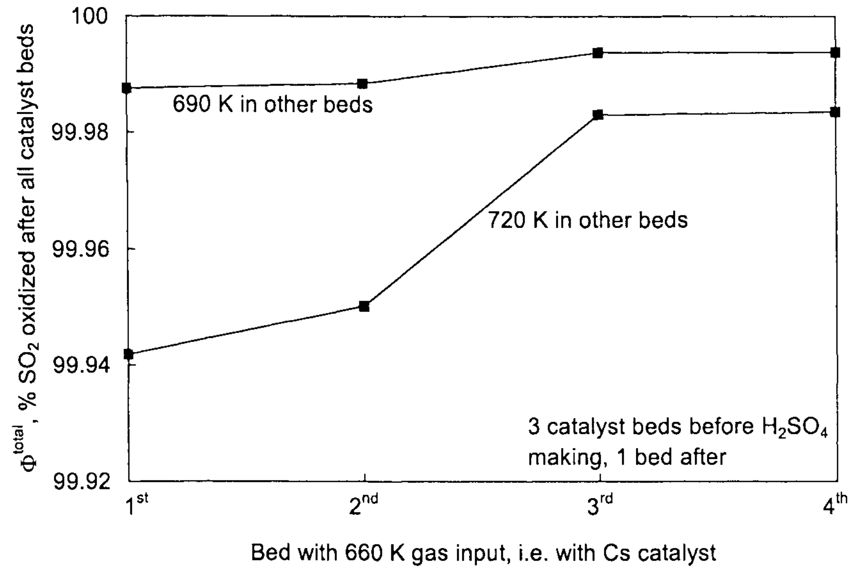

Fig. 20.5. 3 - 1 acid plant with one Cs catalyst bed (660 K gas input) and three K, Na catalyst beds (690 and 720 K). Maximum SO_2 oxidation is obtained with the Cs catalyst in bed 4, i.e. after H_2SO_4 making. Bed 3 (just before H_2SO_4 making) is nearly as good. The calculations are all based on Table 20.1's values – except for gas input temperature.

20.6 Triple Contact Acid Plant

At the time of writing, there are no industrial triple contact acid plants. These plants would be more complex than their double contact counterparts, so they would have to give a significant SO_2 oxidation advantage.

As the following values show, 1 - 1 - 1 acid plants would be slightly less efficient than this chapter's 3 - 1 plants.

3 – 1 double contact	99.99 %	SO_2 oxidation	efficiency
1 - 1 - 1 triple contact	99.97 %	"	"

(all calculations based on Table 20.1 specifications).

This and the complexity of triple contact plants explain why none has been built.

20.7 Summary

Double contact acidmaking is more efficient than single contact acidmaking. This has made it the most used industrial process. The reason for its high efficiency is its efficient oxidation of SO_2 in its after-H_2SO_4-making catalyst bed(s), Chapter 19.

The most efficient double contact plants have one catalyst bed after H_2SO_4 making, remainder before. 3 – 1 plants are more efficient than 2 – 2 plants. 4 – 1 plants are more efficient than 2 – 3 and 3 – 2 plants.

Cool catalyst bed input gas gives high SO_2 oxidation efficiency in single and double contact acid plants. Low deactivation temperature Cs catalyst is beneficial in this respect, Chapters 8 and 12.

Cs catalyst is costly so many acid plants use it in only one catalyst bed. From the SO_2 oxidation efficiency point of view, it is best used after intermediate H_2SO_4 making.

Industrial SO_2 oxidation efficiencies are slightly lower than those in this chapter – because equilibrium is not quite attained in industrial processes. However, the trends in the chapter are instructive as to best double contact practice.

CHAPTER 21

Enthalpies and Enthalpy Transfers

Chapters 10 through 20 indicate that rapid, efficient multi catalyst bed $SO_2 + \frac{1}{2}O_2 \rightarrow SO_3$ oxidation requires:

(a) warm 1st catalyst bed feed gas (~690 K)

(b) cooling of gas between beds and before H_2SO_4 making.

Fig. 21.1 indicates how these requirements are achieved for a single contact sulfur-burning acid plant with 3 catalyst beds. It shows that:

(a) 690 K 1st catalyst bed feed gas is obtained by cooling sulfur burning exit gas in a boiler and steam superheater

(b) 700 K 2nd catalyst bed input gas is obtained by cooling ~890 K 1st catalyst bed exit gas in a second boiler

(c) 710 K 3rd catalyst bed input gas is obtained by cooling ~770 K 2nd catalyst bed exit gas in a steam superheater

(d) 470 K H_2SO_4 making input gas is obtained by cooling ~720 K 3rd catalyst bed exit gas in an economizer (boiler feed water heater).

The final products of the flowsheet are (i) cool SO_3 rich gas ready for H_2SO_4 making and (ii) superheated steam.

Steps (a) to (d) all require transfer of heat to water or steam.

This chapter examines these heat transfers. Its objectives are to calculate:

(a) the enthalpies of (i) catalyst bed input and output gases and (ii) H_2SO_4 making input gas

(b) heat transfers that will give these enthalpies.

These values pave the way for Chapter 22's examination of catalyst bed and H_2SO_4 making temperature control.

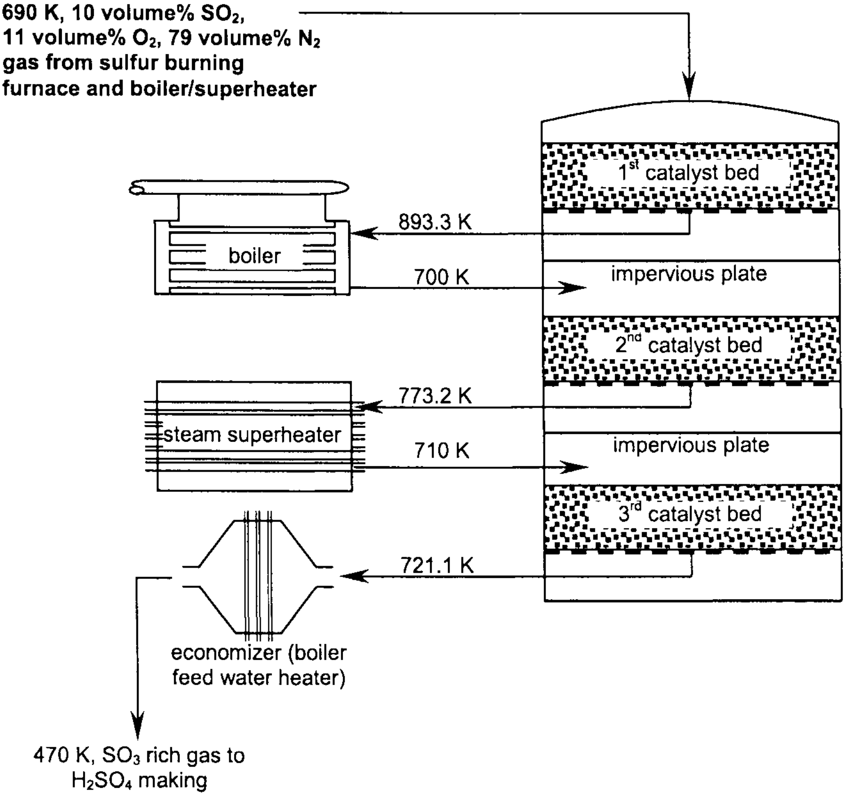

Fig. 21.1. Heat transfer flowsheet for single contact, sulfur burning sulfuric acid plant. It is simpler than industrial plants, which nearly always have 4 catalyst beds rather than 3. The gaseous product is cool, SO_3 rich gas, ready for H_2SO_4 making. The heat transfer product is superheated steam. All calculations in this chapter are based on this figure's feed gas composition and catalyst bed input gas temperatures. All bed pressures are 1.2 bar. The catalyst bed output gas temperatures are the intercept temperatures calculated in Sections 12.2, 15.2 and 16.3.

21.1 Input and Output Gas Enthalpies

Fig. 21.1's catalyst bed input and output gas enthalpies can be calculated directly on our heatup path-equilibrium curve worksheets, Table 21.1. Table 21.1's 3rd catalyst bed input gas enthalpy is, for example:

$$\begin{aligned} H_{\text{input gas}} &= \text{kg-mole } SO_3 \text{ in} * H^{\circ}_{710\atop SO_3} \\ &+ \text{kg-mole } SO_2 \text{ in} * H^{\circ}_{710\atop SO_2} \\ &+ \text{kg-mole } O_2 \text{ in} * H^{\circ}_{710\atop O_2} \\ &+ \text{kg-mole } N_2 \text{ in} * H^{\circ}_{710\atop N_2} \end{aligned}$$

$$\begin{aligned} = \; & B34 * -D28 \\ + \; & B35 * -E28 \\ + \; & B36 * -F28 \\ + \; & B37 * -G28 \end{aligned} \tag{21.1}$$

where B34 etc. are Table 21.1 cell references.

Cells D28-G28 each contain -H°, Eqn. (11.7). This explains their negative signs in Eqn. (21.1).

Table 21.1's cell H43 contains Eqn. (21.1) exactly as shown in the cell beside it. It shows that Fig. 21.1's 3rd catalyst bed input gas enthalpy is:

-25.94 MJ

per kg-mole of 1st catalyst bed feed gas.

21.1.1 Output gas enthalpy

Table 21.1's 3rd catalyst bed output gas enthalpy is calculated the same way. It is described by the equation:

$$\begin{aligned} H_{\text{output gas}} = \; & \text{kg-mole } SO_3 \text{ out} * \underset{SO_3}{H^{\circ}_{721.1}} \\ + \; & \text{kg-mole } SO_2 \text{ out} * \underset{SO_2}{H^{\circ}_{721.1}} \\ + \; & \text{kg-mole } O_2 \text{ out} * \underset{O_2}{H^{\circ}_{721.1}} \\ + \; & \text{kg-mole } N_2 \text{ out} * \underset{N_2}{H^{\circ}_{721.1}} \end{aligned}$$

$$\begin{aligned} = \; & B38 * H28 \\ + \; & B39 * I28 \\ + \; & B40 * J28 \\ + \; & B41 * K28 \end{aligned} \tag{21.2}$$

where 721.1 K is the 3rd catalyst bed intercept temperature.

Table 21.1's cell H44 contains Eqn. (21.2) exactly as shown beside it. It shows that Fig. 21.1's 3rd catalyst bed output gas enthalpy is:

-25.94 MJ

per kg-mole of 1st catalyst bed feed gas.

Table 21.1. Bottom half of Table O.1's 3rd catalyst bed heatup path-equilibrium curve intercept worksheet. Input and output gas enthalpies are shown in rows 43 and 44. Note that they are the same. This is because our heatup path calculations assume no convective, conductive or radiative heat loss during catalytic $SO_2 + \frac{1}{2}O_2 \rightarrow SO_3$ oxidation, Section 11.9. 1st and 2nd catalyst bed enthalpies are calculated similarly – using Tables J.2 and M.2.

	A	B	C	D	E	F	G	H	I	J	K
19	*3rd catalyst bed heatup path matrix. Eqns. 14.6 to 14.8 are from Section 14.6. Eqn. 14.9" is from Appendix K. Eqns. 16.1 to 16.4 are from Section 16.3.*										
20	Equation	description	numerical term =E8 etc.	kg-mole SO_3 **in**	kg-mole SO_2 **in**	kg-mole O_2 **in**	kg-mole N_2 **in**	kg-mole SO_3 **out**	kg-mole SO_2 **out**	kg-mole O_2 **out**	kg-mole N_2 **out**
21	16.1	input SO_3 kg-mole	0.0942	1	0	0	0	0	0	0	0
22	16.2	input SO_2 kg-mole	0.0058	0	1	0	0	0	0	0	0
23	16.3	input O_2 kg-mole	0.0629	0	0	1	0	0	0	0	0
24	16.4	input N_2 kg-mole	0.7900	0	0	0	1	0	0	0	0
25	14.6	S balance	0	-1	-1	0	0	1	1	0	0
26	14.7	O balance	0	-3	-2	-2	0	3	2	2	0
27	14.8	N balance	0	0	0	0	-2	0	0	0	2
28	14.9"	enthalpy balance	0	369.9	277.7	-12.87	-12.28	-369.1	-277.1	13.24	12.63
29											
30			3rd catalyst bed input gas temperature =			710		intercept temperature, cell A14 =		721.1	
31						=K5				=A14	
32											
33	Matrix results equivalent to suggested intercept temperature in cell J30 (and A14)						=-(0.0311*F30-9.797)				
34	kg-mole SO_3 **in**	0.0942									
35	kg-mole SO_2 **in**	0.0058									
36	kg-mole O_2 **in**	0.0629									
37	kg-mole N_2 **in**	0.7900									
38	kg-mole SO_3 **out**	0.0980	heatup path % SO_2 oxidized (Φ) equivalent to 3rd catalyst bed intercept temperature in cell J30 =								
39	kg-mole SO_2 **out**	0.0020	= (1st catalyst bed feed gas kg-mole SO_2 - 3rd catalyst bed kg-mole SO_2 out) * 100 =						98.0	= (G5-B39)/G5*100	(14.1)
40	kg-mole O_2 **out**	0.0610		1st catalyst bed feed gas kg-mole SO_2							
41	kg-mole N_2 **out**	0.7900									
42	all per kg-mole of 1st catalyst bed feed gas										
43							Input gas enthalpy =	-25.94	=B34*-D28+B35*-E28+B36*-F28+B37*-G28		
44							Output gas enthalpy =	-25.94	=B38*H28+B39*I28+B40*J28+B41*K28		
45											
46	Goal Seek calculation										
47	Equilibrium curve % SO_2 oxidized - heatup path % SO_2 oxidized =						0.0	=F11-I39			

21.1.2 First and second bed enthalpies

1st and 2nd catalyst bed input and output gas enthalpies are calculated from Tables J.2 and M.2 exactly as described above. They are summarized in Table 21.2.

21.2 H_2SO_4 Making Input Gas Enthalpy

Fig. 21.1's H_2SO_4-making input SO_3, SO_2, O_2 and N_2 quantities are shown in Table 21.1. They are the 3rd catalyst bed exit (intercept) quantities.

However, their 470 K enthalpies are not shown in the table. They are accounted for by the equation:

$$\begin{aligned} H_{H_2SO_4\,\text{making input gas}} &= \text{kg-mole } SO_3 \text{ out} * (0.07144 * 470 - 420.6) \\ &+ \text{kg-mole } SO_2 \text{ out} * (0.05161 * 470 - 314.3) \\ &+ \text{kg-mole } O_2 \text{ out} * (0.03333 * 470 - 10.79) \\ &+ \text{kg-mole } N_2 \text{ out} * (0.03110 * 470 - 9.797) \qquad (21.3) \\ &= 0.098 * -387.0 \\ &+ 0.002 * -290.0 \\ &+ 0.061 * 4.88 \\ &+ 0.790 * 4.82 \\ &= -34.40 \text{ MJ per kg-mole of 1st catalyst bed feed gas.} \end{aligned}$$

where:

'kg-mole SO_3 out' is kg-mole SO_3 out of the 3rd catalyst bed and into H_2SO_4 making

and:

$(0.07144 * 470 - 420.6)$ is $\underset{SO_3}{H^\circ_{470}}$

and so on.

21.3 Heat Transfers

21.3.1 Heat transfer from 3rd bed exit gas to economizer water

This section calculates how much heat must be removed from Fig. 21.1's:

721.1 K 3rd catalyst bed exit gas

to cool it to the figure's specified:

470 K H_2SO_4 making input gas temperature.

This heat removal is calculated by the equation:

$$Q = |\Delta H| = |H_{H_2SO_4\text{ making input gas}} - H_{3^{rd}\text{ bed exit gas}}| \qquad (21.4).$$

The enthalpies in this equation are those calculated in Sections 21.1.1 and 21.2, giving:

$$Q = |\Delta H| = |-34.40 - (-25.94)|$$

$$= 8.46 \text{ MJ per kg-mole of } 1^{st} \text{ catalyst bed feed gas.}$$

So, per kg-mole of 1st catalyst bed feed gas, 8.46 MJ must be removed from 721.1 K 3rd catalyst bed exit gas to cool it to the specified 470 K H_2SO_4 making input gas temperature. The heat is, of course, transferred to water in Fig. 21.1's economizer.

21.3.2 1 – 2 and 2 – 3 heat transfers

Heat transfers from gas between beds 1 and 2 and 2 and 3 are calculated exactly as described above. They are tabulated in Table 21.2.

Table 21.2. Summary of Fig. 21.1's temperatures, enthalpies and heat transfers. Note the continuing decrease in the gas's enthalpy as heat is transferred from gas to water and steam in Fig. 21.1's boiler, superheater and economizer. All temperatures but the last are from Tables J.2, M.2 and 21.1. Note that a catalyst bed's input enthalpy is always the same as its output enthalpy. This is due to our assumption that there is no conductive, convective or radiative heat loss from the gas.

Gas	Temp. K	Enthalpy#	
1st catalyst bed feed gas	690	-17.31	
1st catalyst bed exit (intercept) gas	893.3	-17.31	
		heat transfer to 1-2 boiler water →	6.50#
2nd catalyst bed input gas	700	-23.81	
2nd catalyst bed exit (intercept) gas	773.2	-23.81	
		heat transfer to superheater steam →	2.13#
3rd catalyst bed input gas	710	-25.94	
3rd catalyst bed exit (intercept) gas	721.1	-25.94	
		heat transfer to economizer water →	8.46#
H_2SO_4 making input gas	470	-34.40	

#MJ per kg-mole of 1st catalyst bed feed gas.

21.4 Heat Transfer Rate

The rate at which heat is transferred from Fig. 21.1's 3rd catalyst bed exit gas to its economizer water is calculated from:

Section 21.3.1's heat transfer amount, MJ per kg-mole of 1st catalyst bed feed gas

and:

a specified 1st catalyst bed feed gas input rate, Nm^3 per hour, e.g. 100 000 Nm^3/hour.

Heat transfer rate is given by the equation:

$$\text{heat transfer rate} = Q * \frac{1^{st} \text{ catalyst bed feed gas input rate, Nm}^3\text{/hr}}{22.4 \text{ Nm}^3 \text{ of feed gas per kg-mole of feed gas}} \qquad (21.5).$$

With Table 21.2's 8.46 MJ economizer heat transfer (Q), it is:

$$\begin{array}{l}3^{rd} \text{ catalyst bed exit} \\ \text{gas to economizer} \\ \text{heat transfer rate}\end{array} =$$

$$= 8.46 \begin{array}{l}\text{MJ per kg-mole} \\ \text{of } 1^{st} \text{ catalyst} \\ \text{bed feed gas}\end{array} * \frac{100\,000 \text{ Nm}^3 \text{ of } 1^{st} \text{ catalyst bed feed gas per hour}}{22.4 \text{ Nm}^3 \text{ of feed gas per kg-mole of feed gas}} \qquad (21.6)$$

$$= 38\,000 \text{ MJ per hour.}$$

21.4.1 Extension

This chapter has examined a very simple acid plant. Its techniques are, however, readily extended to complex industrial acidmaking situations.

21.5 Summary

Catalyst bed gas enthalpies are readily calculated on our heatup path-equilibrium curve intercept worksheets.

These enthalpies are conveniently used to calculate the amount of heat that must be removed to cool a catalyst bed's output gas to a specified temperature.

The enthalpies and heat removal quantities are all calculated per kg-mole of 1st catalyst bed feed gas.

The heat removal quantities (plus 1st catalyst bed feed gas input rate) are readily used to determine the cooling requirements (MJ/hour) of each of Fig. 21.1's gas cooling devices.

The next chapter builds on this information to show how catalyst bed and H_2SO_4 making input gas temperatures are controlled by bypassing gas around the cooling devices.

Problems

21.1 Prepare a table like Table 21.2 for:

12.0 volume% SO_2
13.2 " O_2
74.8 " N_2

1st catalyst bed feed gas and the following catalyst bed gas input temperatures:

1st catalyst bed	675 K
2nd "	685 K
3rd "	695 K.

Assume that:

(a) the pressure in all catalyst beds is 1.2 bar

(b) heatup path-equilibrium curve intercepts are attained in all beds

(c) the 3rd catalyst bed exit gas enters H_2SO_4 making at 470 K.

Hints

1. Use your Problem 12.3, 15.1 and 16.1 spreadsheets to calculate input and output gas enthalpies (as described in Section 21.1).
2. Use your Prob. 16.1 3rd catalyst bed output quantities and Eqn. (21.3) to calculate H_2SO_4 making's input gas enthalpy.

21.2 Calculate the rate, MJ/hour, at which heat must be transferred from 3rd catalyst bed exit gas to economizer water to obtain the above specified 470 K H_2SO_4 making gas. 100 000 Nm^3 per hour of 1st catalyst bed feed gas is entering the 1st catalyst bed.

CHAPTER 22

Control of Gas Temperature by Bypassing

This chapter describes how:

catalyst bed and H_2SO_4 making input gas temperatures

are controlled by bypassing gas around Fig. 21.1's heat transfer equipment.

22.1 Bypassing Principle

The principle of bypassing is that when a portion of a hot gas stream is bypassed around a gas cooling device (e.g. Fig. 21.1's economizer):

the bypassed portion is not cooled.

Then, when the bypassed portion and the cooled portion are recombined (Fig. 22.1), the product gas stream is:

warmer

than when all the gas is being passed through the cooling device.

Most acid plant heat transfer devices are provided with bypass capability, Fig. 22.2.

22.2 Objective

The objective of this chapter is to show how bypassing can be used to adjust the temperatures of acid plant gases. It examines:

(a) how bypassing gas around Fig. 21.1's economizer can be used to adjust the temperature of the economizer's output gas

(b) how bypassing can be used to maintain a constant economizer output gas temperature while the economizer's input gas temperature is varying.

Both calculations also estimate the fraction of economizer input gas that must be bypassed around the economizer to achieve a specified output gas temperature.

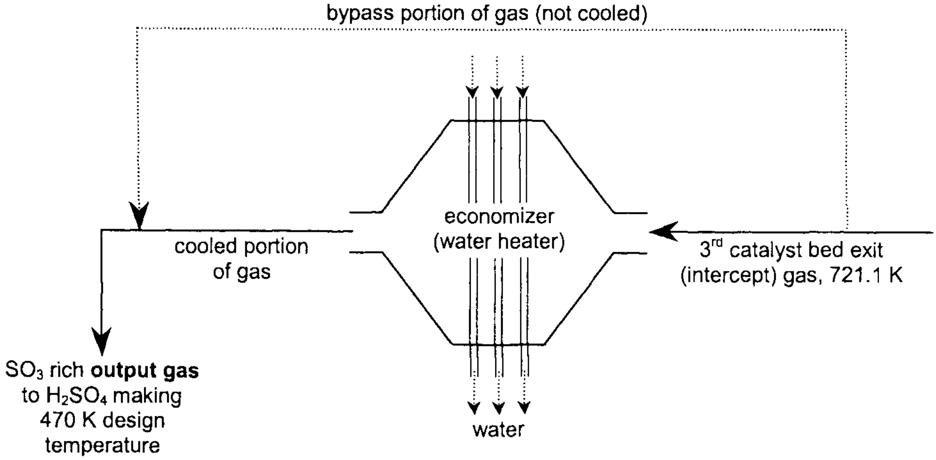

Fig. 22.1. Blowup of Chapter 21's economizer. Bypassing of input gas around the economizer (dotted line) is shown. Bypassing results in a warmer recombined **output gas** stream.

Fig. 22.2. Photograph of gas bypass flue around cross flow gas-to-gas heat exchanger. In this case, the amount of bypass is controlled by manually adjusting a butterfly valve in the bypass flue (note chain below the valve). In most cases, the valve is controlled automatically by a thermocouple placed just beyond the heat exchanger exit gas/bypass gas re-combination point.

22.3 Gas to Economizer Heat Transfer

Fig. 21.1's economizer cools Table 21.1's 3rd catalyst bed exit (intercept) gas from:

721.1 K

to:

470 K (its design output gas temperature).

The gas's enthalpies at 721.1 and 470 K are, Sections 21.1.1 and 21.2:

-25.94 MJ

and

-34.40 MJ

which means that:

8.46 MJ

of heat must be transferred from the 721.1 K economizer input gas to give 470 K output gas, Section 21.3.1.

All enthalpies and heats are per kg-mole of 1st catalyst bed feed gas.

22.3.1 Design heat transfer rate

The Fig. 22.1 economizer's design heat transfer rate with:

(a) the above 8.46 MJ heat transfer per kg-mole of 1st catalyst bed feed gas

and:

(b) 100 000 Nm^3 per hour of 1st catalyst bed feed gas (the flowrate used throughout this chapter)

is:

$$\begin{matrix}3^{rd}\text{ catalyst bed}\\ \text{economizer heat}\\ \text{transfer rate}\end{matrix} = 8.46 \begin{matrix}\text{MJ per kg-mole}\\ \text{of }1^{st}\text{ catalyst}\\ \text{bed feed gas}\end{matrix} * \frac{100\,000\text{ Nm}^3\ 1^{st}\text{ catalyst bed feed gas/hour}}{22.4\text{ Nm}^3\text{ of feed gas per kg-mole of feed gas}}$$

$$= 38\,000\text{ MJ per hour} \qquad (21.6).$$

This value is referred to later in the chapter.

22.4 Heat Transfer Requirement for 480 K Economizer Output Gas

The temperature of Fig. 22.1's economizer output gas can be changed by:

bypassing a portion of the economizer input gas

around the economizer.

This section shows how 480 K output gas is obtained. It calculates:

(a) the enthalpy of 480 K economizer output gas, per kg-mole of 1st catalyst bed feed gas

(b) the amount of heat that must be transferred from 721.1 K 3rd catalyst bed exit gas to give (a)'s enthalpy

(c) the percentage of 3rd catalyst bed exit gas that must be bypassed around the economizer to give (b)'s heat transfer.

22.4.1 Enthalpies and heat transfer

The enthalpy of 721.1 K 3rd catalyst bed exit (intercept) gas is:

-25.94 MJ (Section 21.1.1).

The enthalpy of this gas at 480K is:

-34.07 MJ

(calculated by Eqn. (21.3) with 480 K in place of 470 K).

This means that:

8.13 MJ

must be transferred from 721.1 K economizer input gas to give 480 K **output gas**, Fig. 22.1.

22.5 Changing Heat Transfer by Bypassing

Section 22.3.1 indicates that the Fig. 22.1 economizer has been designed to transfer:

38 000 MJ/hour

which is equivalent to:

8.46 MJ per kg-mole of 1st catalyst bed feed gas.

However, achievement of Section 22.4's specified 480 K economizer output gas requires a transfer of only:

8.13 MJ per kg-mole of 1st catalyst bed feed gas.

22.5.1 Percent bypass

The 8.13 MJ heat transfer required for 480 K output gas is:

$$(8.13/8.46)*100\% = 96\%$$

of the economizer's 8.46 MJ design heat transfer.

Production of 480 K economizer output gas requires, therefore, that:

96% of the 3rd catalyst bed exit gas must be cooled in the economizer

and:

4% must be bypassed around it.

22.6 460 K Economizer Output Gas

This section:

(a) calculates how much heat must be transferred from Fig. 22.1's 721.1 K economizer input gas to give 460 K economizer output gas

(b) indicates how this heat transfer may be obtained.

22.6.1 Enthalpies and heat transfer

The enthalpy of 721.1 K 3rd catalyst bed exit gas is:

-25.94 MJ.

The enthalpy of this gas at 460 K is:

-34.74 MJ (from Eqn. (21.3) with 460 K in place of 470 K).

This means that:

8.80 MJ

of heat must be transferred from 721.1 K gas to cool it to 460 K.

This requirement is greater than the cooling capacity (8.46 MJ) of the Section 22.3.1 economizer. Bypassing of gas around the economizer won't help because bypassing only decreases heat transfer.

This shows that if the temperature of the economizer output gas must be 460 K, the Section 22.3.1 economizer must be enlarged to transfer:

8.80 MJ per kg-mole of 1st catalyst bed feed gas

or more. This 8.80 MJ and 100 000 Nm^3 per hour of 1st catalyst bed feed gas is equivalent to 39 000 MJ/hour, Eqn. (21.6).

22.7 Bypassing for 460, 470 and 480 Economizer Output Gas

Production of 460 K, 470 K and 480 K economizer gas from 721.1 K 3rd catalyst bed exit gas requires transfer of:

8.80 MJ

8.46 MJ

8.13 MJ

all per kg-mole of 1st catalyst bed feed gas. These are equivalent to:

100.0%

95.6%

91.3%

of Section 22.6.1's 39 000 MJ per hour economizer capacity and to bypassing:

0%

4.4%

8.7%

of the gas stream around the economizer.

22.8 Bypassing for 470 K Economizer Output Gas While Input Gas Temperature is Varying

This section shows how Section 22.6.1's 39 000 MJ/hour economizer is used to obtain:

470 K economizer output gas

while its input gas is varying from:

715 to 725 K.

The enthalpies of Table 21.2's 3rd catalyst bed exit gas at 725, 715 and 470 K are:

725 K	-25.81 MJ
715 K	-26.15 MJ
470 K	-34.40 MJ

per kg-mole of Fig 21.1 1st catalyst bed feed gas (calculated with Eqn. (21.3) and the appropriate temperatures).

They indicate that:

(a) cooling 725 K economizer input gas to 470 K requires transfer of:

8.59 MJ

from the gas.

(b) cooling 715 K economizer input gas to 470 K requires transfer of:

8.25 MJ

from the gas.

These are equivalent to 97.6 and 93.8 % of Section 22.6.1's:

8.80 MJ (39 000 MJ/hour)

economizer.

So, operating the economizer to cool its input gas from 725 K to 470 K requires bypassing 2.4% of the gas. Cooling it from 715 K to 470 K requires opening the bypass valve to 6.2%.

Notably, gas is being passed through the bypass flue in both cases. This allows up and down temperature control.

22.9 Industrial Bypassing

This chapter's calculations assume that bypassing is:

100% effective

i.e. that bypassing 10% of a gas stream around a cooling device decreases heat transfer by 10%.

Acid plant designers suggest, however, that industrial bypass efficiency is more closely represented by an equation like:

$$\text{industrial bypass} = (\text{theoretical bypass})^{n} \qquad (22.1)$$

where n = ~1.1.

This means that the industrial bypass required to give Section 22.8's 6.2% theoretical bypass is:

$$\text{industrial bypass} = (6.2\%)^{1.1} \qquad (22.2)$$

$$= 7.4\%$$

22.9.1 Inefficiency explained

Bypassing gas around a cooling device inadvertently:

(a) increases the residence time of the remaining gas in the cooling device

which in turn:

(b) increases heat transfer from this gas to economizer water.

This partially offsets bypassing's heat transfer decrease – lowering its effectiveness.

22.10 Summary

Bypassing various fractions of a gas stream around a cooling device provides control over the device's output gas (Fig. 22.1) temperature.

Operating with gas always flowing in the bypass flue allows the cooling device's exit gas temperature to be adjusted upwards and downwards – by increasing or decreasing the amount the bypass valve is open.

A cooling device should be designed for its maximum anticipated cooling duty, i.e. for:

maximum expected gas flow

and:

maximum expected gas temperature drop.

This permits all lesser cooling duties to be obtained by bypassing.

Also, the bypass flue and control valve should be large enough to give sufficient bypassing for the smallest anticipated cooling duty.

Problems

All heat transfer rates in these problems are based on 100 000 Nm^3 of 1st catalyst bed feed gas per hour.

22.1 Problem 21.2 shows that cooling Prob. 21.1's 710.4 K 3rd catalyst bed exit gas to 470 K requires transfer of:

8.23 MJ per kg of 1st catalyst bed feed gas.

It also shows that with 100 000 Nm^3 per hour of 1st catalyst bed feed gas, this is equivalent to a:

36 740 MJ per hour

economizer.

Determine:

(a) the percentage of economizer input gas that will have to be bypassed around the economizer to give 480 K H_2SO_4 making input gas

(b) the size (MJ per hour) of economizer that will be required to give 460 K H_2SO_4 making input gas (with 100 000 Nm^3 per hour 1st catalyst bed feed gas).

22.2 Industrial practice indicates that Prob. 22.1's 3rd catalyst bed exit gas varies between 705 K to 715 K.

What fraction of Prob. 22.1's 3rd catalyst bed exit gas will have to be bypassed around Prob. 22.1 (b)'s economizer to give 470 K H_2SO_4 making input gas when the economizer input gas is:

(a) 715 K

(b) 710.5 K

(c) 705 K?

Is gas always flowing through the bypass flue?

22.3 What would the industrial (a), (b) and (c) bypasses be if Eqn. (22.2) is obeyed with n = 1.1?

CHAPTER 23

H_2SO_4 Making

Sulfuric acid is made by:

(a) catalytically oxidizing an acid plant's feed $SO_2(g)$ to $SO_3(g)$

(b) making $H_2SO_4(\ell)$ from the resulting $SO_3(g)$.

The reactions are:

$$\underset{\text{in dry feed gas}}{SO_2(g) + \tfrac{1}{2}O_2(g)} \xrightarrow[\text{catalyst}]{\text{700-900 K}} SO_3(g) \qquad (1.1).$$

$$SO_3(g) + \underset{\substack{\text{in strong}\\\text{sulfuric acid}}}{H_2O(\ell)} \xrightarrow{\text{350-380 K}} \underset{\substack{\text{in strengthened}\\\text{sulfuric acid}}}{H_2SO_4(\ell)} \qquad (1.2).$$

Reaction (1.2) produces strengthened sulfuric acid because it consumes $H_2O(\ell)$ and makes $H_2SO_4(\ell)$.

Chapters 10 to 22 examine SO_2 oxidation. This chapter and Chapter 24 examine H_2SO_4 making. They do so from the points of view of:

(a) mass flows, this chapter

and:

(b) acid temperature control, next chapter.

Industrial final-H_2SO_4-making ('absorption') data are also provided, Table 23.2.

Fig. 23.1 is a simplified sulfuric acidmaking flowsheet. Its inputs are:

(a) moist 5 volume% $H_2O(g)$, SO_2, O_2, N_2 gas from gas cleaning and cooling

(b) water.

Its outputs are:

(a) 98 mass% H_2SO_4, 2 mass% H_2O sulfuric acid

(b) dilute SO_2, O_2, N_2 gas.

All other flows are internal.

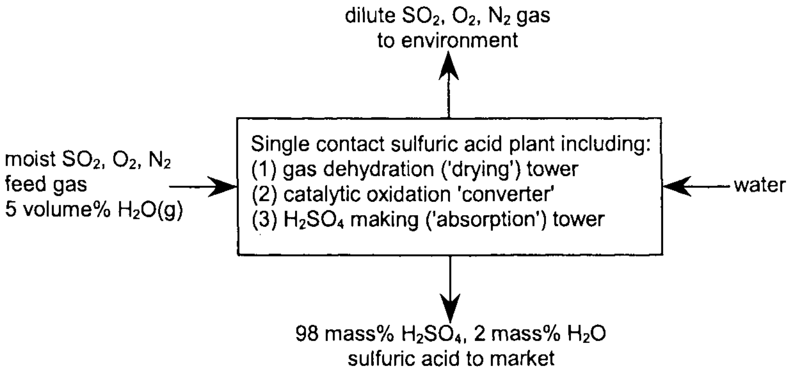

Fig. 23.1. Simplified single contact sulfuric acid production flowsheet. Its inputs are moist feed gas and water. Its outputs are 98 mass% H_2SO_4, 2 mass% H_2O sulfuric acid and dilute SO_2, O_2, N_2 gas. The acid output combines gas dehydration tower acid, H_2SO_4 making tower acid and liquid water. The equivalent sulfur burning acid plant sends moist air (rather than moist feed gas) to dehydration. Appendix V gives an example sulfur burning calculation.

23.1 Objectives

The objectives of this chapter are to calculate:

(a) the mass of 98 mass% H_2SO_4, 2 mass% H_2O sulfuric acid that is produced from Fig. 23.1's inputs

(b) the mass of water needed to make this acid

both per kg-mole of dry 10 volume% SO_2, 11 volume% O_2, 79 volume% N_2 1st catalyst bed feed gas.

Molar and mass balances are used.

23.2 Mass Balances

Acid compositions are given in mass%. It is easier, therefore, to base acid flow calculations on kg rather than kg-mole. This requires, however, that connections be made between the:

molar (gas) calculations of Chapters 10 to 22

and the:

mass (liquid) calculations of this chapter.

The connective calculations are:

conversion of kg-mole SO_3 in H_2SO_4 making tower input gas to kg SO_3.

conversion of kg-mole $H_2O(g)$ in moist acid plant input gas to kg $H_2O(g)$.

Once these conversions are made, the remainder of the calculations can be based on mass.

23.3 SO_3 Input Mass

The gas entering Fig. 23.1's H_2SO_4 making ('absorption') tower is specified to be Section 16.3's 3rd catalyst bed exit gas. It contains:

0.098	kg-mole	SO_3
0.002	"	SO_2
0.061	"	O_2
0.790	"	N_2

per kg-mole of dry 10 volume% SO_2, 11 volume% O_2, 79 volume% N_2 1st catalyst bed feed gas.

Only the SO_3 participates in H_2SO_4 making. It is specified that it all ends up as $H_2SO_4(\ell)$, Reaction (1.2).

The mass of SO_3 equivalent to 0.098 kg-mole is given by the equation:

$$\text{mass } SO_3 = \text{kg-mole } SO_3 * 80 \text{ kg } SO_3 \text{ per kg-mole } SO_3$$

$$= 0.098 * 80$$

$$= 7.84 \text{ kg per kg-mole of dry 1st catalyst bed feed gas} \quad (23.1).$$

(80 is the molecular weight of SO_3.)

23.4 $H_2O(g)$ Input from Moist Acid Plant Input Gas

Fig. 23.1 shows that its moist acid plant input gas contains 5 volume% $H_2O(g)$. The remaining 95 volume% is dry 1st catalyst bed feed gas. These are equivalent to 5 and 95 mole% respectively.

This gas is dehydrated in Fig. 23.1's dehydration tower. Its $H_2O(g)$ reacts with strong sulfuric acid in the tower to form:

slightly weakened sulfuric acid.

The reaction is:

$$\underset{\text{in strong acid}}{H_2O(g) + H_2SO_4(\ell)} \rightarrow \underset{\text{slightly weakened acid}}{H_2SO_4(\ell) + H_2O(\ell)} \qquad (6.2).$$

This section calculates the mass of $H_2O(g)$ in 5 mole% $H_2O(g)$ input gas. It is specified that all of this $H_2O(g)$ ends up in Reaction (6.2)'s slightly weakened acid.

23.4.1 $H_2O(g)$ in moist input gas

The amount of $H_2O(g)$ in Fig. 23.1's moist input gas is given by the equation:

$$\text{kg-mole } H_2O(g) \text{ in moist input gas} = \text{5 mole\% } H_2O(g) \text{ in moist input gas}/100\% * \text{kg-mole moist input gas} \qquad (23.2).$$

Similarly, the quantity of dry 1st catalyst bed feed gas in the moist acid plant input gas is:

$$\text{kg-mole of dry 1}^{st}\text{ catalyst bed feed gas in moist input gas} = \text{95 mole\% dry 1}^{st}\text{ catalyst bed feed gas in moist input gas}/100\% * \text{kg-mole moist input gas} \qquad (23.3).$$

The amount of input $H_2O(g)$ <u>per kg-mole of dry 1st catalyst bed feed gas</u> is obtained by dividing Eqn. (23.2) by Eqn. (23.3), i.e.:

$$\frac{\text{kg-mole } H_2O(g) \text{ in moist input gas}}{\text{kg-mole of dry 1}^{st}\text{ catalyst bed feed gas in moist input gas}} = \frac{5}{95} = 0.0526 \text{ kg-mole } H_2O(g) \text{ per kg-mole of dry 1}^{st}\text{ catalyst bed feed gas} \qquad (23.4).$$

23.4.2 Mass $H_2O(g)$ in moist input gas

Mass $H_2O(g)$ in the above moist gas is given by the equation:

$$\begin{matrix}\text{mass } H_2O(g) \\ \text{in moist acid} \\ \text{plant input gas}\end{matrix} = \begin{matrix}0.0526 \text{ kg-mole of } H_2O(g) \text{ per kg-mole} \\ \text{of dry } 1^{st} \text{ catalyst bed feed gas}\end{matrix} * \begin{matrix}18 \text{ kg } H_2O(g) \\ \text{per kg-mole} \\ \text{of } H_2O(g)\end{matrix}$$

$$= 0.947 \text{ kg } H_2O(g) \text{ per kg-mole of dry } 1^{st} \text{ catalyst bed feed gas} \qquad (23.5).$$

(18 is the molecular weight of H_2O.)

The above sections determine:

(a) mass $SO_3(g)$ entering Fig. 23.1's H_2SO_4 making tower acid

(b) mass $H_2O(g)$ entering Fig. 23.1's dehydration tower acid.

These masses plus mass input liquid water form Fig. 23.1's acid product.

The next sections calculate:

(a) the mass of output 98 mass% H_2SO_4, 2 mass% H_2O sulfuric acid produced by these inputs

(b) the mass of liquid water needed to make this acid product.

23.5 Water for Product Acid

The water entering the Fig. 23.1 acid plant is adjusted to give the plant's specified product, in this case:

98 mass% H_2SO_4
2 mass% H_2O

sulfuric acid.

This water and the $H_2O(g)$ in moist input gas provide all the H_2O for this acid. The H_2O is used for:

(a) the reaction:

$$SO_3(g) \quad + \quad H_2O \quad \rightarrow \quad H_2SO_4(\ell)$$

and:

(b) the 2 mass% H_2O in the product acid.

23.6 Calculation of Mass Water In and Mass Acid Out

This section calculates:

(a) the mass of H_2SO_4 produced from Section 23.3's $SO_3(g)$

(b) the mass of liquid water required to make this H_2SO_4 plus the specified 2 mass% H_2O in the plant's product acid

(c) the total mass of product acid

all per kg-mole of dry 1st catalyst bed feed gas.

The calculations use:

(a) $SO_3(g)$ and $H_2O(g)$ input Eqns. (23.1) and (23.5)

(b) sulfur and total mass balances

(c) a 98 mass% H_2SO_4, 2 mass% H_2O acid composition specification.

The H_2SO_4 making tower's input SO_2, O_2 and N_2 are ignored – because they pass unreacted through the acid plant and into the environment.

23.6.1 S balance

The S mass balance for Fig. 23.1's H_2SO_4 making tower (excluding SO_2) is:

$$\begin{array}{c}\text{mass S in } SO_3 \text{ into}\\ H_2SO_4 \text{ making tower}\end{array} = \text{mass S in product } H_2SO_4$$

Since SO_3 and H_2SO_4 contain 40 mass% and 32.7 mass% S respectively, this equation becomes:

$$40\%/100\% * \begin{array}{c}\text{mass } SO_3 \text{ into}\\ H_2SO_4 \text{ making}\\ \text{tower}\end{array} = 32.7\%/100\% * \text{mass output } H_2SO_4$$

or:

$$0 = -0.4 * \begin{array}{c}\text{mass } SO_3 \text{ into}\\ H_2SO_4 \text{ making}\\ \text{tower}\end{array} + 0.327 * \text{mass output } H_2SO_4 \qquad (23.6).$$

23.6.2 Total mass balance

The total mass balance for Fig. 23.1 (excluding SO_2, O_2 and N_2 in H_2SO_4 making tower input and output gas) is:

$$\text{mass } SO_3 \text{ into } H_2SO_4 \text{ making tower} + \text{mass } H_2O(g) \text{ in} + \text{mass water in} = \text{mass } H_2SO_4 \text{ out} + \text{mass } H_2O \text{ out}$$

or:

$$0 = -\text{mass } SO_3 \text{ into } H_2SO_4 \text{ making tower} - \text{mass } H_2O(g) \text{ in} - \text{mass water in} + \text{mass } H_2SO_4 \text{ out} + \text{mass } H_2O \text{ out} \qquad (23.7).$$

23.6.3 Output acid composition specification

The output acid composition is put into equation form by combining the equations:

$$\text{mass } H_2SO_4 \text{ in output acid} = \frac{98 \text{ mass\% } H_2SO_4 \text{ in output acid}}{100\%} * \text{mass output acid}$$

$$\text{mass } H_2O \text{ in output acid} = \frac{2 \text{ mass\% } H_2O \text{ in output acid}}{100\%} * \text{mass output acid}$$

to give:

$$\frac{\text{mass } H_2SO_4 \text{ in output acid}}{\text{mass } H_2O \text{ in output acid}} = \frac{98}{2}$$

or:

$$2 * \text{mass } H_2SO_4 \text{ in output acid} = 98 * \text{mass } H_2O \text{ in output acid}$$

or:

$$0 = -2 * \text{mass } H_2SO_4 \text{ in output acid} + 98 * \text{mass } H_2O \text{ in output acid} \qquad (23.8).$$

23.6.4 Solving for mass H_2SO_4 out and mass water in

The above four sections contain 5 variables:

mass SO_3 into H_2SO_4 making tower

mass $H_2O(g)$ in

mass water in

mass H_2SO_4 out

mass H_2O out.

They also contain 5 equations, (23.1) and (23.5-23.8). The solutions to all these equations are obtained by solving matrix Table 23.1, as described in Appendix H.

Table 23.1. Matrix for determining the mass of H_2SO_4 produced by the Fig. 23.1 acid plant. The water requirement is also determined. All numerical values are per kg-mole of dry 1st catalyst bed feed gas. The solution to the matrix is given below it.

	A	B	C	D	E	F	G	H
1	Description	equation	numerical term	mass SO_3 into H_2SO_4 making tower	mass H_2O in moist input gas	mass input water	mass H_2SO_4 in output acid	mass H_2O in output acid
2	mass SO_3 into H_2SO_4 making tower	23.1	7.840	1	0	0	0	0
3	mass H_2O in moist feed gas	23.5	0.947	0	1	0	0	0
4	S balance#	23.6	0	-0.4	0	0	0.327	0
5	total mass balance#	23.7	0	-1	-1	-1	1	1
6	output acid composition specification	23.8	0	0	0	0	-2	98

Excluding SO_2, O_2 and N_2 entering and leaving Fig. 23.1's H_2SO_4 making tower.

The solution to the matrix, with all values kg per kg-mole of dry 1st catalyst bed feed gas, is:

mass SO_3 in H_2SO_4 making tower input gas	7.840
mass $H_2O(g)$ in moist input gas	0.947
mass input water	0.999
mass H_2SO_4 in output acid	9.590
mass H_2O in output acid	0.196

These are the only values that satisfy all the equations in the matrix.

23.6.5 Mass output sulfuric acid

Total output acid mass is given by the equation:

mass output acid = mass H_2SO_4 in output acid + mass H_2O in output acid (23.9).

With the above values, it is:

mass output acid = 9.590 + 0.196 = 9.8 kg per kg-mole of dry 1st catalyst bed feed gas.

23.6.6 Flows with 100 000 Nm^3 per hour dry 1st catalyst bed feed gas

The above masses are all per kg-mole of dry 1st catalyst bed feed gas. With 100 000 Nm^3 per hour (4464 kg-mole per hour) of dry 1st catalyst bed feed gas, these masses are equivalent to:

Flow	**kg/hour**
SO_3 in H_2SO_4 making tower input gas	35 000
H_2O in moist input gas	4 200
water in	4 500
H_2SO_4 in output acid	42 800
H_2O in output acid	900
output acid	43 700.

Of course, these flows will double if the 1st catalyst bed feed gas input rate is doubled, etc.

23.7 Interpretations

23.7.1 H_2SO_4 production vs. SO_3 in H_2SO_4 making tower input gas

Fig. 23.2 shows mass H_2SO_4 out of Fig. 23.1's H_2SO_4 making tower as a function of the tower's input SO_3 quantity. H_2SO_4 production (kg) increases linearly with increasing SO_3 input mass (kg).

This is because each kg-mole of SO_3 into the H_2SO_4 making tower produces a kg-mole of H_2SO_4, i.e.:

$$SO_3 + H_2O \longrightarrow H_2SO_4 \qquad (23.10).$$

In terms of mass, each 80 kg of input SO_3 gives 98 kg of output H_2SO_4. This is equivalent to:

$$98/80 = 1.225$$

kg H_2SO_4 out per kg of input SO_3. This is confirmed by the slope of Fig. 23.2's H_2SO_4 making line.

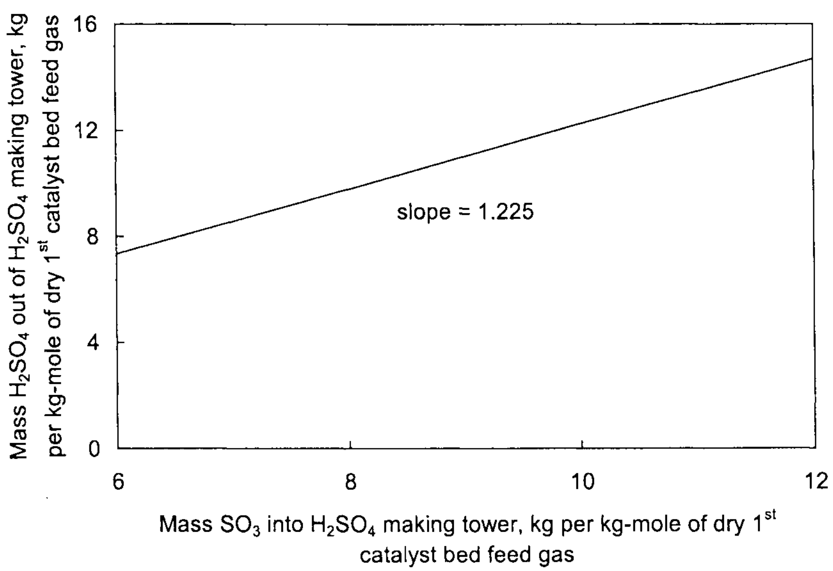

Fig. 23.2. Mass H_2SO_4 out of H_2SO_4 making tower as a function of mass SO_3 into H_2SO_4 making tower. The line is straight with a slope of 1.225 (Section 23.7.1).

23.7.2 Water requirement vs. $H_2O(g)$ in moist input gas

Fig. 23.3 shows Fig. 23.1's acid plant water requirement as a function of volume% $H_2O(g)$ in its moist input gas. As expected, water requirement falls with increasing $H_2O(g)$ in moist feed gas.

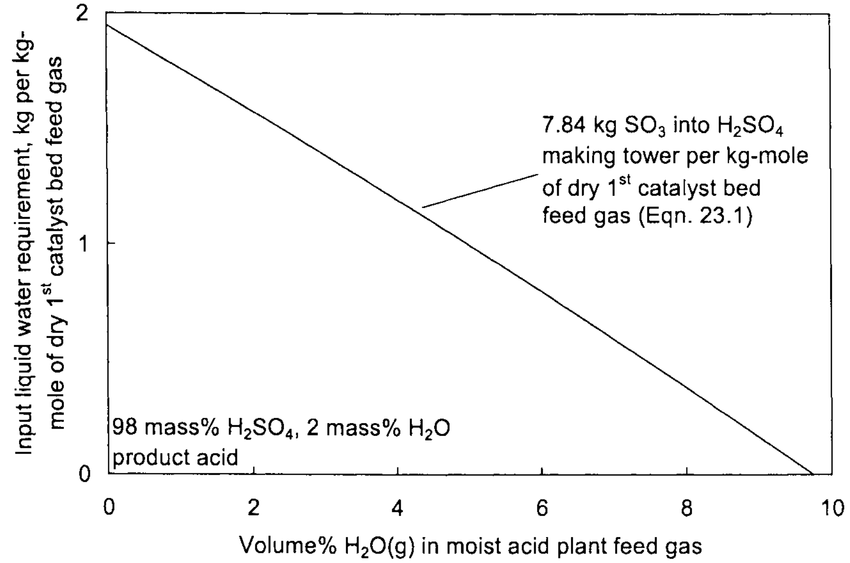

Fig. 23.3. Fig. 23.1 acid plant water requirement as a function of volume% $H_2O(g)$ in acid plant input gas. Water input requirement decreases with increasing volume% $H_2O(g)$. The graph applies only to its specified input SO_3 mass and product acid composition.

Fig. 23.3 also shows that no liquid water is required when the moist input gas contains 9.8 volume% $H_2O(g)$ (under the specific conditions of the Table 23.1 matrix). At this point, all the output acid's H_2O requirement is provided by $H_2O(g)$ in Fig. 23.1's feed gas.

Finally, the figure indicates that moist input gas containing more than 9.8 volume% $H_2O(g)$ cannot produce the specified 98 mass% H_2SO_4 acid – because it brings too much H_2O into the system. 10 volume% $H_2O(g)$ moist input gas would produce, for example, ~97½ mass% H_2SO_4 acid.

23.7.3 Water requirement vs. acid strength

Fig. 23.4 shows the Fig. 21.1 acid plant's water requirement as a function of specified mass% H_2SO_4 in product acid (constant volume% $H_2O(g)$ in moist acid plant input gas).

Water requirement increases with decreasing mass% H_2SO_4 in acid (i.e. with increasing specified mass% H_2O in acid).

Note that liquid water is needed even when the acid plant's product is 100% H_2SO_4. It is needed for the:

$$H_2O + SO_3 \rightarrow H_2SO_4$$

H_2SO_4 making reaction.

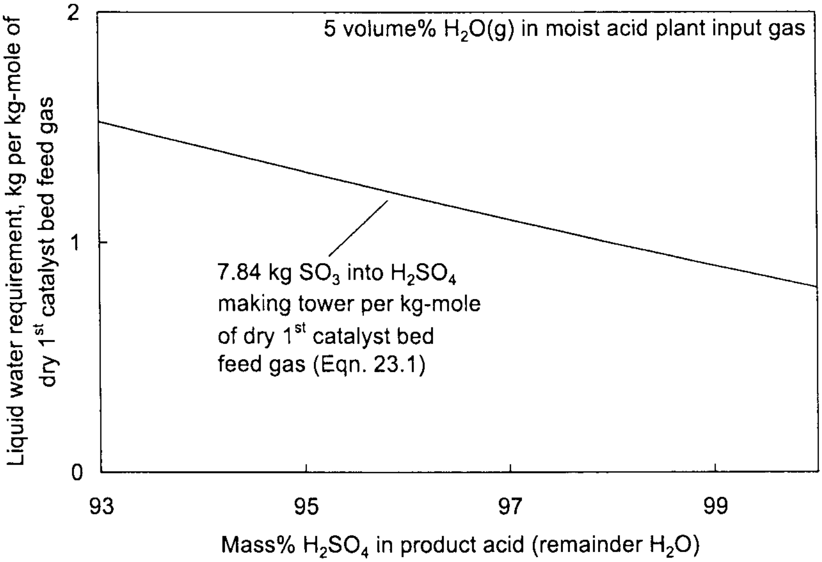

Fig. 23.4. Fig. 23.1 acid plant water requirement as a function of mass% H_2SO_4 in acid plant product acid. Water requirement increases with decreasing specified mass% H_2SO_4 (i.e. with increasing specified mass% H_2O) in acid.

23.7.4 Water requirement vs. mass SO_3 into H_2SO_4 making tower

Fig. 23.5 shows the effect of:

mass SO_3 into H_2SO_4 making tower

on:

acid plant liquid water requirement.

both per kg-mole of dry 1st catalyst bed feed gas. Water requirement increases with increasing mass SO_3.

The increased requirement is made up of:

(a) water needed for Fig. 23.2's increasing H_2SO_4 production, Reaction (23.10)

(b) water for the 2 mass% H_2O in product acid that goes with this increased H_2SO_4 production.

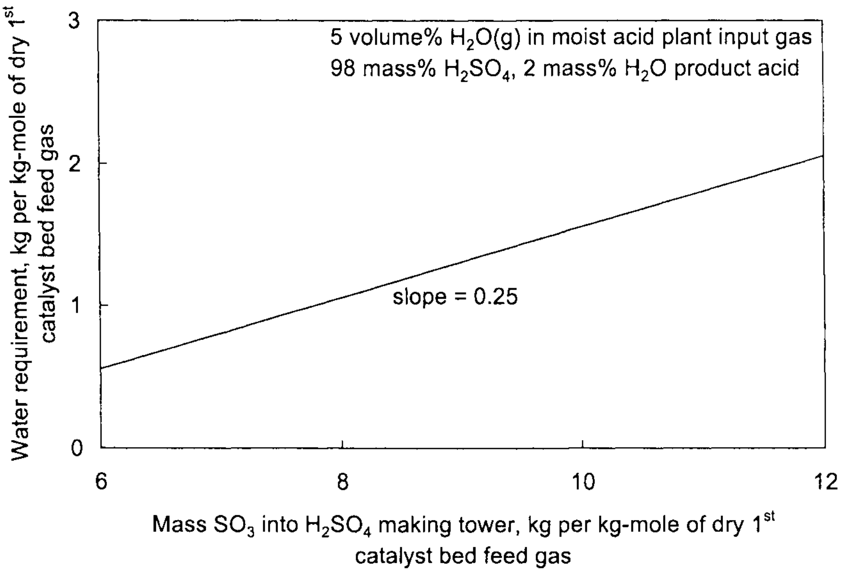

Fig. 23.5. Acid plant water requirement as a function of mass SO_3 into H_2SO_4 making tower. The water requirement increases with increasing SO_3 input mass, Section 23.7.4. With a 100% H_2SO_4 product, the slope is 0.225 (Fig. 23.2). With 2 mass% H_2O, 98 mass% H_2SO_4 product acid, it is 0.25 (as shown). It varies, therefore, with product acid composition.

23.8 Summary

Sulfuric acid compositions are expressed in mass%. For this reason, acidmaking calculations are more easily done with mass (rather than molar) balances.
This chapter uses mass balances to calculate an acid plant's:

(a) H_2SO_4 production

(b) water requirement

(kg per kg-mole of dry 1st catalyst bed feed gas and kg per hour).

H_2SO_4 production increases with increasing SO_3 mass in H_2SO_4 making tower input gas, both per kg-mole of dry 1st catalyst bed feed gas. Acid plant water requirement increases commensurately.

Water requirement also increases with:

(a) decreasing $H_2O(g)$ concentration in moist acid plant feed gas

and

(b) increasing specified mass% H_2O in product acid.

Problem

23.1 The moist gas entering a Fig. 23.1 acid plant contains 6 volume% $H_2O(g)$ and 94 volume% dry 1st catalyst bed feed gas.

The dry portion of input gas contains 12 volume% SO_2, 13.2 volume% O_2 and 74.8 volume% N_2.

This gas is:

(a) dehydrated with strong sulfuric acid

(b) oxidized in 3 catalyst beds

(c) sent to H_2SO_4 making.

The H_2SO_4 making tower input gas (i.e. cooled 3rd catalyst bed exit gas) contains:

0.1183 kg-mole SO_3
0.0017 " " SO_2
0.0728 " " O_2
0.7480 " " N_2

per kg-mole of dry 1st catalyst bed feed gas (Problem 16.1).

The plant is producing 98.5 mass% H_2SO_4, 1.5 mass% H_2O sulfuric acid.

All the input $H_2O(g)$ and all the SO_3 entering the H_2SO_4 making tower end up in the plant's acid product.

Calculate:

(a) the mass of H_2SO_4 produced

(b) the mass of sulfuric acid produced

(c) the mass of input water needed to make this sulfuric acid

all per kg-mole of dry 1st catalyst bed feed gas.

Calculate also the flows of these materials, kg per hour, when 100 000 Nm^3 per hour of dry 1st catalyst bed feed gas are entering the acid plant.

Table 23.2. Details of packed bed H_2SO_4-from-SO_3 plants.

Plant	S1	M2
input gas flowrate, thousand Nm^3/hour	296	110
estimated SO_3 utilization efficiency		99.9
Packed bed details		
number of packed beds	1	1
height * diameter, m	9.85 × 8.3	18.5 × 6.5
construction material	310/304 stainless steel	brick lined carbon steel
ceramic packing	7.5 cm saddles	5.1 & 7.6 cm saddles
packing height, m	2.44	4
acid distributor type	trough and downcomer	buried pipe distributor
mist eliminator type	candles	hanging fiber bed
exit gas mist concentration, g/Nm^3		
acid flowrate, m^3/hour	1060	762
Temperature data, K		
inlet gas	408	463
outlet gas	355	345
inlet acid	355	345
outlet acid	365	356
acid cooling method		plate heat exchanger
Gas composition in, vol.%		
SO_3	0.745	0.42
SO_2	0.04	0.01
O_2	3.9	5.14
CO_2	0	
N_2	95.3	
Gas composition out, vol.%		
SO_3		0
SO_2	0.04	0.01
O_2	3.97	5.16
CO_2	0	
N_2	96.0	
	no tail gas scrubbing	NaOH scrubbing
Acid comp., mass% H_2SO_4		
into tower	98.4	98.5
out of tower	98.5	98.5
Acid plant products, mass% H_2SO_4	98.5	98.5

The data are for FINAL H_2SO_4 making in double contact plants.

Cumerio 1 (Bulgaria)	Cumerio 2 (Bulgaria)	M6
160	150	191
99.98	99.98	99.9
1	1	1
19.2 × 7	21.02 × 7	20.5 × 7.1
brick lined carbon steel	brick lined carbon steel	brick lined carbon steel
7.6 & 5.1 cm saddles	5.1 cm saddles	7.6 cm saddles
3.5	8.5	3.7
Lurgi pipes and tubes	distribution plates	troughs and downcomers
high efficiency candles	candle type	high efficiency candles
750	700	707
453	433	505
355	353	350
355	333	350
384	353	372
shell and tube	shell and tube	shell and tube
0.56	0.45	0.51
0.01	0.014	0.05
8.06	6.12	13.40
0.36	0.31	
91.01	93.11	remainder (inerts)
0.0022	0.0018	
0.027	0.017	0.05
8.1	6.12	13.4
0.36	0.31	
91.51	93.55	
no scrubbing	no scrubbing	no scrubbing
98.5	98.3	98.5
98.55	98.31	98.6
94-98.5	94-98.5	93, 99 oleum (20%)

Table 23.2 (cont.). Details of packed bed H_2SO_4-from-SO_3 plants.

Plant	M4	Asarco Hayden
input gas flowrate, thousand Nm^3/hour	158	170
estimated SO_3 utilization efficiency	99.9	99.9
Packed bed details		
number of packed beds	1	1
height * diameter, m	20.4 × 7.5 (OD)	17.8 × 6.7
construction material	brick lined carbon steel	brick lined carbon steel
ceramic packing	5.1 & 7.6 cm saddles	7.6 cm saddles
packing height, m	5.9	3.66
acid distributor type	submerged distributor pipe	SX troughs
mist eliminator type	Brink mist eliminator (C fiber)	candles
exit gas mist concentration, g/Nm^3	<0.05	
acid flowrate, m^3/hour	940	450
Temperature data, K		
inlet gas	453	455
outlet gas	350	355
inlet acid	350	355
outlet acid	360	377
acid cooling method		
Gas composition in, vol.%		
SO_3	1.1	0.6
SO_2	0.025	0.05
O_2	8.7	7.77
CO_2	3.3	1.2
N_2	remainder	90.4
Gas composition out, vol.%		
SO_3		
SO_2	0.026	0.05
O_2	8.8	7.77
CO_2	3.3	1.2
N_2	remainder	90.9
	no scrubbing	no scrubbing
Acid comp., mass% H_2SO_4		
into tower	98.5	98.0
out of tower		98.5
Acid plant products, mass% H_2SO_4	98.5	93/98

The data are for FINAL H_2SO_4 making in double contact plants.

Phelps Dodge Miami	M1
204	50
99.9	99.9
1	1
21.5 × 8.5	8.5 × 4
carbon steel shell	brick lined carbon steel
5.1 cm saddles and intalox saddles	7.6 cm saddles
5.3	4
pipe and perforated arms	pipe
high efficiency candles	mesh pads (tent and flat)
950	227
516	472-494
348	339-366
348	347-358
375	358-375
	shell and tube
3	
0.15	0.008-0.012
7.25	10.2-12.2
1.1	
88.5	
0	
0.155	0.008-0.012
7.475	10.2-12.2
1.134	1.0
91.236	
scrubbing available, if needed	no scrubbing
98.5	98.5
98.8	98.8
94.5	93.5

Chapter 24

Acid Temperature Control and Heat Recovery

H_2SO_4 is made by the reaction of $SO_3(g)$ with $H_2O(\ell)$ in strong sulfuric acid, i.e.:

$$\underset{\substack{\text{in catalytic}\\\text{oxidation}\\\text{exit gas}}}{SO_3(g)} + \underset{\substack{\text{in strong}\\\text{sulfuric acid}}}{H_2O(\ell)} \xrightarrow{\text{350-380 K}} \underset{\substack{\text{in strengthened}\\\text{sulfuric acid}}}{H_2SO_4(\ell)} \qquad (1.2).$$

The reaction is exothermic. It releases about 130 MJ of heat per kg-mole of $SO_3(g)$.

A result of this is that H_2SO_4 making's output acid is ~25 K warmer than its inlet acid. Fig. 24.1 describes the process.

24.1 Objectives

The objectives of this chapter are to:

(a) show how Fig. 24.1's output acid temperature is calculated

(b) describe the factors which affect this temperature

(c) indicate how output acid is cooled for recycling and shipping

(d) describe how heat-in-acid is recovered as steam.

24.2 Calculation of Output Acid Temperature

This section shows how Fig. 24.1's output acid temperature is calculated. It uses:

(a) Fig. 24.1's temperatures and acid compositions

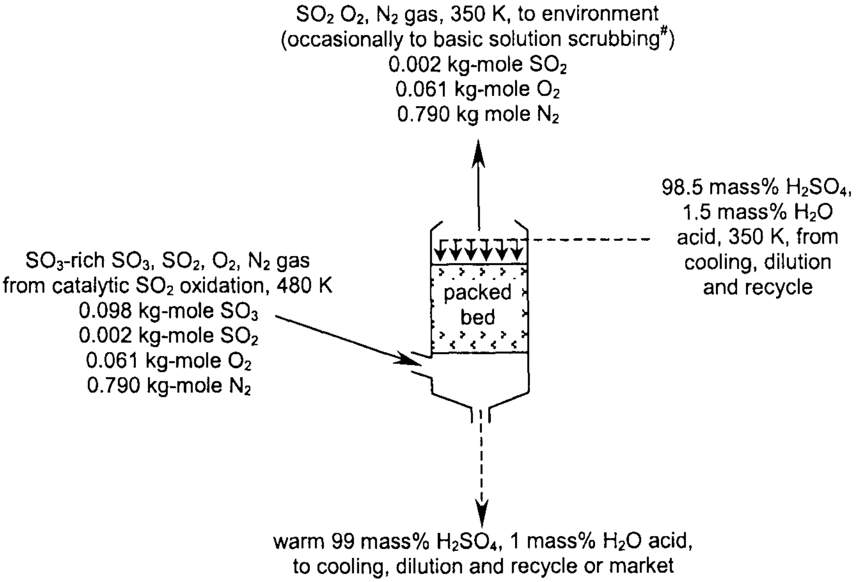

Fig. 24.1. Fig. 23.1's single contact H_2SO_4 making tower. Its temperatures and gas compositions are used in Section 24.1 and 24.2's calculations. The calculations assume that all input $SO_3(g)$ reacts to form $H_2SO_4(\ell)$. Note that output gas temperature = input acid temperature. (#Hay *et al.*, 2003).

(b) Fig. 24.1's input and output gas quantities

(c) mass and enthalpy balances

(d) Appendix G's enthalpy vs. temperature equations

(e) $H_2SO_4(\ell)$-$H_2O(\ell)$ enthalpy of mixing Eqn. (24.2).

Appendix W calculates Fig. 24.1's input and output H_2SO_4 and H_2O masses. They are listed in Table 24.1.

24.2.1 $H_2SO_4(\ell)$-$H_2O(\ell)$ enthalpy-of-mixing

Mixing of $H_2SO_4(\ell)$ and $H_2O(\ell)$ releases heat. This means that the enthalpy of sulfuric acid is lower than the combined enthalpies of its components.

Calorimetric measurements indicate that the enthalpy of mixing $H_2SO_4(\ell)$ and $H_2O(\ell)$ is given by the equation:

$$\underset{\text{MJ per kg-mole of } H_2SO_4}{\Delta H^{\text{mix}}_{H_2SO_4}} = -1.82 * \begin{matrix}\text{mass\% } H_2O \text{ in}\\ \text{sulfuric acid}\end{matrix} \qquad (24.1)$$

(for acid containing up to ~10 mass% H_2O [Duecker and West, 1966]).

Table 24.1. Fig. 24.1's inputs and outputs. Input and output kg-mole of SO_3, SO_2, O_2 and N_2 are from Fig. 24.1. Input and output H_2SO_4 and H_2O masses are calculated in Appendix W. They are all used to calculate Fig. 24.1's output acid temperature. The H° values have been calculated by the equations in Appendix G. (kg-mole H_2SO_4 = kg H_2SO_4/98. kg-mole H_2O = kg H_2O/18)

Substance	mass, kg[#]	kg-mole[#]	specified temperature, K Fig. 24.1	H°, MJ per kg-mole of substance
$SO_3(g)$ **in**		0.098	480	-386.31
$SO_2(g)$ **in**		0.002	480	-289.53
$O_2(g)$ **in**		0.061	480	5.208
$N_2(g)$ **in**		0.790	480	5.131
$H_2SO_4(\ell)$ **in**	360.237	3.676	350	-806.06[##]
$H_2O(\ell)$ **in**	5.486	0.305	350	-281.91
$SO_2(g)$ **out**		0.002	350	-296.24
$O_2(g)$ **out**		0.061	350	0.876
$N_2(g)$ **out**		0.790	350	1.088
$H_2SO_4(\ell)$ **out**	369.827	3.774	?	? [###]
$H_2O(\ell)$ **out**	3.736	0.208	?	?

[#] per kg-mole of 1st catalyst bed feed gas. [##] H, as described by Eqn. (24.2) with 1.5 mass% H_2O in input acid. [###] H, as described by Eqn. (24.2) with 1.0 mass% H_2O in output acid.

The enthalpy of H_2SO_4-in-acid may, therefore, be represented by:

$$H_{T\atop H_2SO_4(\ell)} = H^{\circ}_{T\atop H_2SO_4(\ell)} - 1.82 * \text{mass\% } H_2O \text{ in sulfuric acid} \tag{24.2}$$

(MJ per kg-mole of H_2SO_4).

This equation gives all the heat of mixing to H_2SO_4 rather than to (H_2SO_4 + H_2O). It allows $H^{\circ}_{T\atop H_2O(\ell)}$ to be used without change in our acid temperature calculations.

24.2.2 *H_2SO_4 making enthalpy balance*

The H_2SO_4 making tower enthalpy balance may be written:

$$\begin{matrix}\text{input gas}\\ \text{enthalpy}\end{matrix} + \begin{matrix}\text{input acid}\\ \text{enthalpy}\end{matrix} = \begin{matrix}\text{output gas}\\ \text{enthalpy}\end{matrix} + \begin{matrix}\text{output acid}\\ \text{enthalpy}\end{matrix} + \begin{matrix}\text{conductive, convective}\\ \text{plus radiative heat loss}\end{matrix} \tag{24.3}$$

It is simplified by assuming that:

$$\begin{matrix}\text{conductive, convective}\\ \text{and radiative heat loss}\end{matrix} = 0$$

This gives the final enthalpy equation:

$$\begin{matrix}\text{output acid}\\ \text{enthalpy}\end{matrix} = \left\{\begin{matrix}\text{input gas}\\ \text{enthalpy}\end{matrix} + \begin{matrix}\text{input acid}\\ \text{enthalpy}\end{matrix}\right\} - \begin{matrix}\text{output gas}\\ \text{enthalpy}\end{matrix} \qquad (24.4).$$

24.2.3 Output acid enthalpy

Eqn (24.4) may be expanded to:

$$\text{output }\underline{\text{acid}}\text{ enthalpy} = \begin{aligned}&\left.\begin{aligned}
&\text{kg-mole } SO_3(g)\ \mathbf{in} * H^{\circ}_{\substack{480\,K\\ SO_3(g)}}\\
+\ &\text{kg-mole } SO_2(g)\ \mathbf{in} * H^{\circ}_{\substack{480\,K\\ SO_2(g)}}\\
+\ &\text{kg-mole } O_2(g)\ \mathbf{in} * H^{\circ}_{\substack{480\,K\\ O_2(g)}}\\
+\ &\text{kg-mole } N_2(g)\ \mathbf{in} * H^{\circ}_{\substack{480\,K\\ N_2(g)}}\\
+\ &\text{kg-mole } H_2SO_4(\ell)\ \mathbf{in} * H_{\substack{350\,K\\ H_2SO_4(\ell)}}\\
+\ &\text{kg-mole } H_2O(\ell)\ \mathbf{in} * H^{\circ}_{\substack{350\,K\\ H_2O(\ell)}}
\end{aligned}\right\}\text{input enthalpy}\\
&\left.\begin{aligned}
-\ &\text{kg-mole } SO_2(g)\ \mathbf{out} * H^{\circ}_{\substack{350\,K\\ SO_2(g)}}\\
-\ &\text{kg-mole } O_2(g)\ \mathbf{out} * H^{\circ}_{\substack{350\,K\\ O_2(g)}}\\
-\ &\text{kg-mole } N_2(g)\ \mathbf{out} * H^{\circ}_{\substack{350\,K\\ N_2(g)}}
\end{aligned}\right\}\text{output }\underline{\text{gas}}\text{ enthalpy}\end{aligned}$$

$$(24.5)$$

where the quantities and enthalpies are those listed in Table 24.1.

With Table 24.1's numerical values:

$$\text{output acid enthalpy} = -3094.5\ \begin{matrix}\text{MJ per kg-mole of}\\ 1^{\text{st}}\text{ catalyst bed feed gas}\end{matrix} \qquad (24.6).$$

24.2.4 Output acid temperature

Output acid enthalpy is related to the output quantities and enthalpies of $H_2SO_4(\ell)$ and $H_2O(\ell)$ by the equation:

$$\begin{aligned}\text{Output acid enthalpy} = {} & \text{kg-mole output } H_2SO_4 * H_{\substack{T\,out\\ H_2SO_4\,(\ell)}} \\ & + \text{kg-mole output } H_2O * H^{\circ}_{\substack{T\,out\\ H_2O(\ell)}}\end{aligned} \qquad (24.7).$$

This equation is combined with Table G.1 and Eqn. (24.2) to give:

$$\begin{aligned}\text{Output acid enthalpy} = {} & \begin{matrix}\text{kg-mole}\\ \text{output}\\ H_2SO_4\end{matrix} * \left(0.1485 * T_{out} - 858.3 - 1.82 * \begin{matrix}\text{mass\% } H_2O\\ \text{in output}\\ \text{acid}\end{matrix}\right) \\ & + \begin{matrix}\text{kg-mole}\\ \text{output}\\ H_2O\end{matrix} * (0.07568 * T_{out} - 308.4)\end{aligned} \qquad (24.8)$$

where:

$(0.1485 * T_{out} - 858.3 - 1.82 * \text{mass\% } H_2O \text{ in output acid})$

is the enthalpy (H) of $H_2SO_4(\ell)$ in acid at temperature T_{out}, Appendix G and Eqn. (24.2)

and where:

$0.07568 * T_{out} - 308.4$

is the enthalpy (H°) of $H_2O(\ell)$ at temperature T_{out}, Appendix G (both MJ/kg-mole).

24.2.5 Final enthalpy equation

Substitution of Table 24.1's values of:

kg-mole output H_2SO_4 = 3.774

kg-mole output H_2O = 0.208

(per kg-mole of 1st catalyst bed feed gas) and:

$$\text{mass\% } H_2O \text{ in output acid} = 1.0$$

gives:

$$-3094.5 = 3.774 \begin{matrix}\text{kg-mole}\\ H_2SO_4(\ell)\end{matrix} * \left(0.1485 * T_{out} - 858.3 - 1.82 * 1.0 \begin{matrix}\text{mass\% } H_2O\\ \text{in output}\\ \text{acid}\end{matrix}\right)$$

$$+ 0.208 \begin{matrix}\text{kg-mole}\\ H_2O(\ell)\end{matrix} * (0.07568 * T_{out} - 308.4) \qquad (24.9)$$

from which:

$T_{out} = T_{outlet\ acid} = 374$ K

(as is readily confirmed by inserting 374 K in the right side of Eqn. (24.9).

Perhaps the simplest way to solve Eqn. (24.9) is by the following small Excel Goal Seek calculation.

	A	B	C	D	E	F
1	kg-mole $H_2SO_4(\ell)$ out =	3.774				
2	kg-mole $H_2O(\ell)$ out =	0.208				
3						
4	T_{out} =	374				
5	Output acid enthalpy =	-3094.5	=B1*(0.1485*B4 - 858.3 - 1.82*1) + B2*(0.07568*B4 - 308.4)			

Tools
Goal Seek
Set cell: *B5*
To value: *-3094.5*
By changing cell: *B4*
OK, OK.

24.2.6 Result

The resulting 374 K output acid temperature is 24 K higher than Table 24.1's 350 K input acid temperature. The next few sections examine the factors that affect this output acid temperature.

24.3 Effect of Input Acid Temperature

Fig. 24.2 shows the effect of H_2SO_4 making's input acid temperature on its output acid temperature.

Output acid temperature increases with increasing input acid temperature, but the increase is less than 1:1. This is because:

(a) output acid mass > input acid mass, Table 24.1

(b) output gas temperature (hence output gas enthalpy) increases with increasing input acid temperature (Fig. 24.1) leaving less enthalpy for the output acid.

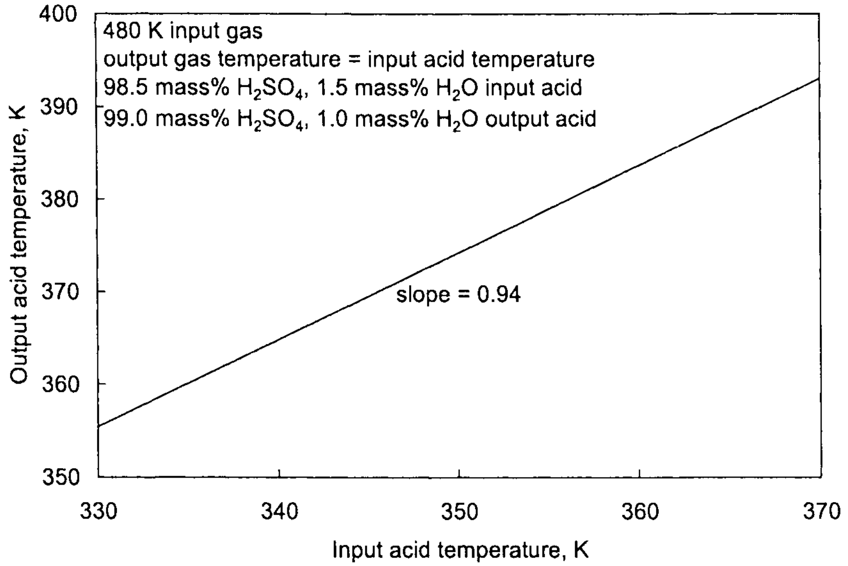

Fig. 24.2. Effect of Fig. 24.1's input acid temperature on its output acid temperature (with Table 24.1's input and output masses). A straight line relationship is shown. Note that the slope is less than 1, as explained in Section 24.3.

24.4. Effect of Input Gas Temperature

Fig. 24.3 shows the effect of H_2SO_4 making's input gas temperature on its output acid temperature. Output acid temperature increases slightly with increasing input gas temperature.

This is because hotter input gas brings slightly more enthalpy to H_2SO_4 making, giving slightly more enthalpy and a slightly higher temperature to the output acid.

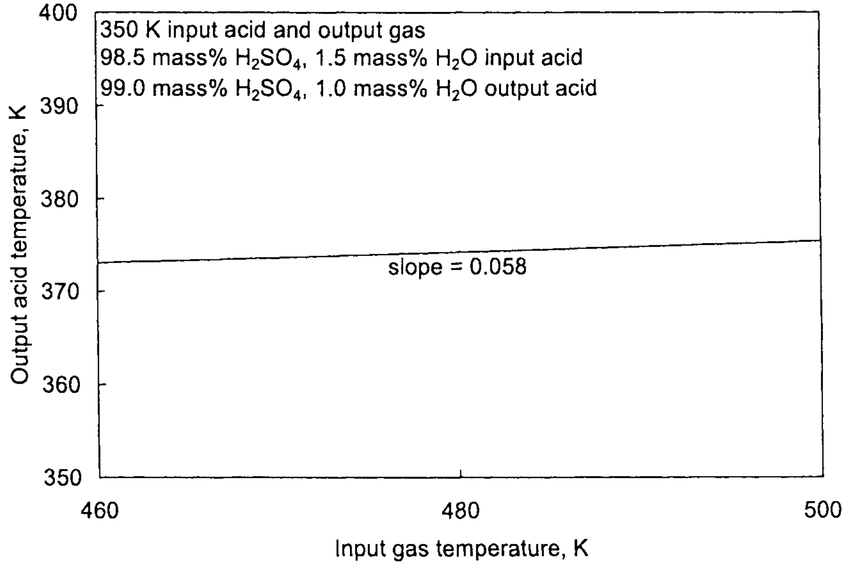

Fig. 24.3. Effect of input gas temperature on Fig. 24.1's output acid temperature (with Table 24.1's input and output masses). Output acid temperature increases slightly with increasing input gas temperature. Output gas temperature remains unaltered at the 350 K input acid temperature.

24.5 Effect of Output Acid Composition on Output Acid Temperature

Fig. 24.4 shows the effect of output acid composition on output acid temperature. Output acid temperature increases with increased mass% H_2SO_4 in output acid. This is because:

(a) the amount of circulating acid decreases with increasing mass% H_2SO_4 in output acid, Fig. W.1

while:

(b) heat release by Reaction (1.2) remains constant

(both per kg-mole of 1st catalyst bed feed gas).

24.6 Effect of Input Gas SO_3 Concentration on Output Acid Temperature

Fig. 24.5 shows the effect of Fig. 24.1's input gas SO_3 concentration on its output acid temperature. Output acid temperature decreases slightly with increasing SO_3-in-input-gas concentration. The smallness of the decrease shows why H_2SO_4 making can accept varying input SO_3 concentrations with an almost constant output acid temperature.

Of course, output acid temperature will increase if mass% H_2SO_4 in output acid is allowed to increase with increasing volume% SO_3 in H_2SO_4 making tower input gas, Fig. 24.4. This is the case when input acid flowrate and mass% H_2SO_4 are kept constant while volume% SO_3 in input gas increases. This is usual industrial practice.

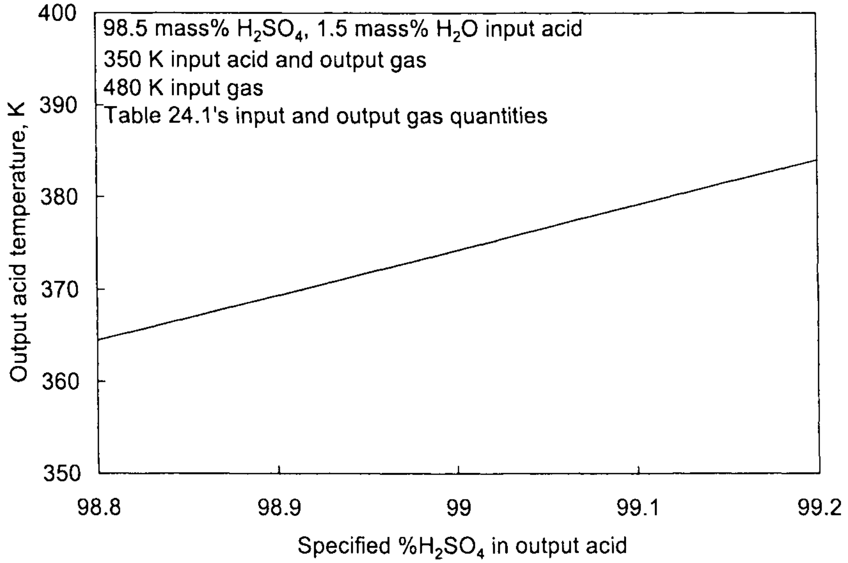

Fig. 24.4. Effect of specified output acid mass% H_2SO_4 on Fig. 24.1's output acid temperature. Output acid temperature increases with increasing output acid % H_2SO_4 as explained in Section 24.6. % H_2SO_4 in output acid is increased by slowing the rate at which acid is cycling through the H_2SO_4 making tower (and vice versa).

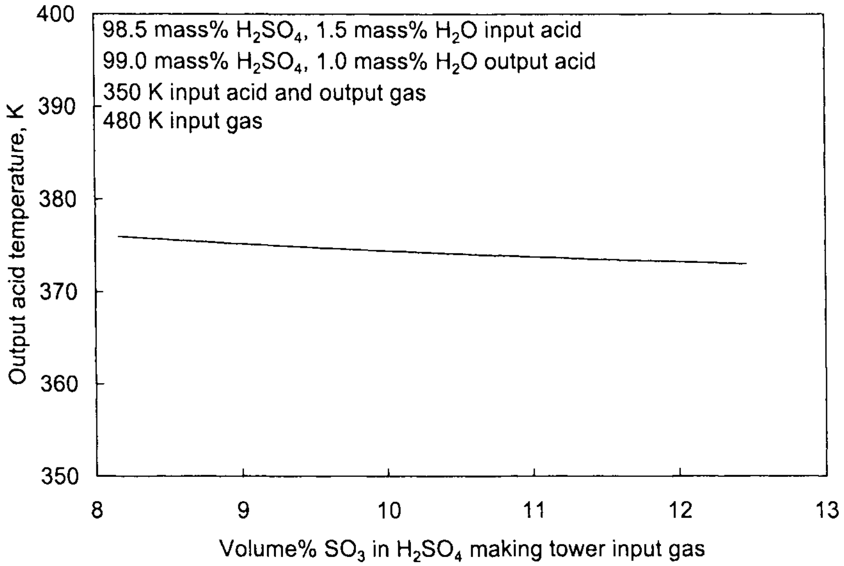

Fig. 24.5. Effect of SO_3(g)-in-input-gas concentration on H_2SO_4 making output acid temperature. Output acid temperature decreases slightly with increasing SO_3(g) concentration. The volume% SO_3 values have been calculated as described in Chapter 16 starting with 8, 9, 10, 11 and 12 volume% SO_2 in 1st catalyst bed feed gas.

24.7 Acid Cooling

The above discussion indicates that acid is heated by Reaction (1.2) as it cycles through the H_2SO_4 making tower. It is evident from this that the recycling acid must be cooled to prevent the system from overheating.

This is done by passing the acid through water cooled:

(a) shell and tube (Figs. 9.5 and 24.6) (Chemetics, 2004)

and

(b) plate and frame (Haslego, 2005)

heat exchangers. Both involve counter current, indirect heat exchange between:

cool water

and:

warm acid.

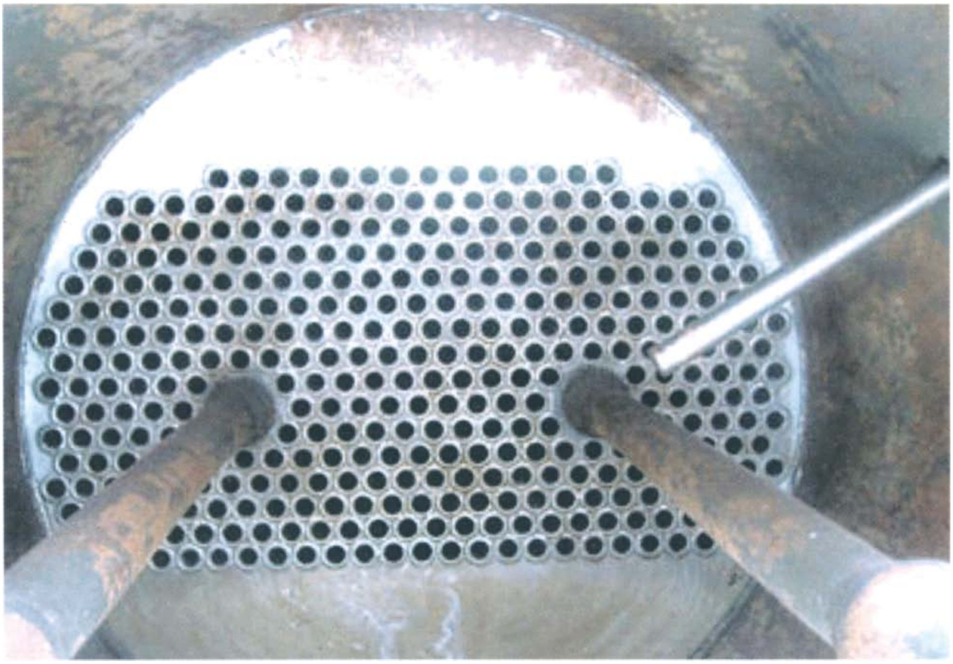

Fig. 24.6. Inside an acid cooler. Fig. 9.5 gives an external view. Tubes start through the tube 'sheet', shown here. They extend almost to the far end of the cooler where there is another tube 'sheet'. Cool water enters at this end and flows through the tubes to the far end. Between the tube 'sheets', the tubes are surrounded by warm acid moving turbulently around them. Heat transfers from the warm acid to the cool water (through the tube walls). The tube entering from the right contains a thermocouple. The polymer tubes in the foreground surround metal rods. The rods are bare between the tube 'sheets'. An electrical potential applied between them and the water tubes anodically protects the tubes against acid side corrosion.

The cooled acid is recycled to the H_2SO_4 making tower or sent to product storage. The warmed water is cooled with atmospheric air and recycled to the acid coolers.

Dehydration tower acid is cooled the same way.

24.8 Target Acid Temperatures

Sulfuric acid:

(a) corrosivity

(b) H_2SO_4, SO_3 and H_2O vapor pressures

increase with increasing acid temperature. It is important, therefore, that acid temperature be kept relatively cool.

Conversely, the rate of H_2SO_4 making Reaction (1.2) decreases with decreasing acid temperature – which means that input acid temperature must not be too cool. 380 K is a typical output acid temperature (~100 K warmer in acid heat to steam recovery plants, next section).

24.9 Recovery of Acid Heat as Steam

The acid cooling described in Section 24.7 is straightforward and efficient but it doesn't make use of hot acid's energy.

Recent acid plants rectify this by recovering much of the acid's heat as steam (for electricity production etc.). All major acid plant designers are working on this technology (Friedman and Friedman, 2004).

Fig. 24.7 describes one version of the process. It is for double contact (Fig. 9.6) acidmaking.

Its core feature is passage of:

hot (~485 K) intermediate H_2SO_4 making tower exit acid

through the tubes of a:

shell and tube water to steam boiler.

The products of the process are:

(a) cool new acid

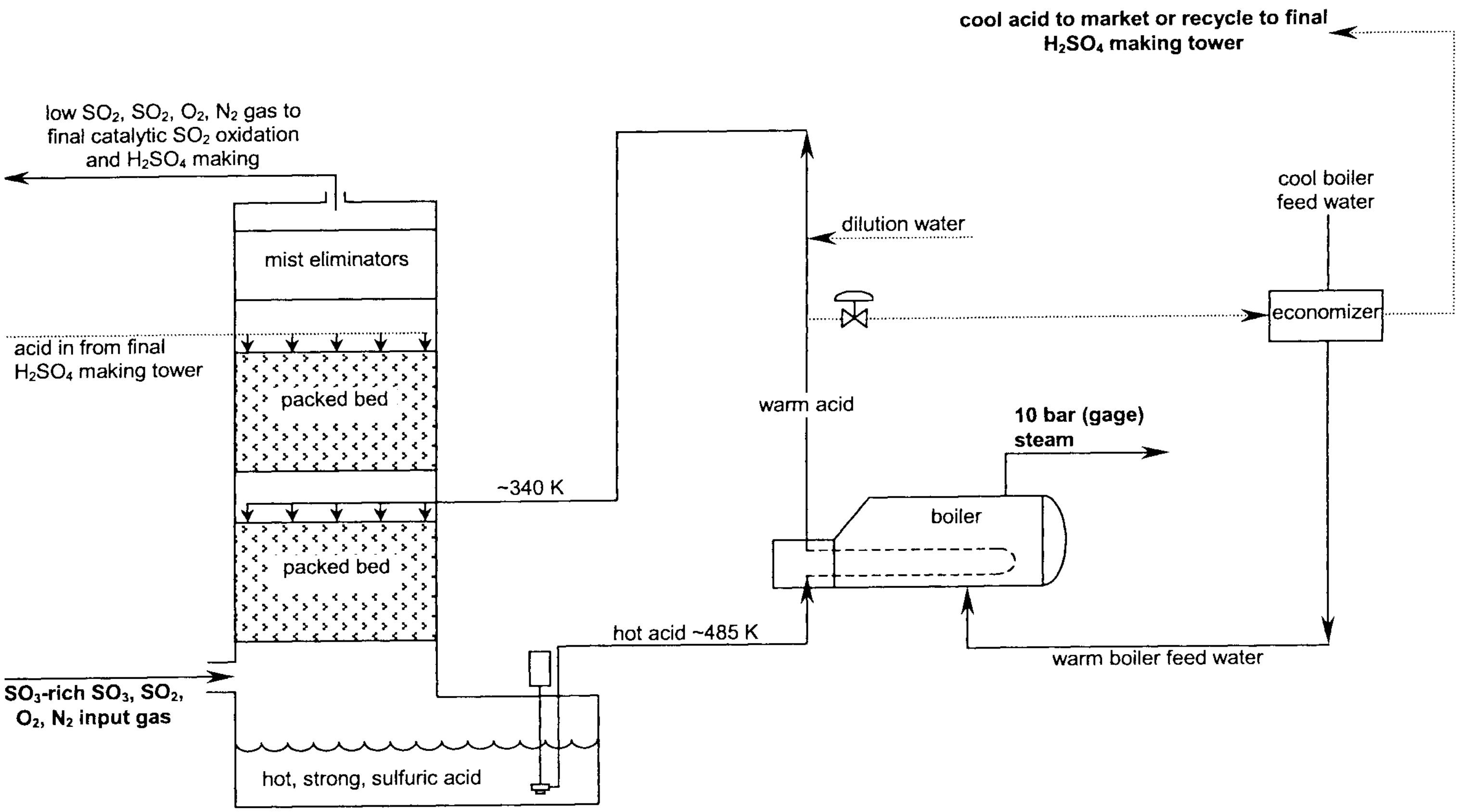

Fig. 24.7. Schematic of acid heat to steam energy recovery system, after Puricelli *et al.*, 1998. It is for intermediate H_2SO_4 making, Fig. 9.6. Note (i) the double packed bed H_2SO_4 making tower and (ii) boiler. Industrial acid heat recovery H_2SO_4 making towers are ~25m high and 10 m diameter. They produce 2000 to 4000 tonnes of H_2SO_4 per day. For photographs see Sulfur, 2004.——— large flows ·············· small flows.

(b) 10 bar (gage) steam.

24.9.1 Double packed bed H_2SO_4 making tower

A second key feature of Fig. 24.7's version of the process is its double packed bed H_2SO_4 making tower – through which:

strong SO_3 gas ascends

strong sulfuric acid descends

around ceramic packing.

Bottom packed bed

The bottom packed bed is fed with slightly diluted return acid from the heat-from-acid boiler. H_2O in the acid reacts with ascending SO_3 gas to form H_2SO_4 by Reaction (1.2). Input acid composition and flowrate are controlled to give hot (~485 K) acid boiler feed, Fig. 24.7.

Top packed bed

The top packed bed is fed with cool acid from the final H_2SO_4 making tower. Its principal purpose is to absorb $H_2SO_4(g)$, $H_2O(g)$ and $SO_3(g)$ rising from the bottom bed's hot acid.

24.9.2 Materials of construction

Passage of hot, strong sulfuric acid though tubes surrounded by hot water and steam requires strongly corrosion resistant materials. Accidental mixing of water and strong acid causes rapid corrosion throughout the H_2SO_4 making system.

Acid flowrates also have to be kept at carefully prescribed velocities.

Alloys currently used in heat-from-acid energy recovery systems are:

anodically protected Saramet® (Aker Kvaerner, www.chemetics.ca)

310 stainless steel (Monsanto Enviro-Chem, www.enviro-chem.com)

(Friedman and Friedman, 2004).

Outokumpu builds a similar heat-from-acid recovery system. It uses a Venturi absorber in place of Fig. 24.7's bottom packed bed (Outokumpu, 2005).

24.10 Summary

$H_2SO_4(\ell)$ is made by the reaction of $SO_3(g)$ with the $H_2O(\ell)$ in strong sulfuric acid.

Heat is released by the reaction, so that H_2SO_4 making's output sulfuric acid is ~25 K warmer than its input acid.

Output acid temperature increases markedly with increasing input acid temperature and decreasing acid circulation rate. Corrosion rates increase with increasing temperature so that excessive temperatures must be avoided.

They are avoided by cooling the recycle acid in water cooled 'shell and tube' or 'plate and frame' heat exchangers.

Acid plants (especially sulfur burning plants) are now often built with 'acid heat to steam' energy recovery systems. These significantly increase acidmaking energy efficiency.

References

Chemetics (2004) Acid coolers, sulphuric acid technology. Brochure distributed at Sulphur 2004 conference, Barcelona, October 24-27, 2004. www.chemetics.com Also personal communication, 2005.

Duecker, W.W. and West, J.R. (1966) *The Manufacture of Sulfuric Acid,* Reinhold Publishing Corporation, New York, 10 11.

Friedman, L.J. and Friedman, S.J. (2004) The wet gas sulphuric acid plant (part 2). *Sulphur*, **293**, July-August 2004, 29 35. www.britishsulphur.com

Haslego, C. (2005) Compact heat exchangers in the phosphate industry, preprint of paper presented at 29th Annual Clearwater Conference (AIChE), Clearwater Florida, June 4, 2005. www.aiche-cf.org www.alfalaval.com

Hay, S., Porretta, F. and Wiggins, B. (2003) Design and start-up of acid plant tail gas scrubber. In *Copper 03-Cobre 03, Proceedings of the Fifth International Conference, Vol. IV (Book 1) Pyrometallurgy of Copper, the Hermann Schwarze Symposium on Copper Pyrometallurgy, Smelting Operations, Ancillary Operations and Furnace Integrity*, ed. Diaz, C., Kapusta, J. and Newman, C., The Metallurgical Society of the Canadian Institute of Mining, Metallurgy and Petroleum, Montreal, 555 566. www.metsoc.org

Puricelli, S.M., Grendel, R.W. and Fries, R.M. (1998) Pollution to power, a case study of the Kennecott sulfuric acid plant. In *Sulfide Smelting '98* ed. Asteljoki, J.A. and Stephens, R.L. TMS, Warrendale, PA 451 462. www.tms.org

Outokumpu (2005) *HEROS, the Outokumpu Technology Heat Recovery System in Sulfuric Acid Plants*, brochure distributed at 29th Annual Clearwater Conference, Clearwater, Florida, June 3 and 4, 2005. www.outokumpu.com

Sulphur (2004) Sulphuric acid equipment update. *Sulphur* **292** (May-June 2004) 33 42. www.britishsulphur.com

Problems

24.1 The inputs to an H_2SO_4 making tower are:

(a) last catalyst bed exit gas (480 K) containing:

0.1183	kg-mole	SO_3
0.0017	"	SO_2
0.0728	"	O_2
0.7480	"	N_2

per kg-mole of 1st catalyst bed feed gas

(b) 98.6 mass% H_2SO_4, 1.4 mass% H_2O sulfuric acid, 350 K.

The outputs are:

(c) exit gas (350 K) containing:

0.0000	kg-mole	SO_3
0.0017	"	SO_2
0.0728	"	O_2
0.7480	"	N_2

per kg-mole of 1st catalyst bed feed gas.

(d) 99.2 mass% H_2SO_4, 0.8 mass% H_2O sulfuric acid.

Calculate the tower's:

1. H_2SO_4 and H_2O input masses, kg
2. H_2SO_4 and H_2O output masses, kg
3. total enthalpy of the inputs, MJ
4. enthalpy of the output gas

(all per kg-mole of 1st catalyst bed feed gas).

Calculate also:

5. the temperature of the tower's output acid (assume that there are no convective, conductive plus radiative heat losses from the tower).

Hints:

Use:

(a) matrix Table W.1 (with appropriate changes) to calculate the H_2SO_4 and H_2O masses

(b) Table 24.1 (with appropriate changes) to calculate the total input enthalpy and gas output enthalpy

(c) Section 24.2 to calculate the output acid temperature.

Appendix A

Sulfuric Acid Properties

A.1 Sulfuric Acid Specific Gravity at Constant Temperature

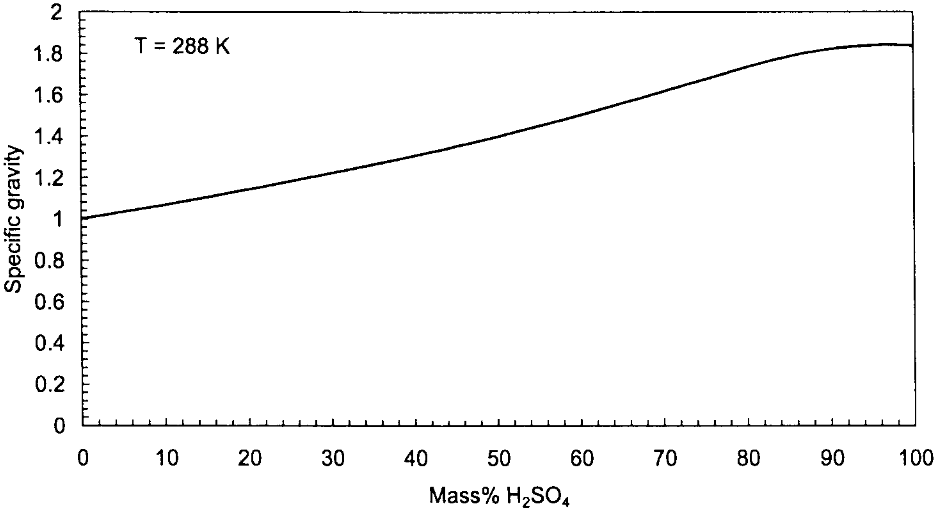

Fig. A.1. Specific gravity of sulfuric acid between 0 and 100 mass% H_2SO_4. Source: *International Critical Tables, Vol. III* (1928) McGraw-Hill Book Co., Inc., New York, 56 57. www.mcgraw-hill.com

A.2 Specific Gravity of Sulfuric Acid at Elevated Temperatures

Table A.1. Specific Gravity of sulfuric acid at various temperatures. Source: *International Critical Tables, Vol. III* (1928) McGraw-Hill Book Co., Inc., New York, 56 57. www.mcgraw-hill.com

Mass %H_2SO_4	303 K	313 K	323 K	333 K	353 K	373 K
100	1.8205	1.8107	1.8013	1.7922	-	-
99	1.8242	1.8145	1.8050	1.7958	-	-
98	1.8261	1.8163	1.8068	1.7976	-	-
97	1.8264	1.8166	1.8071	1.7977	-	-
96	1.8255	1.8157	1.8060	1.7965	-	-
95	1.8236	1.8137	1.8040	1.7944	-	-
94	1.8210	1.8109	1.8011	1.7914	-	-
93	1.8176	1.8074	1.7974	1.7876	1.7681	1.7485
92	1.8136	1.8033	1.7932	1.7832	1.7633	1.7439
91	1.8090	1.7986	1.7883	1.7783	1.7581	1.7388
90	1.8038	1.7933	1.7829	1.7729	1.7525	1.7331
89	1.7979	1.7874	1.7770	1.7669	1.7464	1.7269
88	1.7914	1.7809	1.7705	1.7602	1.7397	1.7202
87	1.7842	1.7736	1.7632	1.7529	1.7324	1.7129
86	1.7763	1.7657	1.7552	1.7449	1.7245	1.7050
85	1.7678	1.7571	1.7466	1.7364	1.7161	1.6966
84	1.7585	1.7479	1.7375	1.7274	1.7072	1.6878
83	1.7487	1.7382	1.7279	1.7179	1.6979	1.6787

A.3 Sulfuric Acid Freezing Points

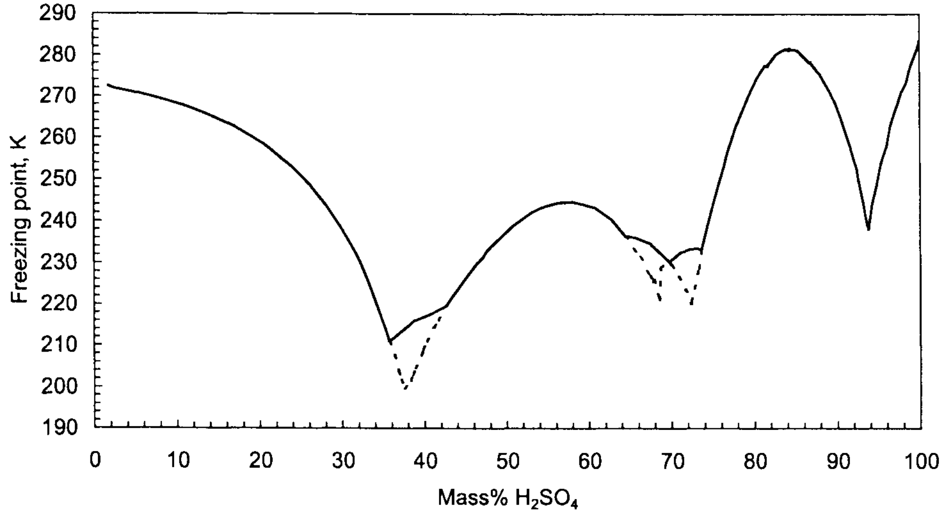

Fig. A.2. Sulfuric acid freezing point temperature versus mass % H_2SO_4 in acid. The dashed lines show metastable phases. Source: Gable, C.M., Betz, H.F. and Maron, S.H. (1950) Phase equilibria of the system sulfur trioxide-water, *Journal of the American Chemical Society*, Vol. 72, 1445 1448. www.chemistry.org

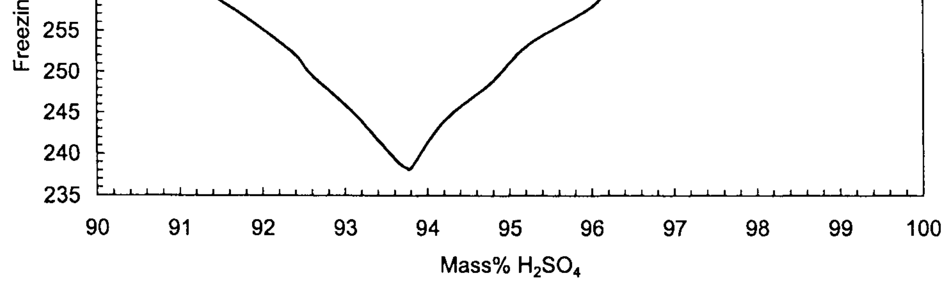

Fig. A.3. Sulfuric acid freezing point temperature versus mass % H_2SO_4 in acid (90-100%). Source: Gable, C.M., Betz, H.F. and Maron, S.H. (1950) Phase equilibria of the system sulfur trioxide-water, *Journal of the American Chemical Society*, Vol. 72, 1445 1448. www.chemistry.org

Table A.2. Sulfuric Acid Freezing Point Data. Sulfuric acid freezing point temperature versus mass % H_2SO_4 in acid. Source: Gable, C.M., Betz, H.F. and Maron, S.H. (1950) Phase equilibria of the system sulfur trioxide-water, *Journal of the American Chemical Society*, Vol. 72, 1445 1448. www.chemistry.org

H_2SO_4 (mass%)	Temperature (K)	H_2SO_4 (mass%)	Temperature (K)	H_2SO_4 (mass%)	Temperature (K)
1.81	272.41	54.16	243.11	84.27	281.16
2.41	271.94	55.37	243.90	84.32	281.57
5.37	270.73	56.36	244.38	84.37	281.38
8.42	269.16	57.64	244.64	84.90	281.28
10.71	267.86	58.09	244.59	85.32	281.10
13.30	265.99	60.04	243.63	86.69	278.24
16.95	262.71	60.76	243.14	86.85	278.27
20.48	258.52	62.78	240.34	87.94	275.40
23.91	253.05	64.46	236.40	88.63	273.00
26.23	248.34	64.69	236.44	89.00	271.64
27.89	244.19	65.68	236.02	89.83	268.36
29.79	238.66	67.47	234.62	90.63	263.82
31.83	231.82	68.98	231.78	91.64	257.68
32.62	228.02	69.70	230.30	92.38	252.28
33.53	223.56	69.74	230.24	92.57	249.83
34.46	218.38	71.18	232.55	93.12	244.76
35.28	213.77	72.32	233.28	93.63	239.16
35.70	211.09	73.13	233.49	93.77	238.14
35.77	211.02	73.68	233.13	93.81	238.39
36.20	211.67	74.33	238.43	94.21	244.06
37.79	214.33	75.08	244.11	94.77	248.54
38.73	215.88	75.91	250.19	95.24	253.37
40.50	217.26	76.59	254.79	96.03	258.09
42.41	219.27	77.04	257.88	96.46	263.05
42.64	219.52	77.95	263.18	97.23	267.57
43.49	222.05	79.33	269.79	97.79	271.02
44.41	224.53	79.71	271.60	98.40	273.46
46.19	229.35	80.34	274.24	98.69	275.80
47.21	231.51	81.40	277.41	99.07	277.97
47.75	233.14	81.69	277.44	99.85	282.17
49.47	236.37	82.72	280.13	99.98	283.37
50.81	238.80	83.61	281.21	100.00	283.35
53.08	242.03	83.90	281.40		

Table A.3. Metastable Sulfuric Acid Freezing Point Data. Metastable sulfuric acid freezing point temperature versus mass% H_2SO_4 in acid. Source: Gable, C.M., Betz, H.F. and Maron, S.H. (1950) Phase equilibria of the system sulfur trioxide-water, *Journal of the American Chemical Society*, Vol. 72, 1445 1448. www.chemistry.org

H_2SO_4 (mass%)	Temperature (K)	H_2SO_4 (mass%)	Temperature (K)	H_2SO_4 (mass%)	Temperature (K)
35.77	211.02	64.46	236.40	69.74	230.24
36.31	207.69	66.27	231.34	70.01	229.50
36.86	203.78	67.45	226.86	70.89	226.71
37.12	201.79	67.80	225.54	71.70	223.65
37.55	199.90	67.91	225.99	72.40	220.15
38.31	201.61	68.56	221.20	72.42	220.85
38.58	203.09	68.71	228.82	72.78	223.92
38.88	204.59	69.74	230.24	73.36	228.85
40.08	209.73			73.68	233.13
39.56	207.71				
41.18	214.41				
41.69	216.28				
42.64	219.52				

A.4. Oleum Specific Gravity

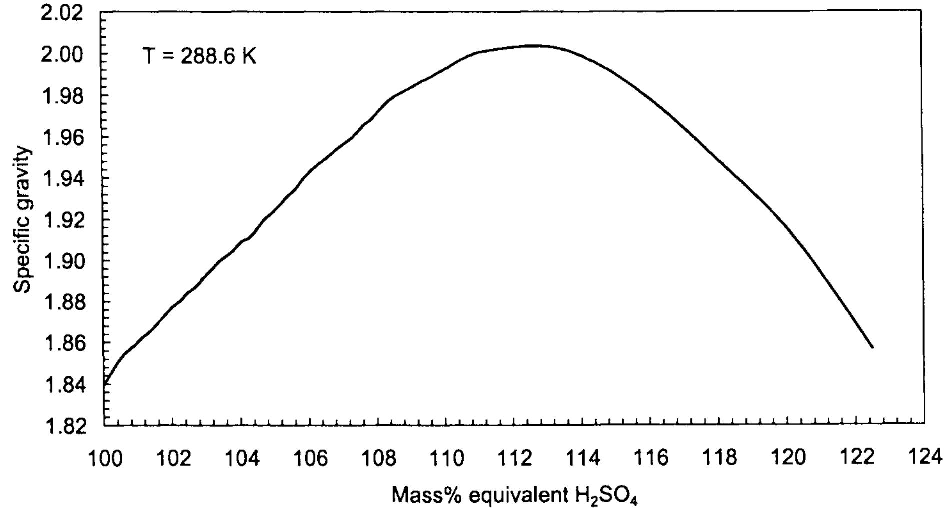

Fig. A.4. Specific Gravity of oleum versus mass% equivalent H_2SO_4. Source: *Chemical Plant Control Data, 8th Ed.* 1963, Chemical Construction Corporation, New York, 43-44.

A.5 Electrical Conductivity of Sulfuric Acid

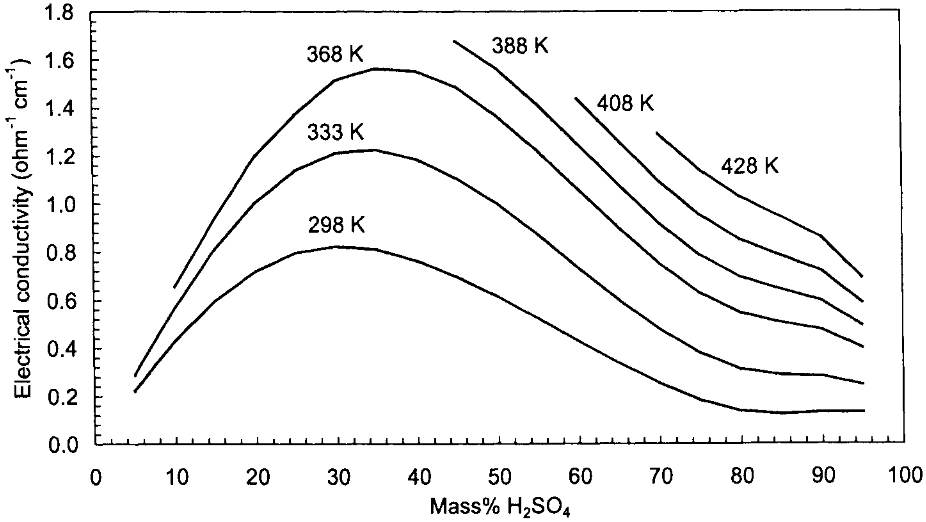

Fig. A.5. Electrical conductivity versus mass% H_2SO_4 in sulfuric acid. Source: Roughton, J.E. (1951) The electrical conductivity of aqueous solutions of sulphuric acid from 25°C to 155°C, *J. Appl. Chem.,I, Supplementary Issue, No. 2.*, 141 144.

A.6 Absolute Viscosity of Sulfuric Acid

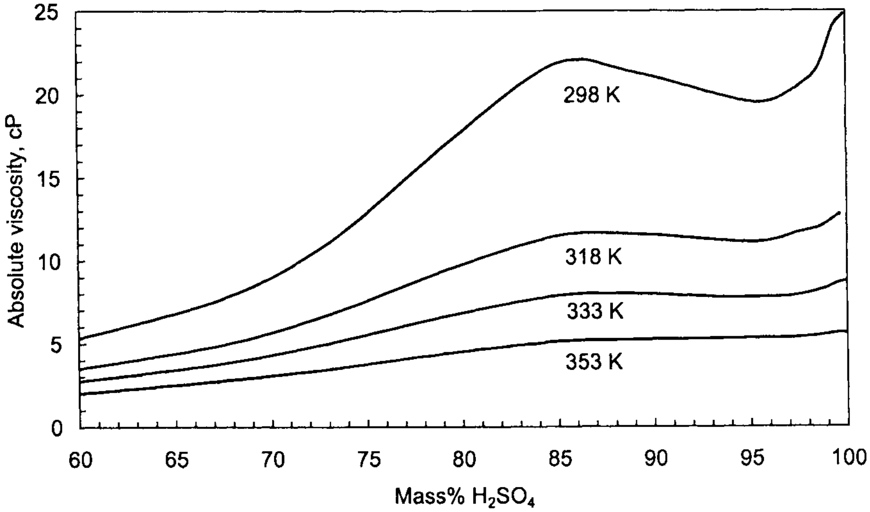

Fig. A.6. Absolute viscosity of sulfuric acid versus mass% H_2SO_4 in sulfuric acid. For viscosity in kg m^{-1} s^{-1}, multiply cP by 0.001. Source: Bright, N.F., Hutchinson, H. and Smith, D., (1946) The viscosity and density of sulfuric acid and oleum, *J. Soc. Chem. Ind.* 65, 385 388.

Appendix B

Derivation of Equilibrium Equation (10.12)

This appendix examines catalytic oxidation of SO_2 in SO_2, O_2, N_2 feed gas by the reaction:

$$\underset{\substack{\text{in feed}\\\text{gas}}}{SO_2(g)} + \underset{\substack{\text{in feed}\\\text{gas}}}{\frac{1}{2}O_2(g)} \rightarrow SO_3(g) \qquad (1.1).$$

It derives equilibrium Eqn. (10.12):

$$K_E = \left(\frac{\Phi^E}{100 - \Phi^E}\right) * \left(\frac{100 - \frac{1}{2}*e*\frac{\Phi^E}{100}}{f - \frac{1}{2}*e*\frac{\Phi^E}{100}}\right)^{\frac{1}{2}} * P_t^{-\frac{1}{2}} \qquad (10.12)$$

from Reaction (1.1)'s equilibrium equation:

$$K_E = \frac{P^E_{SO_3}}{P^E_{SO_2} * \left(P^E_{O_2}\right)^{\frac{1}{2}}} \qquad (10.3)$$

where:

K_E = equilibrium constant, dependent only on temperature, $\text{bar}^{-\frac{1}{2}}$

$P^E_{SO_2}$, $P^E_{O_2}$, $P^E_{SO_3}$ = equilibrium partial pressures of SO_2, O_2 and SO_3, bar

Φ^E = equilibrium *% SO_2 oxidized*, Section 10.1.1

e = volume% SO_2 in Fig. 10.1 feed gas
f = volume% O_2 in Fig. 10.1 feed gas } remainder N_2*

P_t = total equilibrium gas pressure, bar.

---

*CO_2 and Ar behave like N_2, Appendix F. The effects of SO_3-in-feed-gas are examined in Appendix P.

B.1 Modified Equilibrium Equation

$P^E_{SO_2}$, $P^E_{O_2}$ and $P^E_{SO_3}$ in Eqn. (10.3) are related to gas composition by the equations:

$$P^E_{SO_2} = X^E_{SO_2} * P_t \tag{B.1}$$

$$P^E_{O_2} = X^E_{O_2} * P_t \tag{B.2}$$

$$P^E_{SO_3} = X^E_{SO_3} * P_t \tag{B.3}$$

where X^E is equilibrium mole fraction of each gas and P_t is total equilibrium gas pressure. These three equations assume ideal gas behavior (based on the low pressure, ~1 bar, of industrial SO_2 oxidation).

Eqns. (10.3) and (B.1) to (B.3) combine to give:

$$K_E = \frac{X^E_{SO_3}}{X^E_{SO_2} * \left(X^E_{O_2}\right)^{\frac{1}{2}}} * P_t^{-\frac{1}{2}} \tag{B.4}$$

B.2 Mole Fractions Defined

Mole fraction of SO_3 in SO_3, SO_2, O_2, N_2 gas is defined as:

$$X_{SO_3} = \frac{n_{SO_3}}{n_t} = \frac{n_{SO_3}}{n_{SO_3} + n_{SO_2} + n_{O_2} + n_{N_2}} \tag{B.5}$$

where n_t is total kg-mole of gas and n_{SO_3} , n_{SO_2} , n_{O_2} and n_{N_2} and are kg-mole of SO_3, SO_2, O_2 and N_2 in the gas.

Likewise:

$$X_{SO_2} = \frac{n_{SO_2}}{n_t} = \frac{n_{SO_2}}{n_{SO_3} + n_{SO_2} + n_{O_2} + n_{N_2}} \tag{B.6}$$

$$X_{O_2} = \frac{n_{O_2}}{n_t} = \frac{n_{O_2}}{n_{SO_3} + n_{SO_2} + n_{O_2} + n_{N_2}} \tag{B.7}$$

The next six sub-sections use these equations to derive Eqn. (10.12) from Eqn. (B.4). Sulfur, oxygen and nitrogen balances are used.

B.3 Feed and Oxidized Gas Molar Quantities

The derivation is begun by:

(a) specifying that the Fig. 10.1 feed gas contains:

e	volume% SO_2
f	volume% O_2
100 - e - f	volume% N_2

(b) assuming 1 kg-mole of Fig. 10.1 feed gas.

B.3.1 Feed gas molar quantities

The molar quantity of SO_2 in 1 kg-mole of Fig. 10.1 feed gas is given by the equation:

$$\text{kg-mole of } SO_2 \text{ in 1 kg-mole of Fig. 10.1 feed gas} = \frac{\text{mole\% } SO_2 \text{ in feed gas}}{100\%} * 1 \text{ kg-mole of feed gas.}$$

Also, because mole% = volume% (Appendix E):

$$\text{kg-mole of } SO_2 \text{ in 1 kg-mole of Fig. 10.1 feed gas} = \frac{\text{volume\% } SO_2 \text{ in feed gas}}{100\%} * 1 \text{ kg-mole of feed gas}$$

$$= \frac{e}{100} * 1$$

$$= \frac{e}{100} \qquad \text{(B.8).}$$

Likewise:

$$\text{kg-mole of } O_2 \text{ in 1 kg-mole of Fig. 10.1 feed gas} = \frac{f}{100} \qquad \text{(B.9)}$$

$$\text{kg-mole of } N_2 \text{ in 1 kg-mole of Fig. 10.1 feed gas} = \frac{100 - e - f}{100} = 1 - \frac{e}{100} - \frac{f}{100} \qquad \text{(B.10).}$$

B.3.2 Oxidized gas molar quantities

Oxidized gas in the Fig. 10.1 catalyst bed contains:

n_{SO_3}	kg-mole SO_3
n_{SO_2}	kg-mole SO_2
n_{O_2}	kg-mole O_2
n_{N_2}	kg-mole N_2

per kg-mole of Fig. 10.1 feed gas. n_{SO_3}, n_{SO_2} and n_{O_2} vary down the catalyst bed as $SO_2(g) + \frac{1}{2}O_2(g) \rightarrow SO_3(g)$ oxidation proceeds.

B.3.3 Molar balances

S, O and N molar balances are now used to relate Fig. 10.1's feed gas composition to oxidized gas molar quantities. The balances are all based on 1 kg-mole of feed gas.

S balance

The sulfur balance is:

$$\begin{matrix}\text{kg-mole S} \\ \text{in feed gas}\end{matrix} = \begin{matrix}\text{kg-mole S in} \\ \text{oxidized gas}\end{matrix} \qquad \text{(B.11).}$$

1 mole of SO_3 and SO_2 each contain 1 mole of S, so Eqns. (B.11) and (B.8) may be combined to give:

$$1*\frac{e}{100} = 1*n_{SO_3} + 1*n_{SO_2} \qquad \text{(B.12)}$$

or:

$$\frac{e}{100} = n_{SO_3} + n_{SO_2} \qquad \text{(B.13)}$$

or:

$$n_{SO_2} = \frac{e}{100} - n_{SO_3} \qquad \text{(B.14)}$$

where:

$\frac{e}{100}$ = kg-mole of feed SO_2 in Fig. 10.1 feed gas

n_{SO_3} and n_{SO_2} = kg-mole of SO_3 and SO_2 in oxidized gas

(all per kg-mole of Fig. 10.1 feed gas).

O balance

The oxygen balance is:

$$\begin{matrix}\text{kg-mole O} \\ \text{in feed gas}\end{matrix} = \begin{matrix}\text{kg-mole O in} \\ \text{oxidized gas}\end{matrix} \qquad \text{(B.15).}$$

1 mole of SO_3 contains 3 moles of O while 1 mole of SO_2 and O_2 each contain 2 moles of O - so Eqns. (B.15), (B.8) and (B.9) become:

$$2*\frac{e}{100} + 2*\frac{f}{100} = 3*n_{SO_3} + 2*n_{SO_2} + 2*n_{O_2} \qquad \text{(B.16)}$$

where $\frac{f}{100}$ = kg-mole of feed O_2 per kg-mole of Fig. 10.1 feed gas.

Dividing both sides of Eqn. (B.16) by 2 gives:

$$\frac{e}{100} + \frac{f}{100} = \frac{3}{2}*n_{SO_3} + n_{SO_2} + n_{O_2} \qquad \text{(B.17)}$$

or:

$$n_{O_2} = \frac{e}{100} + \frac{f}{100} - \frac{3}{2}*n_{SO_3} - n_{SO_2} \qquad \text{(B.18).}$$

Further, because $n_{SO_2} = \frac{e}{100} - n_{SO_3}$ (Eqn. B.14)

$$n_{O_2} = \frac{e}{100} + \frac{f}{100} - \frac{3}{2}*n_{SO_3} - \left(\frac{e}{100} - n_{SO_3}\right) \qquad \text{(B.19)}$$

$$= \frac{f}{100} - \frac{1}{2}*n_{SO_3} \qquad \text{(B.20)}$$

where n_{SO_3} = kg-mole SO_3 in oxidized catalyst bed gas.

N balance

The nitrogen balance is:

$$\begin{matrix}\text{kg-mole N} \\ \text{in feed gas}\end{matrix} = \begin{matrix}\text{kg-mole N in} \\ \text{oxidized gas}\end{matrix} \tag{B.21}$$

Of course, nitrogen doesn't react during SO_2 oxidation so that it enters and leaves the catalyst as N_2 (only). Each mole of N_2 contains 2 moles of N so that Eqns. (B.21) and (B.10) become:

$$2*\left(1 - \frac{e}{100} - \frac{f}{100}\right) = 2*n_{N_2} \tag{B.22}$$

or:

$$n_{N_2} = 1 - \frac{e}{100} - \frac{f}{100} \tag{B.23}$$

where: $1 - \frac{e}{100} - \frac{f}{100}$ = kg-mole of feed N_2 per kg-mole of Fig. 10.1 feed gas.

Total kg-moles of oxidized gas

Total kg-mole of Fig. 10.1 oxidized gas (per kg-mole of Fig. 10.1 feed gas) is:

$$n_T = n_{SO_3} + n_{SO_2} + n_{O_2} + n_{N_2} \tag{B.24}$$

Combining this with Eqns. (B.14), (B.20) and (B.23) gives:

$$n_T = n_{SO_3} + \left(\frac{e}{100} - n_{SO_3}\right) + \left(\frac{f}{100} - \frac{1}{2} * n_{SO_3}\right) + \left(1 - \frac{e}{100} - \frac{f}{100}\right) \tag{B.25}$$

$$= 1 - \frac{1}{2} * n_{SO_3} \tag{B.26}$$

Note that the$\left(-\frac{1}{2} * n_{SO_3}\right)$ term represents kg-mole of O_2 consumed in oxidizing n_{SO_3} kg-mole of SO_2 to SO_3.

B.4 Mole fractions in oxidized gas

The mole fractions of SO_3, SO_2 and O_2 in Fig. 10.1's oxidized gas are:

$$X_{SO_3} = \frac{n_{SO_3}}{n_t} = \frac{n_{SO_3}}{\left(1 - \frac{1}{2} * n_{SO_3}\right)} \quad \text{from Eqn. (B.26)} \qquad \text{(B.27)}$$

$$X_{SO_2} = \frac{n_{SO_2}}{n_t} = \frac{\left(\frac{e}{100} - n_{SO_3}\right)}{\left(1 - \frac{1}{2} * n_{SO_3}\right)} \quad \text{from Eqn. (B.14) and (B.26)} \qquad \text{(B.28)}$$

$$X_{O_2} = \frac{n_{O_2}}{n_t} = \frac{\left(\frac{f}{100} - \frac{1}{2} * n_{SO_3}\right)}{\left(1 - \frac{1}{2} * n_{SO_3}\right)} \quad \text{from Eqn. (B.20) and (B.26)} \qquad \text{(B.29).}$$

B.5 Equation Applicability

Eqns. (B.5) to (B.29) apply everywhere in the Fig. 10.1 catalyst bed. Of course:

(a) n_{SO_3} increases as feed gas descends the catalyst bed and oxidation proceeds

(b) n_{SO_2} and n_{O_2} decrease as feed gas descends the catalyst bed and oxidation proceeds

(c) n_{N_2} doesn't change in the catalyst bed because N_2 doesn't take part in SO_2 oxidation.

B.6 Equilibrium Equation

Fig. 10.1 describes a catalyst bed in which $SO_2(g) + \frac{1}{2}O_2(g) \rightarrow SO_3(g)$ oxidation comes to equilibrium near the bottom of the bed. Eqn. (B.4) describes this equilibrium in terms of SO_3, SO_2 and O_2 mole fractions, $X^E_{SO_3}$, $X^E_{SO_2}$ and $X^E_{O_2}$

This section shows how the equilibrium values of n_{SO_3}, n_{SO_2} and n_{O_2}, i.e.:

$$n^E_{SO_3}$$

$$n^E_{SO_2}$$

$$n^E_{O_2}$$

are represented in equilibrium Eqn. (B.4) (where E = equilibrium).

B.6.1 Equilibrium mole fractions

At equilibrium, oxidized gas SO_3, SO_2 and O_2 mole fractions are:

(from Eqn. B.27)

$$X^E_{SO_3} = \frac{n^E_{SO_3}}{n^E_t} = \frac{n^E_{SO_3}}{\left(1 - \frac{1}{2}*n^E_{SO_3}\right)} \tag{B.30}$$

(from Eqn. B.28)

$$X^E_{SO_2} = \frac{n^E_{SO_2}}{n^E_t} = \frac{\left(\frac{e}{100} - n^E_{SO_3}\right)}{\left(1 - \frac{1}{2}*n^E_{SO_3}\right)} \tag{B.31}$$

(from Eqn. B.29)

$$X^E_{O_2} = \frac{n^E_{O_2}}{n^E_t} = \frac{\left(\frac{f}{100} - \frac{1}{2}*n^E_{SO_3}\right)}{\left(1 - \frac{1}{2}*n^E_{SO_3}\right)} \tag{B.32).}$$

These equilibrium equations are now combined with Eqn. (B.4) to relate $n^E_{SO_3}$ to equilibrium constant K_E.

B.7 Equilibrium Constant and Molar Quantities

With the Eqn. (B.30)-(B.32) expressions for mole fractions, equilibrium Eqn. (B.4):

$$K_E = \frac{X^E_{SO_3}}{X^E_{SO_2} * \left(X^E_{O_2}\right)^{\frac{1}{2}}} * P_t^{-\frac{1}{2}}$$

becomes:

$$K_E = \frac{\left(\frac{n^E_{SO_3}}{1 - \frac{1}{2}* n^E_{SO_3}}\right)}{\left(\frac{\frac{e}{100} - n^E_{SO_3}}{1 - \frac{1}{2}* n^E_{SO_3}}\right) * \left(\frac{\frac{f}{100} - \frac{1}{2}* n^E_{SO_3}}{1 - \frac{1}{2}* n^E_{SO_3}}\right)^{\frac{1}{2}}} * P_t^{-\frac{1}{2}} \tag{B.33}$$

or, multiplying top and bottom by $\left(1 - \frac{1}{2} * n^E_{SO_3}\right)$

$$K_E = \frac{n^E_{SO_3}}{\left(\frac{e}{100} - n^E_{SO_3}\right) * \left(\frac{\frac{f}{100} - \frac{1}{2} * n^E_{SO_3}}{1 - \frac{1}{2} * n^E_{SO_3}}\right)^{\frac{1}{2}}} * P_t^{-\frac{1}{2}} \qquad \text{(B.34)}$$

or, multiplying top and bottom by $\left(1 - \frac{1}{2} * n^E_{SO_3}\right)^{\frac{1}{2}}$

$$K_E = \frac{n^E_{SO_3} * \left(1 - \frac{1}{2} * n^E_{SO_3}\right)^{\frac{1}{2}}}{\left(\frac{e}{100} - n^E_{SO_3}\right) * \left(\frac{f}{100} - \frac{1}{2} * n^E_{SO_3}\right)^{\frac{1}{2}}} * P_t^{-\frac{1}{2}}$$

or:

$$K_E = \frac{n^E_{SO_3}}{\left(\frac{e}{100} - n^E_{SO_3}\right)} * \left(\frac{1 - \frac{1}{2} * n^E_{SO_3}}{\frac{f}{100} - \frac{1}{2} * n^E_{SO_3}}\right)^{\frac{1}{2}} * P_t^{-\frac{1}{2}} \qquad \text{(B.35)}$$

where $n^E_{SO_3}$ is kg-moles of SO_3 in the Fig. 10.1 equilibrium gas, per kg-mole of feed gas.

This equation is used to calculate $n^E_{SO_3}$ for any given equilibrium constant. $n^E_{SO_2}$ and $n^E_{O_2}$ are then calculated with Eqns. (B.14) and (B.20).

Eqn. (B.35) is written in terms of $n^E_{SO_3}$ (kg-moles SO_3 in equilibrium gas) rather than equilibrium *% SO_2 oxidized* (Φ^E) in Eqn. (10.12). The next section shows how Eqn. (10.12) is derived from Eqn. (B.35).

B.8 Equilibrium $n^E_{SO_3}$ and Φ^E

Eqn. (10.2) defines equilibrium *% SO₂ oxidized* (Φ^E) as:

$$\text{Equilibrium } \%\, SO_2 \text{ oxidized} = \Phi^E = \frac{\text{kg-mole } SO_2 \text{ in feed gas} - \text{kg-mole } SO_2 \text{ in oxidized gas where equilibrium has been attained}}{\text{kg-mole } SO_2 \text{ in feed gas}} * 100 \tag{10.2}$$

or:

$$\Phi^E = \left(\frac{\frac{e}{100} - n^E_{SO_2}}{\frac{e}{100}}\right) * 100 \tag{B.36}$$

where:
e = volume% SO_2 in Fig. 10.1 feed gas
$n^E_{SO_2}$ = kg-mole SO_2 in equilibrium gas per kg-mole of feed gas.

Eqn. (B.36) is expressed in terms of $n^E_{SO_3}$ by combining it with the equilibrium form of Eqn. (B.14), i.e.:

$$n^E_{SO_2} = \frac{e}{100} - n^E_{SO_3} \tag{B.14'}$$

to give:

$$\Phi^E = \left(\frac{\frac{e}{100} - \left(\frac{e}{100} - n^E_{SO_3}\right)}{\frac{e}{100}}\right) * 100$$

or:

$$\Phi^E = \frac{n^E_{SO_3}}{\left(\frac{e}{100}\right)} * 100 \tag{B.37}$$

or:

$$n^E_{SO_3} = \left(\frac{e}{100}\right) * \frac{\Phi^E}{100} \tag{B.38}$$

where:

$n^E_{SO_3}$ = kg-mole SO_3 in equilibrium gas per kg-mole of Fig. 10.1 feed gas
Φ^E = equilibrium *% SO₂ oxidized*, Section 10.1.1
e = volume% SO_2 in Fig. 10.1 feed gas.

B.8.1 Substituting Φ^E for $n^E_{SO_3}$

Substituting $\left(\frac{e}{100}\right)*\frac{\Phi^E}{100}$ for $n^E_{SO_3}$ in Eqn. (B.35) gives:

$$K_E = \left(\frac{\left(\frac{e}{100}\right)*\frac{\Phi^E}{100}}{\frac{e}{100} - \left(\frac{e}{100}\right)*\frac{\Phi^E}{100}}\right)*\left(\frac{1 - \frac{1}{2}*\left(\frac{e}{100}\right)*\frac{\Phi^E}{100}}{\frac{f}{100} - \frac{1}{2}*\left(\frac{e}{100}\right)*\frac{\Phi^E}{100}}\right)^{\frac{1}{2}} *P_t^{-\frac{1}{2}} \qquad (B.39)$$

or:

$$K_E = \left(\frac{\left(\frac{e}{100}\right)*\frac{\Phi^E}{100}}{\frac{e}{100} * \left(1 - \frac{\Phi^E}{100}\right)}\right)*\left(\frac{1 - \frac{1}{2}*\left(\frac{e}{100}\right)*\frac{\Phi^E}{100}}{\frac{f}{100} - \frac{1}{2}*\left(\frac{e}{100}\right)*\frac{\Phi^E}{100}}\right)^{\frac{1}{2}} *P_t^{-\frac{1}{2}} \qquad (B.40)$$

or, dividing top and bottom by $\frac{e}{100}$:

$$K_E = \left(\frac{\frac{\Phi^E}{100}}{\left(1 - \frac{\Phi^E}{100}\right)}\right)*\left(\frac{1 - \frac{1}{2}*\left(\frac{e}{100}\right)*\frac{\Phi^E}{100}}{\frac{f}{100} - \frac{1}{2}*\left(\frac{e}{100}\right)*\frac{\Phi^E}{100}}\right)^{\frac{1}{2}} *P_t^{-\frac{1}{2}} \qquad (B.41)$$

or, multiplying top and bottom by 100:

$$K_E = \left(\frac{\Phi^E}{\left(100 - \Phi^E\right)}\right)*\left(\frac{1 - \frac{1}{2}*\left(\frac{e}{100}\right)*\frac{\Phi^E}{100}}{\frac{f}{100} - \frac{1}{2}*\left(\frac{e}{100}\right)*\frac{\Phi^E}{100}}\right)^{\frac{1}{2}} *P_t^{-\frac{1}{2}} \qquad (B.42)$$

or, multiplying top and bottom by $100^{\frac{1}{2}}$

$$K_E = \left(\frac{\Phi^E}{100 - \Phi^E}\right) * \left(\frac{100 - \frac{1}{2}*e*\frac{\Phi^E}{100}}{f - \frac{1}{2}*e*\frac{\Phi^E}{100}}\right)^{\frac{1}{2}} * P_t^{-\frac{1}{2}} \qquad (10.12).$$

Applications of this equation are described in Sections 10.4 and 10.5.

Appendix C

Free Energy Equations for Equilibrium Curve Calculations

Industrial catalytic $SO_2(g) + \frac{1}{2}O_2(g) \rightarrow SO_3(g)$ oxidation approaches equilibrium at 700 to 900 K. This book's equilibrium calculations require standard free energies over this temperature range. This appendix:

(a) provides the required standard free energies from published data

(b) develops a linear equation which represents standard free energy of reaction as a function of temperature.

The free energy data are from:

Chase, M.W. (1998) *NIST-JANAF Thermochemical Tables, 4th Edition*, American Chemical Society and American Institute of Physics, Woodbury, New York.

Chase provides standard free energies of formation for the reactions:

$$S + \frac{3}{2}O_2(g) \rightarrow SO_3(g) \qquad \Delta_f G^\circ_{SO_3} \qquad \text{(C.1)}$$

$$S + O_2(g) \rightarrow SO_2(g) \qquad \Delta_f G^\circ_{SO_2} \qquad \text{(C.2).}$$

$\Delta G^\circ_{SO_2(g) + \frac{1}{2}O_2(g) \rightarrow SO_3(g)}$ is determined by subtracting Eqn. (C.2) from Eqn. (C.1),

which gives:

$$\frac{1}{2}O_2(g) \rightarrow SO_3(g) - SO_2(g)$$

or:

$$SO_2(g) + \frac{1}{2}O_2(g) \rightarrow SO_3(g)$$

for which:

$$\Delta G^\circ_{SO_2(g) + \frac{1}{2}O_2(g) \rightarrow SO_3(g)} = \Delta_f G^\circ_{SO_3} - \Delta_f G^\circ_{SO_2} \qquad \text{(C.3).}$$

Chase's 700 to 900 K $\Delta_f G^\circ$ values (MJ per kg-mole) for Eqns. (C.1) to (C.3) are:

Temperature T, K	$\Delta_f G^\circ_{SO_3}$	$\Delta_f G^\circ_{SO_2}$	$\Delta G^\circ_{SO_2(g) + \frac{1}{2}O_2(g) \rightarrow SO_3(g)}$ $= \Delta_f G^\circ_{SO_3} - \Delta_f G^\circ_{SO_3}$
700	-332.365	-299.444	-32.921
800	-321.912	-298.370	-23.542
900	-310.258	-296.051	-14.207

Application of Excel's 'Slope' and 'Intercept' functions to the left and right columns gives the linear equation:

$$\Delta G^\circ_{SO_2(g) + \frac{1}{2}O_2(g) \rightarrow SO_3(g)} = 0.09357{*}T - 98.41 \text{ MJ per kg-mole of } SO_3 \qquad (C.4).$$

This equation is used for all of this book's equilibrium calculations.

Appendix D

Preparation of Fig. 10.2 Equilibrium Curve

This appendix uses Eqn. (10.13) to calculate points on the Fig. 10.2 equilibrium curve. The equation is:

$$T_E = \frac{-B}{A + R*\ln\left(\left(\frac{\Phi^E}{100 - \Phi^E}\right) * \left(\frac{100 - \frac{1}{2}*e*\frac{\Phi^E}{100}}{f - \frac{1}{2}*e*\frac{\Phi^E}{100}}\right)^{\frac{1}{2}} * P_t^{-\frac{1}{2}}\right)} \qquad (10.13)$$

where:

T_E = equilibrium temperature, K

A and B = empirical constants relating ΔG°_T for the reaction $SO_2(g) + \frac{1}{2}O_2(g) \rightarrow SO_3(g)$ to temperature, i.e.: $\Delta G^\circ_T = A*T + B$

A = 0.09357 MJ kg-mole SO_2^{-1} K^{-1} (Appendix C)
B = -98.41 MJ/kg-mole SO_2

R = gas constant = 0.008314 MJ kg-mole SO_2^{-1} K^{-1}
Φ^E = equilibrium *% SO_2 oxidized*
e = volume% SO_2 in Fig. 10.1 feed gas } remainder inert
f = volume% O_2 in Fig. 10.1 feed gas } remainder inert
P_t = equilibrium total pressure, bar.

The calculations are done in Excel worksheet Table D.1. The calculation sequence is:

(a) e, f and P_t are entered into cells B2, D2 and D4
(b) a value of Φ^E is entered into cell D6, say 60*% SO_2 oxidized*
(c) Equation (10.13) is placed in cell A9, exactly as shown beside it
(d) the equivalent value of T_E is automatically calculated in cell A9.

(b) and (d) are repeated as desired. Cells A14 to B26 show example results.

Table D.1. Excel spreadsheet for calculating Fig. 10.2 equilibrium points from Eqn. (10.13). The calculation method is described on the previous page. Equilibrium *% SO_2 oxidized* is seen to increase with *decreasing* equilibrium temperature.

	A	B	C	D	E	F	G	H	I
1	Specified feed gas composition								
2	e, volume% SO_2 =	10	f, volume% O_2 =	11	remainder = inert				
3									
4	P_t, specified equilibrium pressure, bar =			1.2					
5									
6	Φ^E, equilibrium % SO_2 oxidized =			60					
7									
8	T_E, equilibrium temperature (K) equivalent to Cell D6's equilibrium % SO_2 oxidized =								
9	923.6	=-(-98.41)/(0.09357+0.008314*LN(D6/(100-D6)*((100-0.5*B2*D6/100)/(D2-0.5*B2*D6/100))^0.5*D4^-0.5))							Eqn. (10.13)
10									
11									
12	Example results for Fig. 10.2								
13	Equilibrium % SO_2 oxidized	Equilibrium temperature, K							
14	30	1030.6							
15	40	990.4							
16	50	955.9							
17	60	923.6							
18	70	890.8							
19	80	854.1							
20	90	805.0							
21	95	765.1							
22	97.5	730.7							
23	99	690.8							
24	99.5	663.6							
25	99.9	608.5							
26	99.95	587.6							

D.1 Integer Temperature Calculations

Table 12.1 is most easily interpolated when the equilibrium curve points have integer temperature values. These points are determined with Table D.1 by means of Excel's Goal Seek tool, next page.

Equilibrium *% SO_2 oxidized* at 895 K is determined, for example, by the sequence:

Tools
Goal Seek
Set cell: A9
To value: 895
Changing cell: D6
OK
OK.

The result is equilibrium *% SO_2 oxidized* = 68.75 % (cell D6) at 895 K (cell A9).
A table of equilibrium points may be prepared by repeating these steps at different temperatures, i.e.:

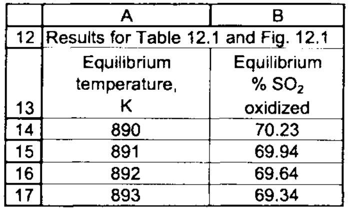

	A	B
12	Results for Table 12.1 and Fig. 12.1	
13	Equilibrium temperature, K	Equilibrium % SO_2 oxidized
14	890	70.23
15	891	69.94
16	892	69.64
17	893	69.34

D.2 2nd and 3rd Catalyst Bed Equilibrium Curves

This appendix's techniques are also used to calculate 2nd and 3rd catalyst bed equilibrium curves, Table 15.1. The calculations require specification of:

(a) the equivalent 1st catalyst feed gas composition, e and f in Eqn. (10.13)

and:

(b) the 2nd or 3rd catalyst bed gas pressure, P_t in Eqn. (10.13).

The applicability of Eqn. (10.13) to 2nd and 3rd catalyst beds is discussed in Section 15.1.

Appendix E

Proof that Volume% = Mole% (for Ideal Gases)

E.1 Definitions

Consider a gas which contains ideal gas A and ideal gas B. Volume% A and volume% B in the gas are defined as:

$$\text{volume\% A} = \left\{\frac{V_A}{V_A + V_B}\right\} * 100\% \qquad \text{(E.1)}$$

$$\text{volume\% B} = \left\{\frac{V_A}{V_A + V_B}\right\} * 100\% \qquad \text{(E.2)}$$

where V_A and V_B are the partial volumes of A and B in the gas, Section E.2. Likewise, mole% A and mole% B are defined for all gases as:

$$\text{mole\% A} = \left\{\frac{n_A}{n_A + n_B}\right\} * 100\% \qquad \text{(E.3)}$$

$$\text{mole\% B} = \left\{\frac{n_A}{n_A + n_B}\right\} * 100\% \qquad \text{(E.4)}$$

where n_A and n_B are moles of A and B in the gas.

E.2 Characterization of Partial Volumes

Consider n_A moles of ideal gas A in a freely expanding/contracting box at constant temperature T° and constant pressure P°. The volume occupied by A is described by the ideal gas law:

$$V_A = \frac{n_A * R * T^\circ}{P^\circ} \qquad \text{(E.5).}$$

Consider also n_B moles of ideal gas B in a freely expanding/contracting box at constant temperature T° and constant pressure P°. The volume occupied by B is:

$$V_B = \frac{n_B * R * T^\circ}{P^\circ} \qquad \text{(E.6).}$$

Remove a wall between the two boxes and join them. Allow the gases to mix. For ideal gases, there is no change in gas volume when the gases mix so that:

$$V_t = V_A + V_B \qquad (E.7).$$

where:

V_t = total volume of gas

V_A = partial volume of ideal gas A

V_B = partial volume of ideal gas B.

Eqns. (E.5) - (E.7) combine to give:

$$V_t = V_A + V_B = \frac{(n_A + n_B)*R*T^\circ}{P^\circ} \qquad (E.8).$$

E.3 Equality of Volume% and Mole%

Volume% A and mole% A are obtained by dividing Eqn. (E.5) by Eqn. (E.8):

to give:

$$\frac{V_A}{V_A + V_B} = \frac{n_A}{n_A + n_B} \qquad (E.9).$$

Both sides of Eqn. (E.9) are then multiplied by 100 to give:

$$\left\{\frac{V_A}{V_A + V_B}\right\}*100 = \left\{\frac{n_A}{n_A + n_B}\right\}*100 \qquad (E.10).$$

The left side of Eqn. (E.10) is volume% A (Eqn. (E.1)) while the right side is mole% A (Eqn. (E.3)) so that the equation becomes:

$$\text{volume\% A} = \text{mole\% A} \qquad (E.11)$$

proving that, for ideal gases, volume% = mole%.

Proof that:

$$\text{volume\% B} = \text{mole\% B} \qquad (E.12)$$

is obtained by dividing Eqn. (E.6) by Eqn. (E.8) and so on.

Appendix F

Effect of CO_2 and Ar on Equilibrium Equations *(None)*

CO_2 is usually present in spent acid decomposition and metallurgical furnace offgases. Most of it passes through gas cooling/cleaning/dehydration and into the Fig. 10.1 catalyst bed. It doesn't take part in catalyst bed oxidation.

This appendix shows that CO_2 has no affect on equilibrium *% SO_2 oxidized* equations, e.g. Eqn. (10.12).

A small amount of Ar is also present in catalytic SO_2 oxidation feed gases. Like CO_2, it has no effect on equilibrium *% SO_2 oxidized* equations.

F.1 CO_2

Proof that CO_2 has no effect on Eqn. (10.12) begins by specifying that Fig. 10.1's feed gas contains:

e	volume% SO_2
f	" " O_2
c	" " CO_2
1 - e - f - c	" " N_2.

Per kg-mole of Fig. 10.1 feed gas, the molar quantities entering the Fig. 10.1 catalyst bed are:

$\frac{e}{100}$	kg-mole SO_2 (Section B.3.1)
$\frac{f}{100}$	" " O_2
$\frac{c}{100}$	" " CO_2
$1 - \frac{e}{100} - \frac{f}{100} - \frac{c}{100}$	" " N_2.

Molar balances

Feed gas CO_2 doesn't change the Appendix B's sulfur molar balance. It remains as:

$$n_{SO_2} = \frac{e}{100} - n_{SO_3} \qquad \text{(B.14)} \quad \textit{unchanged.}$$

CO_2 does, however introduce a carbon molar balance into Appendix B's derivation. It is:

$$\begin{matrix}\text{kg-mole C} \\ \text{in feed gas}\end{matrix} = \begin{matrix}\text{kg-mole C} \\ \text{in exit gas}\end{matrix} \qquad \text{(F.1).}$$

Each mole of CO_2 contains 1 mole of C so Eqn. (F.1) becomes:

$$1*\frac{c}{100} = 1*n_{CO_2}$$

or:

$$n_{CO_2} = \frac{c}{100} \qquad \text{(F.2)}$$

where n_{CO_2} = kg-mole CO_2 in Fig. 10.1 exit gas.

CO_2 changes oxygen molar balance Eqn. (B.16). It becomes:

$$2*\frac{e}{100} + 2*\frac{f}{100} + \mathbf{2*\frac{c}{100}} = 3*n_{SO_3} + 2*n_{SO_2} + 2*n_{O_2} + \mathbf{2*n_{CO_2}}$$

or:

$$n_{O_2} = \frac{e}{100} + \frac{f}{100} + \mathbf{\frac{c}{100}} - \frac{3}{2}*n_{SO_3} - n_{SO_2} - n_{CO_2}$$

Combining this equation with Eqns. (B14) and F(2), i.e. with:

$$n_{SO_2} = \frac{e}{100} - n_{SO_3} \qquad \text{(B.14)}$$

and:

$$n_{CO_2} = \frac{c}{100} \qquad \text{(F.2)}$$

gives:

$$n_{O_2} = \frac{e}{100} + \frac{f}{100} + \frac{c}{100} - \frac{3}{2}n_{SO_3} - \left(\frac{e}{100} - n_{SO_3}\right) - \frac{c}{100}$$

or:

$$= \frac{f}{100} - \frac{1}{2}n_{SO_3} \qquad \text{(B.20) } \textit{unchanged.}$$

N balance Eqn. (B.22) is slightly changed by CO_2 to:

$$2 * \left(1 - \frac{e}{100} - \frac{f}{100} - \frac{c}{100}\right) = 2 * n_{N_2}$$

or:

$$n_{N_2} = 1 - \frac{e}{100} - \frac{f}{100} - \frac{c}{100} \qquad \text{(F.3).}$$

Total kg-mole of exit gas

Including CO_2, the total kg-mole of Fig. 10.1 exit gas is given by:

$$n_t = n_{SO_3} + n_{SO_2} + n_{O_2} + n_{N_2} + n_{CO_2} \qquad \text{(F.4).}$$

Combining this equation with Eqns. (B.14), (B.20), (F.2) and (F.3) gives:

$$n_t = n_{SO_3} + \left(\frac{e}{100} - n_{SO_3}\right) + \left(\frac{f}{100} - \frac{1}{2} * n_{SO_3}\right) + \left(1 - \frac{e}{100} - \frac{f}{100} - \frac{c}{100}\right) + \frac{c}{100}$$

$$= 1 - \frac{1}{2} * n_{SO_3} \qquad \text{(B.26) \textit{unchanged.}}$$

Discussion

Eqns. (B.14), (B.20) and (B.26) are unchanged by CO_2 in Fig. 10.1 feed gas. Consequently, Eqns. (B.27), (B.28), (B.29) and all further developments in Appendix B are also unchanged. So:

Eqn. (10.12) is unaffected by the presence of CO_2 in feed gas.

F.2 Ar

All Fig. 10.1 feed gases contain a small amount of argon. With this Ar, the Section F.1 feed gas may be specified as containing:

e	volume% SO_2
f	" " O_2
c	" " CO_2
a	" " Ar
1 - e - f - c - a	" " N_2.

Per kg-mole of Fig. 10.1 feed gas, the input molar quantities are:

$\frac{e}{100}$	kg-mole SO_2 (Section B.3.1)
$\frac{f}{100}$	" " O_2
$\frac{c}{100}$	" " CO_2
$\frac{a}{100}$	" " Ar
$1 - \frac{e}{100} - \frac{f}{100} - \frac{c}{100} - \frac{a}{100}$	" " N_2.

Molar balances

Section F.1's sulfur and oxygen balances (i.e. Eqns. (B14) and (B20)) are not affected by the presence of Ar in Fig. 10.1's feed gas. Ar does, however, introduce a new molar balance, i.e.:

$$\begin{matrix}\text{kg-mole Ar} \\ \text{in feed gas}\end{matrix} = \begin{matrix}\text{kg-mole Ar} \\ \text{in exit gas}\end{matrix} \tag{F.5}$$

or:

$$\frac{a}{100} = n_{Ar} \tag{F.6}$$

where n_{Ar} = kg-mole Ar in Fig. 10.1 exit gas.

It also changes N balance Eqn. (B.19) to:

$$2*\left(1 - \frac{e}{100} - \frac{f}{100} - \frac{c}{100} - \frac{\mathbf{a}}{\mathbf{100}}\right) = 2*n_{N_2}$$

or:

$$n_{N_2} = 1 - \frac{e}{100} - \frac{f}{100} - \frac{c}{100} - \frac{\mathbf{a}}{\mathbf{100}} \tag{F.7}$$

Total kg-mole of exit gas

Including CO_2 and Ar, total kg-mole of Fig. 10.1 exit gas is given by:

$$n_t = n_{SO_3} + n_{SO_2} + n_{O_2} + n_{N_2} + n_{CO_2} + n_{Ar} \tag{F.8}$$

Combining this with Eqns. (B.14), (B.20), (F.2), (F.6) and (F.7) gives:

$$n_t = n_{SO_3} + \left(\frac{e}{100} - n_{SO_3}\right) + \left(\frac{f}{100} - \frac{1}{2}*n_{SO_3}\right) + \left(1 - \frac{e}{100} - \frac{f}{100} - \frac{c}{100} - \frac{a}{100}\right) + \frac{c}{100} + \frac{a}{100}$$

$$= 1 - \frac{1}{2}*n_{SO_3} \qquad \text{(B.26) } \textit{unchanged.}$$

As with CO_2, Eqns. (B.14), (B.20) and B.26) are unchanged by Ar. Consequently, Eqns. (B.27), (B.28), B29) and all further developments in Appendix B are also unchanged. So Eqn. (10.12) is unaffected by the presence of Ar in Fig. 10.1 feed gas.

F.3 Conclusions

Eqn. (10.12) is unaffected by the presence of N_2, CO_2 and Ar in catalyst bed feed gas. By extension, it is unaffected by all non-reactive gases ('inerts').

Appendix G

Enthalpy Equations for Heatup Path Calculations

Catalytic $SO_2 + \frac{1}{2}O_2 \rightarrow SO_3$ heatup paths range between about 660 K and 900 K. Preparation of these heatup paths requires SO_3, SO_2, O_2, N_2 and CO_2 enthalpy values and equations over this temperature range. This appendix:

(a) calculates the enthalpies of SO_3, SO_2, O_2, N_2 and CO_2 over this range from the data in Chase, 1998[#]

(b) relates these enthalpies to temperature with equations of the form

$H_T^\circ = A*T + B$.

Chase, 1998:

(a) specifies that the enthalpies of elements in their most common state (e.g. $S_{rhombic}$, $O_2(g)$) are zero at 298.15 (the conventional reference temperature, T_r)

and:

(b) gives values for:

$\Delta_f H_{298.15}^\circ$, the standard enthalpy of compound formation at 298.15 K

$(H_T^\circ - H_{298.15}^\circ)$ for elements and compounds, listed as $H^\circ - H^\circ(T_r)$.

The enthalpies of elements and compounds at temperature T are calculated by the equation:

$$H_T^\circ = H_{298.15}^\circ + \left(H_T^\circ - H_{298.15}^\circ\right) \qquad \text{(G.1).}$$

Element enthalpies

$H_{298.15}^\circ$ for elements is zero (see above) so that their enthalpies at temperature T are simply:

$$H_{T\,\text{element}}^\circ = \left(H_T^\circ - H_{298.15}^\circ\right)_{\text{element}} \qquad \text{(G.2)}$$

where Chase, 1998 provides the right hand side values, listed as $H^\circ - H^\circ(T_r)$.

[#] Chase, M.W. (1998) *NIST-JANAF Thermochemical Tables, 4th Edition*, American Chemical Society and American Institute of Physics, Woodbury, New York.

Compound enthalpies (using SO_3 as an example)

$H^\circ_{298.15}$ for compounds is not zero. For SO_3 it is calculated by the equation:

$$\underset{SO_3(g)}{H^\circ_{298.15}} = \Delta_f \underset{SO_3(g)}{H^\circ_{298.15}} + \underset{S(rhombic)}{H^\circ_{298.15}} + \frac{3}{2} * \underset{O_2(g)}{H^\circ_{298.15}} \qquad \text{(G.3).}$$

where $\Delta_f \underset{SO_3(g)}{H^\circ_{298.15}}$ is the enthalpy of formation (298.15 K) of SO_3 from its elements at 298.15 K, i.e.:

$$\underset{298.15}{S_{(rhombic)}} + \frac{3}{2} * O_2(g)_{298.15} \rightarrow SO_3(g)_{298.15}$$

Chase, 1998 provides $\Delta_f H^\circ_{298.15}$ values for each compound to which we add the compound designation, e.g. $\Delta_f \underset{SO_3(g)}{H^\circ_{298.15}}$.

Further:

$$\underset{S(rhombic)}{H^\circ_{298.15}} \quad \text{and} \quad \underset{O_2(g)}{H^\circ_{298.15}}$$

are both zero (because they are elements), so that Eqn. (G.3) reduces to:

$$\underset{SO_3(g)}{H^\circ_{298.15}} = \Delta_f \underset{SO_3(g)}{H^\circ_{298.15}} \qquad \text{(G.4).}$$

Lastly,

$$\underset{SO_3(g)}{H^\circ_T} = \underset{SO_3(g)}{H^\circ_{298.15}} + \left(H^\circ_T - H^\circ_{298.15}\right)_{SO_3(g)} \qquad \text{from (G.1)}$$

which combined with Eqn. (G.4) becomes:

$$\underset{SO_3(g)}{H^\circ_T} = \Delta_f \underset{SO_3(g)}{H^\circ_{298.15}} + \left(H^\circ_T - H^\circ_{298.15}\right)_{SO_3(g)} \qquad \text{(G.5).}$$

where both of the right hand terms are provided by Chase (the latter as $H^\circ - H^\circ(T_r)$.

The enthalpy units in Chase, 1998 are kJ per g-mole. This unit converts one-to-one to MJ per kg-mole, the unit used in this book.

Interestingly, Barin, 1995## provides H°_T values directly. None of the above calculations is necessary when his data are used.

##Barin, I. (1995) *Thermochemical Data of Pure Substances, 3rd Edition*, VCH Publishers Inc., New York.

G.2 An Example – Enthalpy of SO_3(g) at 600 K

Chase, 1998 lists:

$$\Delta_f \underset{SO_3(g)}{H^o_{298.15}} = -395.765 \text{ MJ/kg-mole } SO_3$$

$$\left(H^o_{600} - H^o_{298.15}\right)_{SO_3(g)} = 18.107 \text{ MJ/kg-mole } SO_3.$$

The enthalpy of SO_3(g) at 600 K is, therefore:

$$\underset{SO_3(g)}{H^o_{600}} = \Delta_f \underset{SO_3(g)}{H^o_{298.15}} + \left(H^o_{600} - H^o_{298.15}\right)_{SO_3(g)} \quad \text{(from Eqn. G.5)}$$

$$= -395.765 + 18.107$$

$$= -377.658 \text{ MJ/kg-mole } SO_3$$

as shown in Cell D5 of Table G.1.

G.2 Preparation of Equations

Table G.1 uses Eqn. (G.2), Eqn. (G.5) and Chase, 1998 data to calculate the enthalpies of SO_3, SO_2, O_2, N_2 and CO_2 at 600, 700, 800 and 900 K (and $H_2SO_4(\ell)$ and $H_2O(\ell)$ at 300 to 400 K). It then prepares linear equations (in cells A9, A18, A27, A36, A45, A52 and A63) which relate these enthalpies to temperature over these ranges. Excel's 'Slope' and 'Intercept' functions are used.

Table G.1. Enthalpy data from Chase, 1998# and H^o_T vs temperature equations developed from them. H^o_T is the enthalpy of a pure substance at temperature T.

	A	B	C	D
1	Units in all enthalpy columns: MJ per kg-mole			Eqn. (G.5)
2	**SO_3(g)**			
3	Temperature, K	$\Delta_f H^o_{298.15}$	$H^o_T - H^o_{298.15}$	$H^o_T = \Delta_f H^o_{298.15} + (H^o_T - H^o_{298.15})$
4	298.15	-395.765		
5	600		18.107	-377.658
6	700		24.997	-370.768
7	800		32.160	-363.605
8	900		39.531	-356.234
9	$H^o_{SO3T} = 0.07144*T - 420.6$			
10				
11	**SO_2(g)**			
12	Temperature, K	$\Delta_f H^o_{298.15}$	$H^o_T - H^o_{298.15}$	$H^o_T = \Delta_f H^o_{298.15} + (H^o_T - H^o_{298.15})$
13	298.15	-296.842		
14	600		13.544	-283.298
15	700		18.548	-278.294
16	800		23.721	-273.121
17	900		29.023	-267.819
18	$H^o_{SO2T} = 0.05161*T - 314.3$			

Table G.1 continued.

	A	B	C	D
19	Units in all enthalpy columns: MJ per kg-mole			Eqn. (G.5)
20	**$O_2(g)$**			
21	Temperature, K	$\Delta_f H^o_{298.15}$	$H^o_T - H^o_{298.15}$	$H^o_T = \Delta_f H^o_{298.15} + (H^o_T - H^o_{298.15})$
22	298.15	0		
23	600		9.244	9.244
24	700		12.499	12.499
25	800		15.835	15.835
26	900		19.241	19.241
27	$H^o_{O2T} = 0.03333*T - 10.79$			
28				
29	**$N_2(g)$**			
30	Temperature, K	$\Delta_f H^o_{298.15}$	$H^o_T - H^o_{298.15}$	$H^o_T = \Delta_f H^o_{298.15} + (H^o_T - H^o_{298.15})$
31	298.15	0		
32	600		8.894	8.894
33	700		11.937	11.937
34	800		15.046	15.046
35	900		18.223	18.223
36	$H^o_{N2T} = 0.03110*T - 9.797$			
37				
38	**$CO_2(g)$**			
39	Temperature, K	$\Delta_f H^o_{298.15}$	$H^o_T - H^o_{298.15}$	$H^o_T = \Delta_f H^o_{298.15} + (H^o_T - H^o_{298.15})$
40	298.15	-393.522		
41	600		12.907	-380.615
42	700		17.754	-375.768
43	800		22.806	-370.716
44	900		28.030	-365.492
45	$H^o_{CO2T} = 0.05042*T - 411.0$			
46				
47	**$H_2SO_4(l)$**			
48	Temperature, K	$\Delta_f H^o_{298.15}$	$H^o_T - H^o_{298.15}$	$H^o_T = \Delta_f H^o_{298.15} + (H^o_T - H^o_{298.15})$
49	298.15	-813.989		
50	300		0.257	-813.732
51	400		15.112	-798.877
52	$H^o_{H2SO4(l)T} = 0.1485*T - 858.3$			
53				
54	**$H_2O(l)$**			
55	Temperature, K	$\Delta_f H^o_{298.15}$	$H^o_T - H^o_{298.15}$	$H^o_T = \Delta_f H^o_{298.15} + (H^o_T - H^o_{298.15})$
56	298.15	-285.830		
57	300		0.139	-285.691
58	320		1.646	-284.184
59	340		3.153	-282.677
60	360		4.664	-281.166
61	380		6.182	-279.648
62	400		7.711	-278.119
63	$H^o_{H2O(l)T} = 0.07568*T - 308.4$			

Appendix H

Matrix Solving
Using Tables 11.2 and 14.2 as Examples

1. Put Table 11.2 into an Excel spreadsheet with the top of the numerical term column (0.10) in cell C2. The matrix covers cells C2 to J8. Label as shown in Table 11.2.

2. Select cells B13 to B19 (by, for example, selecting cell B13, holding down the Shift key and arrowing down to cell B19).

3. Leave these cells selected then type ***=mmult(minverse(D2:J8),C2:C8)*** then simultaneously press **Ctrl Shift Enter**.

4. Cells B13-B19 contain the solution to the matrix. Label as shown in Table 11.2.

Subsequent problems can be solved without repeating the above steps. The Section 11.13 example problem is solved, for example, by putting 0.130, 0.143 and 0.727 into cells C2, C3 and C4 respectively. The solution appears automatically in cells B13-B19.

Table 14.2's matrix has 1 more column than Table 11.2 – and 1 more row. This means that instruction 2 (above) must select 8 cells instead of 7, say B20 to B27 in Table 14.2.

Table 14.2's solving instruction is:
Leave cells B20 through B27 selected then type ***=mmult(minverse(D8:K15),C8:C15)*** then simultaneously press **Ctrl Shift Enter**.

Appendix I

Enthalpy Equations in Heatup Path Matrix Cells

Heatup path calculations are simplified by putting enthalpy-as-a-function-of-temperature equations in cells D8-J8 of matrix Table 11.2. The equations are listed in Appendix G. They change Eqn. (11.7) to:

$$\begin{aligned}
0 \quad = \quad & -\text{kg-mole } SO_2 \ \mathbf{in} * (0.05161 * T_{\text{feed}} - 314.3) \\
& -\text{kg-mole } O_2 \ \mathbf{in} * (0.03333 * T_{\text{feed}} - 10.79) \\
& -\text{kg-mole } N_2 \ \mathbf{in} * (0.03110 * T_{\text{feed}} - 9.797) \\
& +\text{kg-mole } SO_3 \ \mathbf{out} * (0.07144 * T_L - 420.6) \\
& +\text{kg-mole } SO_2 \ \mathbf{out} * (0.05161 * T_L - 314.3) \\
& +\text{kg-mole } O_2 \ \mathbf{out} * (0.03333 * T_L - 10.79) \\
& +\text{kg-mole } N_2 \ \mathbf{out} * (0.03110 * T_L - 9.797) \qquad \text{(11.7")}
\end{aligned}$$

where:

$(0.05161 * T - 314.3) = H^{\circ}_{T\ SO_2}$ etc.

T_{feed} = Fig. 11.3 feed gas temperature, K
T_L = Fig. 11.3 level L gas temperature, K.

As shown in Table I.1, Eqn. (11.7") is put into matrix Table 11.2 by:

(a) inserting numerical values of T_{feed} and T_L into cells F10 and J10
(b) putting the Eqn (11.7") enthalpy terms into cells D8-J8 so that:

cell D8 contains = -(0.05161*F10 - 314.3)
" E8 " " = -(0.03333*F10 - 10.79) note the - signs
" F8 " " = -(0.03110*F10 - 9.797)
" G8 " " = (0.07144*J10 - 420.6)
" H8 " " = (0.05161*J10 - 314.3)
" I8 " " = (0.03333*J10 - 10.79)
" J8 " " = (0.03110*J10 - 9.797).

Insertion of these equations into Table 11.2 (with 690 K and 820 K in cells F10 and J10) automatically gives the Table 11.2 result, as shown below. The temperatures in cells F10 and J10 can then be changed at will – and new heatup path points automatically calculated. Example results are shown after Table I.1. Matrix solving is described in Appendix H.

Table I.1. Matrix Table 11.2 with Eqn. (11.7") enthalpy equations in cells D8-J8, see above. The in-cell equations refer to T_{feed} in cell F10 and T_L in cell J10. Feed gas quantities in cells C2-C4 can also be changed at will as described in Section 11.13. Refer to Table 11.2 for other details.

	A	B	C	D	E	F	G	H	I	J
1	Equation	description	numerical term	kg-mole SO_2 **in**	kg-mole O_2 **in**	kg-mole N_2 **in**	kg-mole SO_3 **out**	kg-mole SO_2 **out**	kg-mole O_2 **out**	kg-mole N_2 **out**
2	11.1	feed SO_2 kg-mole	0.10	1	0	0	0	0	0	0
3	11.2	feed O_2 kg-mole	0.11	0	1	0	0	0	0	0
4	11.3	feed N_2 kg-mole	0.79	0	0	1	0	0	0	0
5	11.4	S balance	0	-1	0	0	1	1	0	0
6	11.5	O balance	0	-2	-2	0	3	2	2	0
7	11.6	N balance	0	0	0	-2	0	0	0	2
8	11.7"	enthalpy balance	0	278.7	-12.21	-11.66	-362.0	-272.0	16.54	15.71
9										
10				Fig. 11.3 feed gas temperature, K =		690		Fig. 11.3 level L gas temp, K =		820
11										
12	Matrix results per kg-mole of feed gas					contains	=0.07144*J10-420.6			
13	kg-mole SO_2 **in**	0.1000								
14	kg-mole O_2 **in**	0.1100								
15	kg-mole N_2 **in**	0.7900								
16	kg-mole SO_3 **out**	0.0442			% SO_2 oxidized at level L =	((kg-mole SO_2 **in** - kg-mole SO_2 **out**)/kg-mole SO_2 **in**)*100				(Eqn. 10.1)
17	kg-mole SO_2 **out**	0.0558			=	(B13-B17)/B13*100	=	44.2		
18	kg-mole O_2 **out**	0.0879								
19	kg-mole N_2 **out**	0.7900								

I.1 Example Results

Table I.1 automatically shows that:

an 820 K heatup path temperature

with:

10 volume% SO_2, 11 volume% O_2, 79 volume% N_2, 690 K feed gas

is equivalent to:

44.2 % oxidation of the feed gas's SO_2

in the Fig. 11.3 catalyst bed. This is one point on the feed gas's heatup path.

Other points may be calculated by:

(a) incrementally changing the cell J10 temperature

(b) tabulating these temperatures and their equivalent cell H17 *% SO_2 oxidized* values.

Table 11.3/Fig. 11.1 points have been calculated this way. A few of them are:

	A	B	C
21		Fig. 11.3 level L temperature, K	% SO_2 oxidized at level L
22		690	0.0
23		710	6.8
24		730	13.5

Table 12.1/Fig. 12.1 heatup path points have also been calculated this way. A few are:

	A	B	C
21		Fig. 11.3 level L temperature, K	% SO_2 oxidized at level L
22		890	68.09
23		891	68.44
24		892	68.78

Appendix J

Heatup Path-Equilibrium Curve Intercept Calculations

Figs. 11.7 and 12.1 indicate that maximum SO_2 oxidation in a catalyst bed occurs where a feed gas's:

heatup path

intercepts its:

equilibrium curve.

The point of interception may be determined:

(a) by re-doing Table 12.1's calculations every 0.1 K

(b) iteratively, using Excel's Goal Seek tool.

This appendix describes (b).

J.1 Calculation Strategy

Our iterative intercept strategy is to find the temperature at which a feed gas's:

heatup path *% SO_2 oxidized*, Φ.

equals its:

equilibrium curve *% SO_2 oxidized*, Φ^E.

This temperature and its equivalent *% SO_2 oxidized* define the intercept point. The next several pages provide an intercept calculation worksheet and instructions. The worksheet is for the specific case of:

10 volume% SO_2

11 volume% O_2

79 volume% N_2

690 K

feed gas and 1.2 bar gas pressure. It is easily altered for different pressures and gas compositions and temperatures. All calculations are based on 1 kg-mole of 1st catalyst bed feed gas.

J.2 Worksheet

The top of worksheet Table J.1 is similar to equilibrium curve worksheet Table D.1. Its main components are:

(a) an equilibrium curve *% SO_2 oxidized* value in cell F11

(b) Eqn. (10.13) in cell A14 (as shown to the right of that cell)

(c) equilibrium pressure P_t specified in cell K6.

The middle of the worksheet is similar to heatup path Table I.1. Its main components are:

(a) a matrix which contains Eqns. (11.1) to (11.6) – and Eqn. (11.7") with enthalpy equations in cells D28-J28

(b) feed gas temperature in cell F30 (copied from cell K5)

(c) intercept gas temperature in cell J30 (copied from cell A14)

(d) a matrix results column like that in Table I.1

(e) a heatup path *% SO_2 oxidized* value calculated in cell I39 from the matrix results.

The bottom of Table J.1 is the iterative part of the worksheet. It:

(a) subtracts:

heatup path *% SO_2 oxidized* (cell I39)

from

equilibrium curve *% SO_2 oxidized* (cell F11)

in cell G47

then:

(b) uses Excel's Goal Seek tool to determine the value of:

equilibrium curve *% SO_2 oxidized* in cell F11

which gives a zero value to cell G47.

The Goal Seek procedure is described in Section J.4.

J.3 Intercept Worksheet Preparation Instructions

1. Feed gas volume% SO_2, O_2 and N_2 are entered into cells G3, I3 and K3. Feed gas temperature is entered into cell K5. Total gas pressure is entered into cell K6.

2. Feed kg-mole SO_2, O_2 and N_2 are calculated in cells G8, I8 and K8 as shown. They are all per kg-mole of feed gas. Feed kg-mole SO_2 is repeated in cell G5 (for later 2nd catalyst bed calculations).

3. A suggested equilibrium curve intercept *% SO_2 oxidized* value is entered in cell F11 (perhaps 69% from Table 12.1).

4. Eqn. (10.13) is entered in Cell A14 as shown.

5. Steps 3 and 4 automatically calculate the equilibrium curve temperature (cell A14) equivalent to the *% SO_2 oxidized* value in cell F11. The cell A14 temperature is automatically copied into cell J30. This links the equilibrium curve and heatup path calculations.

6. A heatup path matrix is entered as described in Tables 11.2 and I.1. Cells D28 to J28 contain enthalpy-as-a-function-of-temperature equations, Table I.1. Cells C22 to C24 contain input kg-mole SO_2, O_2 and N_2, Section 11.13.

7. The matrix is solved as described in Appendix H. The procedure is: select cell B35, shift-arrow down to cell B41, type ***mmult(minverse(D22:J28),C22:C28)*** then simultaneously press **Ctrl Shift Enter**. This is the only time the matrix must be solved.

8. Eqn. (10.1) is entered in cell I39. This automatically uses the step 7 results to calculate the heatup path *% SO_2 oxidized* value equivalent to:

   cell J30's (hence cell A14's) intercept temperature.

9. At his point, equilibrium curve temperature = heatup path temperature. But equilibrium curve *% SO_2 oxidized* (cell F11) $\neq$ heatup path *% SO_2 oxidized* (cell I39). So this is not the intercept.

The 'actual' intercept value is determined by the Goal Seek calculation in Section J.4.

Table J.1. Worksheet for calculating 1st catalyst bed heatup path-equilibrium curve intercept. Preparation instructions are given in Section J.3. Operating instructions are given in Section J.4. Notice that equilibrium curve *% SO$_2$ oxidized* (cell F11) ≠ heatup path *% SO$_2$ oxidized* (cell I39). So 894.2 K in cells A14 and J30 is not the intercept temperature. The intercept value is calculated in Table J.2.

	A	B	C	D	E	F	G	H	I	J	K
1	**1ST CATALYST BED**							**All quantities are per kg-mole of 1st catalyst bed feed gas**			
2											
3	1st catalyst bed feed gas composition from Fig. 11.2					e, volume% SO$_2$ =	10	f, volume% O$_2$ =	11	volume% N$_2$ =	79
4											
5	1st catalyst bed feed **kg-mole** SO$_2$ (for Eqn. (10.1) = e/100 = G3/100 (Eqn. 11.1)						0.1			feed gas temperature, K =	690
6										catalyst bed pressure P$_t$, bar =	1.2
7											
8	1st catalyst bed feed **kg-mole** from above feed gas composition, Eqn. (11.1) etc.					SO$_2$ =	0.1	O$_2$ =	0.11	N$_2$ =	0.79
9							= e/100 =G3/100		=f/100 =I3/100		=K3/100
10											
11	Suggested equilibrium curve intercept % SO$_2$ oxidized, Φ^E =					69.0					
12											
13	Equilibrium curve temperature equivalent to cell F11's suggested % SO$_2$ oxidized, Eqn. (10.13)										
14	894.2	=-(-98.41)/(0.09357+0.008314*LN(F11/(100-F11)*((100-0.5*G3*F11/100)/(I3-0.5*G3*F11/100))^0.5*K6^-0.5))						(10.13)			
15											
16											
17											
18											
19											
20	*Heatup path matrix (**In** means 'in feed gas', **out** means 'in intercept gas')*										
21	Equation	description	numerical term =G8 etc.	kg-mole SO$_2$ **in**	kg-mole O$_2$ **in**	kg-mole N$_2$ **in**	kg-mole SO$_3$ **out**	kg-mole SO$_2$ **out**	kg-mole O$_2$ **out**	kg-mole N$_2$ **out**	
22	11.1	feed SO$_2$ kg-mole	0.10	1	0	0	0	0	0	0	
23	11.2	feed O$_2$ kg-mole	0.11	0	1	0	0	0	0	0	
24	11.3	feed N$_2$ kg-mole	0.79	0	0	1	0	0	0	0	
25	11.4	S balance	0	-1	0	0	1	1	0	0	
26	11.5	O balance	0	-2	-2	0	3	2	2	0	
27	11.6	N balance	0	0	0	-2	0	0	0	2	
28	11.7"	enthalpy balance	0	278.7	-12.21	-11.66	-356.7	-268.2	19.01	18.01	
29											
30					feed gas temperature =	690			intercept temperature from cell A14 =	894.2	
31						=K5				=A14	
32											
33							=0.07144*J30-420.6	from Appendix G			
34	Matrix results equivalent to suggested intercept temperature in cell J30 (and A14)										
35	kg-mole SO$_2$ in	0.1000									
36	kg-mole O$_2$ in	0.1100									
37	kg-mole N$_2$ in	0.7900									
38	kg-mole SO$_3$ out	0.0695			heatup path % SO$_2$ oxidized (Φ) equivalent to intercept temperature in cells J30 and A14 =						
39	kg-mole SO$_2$ out	0.0305			(kg-mole SO$_2$ in - kg-mole SO$_2$ out)/kg-mole SO$_2$ in*100 =				69.5	=(G5-B39)/G5*100	(10.1)
40	kg-mole O$_2$ out	0.0752									
41	kg-mole N$_2$ out	0.7900									
42	all per kg-mole of feed gas										
43											
44											
45											
46	Goal Seek calculation										
47	Equilibrium curve % SO$_2$ oxidized - heatup path % SO$_2$ oxidized =						-0.5	=F11-I39			

J.4 Goal Seek Instructions

Table J.1 is set up so that equilibrium curve temperature always = heatup path temperature. The only remaining question is at what temperature does:

heatup path *% SO_2 oxidized* = equilibrium curve *% SO_2 oxidized*?

This is determined by:

1. Putting 'equilibrium curve '*% SO_2 oxidized* - heatup path *% SO_2 oxidized*' in cell G47, as shown.
2. Using Goal Seek to adjust:

equilibrium curve *% SO_2 oxidized* (cell F11)

until cell G47 = zero, i.e. until:

heatup path *% SO_2 oxidized* = equilibrium curve *% SO_2 oxidized*.

The Goal Seek procedure is:

Tools
Goal Seek
Set cell: G47
To value: 0
Changing cell: F11
OK
OK.

The results are shown in worksheet Table J.2. The intercept point is 69.2 *% SO_2 oxidized* (in cells F11 and I39), 893.3 K (in cells A14 and J30) – as is readily checked by comparison with Table 12.1.

Intercept kg-mole SO_3, SO_2, O_2 and N_2 (per kg-mole of feed gas) are also provided in cells B38 to B41. They are used in Chapter 14 and 15's multi-catalyst bed calculations.

J.5 Another Example

Table J.3 is a worksheet for 13 volume% SO_2, 14.3 volume% O_2 and 72.7 volume% N_2, 690 K feed gas and a 1.2 bar equilibrium pressure. The heatup path-equilibrium curve intercept for this new gas is determined by:

(a) entering these new specifications in cells G3, I3, K3, K5 and K6

(b) repeating Section J.4's Goal Seek instructions.

Table J.2. Table J.1 worksheet after Goal Seek has found the heatup path-equilibrium curve intercept: 893.3 K, 69.2% *SO_2 oxidized.*

	A	B	C	D	E	F	G	H	I	J	K
1	**1ST CATALYST BED**							**All quantities are per kg-mole of 1st catalyst bed feed gas**			
2											
3	1st catalyst bed feed gas composition from Fig. 11.2					e, volume% SO_2 =	10	f, volume% O_2 =	11	volume% N_2 =	79
4											
5	1st catalyst bed feed **kg-mole** SO_2 (for Eqn. (10.1) = e/100 = G3/100 (Eqn. 11.1)						0.1		feed gas temperature, K =		690
6									catalyst bed pressure P_t, bar =		1.2
7											
8	1st catalyst bed feed **kg-mole** from above feed gas composition, Eqn. (11.1) etc.					SO_2 =	0.1	O_2 =	0.11	N_2 =	0.79
9							= e/100 =G3/100		=f/100 =I3/100		=K3/100
10											
11	Suggested equilibrium curve intercept % SO_2 oxidized, Φ^E =					69.2					
12											
13	Equilibrium curve temperature equivalent to cell F11's suggested % SO_2 oxidized, Eqn. (10.13)										
14	893.3	=-(-98.41)/(0.09357+0.008314*LN(F11/(100-F11)*((100-0.5*G3*F11/100)/(I3-0.5*G3*F11/100))^0.5*K6^-0.5))						(10.13)			
15											
16											
17											
18											
19											
20	*Heatup path matrix (**in** means 'in feed gas', **out** means 'in intercept gas')*										
21	Equation		numerical term =G8 etc.	kg-mole SO_2 **in**	kg-mole O_2 **in**	kg-mole N_2 **in**	kg-mole SO_3 **out**	kg-mole SO_2 **out**	kg-mole O_2 **out**	kg-mole N_2 **out**	
22	11.1	feed SO_2 kg-mole	0.10	1	0	0	0	0	0	0	
23	11.2	feed O_2 kg-mole	0.11	0	1	0	0	0	0	0	
24	11.3	feed N_2 kg-mole	0.79	0	0	1	0	0	0	0	
25	11.4	S balance	0	-1	0	0	1	1	0	0	
26	11.5	O balance	0	-2	-2	0	3	2	2	0	
27	11.6	N balance	0	0	0	-2	0	0	0	2	
28	11.7*	enthalpy balance	0	278.7	-12.21	-11.66	-356.8	-268.2	18.99	17.99	
29											
30					feed gas temperature =	690		intercept temperature from cell A14 =		893.3	
31						=K5				=A14	
32											
33							=0.07144*J30-420.6	from Appendix G			
34	Matrix results equivalent to suggested intercept temperature in cell J30 (and A14)										
35	kg-mole SO_2 **in**	0.1000									
36	kg-mole O_2 **in**	0.1100									
37	kg-mole N_2 **in**	0.7900									
38	kg-mole SO_3 **out**	0.0692			heatup path % SO_2 oxidized (Φ) equivalent to intercept temperature in cells J30 and A14 =						
39	kg-mole SO_2 **out**	0.0308			(kg-mole SO_2 **in** - kg-mole SO_2 **out**)/kg-mole SO_2 **in***100 =				69.2	=(G5-B39)/G5*100	(10.1)
40	kg-mole O_2 **out**	0.0754									
41	kg-mole N_2 **out**	0.7900									
42	all per *kg-mole of feed gas*										
43											
44											
45											
46	Goal Seek calculation										
47	Equilibrium curve % SO_2 oxidized - heatup path % SO_2 oxidized =						0.0	=F11-I39			

Table J.3. Worksheet for 13 volume% SO_2, 14.3 volume% O_2, 72.7 volume% N_2, 690 K feed gas (1.2 bar) after Goal Seek has found the intercept.

	A	B	C	D	E	F	G	H	I	J	K
1	**1ST CATALYST BED**							**All quantities are per kg-mole of 1st catalyst bed feed gas**			
2											
3	1st catalyst bed feed gas specification					e, volume% SO_2 =	13.0	f, volume% O_2 =	14.3	volume% N_2 =	72.7
4											
5	1st catalyst bed feed kg-mole SO2 = e/100 = G3/100 =			Eqn. (11.1)			0.13		feed gas temperature, K =		690
6									gas pressure in bed P_1, bar =		1.2
7											
8	1st catalyst bed feed kg-mole from feed gas composition					kg-mole SO_2 =	0.13	kg-mole O_2 =	0.143	kg-mole N_2 =	0.727
9							= e/100 =G3/100		=f/100 =I3/100		=K3/100
10											
11	Equilibrium curve intercept % SO_2 oxidized =					62.7					
12											
13	Equilibrium curve temperature equivalent to cell F11's suggested % SO_2 oxidized, from Eqn. (10.13)										
14	924.5	=-(-98.41)/(0.09357+0.008314*LN(F11/(100-F11)*((100-0.5*G3*F11/100)/(I3-0.5*G3*F11/100))^0.5*K6^-0.5))						(10.13)			
15											
16											
17											
18											
19											
20	*Heatup path matrix (**in** means 'in feed gas', **out** means 'in intercept gas')*										
21	Equation	description	numerical term =G8 etc.	kg-mole SO_2 **in**	kg-mole O_2 **in**	kg-mole N_2 **in**	kg-mole SO_3 **out**	kg-mole SO_2 **out**	kg-mole O_2 **out**	kg-mole N_2 **out**	
22		feed SO_2 kg-mole	0.130	1	0	0	0	0	0	0	
23		feed O_2 kg-mole	0.143	0	1	0	0	0	0	0	
24		feed N_2 kg-mole	0.727	0	0	1	0	0	0	0	
25	11.4	S balance	0	-1	0	0	1	1	0	0	
26	11.5	O balance	0	-2	-2	0	3	2	2	0	
27	11.6	N balance	0	0	0	-2	0	0	0	2	
28	11.7*	enthalpy balance	0	278.7	-12.21	-11.66	-354.6	-266.6	20.02	18.95	
29											
30					feed gas temperature =	690			intercept temperature from cell A10 =	924.5	
31						=K5				=A14	
32											
33							=0.07144*J30-420.6	from Appendix AHUP			
34	Matrix results equivalent to suggested intercept temperature in cell J30 (and A14)										
35	kg-mole SO_2 **in**	0.1300									
36	kg-mole O_2 **in**	0.1430									
37	kg-mole N_2 **in**	0.7270									
38	kg-mole SO_3 **out**	0.0816							% SO_2 oxidized equivalent to intercept temperature in cells J30 and A14 =		
39	kg-mole SO_2 **out**	0.0484						(kg-mole SO_2 **in** - kg-mole SO_2 **out**)/kg-mole SO_2 **in***100 =	62.7	=(G5-B39)/G5*100	(10.2)
40	kg-mole O_2 **out**	0.1022									
41	kg-mole N_2 **out**	0.7270									
42	all per kg-mole of feed gas										
43											
44											
45											
46	Goal Seek calculation										
47	Equilibrium curve % SO_2 oxidized - heatup path % SO_2 oxidized =						0.0	=F11-I39			

Appendix K

2nd Catalyst Bed Heatup Path Calculations

Table K.1 shows a 2nd catalyst bed heatup path matrix with enthalpy-as-a-function-of-temperature equations in cells D15 to K15. The only difference between this matrix and the Table 14.2 matrix is that Eqn. 14.9 in row 15 has been changed to:

$$
\begin{aligned}
0 \quad = \quad & -\text{kg-mole } SO_3 \ \textbf{in} * (0.07144 * T_{\text{input}} - 420.6) \\
& -\text{kg-mole } SO_2 \ \textbf{in} * (0.05161 * T_{\text{input}} - 314.3) \\
& -\text{kg-mole } O_2 \ \textbf{in} * (0.03333 * T_{\text{input}} - 10.79) \\
& -\text{kg-mole } N_2 \ \textbf{in} * (0.03110 * T_{\text{input}} - 9.797) \\
& +\text{kg-mole } SO_3 \ \textbf{out} * (0.07144 * T_L - 420.6) \\
& +\text{kg-mole } SO_2 \ \textbf{out} * (0.05161 * T_L - 314.3) \\
& +\text{kg-mole } O_2 \ \textbf{out} * (0.03333 * T_L - 10.79) \\
& +\text{kg-mole } N_2 \ \textbf{out} * (0.03110 * T_L - 9.797) \qquad (14.9'')
\end{aligned}
$$

where:

$(0.07144 * T - 420.6) = H^{\circ}_{T\ SO_3}$ etc.

T_{input} = Fig. 14.2's 2nd catalyst bed input gas temperature, K
T_L = Fig. 14.2's 2nd catalyst bed level L gas temperature, K.
Eqn. (14.9") is put into Table 14.2's solved matrix by:

(a) inserting numerical values of T_{input} and T_L into cells F17 and J17

(b) putting the Eqn (14.9") enthalpy terms into cells D15 to K15 so that:

cell D15 contains = -(0.07144 * F17 - 420.6)
" E15 " " = -(0.05161 * F17 - 314.3)
" F15 " " = -(0.03333 * F17 - 10.79) } Note the (-) signs
" G15 " " = -(0.03110 * F17 - 9.797)
" H15 " " = (0.07144 * J17 - 420.6)
" I15 " " = (0.05161 * J17 - 314.3)
" J15 " " = (0.03333 * J17 - 10.79)
" K15 " " = (0.03110 * J17 - 9.797).

Insertion of these terms (with 700 K and 760 K in cells F17 and J17) automatically gives the same result as in Table 14.2. The temperatures in cells F17 and J17 can now be changed at will – and heatup path points automatically calculated. Example results are shown below the worksheet.

Table K.1 Table 14.2 with (i) input and level L temperatures in cells F17 and J17 and (ii) enthalpy equations in cells D15 to K15. A change in either temperature automatically gives a new *% SO_2 oxidized* result.

	A	B	C	D	E	F	G	H	I	J	K
1	**All calculations are based on 1 kg-mole of 1st catalyst bed feed gas.**										
2	kg-mole SO_2 in 1 kg-mole of 1st catalyst bed feed gas			0.1							
3											
4											
5											
6	**2nd catalyst bed matrix**										
7	Equation	description	numerical term	kg-mole SO_3 **in**	kg-mole SO_2 **in**	kg-mole O_2 **in**	kg-mole N_2 **in**	kg-mole SO_3 **out**	kg-mole SO_2 **out**	kg-mole O_2 **out**	kg-mole N_2 **out**
8	14.2	input SO_3 kg-mole	0.0692	1	0	0	0	0	0	0	0
9	14.3	input SO_2 kg-mole	0.0308	0	1	0	0	0	0	0	0
10	14.4	input O_2 kg-mole	0.0754	0	0	1	0	0	0	0	0
11	14.5	input N_2 kg-mole	0.7900	0	0	0	1	0	0	0	0
12	14.6	S balance	0	-1	-1	0	0	1	1	0	0
13	14.7	O balance	0	-3	-2	-2	0	3	2	2	0
14	14.8	N balance	0	0	0	0	-2	0	0	0	2
15	14.9"	enthalpy balance	0	370.6	278.2	-12.54	-11.97	-366.3	-275.1	14.54	13.84
16											
17				Fig. 14.2 input gas temperature =		700		heatup path temperature =		760	
18											
19	Heatup path result per kg-mole of 1st catalyst bed feed gas					contains =-(0.0311*F17-9.797)					
20	kg-mole SO_3 **in**	0.0692									
21	kg-mole SO_2 **in**	0.0308									
22	kg-mole O_2 **in**	0.0754		% SO_2 oxidized at cell J17		kg-mole SO_2 in 1st		kg-mole SO_2 at heatup path			
23	kg-mole N_2 **in**	0.7900		heatup path temper-		= catalyst bed feed gas - temperature in 2nd catalyst bed * 100					
24	kg-mole SO_3 **out**	0.0897		ature in 2nd catalyst bed			kg-mole SO_2 in 1st catalyst bed feed gas				
25	kg-mole SO_2 **out**	0.0103					=(D2-B25)/D2*100 =	89.7	% SO_2 oxidized		
26	kg-mole O_2 **out**	0.0652									
27	kg-mole N_2 **out**	0.7900									

Several Table 14.3/Fig. 14.3 heatup path points calculated with the above worksheet are:

	A	B	C
30		Fig. 14.2 level L temperature, K	% SO_2 oxidized at level L
31		700	69.2
32		705	70.9
33		710	72.6

Appendix L

Equilibrium Equation for Multi-Catalyst Bed SO_2 Oxidation

This appendix shows that the equilibrium equation developed for the 1st catalyst bed of a multi-catalyst bed 'converter' (Eqn. 10.13) also applies to the converter's:

2nd, 3rd (and 4th) pre-H_2SO_4-making catalyst beds.

It also indicates that the 1st catalyst bed equation does not apply to beds which follow:

(a) selective removal of SO_3(g) during H_2SO_4 making, Reaction (1.2)

or:

(b) addition of air between beds (as is occasionally done industrially).

L.1 Proof

Examination of Appendix B and Chapter 10 shows that if the:

kg-mole S
kg-mole O
kg-mole N

inputs to a 2nd catalyst bed are the same as those entering the preceding 1st catalyst bed (per kg-mole of 1st catalyst bed feed gas), then:

equilibrium Eqn. (10.13) applies to both beds.

These 1st and 2nd bed inputs are, of course, the same if nothing is added to or removed from the gas as it passes between the beds. Industrially this is almost always the case so that Eqn. (10.13) almost always applies to both beds.

The following empirical calculation serves to emphasize this point.

Table J.2 shows that 1 kg-mole of its 1st catalyst bed feed gas contains:

$$0.10 \text{ kg-mole } SO_2 = \frac{e}{100}$$

$$0.11 \text{ kg-mole } O_2 = \frac{f}{100}$$

$$0.79 \text{ kg-mole } N_2 = 1 - \frac{e}{100} - \frac{f}{100}$$

where e and f are volume% SO_2 and O_2 in the 1st catalyst bed feed gas.

kg-mole S, O and N equivalent to the above quantities are (Section B.3.1):

$$\text{kg-mole S} = 1*\frac{e}{100} = 0.10$$

$$\text{kg-mole O} = 2*\frac{e}{100} + 2*\frac{f}{100} = 0.42$$

$$\text{kg-mole N} = 2*\left(1 - \frac{e}{100} - \frac{f}{100}\right) = 1.58$$

Table J.2 also shows that the 1st catalyst bed exit (intercept) gas contains:

0.0692 kg-mole SO_3
0.0308 kg-mole SO_2
0.0754 kg-mole O_2
0.7900 kg-mole N_2

which are equivalent to:

$$\text{kg-mole S} = 1*0.0692 \text{ kg-mole } SO_3 + 1*0.0308 \text{ kg-mole } SO_2 = 0.10$$

$$\begin{aligned}\text{kg-mole O} = {} & 3*0.0692 \text{ kg-mole } SO_3 \\ & + 2*0.0308 \text{ kg-mole } SO_2 \\ & + 2*0.0754 \text{ kg-mole } O_2 = 0.42\end{aligned}$$

$$\text{kg-mole N} = 2*0.79 \text{ kg-mole } N_2 = 1.58$$

(all per kg-mole of 1st catalyst bed feed gas).

This exit gas flows without addition or removal through its gas cooler and into the 2nd catalyst bed – which leads to the conclusions that:

(a)

$$\frac{\text{kg-mole S into}}{\text{1st catalyst bed}} = \frac{\text{kg-mole S into}}{\text{2nd catalyst bed}} = 0.10 = 1*\frac{e}{100} \qquad \text{(L.1)}$$

$$\frac{\text{kg-mole O into}}{\text{1st catalyst bed}} = \frac{\text{kg-mole O into}}{\text{2nd catalyst bed}} = 0.42 = 2*\frac{e}{100} + 2*\frac{f}{100} \qquad \text{(L.2)}$$

$$\frac{\text{kg-mole N into}}{\text{1st catalyst bed}} = \frac{\text{kg-mole N into}}{\text{2nd catalyst bed}} = 1.58 = 2*\left(1 - \frac{e}{100} - \frac{f}{100}\right). \qquad \text{(L.3)}$$

(b) Eqn. (10.13) therefore applies to both catalyst beds.

Item (b) arises because Eqns. (B14), (B20), (B23) (B26) (and all subsequent Appendix B equations) are the same for both catalyst beds.

The above calculation can be generalized to a series of catalyst beds as long as nothing is added to or removed from the gas stream between beds.

L.2 Inapplicability

1st catalyst bed equilibrium Eqn. (10.13) does <u>not</u>, however, apply to beds which follow:

(a) selective removal of SO_3 during H_2SO_4-making

(b) addition of air between beds.

This is because Eqns. (L.1), (L.2) and (L.3), hence Eqns. (B.14), (B.20), (B23) and (B.26) would not apply to bed 2 (and subsequent beds) if SO_3 were removed or air were added between beds 1 and 2.

Appendix M

2nd Catalyst Bed Intercept Calculations

Chapter 15 indicates that maximum SO_2 oxidation in a 2nd catalyst bed occurs where the bed's:

heatup path

intercepts its

equilibrium curve.

The point of interception may be determined:

(a) by interpolation, Table 15.1
(b) iteratively with Excel's Goal Seek tool, described here.

M.1 Calculation Strategy

Our iteration strategy here is much like that in Appendix J. It consists of finding the temperature at which a 2nd catalyst bed's:

equilibrium curve *% SO_2 oxidized*, Φ^E

is the same as its

heatup path *% SO_2 oxidized*, Φ.

This temperature and its equivalent *% SO_2 oxidized* define the 2nd catalyst bed intercept point.

All calculations in this appendix are based on the gas composition, temperature and pressure specifications in Fig. 14.2. The calculations are all per kg-mole of 1st catalyst bed feed gas.

M.2 Specifications (Fig. 14.2)

This appendix's specifications are:

1st catalyst bed feed gas composition:

10 volume% SO_2, 11 volume% O_2, 79 volume% N_2

2nd catalyst bed input gas quantities:

0.0692 kg-mole SO_3
0.0308 kg-mole SO_2
0.0754 kg-mole O_2
0.7900 kg-mole N_2

per kg-mole of 1st catalyst bed feed gas.

2nd catalyst bed gas input temperature and bed pressure:

700 K 1.2 bar

M.3 Worksheet

All quantities are per kg-mole of 1st catalyst bed feed gas.

The 2nd catalyst bed intercept worksheet (below) is prepared as follows:

1. *1st catalyst bed feed* gas volume % SO_2 and volume% O_2 are entered in cells G3 and I3. 1st catalyst bed input kg-mole SO_2 is calculated in cell G5.
2. 2nd catalyst bed input gas quantities are entered in cells E8, G8, I8 and K8. They are Fig. 14.2's 1st catalyst bed intercept quantities. They are automatically copied into cells C21-C24.
3. 2nd catalyst bed gas input temperature and catalyst bed pressure are entered in cells K5 and K6.
4. An equilibrium curve intercept *% SO_2 oxidized* is suggested in cell F11 (perhaps 94% from Table 15.1).
5. Eqn. (10.13) is entered in cell A14 as shown beside the cell.
6. Steps 4 and 5 automatically calculate the cell A14 equilibrium curve temperature that is equivalent to cell F11's *% SO_2 oxidized*. The cell A14 temperature is then automatically copied into cell J30, as shown. This links the 2nd bed equilibrium curve and heatup path calculations.
7. The Appendix K heatup path matrix is entered into cells C21 to K28. Cells D28 to K28 contain enthalpy-as-a-function-of-temperature equations, Appendix K ($-H^\circ_T$ in cells D28 to G28). Cells C21 to C24 contain Fig. 14.2's 2nd catalyst bed input kg-mole SO_3, SO_2, O_2 and N_2.
8. The matrix is solved as described in Appendix H. The procedure is: select cell B34, shift-arrow down to cell B41. With these cells still selected, type ***mmult(minverse(D21:K28),C21:C28)*** then simultaneously press **Ctrl Shift Enter**
9. Eqn. (14.1) is entered in cell I39 as shown beside it. This automatically uses step 8's results to calculate the heatup path *% SO_2 oxidized* equivalent to cell J30's (hence cell A14's) intercept temperature.
10. At this point, equilibrium curve temperature = heatup path temperature. But equilibrium curve *% SO_2 oxidized* (cell F11) $\neq$ heatup path *% SO_2 oxidized* (cell I39). So this is not the intercept.

The actual 2nd catalyst bed intercept value is determined by the Goal Seek calculation in Section M.4.

Table M.1. Worksheet for determining 2nd catalyst bed heatup path-equilibrium curve intercept. The non-zero 'equilibrium curve *% SO_2 oxidized* - heatup path *% SO_2 oxidized*' value in cell G47 indicates that cell F11's suggested 94% *SO_2 oxidized* is not the intercept value. The actual intercept value is calculated in Table M.2.

	A	B	C	D	E	F	G	H	I	J	K
1	**2nd CATALYST BED**							**All quantities are per kg-mole of 1st catalyst bed feed gas**			
2											
3	1st catalyst bed feed gas specifications from Fig. 14.2					e, volume% SO_2 =	10	f, volume% O_2 =	11		
4											
5	1st catalyst bed feed **kg-mole** SO_2 (for Eqn. (14.1) = e/100 = G3/100				Eqn. (11.1)		0.1	2nd catalyst bed input gas temperature, K =			700
6								2nd catalyst bed pressure P_t, bar =			1.2
7											
8	2nd catalyst bed input **kg-mole** from Fig. 14.2			SO_3 =	0.0692	SO_2 =	0.0308	O_2 =	0.0754	N_2 =	0.79
9											
10											
11	Suggested 2nd catalyst bed equilibrium curve intercept % SO_2 oxidized, Φ^E =					94.0					
12											
13	2nd catalyst bed equilibrium curve temperature equivalent to cell F11's % SO_2 oxidized, from Eqn. (10.13)										
14	775.0	=-(-98.41)/(0.09357+0.008314*LN(F11/(100-F11)*((100-0.5*G3*F11/100)/(I3-0.5*G3*F11/100))^0.5*K6^-0.5))							(10.13)		
15											
16											
17											
18											
19	*2nd catalyst bed heatup path matrix. Eqns. 14.2 to 14.8 are from Sections 14.5 and 14.6. Eqn. 14.9" from Appendix K.*										
20	Equation	description	numerical term =E8 etc.	kg-mole SO_3 **in**	kg-mole SO_2 **in**	kg-mole O_2 **in**	kg-mole N_2 **in**	kg-mole SO_3 **out**	kg-mole SO_2 **out**	kg-mole O_2 **out**	kg-mole N_2 **out**
21	14.2	input SO_3 kg-mole	0.0692	1	0	0	0	0	0	0	0
22	14.3	input SO_2 kg-mole	0.0308	0	1	0	0	0	0	0	0
23	14.4	input O_2 kg-mole	0.0754	0	0	1	0	0	0	0	0
24	14.5	input N_2 kg-mole	0.7900	0	0	0	1	0	0	0	0
25	14.6	S balance	0	-1	-1	0	0	1	1	0	0
26	14.7	O balance	0	-3	-2	-2	0	3	2	2	0
27	14.8	N balance	0	0	0	0	-2	0	0	0	2
28	14.9"	enthalpy balance	0	370.6	278.2	-12.54	-11.97	-365.2	-274.3	15.04	14.31
29											
30			2nd catalyst bed input gas temperature =			700		intercept temperature, cell A14 =		775.0	
31						=K5				=A14	
32											
33	Matrix results equivalent to suggested intercept temperature in cell J30 (and A14)						=-(0.0311*F30-9.797)	(Appendix AHUP)			
34	kg-mole SO_3 **in**	0.0692									
35	kg-mole SO_2 **in**	0.0308									
36	kg-mole O_2 **in**	0.0754									
37	kg-mole N_2 **in**	0.7900									
38	kg-mole SO_3 **out**	0.0948	heatup path % SO_2 oxidized (Φ) equivalent to intercept temperature in cell J30 =								
39	kg-mole SO_2 **out**	0.0052	= (<u>1st catalyst bed feed gas kg-mole SO_2 - 2nd catalyst bed kg-mole SO_2 out)</u> * 100 =						94.8	= (G5-B39)/G5*100	(14.1)
40	kg-mole O_2 **out**	0.0626			1st catalyst bed feed gas kg-mole SO_2						
41	kg-mole N_2 **out**	0.7900									
42	all per kg-mole of 1st catalyst bed feed gas										
43											
44											
45											
46	Goal Seek calculation										
47	Equilibrium curve % SO_2 oxidized - heatup path % SO_2 oxidized =						-0.8	=F11-I39			

M.4 Goal Seek Instructions

Table M.1 is set up so that equilibrium curve temperature always = heatup path temperature. The only remaining question is at what temperature does:

heatup path *% SO_2 oxidized* = equilibrium curve *% SO_2 oxidized?*

This is determined by:

1. Putting 'equilibrium curve *% SO_2 oxidized* - heatup path *% SO_2 oxidized*' in cell G47, as shown in Table M.1.

2. Using Goal Seek to adjust:

   equilibrium curve *% SO_2 oxidized* (cell F11)

until cell G47 = zero, i.e. until:

heatup path *% SO_2 oxidized* = equilibrium curve *% SO_2 oxidized.*

The Goal Seek procedure is:

Tools
Goal Seek
Set Cell **G47**
To Value **0**
Changing Cell **F11**
OK
OK.

The results are shown in Table M.2. The intercept point is 94.2% SO_2 oxidized (in cells F11 and I39), 773.2 K (in cells A14 and J30) – as is readily checked with Table 15.1.

Table M.2. Table M.1 after Goal Seek has found the intercept. It is 773.2 K (cells A14 and J30), 94.2% *SO_2 oxidized* (cells F11 and I39). This result is the same as that obtained by interpolating Table 15.1's temperature-*% SO_2 oxidized* values.

	A	B	C	D	E	F	G	H	I	J	K
1	**2^{nd} CATALYST BED**							**All quantities are per kg-mole of 1^{st} catalyst bed feed gas**			
2											
3	1^{st} catalyst bed feed gas specifications from Fig. 14.2					e, volume% SO_2 =	10	f, volume% O_2 =	11		
4											
5	1^{st} catalyst bed feed **kg-mole** SO_2 (for Eqn. (14.1) = e/100 = G3/100				Eqn. (11.1)		0.1	2nd catalyst bed input gas temperature, K =			700
6								2nd catalyst bed pressure P_t, bar =			1.2
7											
8	2^{nd} catalyst bed input **kg-mole** from Fig. 14.2			SO_3 =	0.0692	SO_2 =	0.0308	O_2 =	0.0754	N_2 =	0.79
9											
10											
11	Suggested 2^{nd} catalyst bed equilibrium curve intercept % SO_2 oxidized, Φ^E =					94.2					
12											
13	2^{nd} catalyst bed equilibrium curve temperature equivalent to cell F11's % SO_2 oxidized, from Eqn. (10.13)										
14	773.2	=-(-98.41)/(0.09357+0.008314*LN(F11/(100-F11)*((100-0.5*G3*F11/100)/(I3-0.5*G3*F11/100))^0.5*K6^-0.5))							(10.13)		
15											
16											
17											
18											
19	*2^{nd} catalyst bed heatup path matrix. Eqns. 14.2 to 14.8 are from Sections 14.5 and 14.6. Eqn. 14.9" is from Appendix K.*										
20	Equation	description	numerical term =E8 etc.	kg-mole SO_3 **in**	kg-mole SO_2 **in**	kg-mole O_2 **in**	kg-mole N_2 **in**	kg-mole SO_3 **out**	kg-mole SO_2 **out**	kg-mole O_2 **out**	kg-mole N_2 **out**
21	14.2	input SO_3 kg-mole	0.0692	1	0	0	0	0	0	0	0
22	14.3	input SO_2 kg-mole	0.0308	0	1	0	0	0	0	0	0
23	14.4	input O_2 kg-mole	0.0754	0	0	1	0	0	0	0	0
24	14.5	input N_2 kg-mole	0.7900	0	0	0	1	0	0	0	0
25	14.6	S balance	0	-1	-1	0	0	1	1	0	0
26	14.7	O balance	0	-3	-2	-2	0	3	2	2	0
27	14.8	N balance	0	0	0	0	-2	0	0	0	2
28	14.9"	enthalpy balance	0	370.6	278.2	-12.54	-11.97	-365.4	-274.4	14.98	14.25
29											
30			2nd catalyst bed input gas temperature =			700		intercept temperature, cell A14 =		773.2	
31						=K5				=A14	
32											
33	Matrix results equivalent to suggested intercept temperature in cell J30 (and A14)						=-(0.0311*F30-9.797)	(Appendix AHUP)			
34	kg-mole SO_3 **in**	0.0692									
35	kg-mole SO_2 **in**	0.0308									
36	kg-mole O_2 **in**	0.0754									
37	kg-mole N_2 **in**	0.7900									
38	kg-mole SO_3 **out**	0.0942		heatup path% SO_2 oxidized (Φ) equivalent to intercept temperature in cell J30 =							
39	kg-mole SO_2 **out**	0.0058		= (<u>1^{st} catalyst bed feed gas kg-mole SO_2 - 2^{nd} catalyst bed kg-mole SO_2 out</u>) * 100 =					94.2	= (G5-B39)/G5*100	(14.1)
40	kg-mole O_2 **out**	0.0629			1^{st} catalyst bed feed gas kg-mole SO_2						
41	kg-mole N_2 **out**	0.7900									
42	all per kg-mole of 1st catalyst bed feed gas										
43											
44											
45											
46	Goal Seek calculation										
47	Equilibrium curve % SO_2 oxidized - heatup path % SO_2 oxidized =						0.0	=F11-I39			

Appendix N

3^{rd} Catalyst Bed Heatup Path Worksheet

Table N.1 is a 3^{rd} catalyst bed heatup path worksheet. It is a copy of worksheet Table K.1# with:

(a) Eqns. (16.1) to (16.4) in place of Eqns. (14.2) to (14.5), rows 8 to 11

(b) Chapter 16's 710 K 3^{rd} catalyst bed input gas temperature in cell F17

(c) a 715 K 3^{rd} bed heatup path temperature in cell J17

(d) 3^{rd} instead of 2^{nd} in all captions.

With these changes, the worksheet automatically gives the result that 715 K in the 3^{rd} catalyst bed is generated by a total of 95.9% SO_2 oxidation (including oxidation in the preceding 1^{st} and 2^{nd} beds), cell H25.

The table's matrix doesn't have to be re-solved for this or any other calculation. A few other heatup path points are:

	M	N
31	**Fig. 16.2 level L temperature, K**	**% SO_2 oxidized at level L**
32	710	94.20
33	712	94.89
34	714	95.57
35	716	96.25

#Steps for copying the worksheet are:
Edit
Move or Copy Sheet
To book: ***(new book)***
Create a copy ✓
OK.

Changes (a) – (d) are then made. Finally, the worksheet is saved in the Chapter 16 file with an appropriate name, e.g. Table N.1.

Table N.1. 3rd catalyst bed heatup path matrix with enthalpy equations in cells D15-K15. The numerical quantities in cells C8-C11 are Table M.2's 2nd catalyst bed intercept quantities.

	A	B	C	D	E	F	G	H	I	J	K
1	**All calculations are based on 1 kg-mole of 1st catalyst bed feed gas.**										
2	kg-mole SO_2 in 1 kg-mole of 1st catalyst bed feed gas			0.1							
3											
4											
5											
6	**3rd catalyst bed matrix**										
7	Equation	description	numerical term	kg-mole SO_3 **in**	kg-mole SO_2 **in**	kg-mole O_2 **in**	kg-mole N_2 **in**	kg-mole SO_3 **out**	kg-mole SO_2 **out**	kg-mole O_2 **out**	kg-mole N_2 **out**
8	16.1	input SO_3 kg-mole	0.0942	1	0	0	0	0	0	0	0
9	16.2	input SO_2 kg-mole	0.0058	0	1	0	0	0	0	0	0
10	16.3	input O_2 kg-mole	0.0629	0	0	1	0	0	0	0	0
11	16.4	input N_2 kg-mole	0.7900	0	0	0	1	0	0	0	0
12	14.6	S balance	0	-1	-1	0	0	1	1	0	0
13	14.7	O balance	0	-3	-2	-2	0	3	2	2	0
14	14.8	N balance	0	0	0	0	-2	0	0	0	2
15	14.9"	enthalpy balance	0	369.9	277.7	-12.87	-12.28	-369.5	-277.4	13.04	12.44
16											
17					Fig. 16.2 input gas temperature =	710			heatup path temperature =	715	
18											
19	Heatup path result per kg-mole of 1st catalyst bed feed gas					contains	=-(0.0311*F17-9.797)				
20	kg-mole SO_3 **in**	0.0942									
21	kg-mole SO_2 **in**	0.0058									
22	kg-mole O_2 **in**	0.0629		% SO_2 oxidized at cell J17		kg-mole SO_2 in 1st	kg-mole SO_2 at heatup path				
23	kg-mole N_2 **in**	0.7900		heatup path temper-		= catalyst bed feed gas - temperature in 3rd catalyst bed * 100				(14.1)	
24	kg-mole SO_3 **out**	0.0959		ature in 3rd catalyst bed		kg-mole SO_2 in 1st catalyst bed feed gas					
25	kg-mole SO_2 **out**	0.0041					=(D2-B25)/D2*100 =	95.9	% SO_2 oxidized		
26	kg-mole O_2 **out**	0.0620									
27	kg-mole N_2 **out**	0.7900									

Appendix O

3rd Catalyst Bed Intercept Worksheet

Table O.1 is a 3rd catalyst bed heatup path-equilibrium curve intercept worksheet. It is a copy of Table M.2[#] with:

(a) Fig. 16.2's 3rd catalyst bed input gas quantities in cells E8, G8, I8 and K8

(b) Eqns. (16.1) to (16.4) in place of Eqns. (14.2) to (14.5), rows 21 to 24

(c) Fig. 16.2's specified 710 K 3rd catalyst bed input gas temperature in cell K5 and its specified 1.2 bar 3rd bed pressure in cell K6

(d) 3rd instead of 2nd in all captions.

The worksheet is operated exactly like worksheet Table M.2. The result is shown in Table O.1. It indicates that the 3rd catalyst bed intercept point under Fig. 16.2's specified conditions is:

721.1 K, 98.0% *SO_2 oxidized* (after 3 beds).

[#] Copied as described in Appendix N.

Table O.1. 3rd catalyst bed intercept worksheet after Appendix M's Goal Seek instructions have been carried out. The intercept is shown to be 721.1 K, 98.0% *SO_2 oxidized* – which gives a zero value in cell G47.

	A	B	C	D	E	F	G	H	I	J	K
1	**3RD CATALYST BED**							**All quantities are per kg-mole of 1st catalyst bed feed gas**			
2											
3	1st catalyst bed feed gas composition from Fig. 11.2					e, volume% SO_2 =	10	f, volume% O_2 =	11		
4											
5	1st catalyst bed feed **kg-mole** SO_2 (for Eqn. (14.1) = e/100 = G3/100				(Eqn. (11.1)		0.1	3rd catalyst bed input gas temperature, K =			710
6										3rd catalyst bed pressure P_t, bar =	1.2
7											
8	3rd catalyst bed input **kg-mole** from Section 15.2.4			SO_3 =	0.0942	SO_2 =	0.0058	O_2 =	0.0629	N_2 =	0.79
9											
10											
11	Suggested 3rd catalyst bed equilibrium curve intercept % SO_2 oxidized, Φ^E =					98.0					
12											
13	3rd catalyst bed equilibrium curve temperature equivalent to cell F11's % SO_2 oxidized, Eqn. (10.13)										
14	721.1	=-(-98.41)/(0.09357+0.008314*LN(F11/(100-F11)*((100-0.5*G3*F11/100)/(I3-0.5*G3*F11/100))^0.5*K6^-0.5))							(10.13)		
15											
16											
17											
18											
19	*3rd catalyst bed heatup path matrix. Eqns. 14.6 to 14.8 are from Section 14.6. Eqn. 14.9" is from Appendix K. Eqns. 16.1 to 16.4 are from Section 16.2.*										
20	Equation	description	numerical term =E8 etc.	kg-mole SO_3 **in**	kg-mole SO_2 **in**	kg-mole O_2 **in**	kg-mole N_2 **in**	kg-mole SO_3 **out**	kg-mole SO_2 **out**	kg-mole O_2 **out**	kg-mole N_2 **out**
21	16.1	input SO_3 kg-mole	0.0942	1	0	0	0	0	0	0	0
22	16.2	input SO_2 kg-mole	0.0058	0	1	0	0	0	0	0	0
23	16.3	input O_2 kg-mole	0.0629	0	0	1	0	0	0	0	0
24	16.4	input N_2 kg-mole	0.7900	0	0	0	1	0	0	0	0
25	14.6	S balance	0	-1	-1	0	0	1	1	0	0
26	14.7	O balance	0	-3	-2	-2	0	3	2	2	0
27	14.8	N balance	0	0	0	0	-2	0	0	0	2
28	14.9"	enthalpy balance	0	369.9	277.7	-12.87	-12.28	-369.1	-277.1	13.24	12.63
29											
30			3rd catalyst bed input gas temperature =			710		intercept temperature, cell A14 =		721.1	
31						=K5				=A14	
32											
33	Matrix results equivalent to suggested intercept temperature in cell J30 (and A14)						=-(0.0311*F30-9.797)	(Appendix G)			
34	kg-mole SO_3 **in**	0.0942									
35	kg-mole SO_2 **in**	0.0058									
36	kg-mole O_2 **in**	0.0629									
37	kg-mole N_2 **in**	0.7900									
38	kg-mole SO_3 **out**	0.0980	heatup path % SO_2 oxidized (Φ) equivalent to 3rd catalyst bed intercept temperature in cell J30 =								
39	kg-mole SO_2 **out**	0.0020	= (1st catalyst bed feed gas kg-mole SO_2 - 3rd catalyst bed kg-mole SO_2 out) * 100 =						98.0	= (G5-B39)/G5*100	(14.1)
40	kg-mole O_2 **out**	0.0610		1st catalyst bed feed gas kg-mole SO_2							
41	kg-mole N_2 **out**	0.7900									
42	all per kg-mole of 1st catalyst bed feed gas										
43											
44											
45											
46	Goal Seek calculation										
47	Equilibrium curve % SO_2 oxidized - heatup path % SO_2 oxidized =						0.0	=F11-I39			

Appendix P

Effect of SO_3 in Fig. 10.1 Feed Gas on Equilibrium Equations

About 2% of (SO_2 + SO_3) in sulfur-burning furnace/waste heat boiler offgas is SO_3. Sulfur burning offgas isn't water quenched/cleaned so its SO_3 isn't absorbed. It enters the Fig. 10.1 catalyst bed.

This appendix describes how SO_3-in-feed-gas affects equilibrium Equations (10.12) and (10.13).

Including SO_3, Fig. 10.1's feed gas contains:

d	volume% SO_3
e	" " SO_2
f	" " O_2
100 - d - e - f	" " N_2.

Per kg-mole of Fig. 10.1 feed gas, the input molar quantities are:

$\frac{d}{100}$	kg-mole SO_3 (Section B.3.1)
$\frac{e}{100}$	" " SO_2
$\frac{f}{100}$	" " O_2
$1 - \frac{d}{100} - \frac{e}{100} - \frac{f}{100}$	" " N_2.

P.1 Molar balances

Sulfur

SO_3 in Fig. 10.1 feed gas changes Appendix B's sulfur balance:

$$\begin{matrix}\text{kg-mole S} \\ \text{in feed gas}\end{matrix} = \begin{matrix}\text{kg-mole S} \\ \text{in oxidized gas}\end{matrix} \tag{B.11}$$

to:

$$1*\frac{d}{100} + 1*\frac{e}{100} = 1*n_{SO_3} + 1*n_{SO_2}$$

or:

$$\frac{\mathbf{d}}{\mathbf{100}} + \frac{e}{100} = n_{SO_3} + n_{SO_2}$$

or:

$$n_{SO_2} = \frac{\mathbf{d}}{\mathbf{100}} + \frac{e}{100} - n_{SO_3} \qquad (P.1)$$

Oxygen

SO_3 in Fig. 10.1 feed gas changes its oxygen balance:

$$\begin{matrix}\text{kg-mole O}\\ \text{in feed gas}\end{matrix} = \begin{matrix}\text{kg-mole O}\\ \text{in oxidized gas}\end{matrix} \qquad (B.15).$$

to:

$$3*\frac{\mathbf{d}}{\mathbf{100}} + 2*\frac{e}{100} + 2*\frac{f}{100} = 3*n_{SO_3} + 2*n_{SO_2} + 2*n_{O_2}$$

or:

$$\frac{\mathbf{3}}{\mathbf{2}}*\left(\frac{\mathbf{d}}{\mathbf{100}}\right) + \frac{e}{100} + \frac{f}{100} = \frac{3}{2}*n_{SO_3} + n_{SO_2} + n_{O_2}$$

or:

$$n_{O_2} = \frac{3}{2}*\left(\frac{d}{100}\right) + \frac{e}{100} + \frac{f}{100} - \frac{3}{2}*n_{SO_3} - n_{SO_2}$$

Further, because $n_{SO_2} = \frac{d}{100} + \frac{e}{100} - n_{SO_3}$ (Eqn. [P.1])

$$n_{O_2} = \frac{3}{2}*\left(\frac{d}{100}\right) + \frac{e}{100} + \frac{f}{100} - \frac{3}{2}*n_{SO_3} - \left(\frac{d}{100} + \frac{e}{100} - n_{SO_3}\right)$$

or:

$$= \frac{f}{100} + \frac{\mathbf{1}}{\mathbf{2}}*\frac{\mathbf{d}}{\mathbf{100}} - \frac{1}{2}*n_{SO_3} \qquad (P.2)$$

Nitrogen

SO_3 in feed gas changes N balance Eqn.(B.22) slightly to:

$$2*\left(1 - \frac{d}{100} - \frac{e}{100} - \frac{f}{100}\right) = 2*n_{N_2}$$

or:

$$n_{N_2} = 1 - \frac{d}{100} - \frac{e}{100} - \frac{f}{100} \qquad (P.3).$$

P.2 Total kg-mole of oxidized gas

Total kg-mole of oxidized gas is still given by Eqn. (B.24), i.e.:

$$n_t = n_{SO_3} + n_{SO_2} + n_{O_2} + n_{N_2}$$

Combining this with Eqns. (P.1), (P.2) and (P.3) gives:

$$n_t = n_{SO_3} + \left(\frac{d}{100} + \frac{e}{100} - n_{SO_3}\right) + \left(\frac{f}{100} + \frac{1}{2}*\frac{d}{100} - \frac{1}{2}*n_{SO_3}\right) + \left(1 - \frac{d}{100} - \frac{e}{100} - \frac{f}{100}\right)$$

$$= 1 + \frac{1}{2}*\frac{d}{100} - \frac{1}{2}*n_{SO_3} \qquad (P.4).$$

P.3 Mole fractions in oxidized gas

With SO_3-in-feed gas, the mole fractions of SO_3, SO_2 and O_2 in Fig. 10.1 oxidized gas are:

$$X_{SO_3} = \frac{n_{SO_3}}{n_t} = \frac{n_{SO_3}}{\left(1 + \frac{1}{2}*\frac{d}{100} - \frac{1}{2}*n_{SO_3}\right)} \quad \text{from Eqn. (P.4)} \qquad (P.5)$$

$$X_{SO_2} = \frac{n_{SO_2}}{n_t} = \frac{\frac{d}{100} + \frac{e}{100} - n_{SO_3}}{\left(1 + \frac{1}{2}*\frac{d}{100} - \frac{1}{2}*n_{SO_3}\right)} \quad \text{from Eqns. (P.1) and (P.4)} \qquad (P.6)$$

$$X_{O_2} = \frac{n_{O_2}}{n_t} = \frac{\frac{f}{100} + \frac{1}{2}*\frac{d}{100} - \frac{1}{2}*n_{SO_3}}{\left(1 + \frac{1}{2}*\frac{d}{100} - \frac{1}{2}*n_{SO_3}\right)} \quad \text{from Eqns. (P.2) and (P.4)} \qquad (P.7).$$

P.4 New equilibrium equation

With the Eqns. (P.5) to (P.7) expressions for mole fraction, equilibrium Eqn. (B.4)

$$K_E = \frac{X^E_{SO_3}}{X^E_{SO_2} * \left(X^E_{O_2}\right)^{\frac{1}{2}}} * P_t^{-\frac{1}{2}} \qquad (B.4).$$

becomes:

$$K_E = \frac{\left(\dfrac{n_{SO_3}^E}{1 + \frac{1}{2}*\frac{d}{100} - \frac{1}{2}*n_{SO_3}^E}\right)}{\left(\dfrac{\frac{d}{100} + \frac{e}{100} - n_{SO_3}^E}{1 + \frac{1}{2}*\frac{d}{100} - \frac{1}{2}*n_{SO_3}^E}\right)*\left(\dfrac{\frac{f}{100} + \frac{1}{2}*\frac{d}{100} - \frac{1}{2}*n_{SO_3}^E}{1 + \frac{1}{2}*\frac{d}{100} - \frac{1}{2}*n_{SO_3}^E}\right)^{\frac{1}{2}}} * P_t^{-\frac{1}{2}} \qquad (P.8)$$

or, multiplying top and bottom by $1 + \frac{1}{2}*\frac{d}{100} - \frac{1}{2}*n_{SO_3}^E$

$$K_E = \frac{n_{SO_3}^E}{\left(\frac{d}{100} + \frac{e}{100} - n_{SO_3}^E\right)*\left(\dfrac{\frac{f}{100} + \frac{1}{2}*\frac{d}{100} - \frac{1}{2}*n_{SO_3}^E}{1 + \frac{1}{2}*\frac{d}{100} - \frac{1}{2}*n_{SO_3}^E}\right)^{\frac{1}{2}}} * P_t^{-\frac{1}{2}} \qquad (P.9)$$

or, multiplying top and bottom by: $\left(1 + \frac{1}{2}*\frac{d}{100} - \frac{1}{2}*n_{SO_3}^E\right)^{\frac{1}{2}}$

$$K_E = \frac{n_{SO_3}^E*\left(1 + \frac{1}{2}*\frac{d}{100} - \frac{1}{2}*n_{SO_3}^E\right)^{\frac{1}{2}}}{\left(\frac{d}{100} + \frac{e}{100} - n_{SO_3}^E\right)*\left(\frac{f}{100} + \frac{1}{2}*\frac{d}{100} - \frac{1}{2}*n_{SO_3}^E\right)^{\frac{1}{2}}} * P_t^{-\frac{1}{2}}$$

or:

$$K_E = \left(\frac{n_{SO_3}^E}{\frac{d}{100} + \frac{e}{100} - n_{SO_3}^E}\right)*\left(\frac{1 + \frac{1}{2}*\frac{d}{100} - \frac{1}{2}*n_{SO_3}^E}{\frac{f}{100} + \frac{1}{2}*\frac{d}{100} - \frac{1}{2}*n_{SO_3}^E}\right)^{\frac{1}{2}} * P_t^{-\frac{1}{2}} \qquad (P.10).$$

Eqn. (P.10) is written in terms of $n_{SO_3}^E$. The next few sections show how it is expressed in terms of *% SO_2 oxidized.*

P.5 *%SO₂ oxidized* in Equilibrium Equation

Equilibrium *% SO_2 oxidized* with SO_3 in feed gas is defined exactly as in Section B.8 and Chapter 10. The definition is:

$$\text{Equilibrium } \%SO_2 \text{ oxidized} = \Phi^E = \frac{\text{kg-mole } SO_2 \text{ in feed gas} - \text{kg-mole } SO_2 \text{ in oxidized gas where equilibrium has been attained}}{\text{kg-mole } SO_2 \text{ in feed gas}} * 100 \tag{10.2}$$

or:

$$\Phi^E = \left(\frac{\frac{e}{100} - n^E_{SO_2}}{\frac{e}{100}} \right) * 100 \tag{B.36}$$

Eqn. (B.36) is expressed in terms of $n^E_{SO_3}$ by combining it with the equilibrium form of Eqn. (P.1), i.e.:

$$n^E_{SO_2} = \frac{d}{100} + \frac{e}{100} - n^E_{SO_3}$$

to give:

$$\text{Equilibrium } \%SO_2 \text{ oxidized} = \Phi^E = \left(\frac{\frac{e}{100} - \left(\frac{d}{100} + \frac{e}{100} - n^E_{SO_3} \right)}{\frac{e}{100}} \right) * 100 \tag{P.11}$$

or:

$$\Phi^E = \left(\frac{n^E_{SO_3} - \frac{d}{100}}{\frac{e}{100}} \right) * 100 \tag{P.12}$$

or:

$$\left(\frac{e}{100} \right) * \frac{\Phi^E}{100} = n^E_{SO_3} - \frac{d}{100} \tag{P.13}$$

or:

$$n^E_{SO_3} = \frac{d}{100} + \left(\frac{e}{100} \right) * \frac{\Phi^E}{100} \tag{P.14}$$

Substituting the right side of Eqn. (P.14) for $n^E_{SO_3}$ in Eqn. (P.10) gives:

$$K_E =$$

$$\left(\frac{\frac{d}{100}+\left(\frac{e}{100}\right)*\frac{\Phi^E}{100}}{\frac{d}{100}+\frac{e}{100}-\left(\frac{d}{100}+\left(\frac{e}{100}\right)*\frac{\Phi^E}{100}\right)}\right)*\left(\frac{1+\frac{1}{2}*\frac{d}{100}-\frac{1}{2}*\left(\frac{d}{100}+\left(\frac{e}{100}\right)*\frac{\Phi^E}{100}\right)}{\frac{f}{100}+\frac{1}{2}*\frac{d}{100}-\frac{1}{2}*\left(\frac{d}{100}+\left(\frac{e}{100}\right)*\frac{\Phi^E}{100}\right)}\right)^{\frac{1}{2}}*P_t^{-\frac{1}{2}} \tag{P.15}$$

or, rearranging the bottom left term:

$$K_E = \left(\frac{\frac{d}{100}+\left(\frac{e}{100}\right)*\frac{\Phi^E}{100}}{\frac{e}{100}-\left(\frac{e}{100}\right)*\frac{\Phi^E}{100}}\right)*\left(\frac{1+\frac{1}{2}*\frac{d}{100}-\frac{1}{2}*\left(\frac{d}{100}+\left(\frac{e}{100}\right)*\frac{\Phi^E}{100}\right)}{\frac{f}{100}+\frac{1}{2}*\frac{d}{100}-\frac{1}{2}*\left(\frac{d}{100}+\left(\frac{e}{100}\right)*\frac{\Phi^E}{100}\right)}\right)^{\frac{1}{2}}*P_t^{-\frac{1}{2}} \tag{P.16}$$

or:

$$K_E = \left(\frac{\frac{d}{100}+\left(\frac{e}{100}\right)*\frac{\Phi^E}{100}}{\left(\frac{e}{100}\right)*\left(1-\frac{\Phi^E}{100}\right)}\right)*\left(\frac{1-\frac{1}{2}*\left(\frac{e}{100}\right)*\frac{\Phi^E}{100}}{\frac{f}{100}-\frac{1}{2}*\left(\frac{e}{100}\right)*\frac{\Phi^E}{100}}\right)^{\frac{1}{2}}*P_t^{-\frac{1}{2}} \tag{P.17}$$

and, multiplying top and bottom by 100:

$$K_E = \left(\frac{d+e*\frac{\Phi^E}{100}}{e*\left(1-\frac{\Phi^E}{100}\right)}\right)*\left(\frac{1-\frac{1}{2}*\left(\frac{e}{100}\right)*\frac{\Phi^E}{100}}{\frac{f}{100}-\frac{1}{2}*\left(\frac{e}{100}\right)*\frac{\Phi^E}{100}}\right)^{\frac{1}{2}}*P_t^{-\frac{1}{2}} \tag{P.18}$$

or, multiplying top and bottom by $100^{\frac{1}{2}}$

$$K_E = \left(\frac{d+e*\frac{\Phi^E}{100}}{e*\left(1-\frac{\Phi^E}{100}\right)}\right)*\left(\frac{100-\frac{1}{2}*e*\frac{\Phi^E}{100}}{f-\frac{1}{2}*e*\frac{\Phi^E}{100}}\right)^{\frac{1}{2}}*P_t^{-\frac{1}{2}} \tag{P.19}$$

Comparison of Eqn. (P.19) with Eqns. (B41) and (10.12) shows that the only difference between the two is the presence of *d* (volume% SO_3 in feed gas) in the top left term.

The meanings of the terms are also clear:

$e*\frac{\Phi^E}{100}$	represents the equilibrium amount of SO_2 oxidized to SO_3 in the catalyst bed
upper left term	represents equilibrium production of SO_3 in the catalyst bed + the amount of SO_3 in the original feed gas
lower left term	represents amount of SO_2 remaining after equilibrium oxidation of SO_2 to SO_3 in the catalyst bed
upper right term	represents the total amount of gas remaining after equilibrium oxidation of SO_2 to SO_3 because each mole of SO_2 oxidized consumes 0.5 mole of O_2
lower right term	represents the amount of O_2 remaining after equilibrium oxidation of SO_2 to SO_3 because each mole of SO_2 oxidized consumes 0.5 mole of O_2.

P.6 Equilibrium *% SO_2 Oxidized* as a Function of Temperature

The effect of temperature on equilibrium *% SO_2 oxidized* is determined by combining Eqns. (P.19) and (10.11), i.e.:

$$T_E = \frac{-B}{A + R*\ln(K_E)}$$

(as described in Section 10.3)

where:

T_E = equilibrium temperature

A and B = empirical constants for relating $\Delta_f G^\circ_{SO_2(g)+\frac{1}{2}O_2(g)\rightarrow SO_3(g)}$ to temperature,

Section 10.3 and Appendix C:

$A = 0.09357$ MJ kg-mole SO_2^{-1} K^{-1}

$B = -98.41$ MJ/kg-mole SO_2.

The result is:

$$T_E = \frac{-B}{A + R*\ln\left(\left(\frac{d + e*\frac{\Phi^E}{100}}{e*\left(1 - \frac{\Phi^E}{100}\right)}\right) * \left(\frac{100 - \frac{1}{2}*e*\frac{\Phi^E}{100}}{f - \frac{1}{2}*e*\frac{\Phi^E}{100}}\right)^{\frac{1}{2}} * P_t^{-\frac{1}{2}}\right)} \quad (17.1).$$

Appendix Q

SO_3-in-Feed-Gas Intercept Worksheet

Table Q.1 is a 1st catalyst bed worksheet for calculating heatup path-equilibrium curve intercepts with SO_3-in-feed-gas. The worksheet is similar to those in Appendices M and O.

Preparation instructions

1. Enter the data, equations and matrix as shown. This might be done by (i) copying Table O.1 and (ii) making appropriate changes to the copy. Copying instructions are given in Appendix N.
2. Suggest an equilibrium curve *% SO_2 oxidized* value in cell F11, say 65%.
3. Enter equilibrium curve Eqn. (17.1) into cell A14 as shown, not Eqn. (10.13).
4. Solve the matrix as described in Appendix M. Once solved, the matrix doesn't need re-solving.

Operating instructions

1. Find the intercept by means of Section M.4's Goal Seek instructions.

Result

The result is as shown in the worksheet – the intercept is 890.3 K, 69.7*% SO_2 oxidized*.

Other calculations

Catalyst bed pressure, feed gas composition and feed gas input temperature can now be changed at will. Only the Goal Seek procedure needs to be repeated to find the new intercept.

Comment

SO_3, SO_2, O_2 and N_2 input quantities are represented in Table Q.1's matrix by Eqns. (17.2), (17.3), (11.2) and (11.3). A more general representation is:

kg-mole SO_3 **in** = E8   kg-mole SO_2 **in** = G8   kg-mole O_2 **in** = I8   kg-mole N_2 **in** = K8
where E8 etc. are cell designations

This causes any change in feed gas composition (Cells E2, G2, I2, K2) to be reflected in the matrix. It allows new intercepts to be calculated at will (using only Goal Seek).

Table Q.1. 1st catalyst bed intercept calculation worksheet with SO_3 in feed gas. The use of Eqn. (17.1) in cell A14 is notable. Cells D28 to G28 contain -*H°* values. Cells H28 to K28 contain H° values.

	A	B	C	D	E	F	G	H	I	J	K
1	**1ST CATALYST BED**							**All quantities are per kg-mole of 1st catalyst bed feed gas**			
2											
3	1st bed feed gas specification, Section 17.1.2			d, volume% SO_3 =	0.2	e, volume% SO_2 =	9.8	f, volume% O_2 =	11	volume% N_2 =	79
4											
5	1st catalyst bed feed **kg-mole** SO_2 (for Eqn. (14.1) = e/100 = G3/100				(Eqn. 17.2)		0.098	1st catalyst bed input gas temperature, K =			690
6								1st catalyst bed pressure P_1, bar =			1.2
7	1st catalyst bed input **kg-mole** from above feed gas specification, Eqn. (17.2) etc.										
8				SO_3 =	0.002	SO_2 =	0.098	O_2 =	0.11	N_2 =	0.79
9					=d/100=E3/100		=e/100=G3/100		=f/100=I3/100		=K3/100
10											
11	Suggested equilibrium curve intercept % SO_2 oxidized, Φ^E =					69.7					
12											
13	Equilibrium curve temperature equivalent to cell F11's % SO_2 oxidized, from Eqn. (17.1)										
14	890.3	=-(-98.41)/(0.09357+0.008314*LN((E3+G3*F11/100)/(G3*(1-F11/100))*((100-0.5*G3*F11/100)/(I3-0.5*G3*F11/100))^0.5*K6^-0.5))								(17.1)	
15											
16											
17											
18											
19	*1st catalyst bed heatup path matrix (**In** means 'in input gas', **out** means 'in intercept gas').*										
20	Equation	description	numerical term =E8 etc.	kg-mole SO_3 **In**	kg-mole SO_2 **In**	kg-mole O_2 **In**	kg-mole N_2 **In**	kg-mole SO_3 **out**	kg-mole SO_2 **out**	kg-mole O_2 **out**	kg-mole N_2 **out**
21	17.2	input SO_3 kg-mole	0.0020	1	0	0	0	0	0	0	0
22	17.3	input SO_2 kg-mole	0.0980	0	1	0	0	0	0	0	0
23	11.2	input O_2 kg-mole	0.1100	0	0	1	0	0	0	0	0
24	11.3	input N_2 kg-mole	0.7900	0	0	0	1	0	0	0	0
25	14.6	S balance	0	-1	-1	0	0	1	1	0	0
26	14.7	O balance	0	-3	-2	-2	0	3	2	2	0
27	11.6	N balance	0	0	0	0	-2	0	0	0	2
28		enthalpy balance	0	371.3	278.7	-12.21	-11.66	-357.0	-268.4	18.88	17.89
29											
30					feed gas temperature =	690		intercept temperature, cell A14 =		890.3	
31						=K5				=A14	
32											
33	Matrix results equivalent to suggested intercept temperature in cell J30 (and A14)						=-(0.0311*F30-9.797)				
34	kg-mole SO_3 **In**	0.0020									
35	kg-mole SO_2 **In**	0.0980									
36	kg-mole O_2 **In**	0.1100									
37	kg-mole N_2 **In**	0.7900									
38	kg-mole SO_3 **out**	0.0703			heatup path % SO_2 oxidized (Φ) equivalent to intercept temperature in cells J30 and A14 =						
39	kg-mole SO_2 **out**	0.0297			= (kg-mole SO_2 **In** - kg-mole SO_2 **out**)/kg-mole SO_2 **In***100 =				69.7	=(G5-B39)/G5*100	(14.1)
40	kg-mole O_2 **out**	0.0759									
41	kg-mole N_2 **out**	0.7900									
42	all per kg-mole of 1st catalyst bed feed gas										
43											
44											
45											
46	Goal Seek calculation										
47	Equilibrium curve % SO_2 oxidized - heatup path % SO_2 oxidized =						0.0	=F11-I39			

Appendix R

CO_2- and SO_3-in-Feed-Gas Intercept Worksheet

Table R.1 is a worksheet for calculating 1st catalyst bed heatup path-equilibrium curve intercepts with CO_2 and SO_3 in feed gas. It is similar to that in Appendix Q.

This is the final form of our 1st catalyst bed worksheets. It can be used for all of the book's 1st catalyst bed calculations.

Preparation instructions

1. Enter the data, equations and matrix as shown. This might be done by (i) copying Table Q.1 and by (ii) making appropriate changes to the copy. CO_2 enlarges the matrix so that it has to be re-solved (once) as described in Appendix H.
2. Suggest an equilibrium curve *% SO_2 oxidized* value in cell F11, say 65%.
3. Enter Eqn. (17.1) into cell A14, as shown.
4. Solve the matrix as described in Appendix H.

The worksheet is now ready to operate.

Operating instructions

1. Find the intercept using Section M.4's Goal Seek instructions.

Result

As shown, the intercept with 10% CO_2 in feed gas is:

887.2 K, 71.0% *SO_2 oxidized.*

Other Calculations

The worksheet is readily used for other specified bed pressures and input gas compositions and temperatures. Once the new data are entered, only Goal Seek is required.

Table R.1. 1st catalyst bed intercept calculations with <u>SO$_3$ and CO$_2$</u> in feed gas. Note the 2 new CO$_2$ columns, new input CO$_2$ and C balance rows and 2 new CO$_2$ result rows. The use of Eqn (17.1) in cell A14 is notable. Cells D28-H28 contain –H° values. Cells I28-M28 contain H° values.

	A	B	C	D	E	F	G	H	I	J	K	L	M
1	**1ST CATALYST BED**							**All quantities are per kg-mole of 1st catalyst bed feed gas**					
2													
3	1st bed feed gas specification, Section 17.3			d,vol% SO$_3$ =	0	e,vol% SO$_2$ =	10	f,vol% O$_2$ =	11	vol% N$_2$ =	69	vol% CO$_2$=	10
4													
5	1st catalyst bed feed **kg-mole** SO$_2$ (for Eqn. (14.1) = e/100 = G3/100				(Eqn. 11.1)		0.1		feed gas temperature, K =		690		
6									bed gas pressure, bar =		1.2		
7	1st catalyst bed feed gas **kg-mole** from feed gas specification, Eqn. (11.1) etc.												
8				SO$_3$ =	0	SO$_2$ =	0.1	O$_2$ =	0.11	N$_2$ =	0.69	CO$_2$ =	0.1
9					= d/100 =E3/100		= e/100 =G3/100		= f/100 =I3/100		=K3/100		=M3/100
10													
11	Suggested equilibrium curve intercept % SO$_2$ oxidized, Φ^E =					71.0							
12													
13	Equilibrium curve temperature equivalent to cell F11's % SO$_2$ oxidized, from Eqn. (17.1)												
14	887.2	=-(-98.41)/(0.09357+0.008314*LN((E3+G3*F11/100)/(G3*(1-F11/100))*((100-0.5*G3*F11/100)/(I3-0.5*G3*F11/100))^0.5*K6^-0.5))											(17.1)
15													
16													
17	*1st catalyst bed heatup path matrix (**in** means 'in input gas', **out** means 'in intercept gas')*												
18	Equation	Description	numerical term	kg-mole SO$_3$ **in**	kg-mole SO$_2$ **in**	kg-mole O$_2$ **in**	kg-mole N$_2$ **in**	kg-mole CO$_2$ **in**	kg-mole SO$_3$ **out**	kg-mole SO$_2$ **out**	kg-mole O$_2$ **out**	kg-mole N$_2$ **out**	kg-mole CO$_2$ **out**
19		input SO$_3$ kg-mole	0	1	0	0	0	0	0	0	0	0	0
20	11.1	input SO$_2$ kg-mole	0.1000	0	1	0	0	0	0	0	0	0	0
21	11.2	input O$_2$ kg-mole	0.1100	0	0	1	0	0	0	0	0	0	0
22	17.8	input N$_2$ kg-mole	0.6900	0	0	0	1	0	0	0	0	0	0
23	17.4	input CO$_2$ kg-mole	0.1000	0	0	0	0	1	0	0	0	0	0
24	14.6	S balance	0	-1	-1	0	0	0	1	1	0	0	0
25	17.6	O balance	0	-3	-2	-2	0	-2	3	2	2	0	2
26	11.6	N balance	0	0	0	0	-2	0	0	0	0	2	0
27	17.5	C balance	0	0	0	0	0	-1	0	0	0	0	1
28	17.7	enthalpy balance	0	371.3	278.7	-12.21	-11.66	376.2	-357.2	-268.5	18.78	17.80	-366.3
29													
30				feed gas temperature =		690		intercept temperature, cell A14 =		887.2			
31						=K5				=A14			
32	Matrix results equivalent to intercept temperature in cell J30 (and A14)												
33	kg-mole SO$_3$ **in**	0.0000				=-(0.0311*F30-9.797)							
34	kg-mole SO$_2$ **in**	0.1000											
35	kg-mole O$_2$ **in**	0.1100											
36	kg-mole N$_2$ **in**	0.6900											
37	kg-mole CO$_2$ **in**	0.1000											
38	kg-mole SO$_3$ **out**	0.0710		heatup path % SO$_2$ oxidized (Φ) equivalent to intercept temperature in cell J30 and A14 =									
39	kg-mole SO$_2$ **out**	0.0290		= (kg-mole SO$_2$ **in** - kg-mole SO$_2$ **out**)/kg-mole SO$_2$ **in***100 =					71.0	= (G5-B39)/G5*100		(14.1)	
40	kg-mole O$_2$ **out**	0.0745											
41	kg-mole N$_2$ **out**	0.6900											
42	kg-mole CO$_2$ **out**	0.1000											
43	all per kg-mole of 1st catalyst bed feed gas												
44													
45													
46	Goal Seek calculation												
47	Equilibrium curve % SO$_2$ oxidized - heatup path % SO$_2$ oxidized =						0.0	=F11-I39					

Appendix S

3-Catalyst-Bed 'Converter' Calculations[#]

All calculations in this appendix are per kg-mole of 1st catalyst bed feed gas. They are based on the specifications in Table 18.1 This appendix shows how 3-catalyst-bed 'converter' calculations are done. Three areas in the same Excel worksheet are used, Tables S.1, S.2 and S.3. The 3 beds are linked by kg-mole SO_3, SO_2, O_2, N_2 and CO_2 passing between beds 1 and 2 and beds 2 and 3.

Each area is arranged so that the same cells in all three areas have the same meaning. For example, cells K6, AK6 and BK6 all contain catalyst bed pressure.

The objectives of the 3-bed calculations are to determine, for any set of Table 18.1 specifications:

(a) the percentage of feed SO_2 that is oxidized to SO_3 after the feed gas has passed through 3 catalyst beds

(b) kg-mole of SO_3, SO_2, O_2, N_2 and CO_2 departing the 3rd catalyst bed. These kg-mole values are used for Chapter 19's double contact acid plant calculations.

S.1 1st Catalyst Bed Calculations (Cells A1 through M47)

The objectives of the 1st catalyst bed worksheet area are to calculate:

(a) 1st bed heatup path-equilibrium curve intercept temperature and *% SO_2 oxidized*

(b) kg-mole of SO_3, SO_2, O_2, N_2 and CO_2 in the 1st bed intercept gas, per kg-mole of feed gas. These kg-mole pass between the 1st and 2nd catalyst beds.

Setup and Operation

The 1st catalyst bed worksheet area is set up exactly like Table R.1. It may be copied from that table as described in Appendix N. Only the feed gas composition specification is different, Table 18.1. The intercept is found by Section M.4's Goal Seek procedure (Appendix M). The results are 893.3 K, 69.2 *% SO_2 oxidized* and:

0.0692 kg-mole SO_3	0.0308 kg-mole SO_2	0.0754 kg-mole O_2	0.79 kg-mole N_2	0 kg-mole CO_2

in the intercept gas (as confirmed by Section 12.2).

These intercept quantities are automatically copied into the 2nd catalyst bed worksheet area as described in the next section.

[#] A 4th catalyst bed worksheet is added at the end of this appendix. It is used to prepare Fig. 19.7.

	A	B	C	D	E	F	G	H	I	J	K	L	M
1	**TABLE S.1, 1ST CATALYST BED**							**All quantities are per kg-mole of 1st catalyst bed feed gas**					
2													
3	1st bed feed gas specification, Table 18.1			d,vol% SO_3 =	0	e,vol% SO_2 =	10	f,vol% O_2 =	11	vol% N_2 =	79	vol% CO_2=	0
4													
5	1st catalyst bed feed **kg-mole** SO_2 (for Eqn. (14.1) = e/100 = G3/100				(Eqn. 11.1)		0.1		feed gas temperature, K =		690		
6								catalyst bed gas pressure, bar =			1.2		
7	1st catalyst bed feed gas **kg-mole** from feed gas specification, Eqn. (11.1) etc.												
8				SO_3 =	0	SO_2 =	0.1	O_2 =	0.11	N_2 =	0.79	CO_2 =	0
9					= d/100 =E3/100		= e/100 =G3/100		= f/100 =I3/100		=K3/100		=M3/100
10													
11	Suggested equilibrium curve intercept % SO_2 oxidized, Φ^E =					69.2							
12													
13	Equilibrium curve temperature equivalent to cell F11's % SO_2 oxidized, Eqn. (17.1)												
14	893.3	=-(-98.41)/(0.09357+0.008314*LN((E3+G3*F11/100)/(G3*(1-F11/100))*((100-0.5*G3*F11/100)/(I3-0.5*G3*F11/100))^0.5*K6^-0.5))											(17.1)
15													
16													
17	*1st catalyst bed heatup path matrix (**in** means 'in input gas', **out** means 'in intercept gas')*												
18	Equation	description	number = E8 etc.	kg-mole SO_3 **in**	kg-mole SO_2 **in**	kg-mole O_2 **in**	kg-mole N_2 **in**	kg-mole CO_2 **in**	kg-mole SO_3 **out**	kg-mole SO_2 **out**	kg-mole O_2 **out**	kg-mole N_2 **out**	kg-mole CO_2 **out**
19		input SO_3 kg-mole	0	1	0	0	0	0	0	0	0	0	0
20	11.1	input SO_2 kg-mole	0.1000	0	1	0	0	0	0	0	0	0	0
21	11.2	input O_2 kg-mole	0.1100	0	0	1	0	0	0	0	0	0	0
22	11.3	input N_2 kg-mole	0.7900	0	0	0	1	0	0	0	0	0	0
23		input CO_2 kg-mole	0.0000	0	0	0	0	1	0	0	0	0	0
24	14.6	S balance	0	-1	-1	0	0	0	1	1	0	0	0
25	17.6	O balance	0	-3	-2	-2	0	-2	3	2	2	0	2
26	11.6	N balance	0	0	0	0	-2	0	0	0	0	2	0
27	17.5	C balance	0	0	0	0	0	-1	0	0	0	0	1
28	17.7	enthalpy balance	0	371.3	278.7	-12.21	-11.66	376.2	-356.8	-268.2	18.99	17.99	-366.0
29													
30				feed gas temperature =		690	intercept temperature, cell A14 =			893.3			
31						=K5				=A14			
32	Matrix results equivalent to intercept temperature in cell J30 (and A14)												
33	kg-mole SO_3 **in**	0.0000				=-(0.0311*F30-9.797)							
34	kg-mole SO_2 **in**	0.1000											
35	kg-mole O_2 **in**	0.1100											
36	kg-mole N_2 **in**	0.7900											
37	kg-mole CO_2 **in**	0.0000											
38	kg-mole SO_3 **out**	0.0692											
39	kg-mole SO_2 **out**	0.0308			Heatup path % SO_2 oxidized (Φ) equivalent to intercept temperature in cells J30 and A14			=	69.2	= (G5-B39)/G5*100		(14.1)	
40	kg-mole O_2 **out**	0.0754								=% SO_2 oxidized after 1st catalyst bed			
41	kg-mole N_2 **out**	0.7900											
42	kg-mole CO_2 **out**	0.0000											
43	all per kg-mole of 1st catalyst bed feed gas												
44													
45													
46	Goal Seek calculation												
47	Equilibrium curve % SO_2 oxidized - heatup path % SO_2 oxidized =						0.0	=F11-I39					

S.2 2nd Catalyst Bed Calculations (Cells AA1 through AM47)

The objectives of the 2nd catalyst bed worksheet area are to:

(a) automatically copy 1st catalyst bed exit (intercept) gas quantities into the 2nd catalyst bed worksheet area

and to determine 2nd catalyst bed:

(b) heatup path-equilibrium curve intercept temperature and *% SO_2 oxidized*

(c) kg-mole SO_3, SO_2, O_2, N_2 and CO_2 in intercept gas

with 1st catalyst bed exit gas as 2nd catalyst bed feed gas.

Setup and Operation

The 2nd catalyst bed worksheet area is set up much like the 1st (with a different input gas temperature, Table 18.1). The distinctive difference is that the input quantities in row 8 are 1st catalyst bed exit (intercept) gas quantities from Table S.1 cells B38 through B42. The latter are automatically copied into the 2nd catalyst bed area by the instructions:

=B38 in cell AE8
=B39 in cell AG8
=B40 in cell AI8
=B41 in cell AK8
=B42 in cell AM8.

The 2nd bed intercept is then found by Section M.4's Goal Seek procedure. The intercept results are 773.1 K, 94.2*% SO_2 oxidized* and:

0.0942 kg-mole SO_3
0.0058 kg-mole SO_2
0.0629 kg-mole O_2
0.7900 kg-mole N_2
0.0000 kg-mole CO_2

in 2nd catalyst bed intercept gas (as confirmed by Section 15.2.2).

These gas quantities are automatically copied into the 3rd catalyst bed area as described in the next section.

	AA	AB	AC	AD	AE	AF	AG	AH	AI	AJ	AK	AL	AM
1	**TABLE S.2, 2ND CATALYST BED**							**All quantities are per kg-mole of 1st catalyst bed feed gas**					
2													
3	1st bed feed gas specification, Table 18.1			d,vol% SO_3 =	0	e,vol% SO_2 =	10	f,vol% O_2 =	11				
4													
5	1st catalyst bed feed **kg-mole** SO_2 (for Eqn. (14.1) = e/100 = AG3/100					(Eqn. 11.1)	0.1			input gas temperature, K =	700		
6										catalyst bed gas pressure, bar =	1.2		
7	2nd catalyst bed feed gas **kg-mole** from cell B38-B42 1st catalyst bed intercept data												
8				SO_3 =	0.0692	SO_2 =	0.0308	O_2 =	0.0754	N_2 =	0.7900	CO_2 =	0.0000
9					=B38		=B39		=B40		=B41		=B42
10													
11	Suggested equilibrium curve intercept % SO_2 oxidized, Φ^E =					94.2							
12													
13	2nd catalyst bed equilibrium curve temperature equivalent to cell AF11's % SO_2 oxidized, Eqn. (17.1)												
14	773.1	=-(-98.41)/(0.09357+0.008314*LN((AE3+AG3*AF11/100)/(AG3*(1-AF11/100))*((100-0.5*AG3*AF11/100)/(AI3-0.5*AG3*AF11/100))^0.5*AK6^-0.5))											(17.1)
15													
16													
17	*2nd catalyst bed heatup path matrix (**In** means 'in input gas', **out** means 'in intercept gas')*												
18	Equation	description	number = AE8 etc.	kg-mole SO_3 **in**	kg-mole SO_2 **in**	kg-mole O_2 **in**	kg-mole N_2 **in**	kg-mole CO_2 **in**	kg-mole SO_3 **out**	kg-mole SO_2 **out**	kg-mole O_2 **out**	kg-mole N_2 **out**	kg-mole CO_2 **out**
19	14.2	input SO_3 kg-mole	0.0692	1	0	0	0	0	0	0	0	0	0
20	14.3	input SO_2 kg-mole	0.0308	0	1	0	0	0	0	0	0	0	0
21	14.4	input O_2 kg-mole	0.0754	0	0	1	0	0	0	0	0	0	0
22	14.5	input N_2 kg-mole	0.7900	0	0	0	1	0	0	0	0	0	0
23		input CO_2 kg-mole	0.0000	0	0	0	0	1	0	0	0	0	0
24	14.6	S balance	0	-1	-1	0	0	0	1	1	0	0	0
25	17.6	O balance	0	-3	-2	-2	0	-2	3	2	2	0	2
26	11.6	N balance	0	0	0	0	-2	0	0	0	0	2	0
27	17.5	C balance	0	0	0	0	0	-1	0	0	0	0	1
28	17.7	enthalpy balance	0	370.6	278.2	-12.54	-11.97	375.7	-365.4	-274.4	14.98	14.25	-372.0
29													
30					input gas temperature =	700			intercept temperature, cell AA14 =	773.1			
31						=AK5				=AA14			
32	Matrix results equivalent to intercept temperature in cell AJ30 (and AA14)												
33	kg-mole SO_3 **in**	0.0692				=-(0.0311*AF30-9.797)							
34	kg-mole SO_2 **in**	0.0308											
35	kg-mole O_2 **in**	0.0754											
36	kg-mole N_2 **in**	0.7900											
37	kg-mole CO_2 **in**	0.0000											
38	kg-mole SO_3 **out**	0.0942											
39	kg-mole SO_2 **out**	0.0058			Heatup path % SO_2 oxidized (Φ) equivalent to			=	94.2	= (AG5-AB39)/AG5*100		(14.1)	
40	kg-mole O_2 **out**	0.0629			intercept temperature in cells AJ30 and AA14					= total % SO_2 oxidized after 1stand 2nd catalyst beds			
41	kg-mole N_2 **out**	0.7900											
42	kg-mole CO_2 **out**	0.0000											
43	all per kg-mole of 1st catalyst bed feed gas												
44													
45													
46	Goal Seek calculation												
47	Equilibrium curve % SO_2 oxidized - heatup path % SO_2 oxidized =						0.0	=AF11-AI39					

S.3 3rd Catalyst Bed Calculations (cells BA1 through BM47)

The objectives of the 3rd catalyst bed area are to:

(a) automatically copy 2nd catalyst bed exit (intercept) gas quantities into the 3rd catalyst bed worksheet area

and to determine 3rd catalyst bed:

(b) heatup path-equilibrium curve intercept temperature and *% SO_2 oxidized*

(c) kg-mole of SO_3, SO_2, O_2, N_2 and CO_2 in intercept gas (for Chapter 19's calculations)

with 2nd catalyst bed exit gas as 3rd catalyst bed input gas.

Setup and Operation

The 3rd catalyst bed worksheet area is set up like the 2nd (with a different input gas temperature, Table 18.1). The row 8 quantities are automatically copied from the 2nd bed area by the instructions:

=AB38	in cell BE8
=AB39	in cell BG8
=AB40	in cell BI8
=AB41	in cell BK8
=AB42	in cell BM8.

The 3rd catalyst bed intercept is found by means of Section M.4's Goal Seek procedure. The results are 721.0 K, 98.0*% SO_2 oxidized* and:

0.098 kg-mole SO_3
0.002 kg-mole SO_2
0.061 kg-mole O_2
0.79 kg-mole N_2
0 kg-mole CO_2

in 3rd catalyst bed intercept gas (as confirmed by Section 16.3). This gas now goes to cooling and H_2SO_4-making, Chapter 19.

	BA	BB	BC	BD	BE	BF	BG	BH	BI	BJ	BK	BL	BM
1	**TABLE S.3, 3RD CATALYST BED**							**All quantities are per kg-mole of 1st catalyst bed feed gas**					
2													
3	1st bed feed gas specification, Table 18.1			d,vol% SO_3 =	0	e,vol% SO_2 =	10	f,vol% O_2 =	11				
4													
5	1st catalyst bed feed **kg-mole** SO_2 (for Eqn. (14.1) = e/100 = BG3/100					(Eqn. 11.1)	0.1			input gas temperature, K =	710		
6										catalyst bed gas pressure, bar =	1.2		
7	3rd catalyst bed feed gas **kg-mole** from cell AB38-AB42 2nd catalyst bed intercept data												
8				SO_3 =	0.0942	SO_2 =	0.0058	O_2 =	0.0629	N_2 =	0.7900	CO_2 =	0.0000
9					=AB38		=AB39		=AB40		=AB41		=AB42
10													
11	Suggested equilibrium curve intercept % SO_2 oxidized, Φ^E =					98.0							
12													
13	3rd catalyst bed equilibrium curve temperature equivalent to cell BF11's % SO_2 oxidized, Eqn. (17.1)												
14	721.0	=-(-98.41)/(0.09357+0.008314*LN((BE3+BG3*BF11/100)/(BG3*(1-BF11/100))*((100-0.5*BG3*BF11/100)/(BI3-0.5*BG3*BF11/100))^0.5*BK6^-0.5))											(17.1)
15													
16													
17	*3rd catalyst bed heatup path matrix (**in** means 'in input gas', **out** means 'in intercept gas')*												
18	Equation	description	number = BE8 etc.	kg-mole SO_3 **in**	kg-mole SO_2 **in**	kg-mole O_2 **in**	kg-mole N_2 **in**	kg-mole CO_2 **in**	kg-mole SO_3 **out**	kg-mole SO_2 **out**	kg-mole O_2 **out**	kg-mole N_2 **out**	kg-mole CO_2 **out**
19	16.1	input SO_3 kg-mole	0.0942	1	0	0	0	0	0	0	0	0	0
20	16.2	input SO_2 kg-mole	0.0058	0	1	0	0	0	0	0	0	0	0
21	16.3	input O_2 kg-mole	0.0629	0	0	1	0	0	0	0	0	0	0
22	16.4	input N_2 kg-mole	0.7900	0	0	0	1	0	0	0	0	0	0
23		input CO_2 kg-mole	0.0000	0	0	0	0	1	0	0	0	0	0
24	14.6	S balance	0	-1	-1	0	0	0	1	1	0	0	0
25	17.6	O balance	0	-3	-2	-2	0	-2	3	2	2	0	2
26	11.6	N balance	0	0	0	0	-2	0	0	0	0	2	0
27	17.5	C balance	0	0	0	0	0	-1	0	0	0	0	1
28	17.7	enthalpy balance	0	369.9	277.7	-12.87	-12.28	375.2	-369.1	-277.1	13.24	12.63	-374.6
29													
30					input gas temperature =	710			intercept temperature, cell BA14 =	721.0			
31						=BK5				=BA14			
32	Matrix results equivalent to intercept temperature in cell BJ30 (and BA14)												
33	kg-mole SO_3 **in**	0.0942				=-(0.0311*BF30-9.797)							
34	kg-mole SO_2 **in**	0.0058											
35	kg-mole O_2 **in**	0.0629											
36	kg-mole N_2 **in**	0.7900											
37	kg-mole CO_2 **in**	0.0000											
38	kg-mole SO_3 **out**	0.0980											
39	kg-mole SO_2 **out**	0.0020			Heatup path % SO_2 oxidized (Φ) equivalent to			=	98.0	= (BG5-BB39)/BG5*100		(14.1)	
40	kg-mole O_2 **out**	0.0610			intercept temperature in cells BJ30 and BA14					= total % SO_2 oxidized after 1st, 2nd and 3rd catalyst beds			
41	kg-mole N_2 **out**	0.7900											
42	kg-mole CO_2 **out**	0.0000											
43	all per kg-mole of 1st catalyst bed feed gas												
44													
45													
46	Goal Seek calculation												
47	Equilibrium curve % SO_2 oxidized - heatup path % SO_2 oxidized =						0.0	=BF11-BI39					

	CA	CB	CC	CD	CE	CF	CG	CH	CI	CJ	CK	CL	CM
1	**TABLE S.4, 4TH CATALYST BED**							**All quantities are per kg-mole of 1st catalyst bed feed gas**					
2													
3	1st bed feed gas specification, Table 18.1			d, vol% SO_3 =	0	e,vol% SO_2 =	10	f, vol% O_2 =	11				
4													
5	1st catalyst bed feed **kg-mole** SO_2 = e/100 = CG3/100			(Eqn. 11.1)			0.1		input gas temperature, K =		690		
6										catalyst bed gas pressure, bar =	1.2		
7	4th catalyst bed feed gas **kg-mole** from cell BB38-BB42 2nd catalyst bed intercept data												
8				SO_3 =	0.0980	SO_2 =	0.0020	O_2 =	0.0610	N_2 =	0.7900	CO_2 =	0.0000
9					=BB38		=BB39		=BB40		=BB41		=BB42
10													
11	Suggested equilibrium curve intercept % SO_2 oxidized, Φ^E =					98.9							
12													
13	4th catalyst bed equilibrium curve temperature equivalent to cell CF11's % SO_2 oxidized, Eqn. (17.1)												
14	692.8	=-(-98.41)/(0.09357+0.008314*LN((CE3+CG3*CF11/100)/(CG3*(1-CF11/100))*((100-0.5*CG3*CF11/100)/(CI3-0.5*CG3*CF11/100))^0.5*CK6^-0.5))											(17.1)
15													
16													
17	*4th catalyst bed heatup path matrix (**in** means 'in input gas', **out** means 'in intercept gas')*												
18	Equation	description	number = CE8 etc.	kg-mole SO_3 **in**	kg-mole SO_2 **in**	kg-mole O_2 **in**	kg-mole N_2 **in**	kg-mole CO_2 **in**	kg-mole SO_3 **out**	kg-mole SO_2 **out**	kg-mole O_2 **out**	kg-mole N_2 **out**	kg-mole CO_2 **out**
19		input SO_3 kg-mole	0.0980	1	0	0	0	0	0	0	0	0	0
20		input SO_2 kg-mole	0.0020	0	1	0	0	0	0	0	0	0	0
21		input O_2 kg-mole	0.0610	0	0	1	0	0	0	0	0	0	0
22		input N_2 kg-mole	0.7900	0	0	0	1	0	0	0	0	0	0
23		input CO_2 kg-mole	0.0000	0	0	0	0	1	0	0	0	0	0
24	14.6	S balance	0	-1	-1	0	0	0	1	1	0	0	0
25	17.6	O balance	0	-3	-2	-2	0	-2	3	2	2	0	2
26	11.6	N balance	0	0	0	0	-2	0	0	0	0	2	0
27	17.5	C balance	0	0	0	0	0	-1	0	0	0	0	1
28	17.7	enthalpy balance	0	371.3	278.7	-12.21	-11.66	376.2	-371.1	-278.5	12.30	11.75	-376.1
29													
30					input gas temperature =	690			intercept temperature, cell CA14 =	692.8			
31						=CK5				=CA14			
32	Matrix results equivalent to intercept temperature in cell CJ30 (and CA14)												
33	kg-mole SO_3 **in**	0.0980				=-(0.0311*CF30-9.797)							
34	kg-mole SO_2 **in**	0.0020											
35	kg-mole O_2 **in**	0.0610											
36	kg-mole N_2 **in**	0.7900											
37	kg-mole CO_2 **in**	0.0000											
38	kg-mole SO_3 **out**	0.0989											
39	kg-mole SO_2 **out**	0.0011			Heatup path % SO_2 oxidized (Φ) equivalent to intercept temperature in cells CJ30 and CA14			=	98.9	= (CG5-CB39)/CG5*100		(10.2)	
40	kg-mole O_2 **out**	0.0605								= total % SO_2 oxidized after 1st, 2nd, 3rd & 4th catalyst beds			
41	kg-mole N_2 **out**	0.7900											
42	kg-mole CO_2 **out**	0.0000											
43	all per kg-mole of 1st catalyst bed feed gas												
44													
45													
46	Goal Seek calculation												
47	Equilibrium curve % SO_2 oxidized - heatup path % SO_2 oxidized =						0.0	=CF11-CI39					

Appendix T

Worksheet for Calculating After-Intermediate-H_2SO_4-Making Heatup Path Equilibrium Curve Intercepts

A worksheet for calculating after-intermediate-H_2SO_4-making heatup path-equilibrium curve intercepts is shown on the following page. It uses Fig. 19.2's after-intermediate-H_2SO_4-making catalyst bed input gas composition, quantities and temperature (P_t = 1.2 bar). It calculates the percentage of after H_2SO_4 making catalyst bed input SO_2 that is oxidized to SO_3 when the intercept is attained, Eqn. 19.3. Operating instructions are given in Appendix J.

	A	B	C	D	E	F	G	H	I	J	K
1	**1ST AFTER-H_2SO_4-MAKING CATALYST BED**						**All quantities are per kg-mole of 1st before-H_2SO_4-making catalyst bed feed gas**				
2											
3	1st after-H_2SO_4-making catalyst bed input gas composition, Section 19.4.1					e', volume% SO_2 =	0.234	f', volume% O_2 =	7.15		
4											
5	1st after-H_2SO_4-making catalyst bed input **kg-mole** SO_2, Section 19.3						0.002		feed gas temperature, K =		690
6									gas pressure in bed P_t, bar =		1.2
7											
8	1st after-H_2SO_4-making catalyst bed input **kg-mole**, Section 19.3					SO_2 =	0.002	O_2 =	0.061	N_2 =	0.79
9											
10											
11	Suggested after-H_2SO_4-making equilibrium curve intercept % SO_2 oxidized, $\Phi^{E_{after}}$ =					98.9					
12											
13	Equilibrium curve temperature equivalent to cell F11's suggested % SO_2 oxidized, Eqn. (19.1)										
14	697.3	=-(-98.41)/(0.09357+0.008314*LN(F11/(100-F11)*((100-0.5*G3*F11/100)/(I3-0.5*G3*F11/100))^0.5*K6^-0.5))						(19.1)			
15											
16											
17											
18											
19											
20	*Heatup path matrix (**In** means 'in feed gas', **out** means 'in intercept gas')*										
21	Equation	description	numerical term =G8 etc.	kg-mole SO_2 **in**	kg-mole O_2 **in**	kg-mole N_2 **in**	kg-mole SO_3 **out**	kg-mole SO_2 **out**	kg-mole O_2 **out**	kg-mole N_2 **out**	
22	19.4	feed SO_2 kg-mole	0.0020	1	0	0	0	0	0	0	
23	19.5	feed O_2 kg-mole	0.0610	0	1	0	0	0	0	0	
24	19.6	feed N_2 kg-mole	0.7900	0	0	1	0	0	0	0	
25	11.4	S balance	0	-1	0	0	1	1	0	0	
26	11.5	O balance	0	-2	-2	0	3	2	2	0	
27	11.6	N balance	0	0	0	-2	0	0	0	2	
28		enthalpy balance	0	278.7	-12.21	-11.66	-370.8	-278.3	12.45	11.89	
29											
30					input gas temperature =	690		intercept temperature from cell A14 =		697.3	
31						=K5				=A14	
32											
33							=0.07144*J30-420.6				
34	Matrix results equivalent to suggested intercept temperature in cell J30 (and A14)										
35	kg-mole SO_2 **in**	0.0020									
36	kg-mole O_2 **in**	0.0610									
37	kg-mole N_2 **in**	0.7900									
38	kg-mole SO_3 **out**	0.001978	heatup path % SO_2 oxidized (Φ^{after}) equivalent to intercept temperature in cell J30 and A14 =								
39	kg-mole SO_2 **out**	0.000022	= (kg-mole SO_2 in 1st after-H_2SO_4-making catalyst bed input gas - kg-mole SO_2 **out**)*100 =						98.9	=(G5-B39)/G5*100	(19.2)
40	kg-mole O_2 **out**	0.060011	kg-mole SO_2 in 1st after-H_2SO_4-making catalyst bed input gas							= % of 1st after-H_2SO_4-making	
41	kg-mole N_2 **out**	0.790000								catalyst input SO_2 that is	
42	all per kg-mole of 1st before-H_2SO_4-making feed gas									oxidized in this catalyst bed	
43											
44											
45											
46	Goal Seek calculation										
47	Equilibrium curve % SO_2 oxidized - heatup path % SO_2 oxidized =						0.0	=F11-I39			

Appendix U

After-H_2SO_4-Making SO_2 Oxidation with SO_3 and CO_2 in Input Gas

All quantities in this appendix are per kg-mole of 1st before-H_2SO_4-making catalyst bed feed gas.

Chapter 19's SO_2 oxidation calculations assume that 100% of the SO_3 entering H_2SO_4 making reacts to form $H_2SO_4(\ell)$. This appendix's calculations remove that restriction. They also consider CO_2 in feed gas.

The objectives of the calculations are to determine a 1st after-H_2SO_4-making catalyst bed's:

(a) intercept temperature and *% SO_2 oxidized*, Φ^{Eafter}
(b) intercept SO_3, SO_2, O_2, N_2 and CO_2 quantities

with SO_3 and CO_2 in after-H_2SO_4-making input gas.

Total *% SO_2 oxidized* after:

3 before-H_2SO_4-making catalyst beds
1 after-H_2SO_4-making catalyst bed

is also calculated, Section U.6.

U.1 Equilibrium equation with SO_3 in after-H_2SO_4-making input gas

The after-H_2SO_4-making $SO_2(g) + \frac{1}{2}O_2(g) \rightarrow SO_3(g)$ equilibrium equation is:

$$T_E = \frac{-B}{A + R*\ln\left(\left(\dfrac{d' + e' * \dfrac{\Phi^{\text{Eafter}}}{100}}{e' * \left(1 - \dfrac{\Phi^{\text{Eafter}}}{100}\right)}\right) * \left(\dfrac{100 - \dfrac{1}{2}*e' * \dfrac{\Phi^{\text{Eafter}}}{100}}{f' - \dfrac{1}{2}*e' * \dfrac{\Phi^{\text{Eafter}}}{100}}\right)^{\frac{1}{2}} * P_t^{-\frac{1}{2}}\right)} \qquad \text{(U.1)}$$

where:

T_E = equilibrium temperature, K

A and B = empirical constants for calculating $\Delta G^\circ_{SO_2(g) + \frac{1}{2}O_2(g) \rightarrow SO_3(g)}$ from temperature, Eqn. (10.9) and Appendix C

$A = 0.09357$ MJ kg-mole $SO_2^{-1}K^{-1}$
$B = -98.41$ MJ/kg-mole SO_2

R = gas constant, 0.008314 MJ/kg-mole SO_2.

d' = volume% SO_3 in 1st after H_2SO_4-making catalyst bed feed gas
e' = volume% SO_2 " " " " "
f' = volume% O_2 " " " " "

$\left.\right\}$ remainder CO_2 and N_2

$\Phi^{E\text{after}}$ = equilibrium *% SO_2 oxidized*, Section 19.4.2
P_t = total gas pressure, bar

It is exactly analogous to Eqn. (17.1) and is derived the same way.

U.2 H_2SO_4-Making Input Gas Quantity Specification

H_2SO_4-making input gas is specified to be the same as in Fig. 19.2, i.e.:

0.098 kg-mole SO_3
0.002 kg-mole SO_2
0.061 kg-mole O_2
0.790 kg-mole N_2
0.000 kg-mole CO_2

U.3 H_2SO_4-Making Exit Gas Quantity Calculation

Chapter 19 assumes that 100% of H_2SO_4-making input SO_3 is made into $H_2SO_4(\ell)$. This appendix assumes that 99.9% of the SO_3 is made into $H_2SO_4(\ell)$, i.e. that 0.1% remains in H_2SO_4-making exit gas. The exit gas contains, therefore:

$$\frac{0.1\%}{100\%} * 0.098 \text{ kg-mole } SO_3 \text{ into } H_2SO_4 \text{ making} = 0.0001 \text{ kg-mole } SO_3$$

plus:
0.002 " " SO_2
0.061 " " O_2
0.790 " " N_2
0.000 " " CO_2
0.8531 total kg-mole.

This gas is goes forward to further SO_2 oxidation in a 1st after-H_2SO_4-making catalyst bed.

U.4 Calculation of H_2SO_4-Making Exit Gas Volume Percents

The composition of the H_2SO_4-making exit gas is calculated as described in Section 19.4.1, e.g.:

$$\text{volume\% } SO_3 = \text{mole\% } SO_3 = \frac{\text{kg-mole } SO_3}{\text{total kg-mole gas}} * 100\%$$

$$= \frac{0.0001}{0.8531} * 100 = 0.012 \text{ volume\% } SO_3 = d'$$

Volume% SO_2 and O_2 are calculated similarly to be:

0.234 " " SO_2 = e'
7.15 " " O_2 = f'.

The above after-H_2SO_4-making kg-mole and volume % values are the starting points for this appendix's after-H_2SO_4-making intercept calculations. The calculations are described in the next two sections.

U.5 Worksheet Construction and Operation

Table U.1 shows an after-H_2SO_4-making intercept calculation worksheet. It is much like Table R.1. It includes SO_3 and CO_2 in catalyst bed input gas. Preparation and use instructions are:

1. In Excel, make a copy of Table R.1 by:

   Edit
   Move or Copy Sheet
   Create a copy ✓
   To book: (*new book*)
   OK.
2. Enter Section U4's 1st after-H_2SO_4-making catalyst bed input volume% SO_3, SO_2 and O_2 into cells E3, G3 and I3 (empty cells J3 through M3)
3. Enter Section U.3's 1st after-H_2SO_4-making catalyst bed input kg-mole SO_3, SO_2, O_2, N_2 and CO_2 into cells E8, G8, I8, K8 & M8.
4. Re-enter Section U.3's 1st after-H_2SO_4-making catalyst bed input kg-mole SO_2 into cell G5 (for possible 2nd after-H_2SO_4-making catalyst bed calculations).
5. Enter gas input temperature and bed pressure in cells K5 and K6. Label all cells as shown.
6. Estimate an intercept *% SO_2 oxidized* (Φ^{Eafter}) value in cell F11 (perhaps 99% from Table 19.2).
7. Enter Eqn. U.1 into cell A14, exactly as shown in cell B14.
8. Use Goal Seek to find the actual intercept *% SO_2 oxidized* (Φ^{Eafter}) – by the instructions:

Tools
Goal Seek
Set cell: G47
To value: 0
Changing cell: F11
OK
OK.

The results are shown in worksheet Table U.1. The intercept point is 98.8 *% SO_2 oxidized* (Φ^{Eafter} in cells F11 and I39), 697.3 K (in cells A14 and J30).

Table U.1. Excel worksheet for calculating after-H_2SO_4-making heatup path/equilibrium curve intercept with SO_3 and CO_2 in input gas.[S]

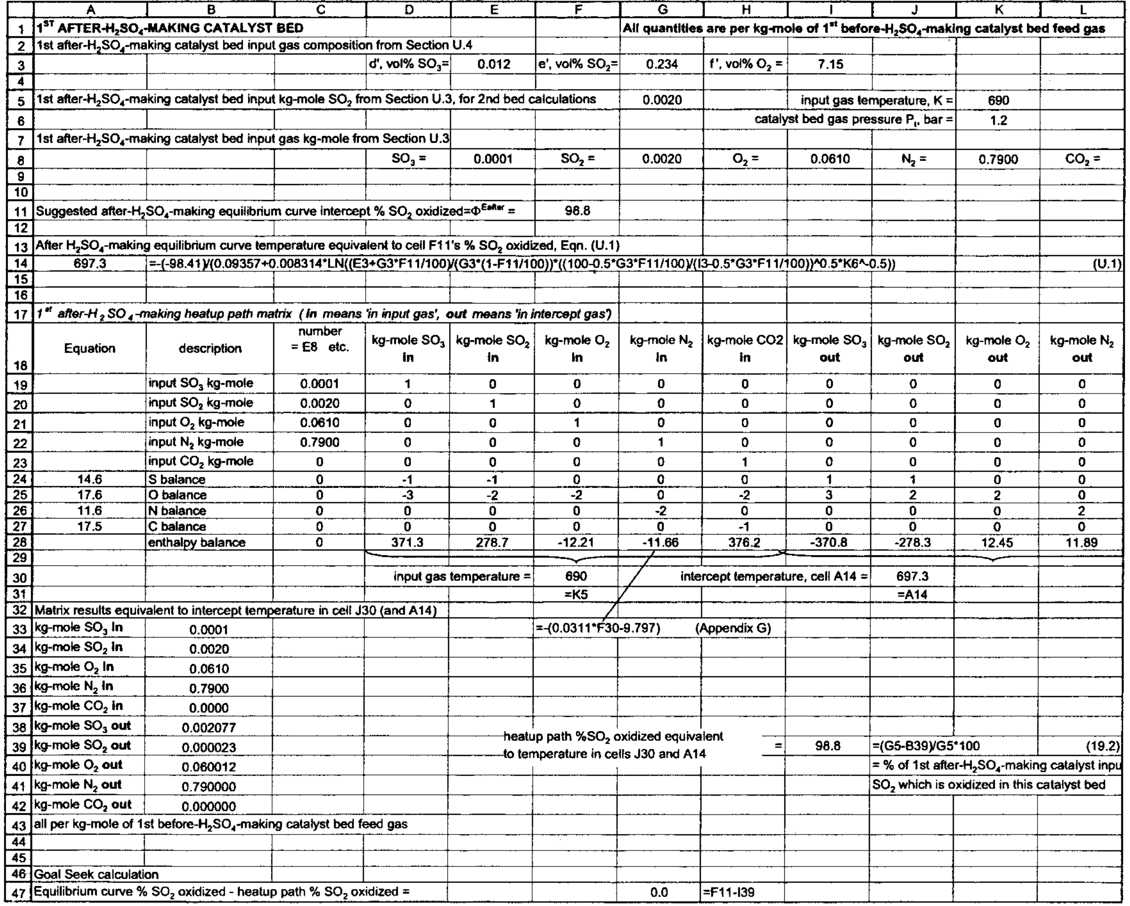

	A	B	C	D	E	F	G	H	I	J	K	L
1	**1ST AFTER-H_2SO_4-MAKING CATALYST BED**						**All quantities are per kg-mole of 1st before-H_2SO_4-making catalyst bed feed gas**					
2	1st after-H_2SO_4-making catalyst bed input gas composition from Section U.4											
3				d', vol% SO_3=	0.012	e', vol% SO_2=	0.234	f', vol% O_2 =	7.15			
4												
5	1st after-H_2SO_4-making catalyst bed input kg-mole SO_2 from Section U.3, for 2nd bed calculations						0.0020			input gas temperature, K =	690	
6										catalyst bed gas pressure P_t, bar =	1.2	
7	1st after-H_2SO_4-making catalyst bed input gas kg-mole from Section U.3											
8				SO_3 =	0.0001	SO_2 =	0.0020	O_2 =	0.0610	N_2 =	0.7900	CO_2 =
9												
10												
11	Suggested after-H_2SO_4-making equilibrium curve intercept % SO_2 oxidized=$\Phi^{E after}$ =					98.8						
12												
13	After H_2SO_4-making equilibrium curve temperature equivalent to cell F11's % SO_2 oxidized, Eqn. (U.1)											
14	697.3	=-(-98.41)/(0.09357+0.008314*LN((E3+G3*F11/100)/(G3*(1-F11/100))*((100-0.5*G3*F11/100)/(I3-0.5*G3*F11/100))^0.5*K6^-0.5))										(U.1)
15												
16												
17	*1st after-H_2SO_4-making heatup path matrix (**in** means 'in input gas', **out** means 'in intercept gas')*											
18	Equation	description	number = E8 etc.	kg-mole SO_3 **in**	kg-mole SO_2 **in**	kg-mole O_2 **in**	kg-mole N_2 **in**	kg-mole CO2 **in**	kg-mole SO_3 **out**	kg-mole SO_2 **out**	kg-mole O_2 **out**	kg-mole N_2 **out**
19		input SO_3 kg-mole	0.0001	1	0	0	0	0	0	0	0	0
20		input SO_2 kg-mole	0.0020	0	1	0	0	0	0	0	0	0
21		input O_2 kg-mole	0.0610	0	0	1	0	0	0	0	0	0
22		input N_2 kg-mole	0.7900	0	0	0	1	0	0	0	0	0
23		input CO_2 kg-mole	0	0	0	0	0	1	0	0	0	0
24	14.6	S balance	0	-1	-1	0	0	0	1	1	0	0
25	17.6	O balance	0	-3	-2	-2	0	-2	3	2	2	0
26	11.6	N balance	0	0	0	0	-2	0	0	0	0	2
27	17.5	C balance	0	0	0	0	0	-1	0	0	0	0
28		enthalpy balance	0	371.3	278.7	-12.21	-11.66	376.2	-370.8	-278.3	12.45	11.89
29												
30					input gas temperature =	690			intercept temperature, cell A14 =	697.3		
31						=K5				=A14		
32	Matrix results equivalent to intercept temperature in cell J30 (and A14)											
33	kg-mole SO_3 **in**	0.0001				=-(0.0311*F30-9.797)		(Appendix G)				
34	kg-mole SO_2 **in**	0.0020										
35	kg-mole O_2 **in**	0.0610										
36	kg-mole N_2 **in**	0.7900										
37	kg-mole CO_2 **in**	0.0000										
38	kg-mole SO_3 **out**	0.002077										
39	kg-mole SO_2 **out**	0.000023			heatup path %SO_2 oxidized equivalent to temperature in cells J30 and A14			=	98.8	=(G5-B39)/G5*100		(19.2)
40	kg-mole O_2 **out**	0.060012								= % of 1st after-H_2SO_4-making catalyst inpu		
41	kg-mole N_2 **out**	0.790000								SO_2 which is oxidized in this catalyst bed		
42	kg-mole CO_2 **out**	0.000000										
43	all per kg-mole of 1st before-H_2SO_4-making catalyst bed feed gas											
44												
45												
46	Goal Seek calculation											
47	Equilibrium curve % SO_2 oxidized - heatup path % SO_2 oxidized =						0.0	=F11-I39				

U.6 Calculation of *% SO_2 Oxidized* After All Catalyst Beds

Section 19.7 describes calculation of after-all-catalyst-bed SO_2 oxidation efficiency. The equation is:

$$\%SO_2\ oxidized = \Phi^{\text{total}} = \frac{\begin{matrix}\text{kg-mole SO}_2\text{ in 1}^{\text{st}} \\ \text{catalyst bed feed gas}\end{matrix} - \begin{matrix}\text{kg-mole SO}_2\text{ in last} \\ \text{catalyst bed exit gas}\end{matrix}}{\text{kg-mole SO}_2\text{ in 1}^{\text{st}}\text{ catalyst bed feed gas}} * 100 \qquad (19.7).$$

This appendix repeats this calculation. Its data are:

from Fig. 19.2: **kg-mole SO_2 in 1st catalyst bed feed gas = 0.1**

from Table U.1: **kg-mole SO_2 in after-H_2SO_4-making catalyst bed exit gas = 0.000023**

so that:

total % SO_2 oxidized after 3 before-H_2SO_4-making beds and 1 after-H_2SO_4-making catalyst bed $= \dfrac{(0.1\ -\ 0.000023)}{0.1} * 100\% = 99.98\%.$

This result is virtually the same as with no SO_3 in 1st after-H_2SO_4-making input gas, Section 19.7.

Appendix V

Moist Air in H_2SO_4 Making Calculations

Chapter 23 examines the input of moist metallurgical and spent acid regeneration gases into Fig. 23.1's dehydration tower. It quantifies the amount of $H_2O(g)$ that enters dehydration tower acid:

per kg-mole of dry 1st catalyst bed feed gas.

This appendix examines $H_2O(g)$ in sulfur burning acid plants. It:

(a) shows that sulfur burning plants dehydrate sulfur burning air rather than cleaned furnace offgas

(b) quantifies the amount of $H_2O(g)$ that enters dehydration tower acid

per kg-mole of dry air

and:

per kg-mole of dry 1st catalyst bed feed gas.

Fig. V.1 depicts the feed end of a sulfur burning sulfuric acid plant.

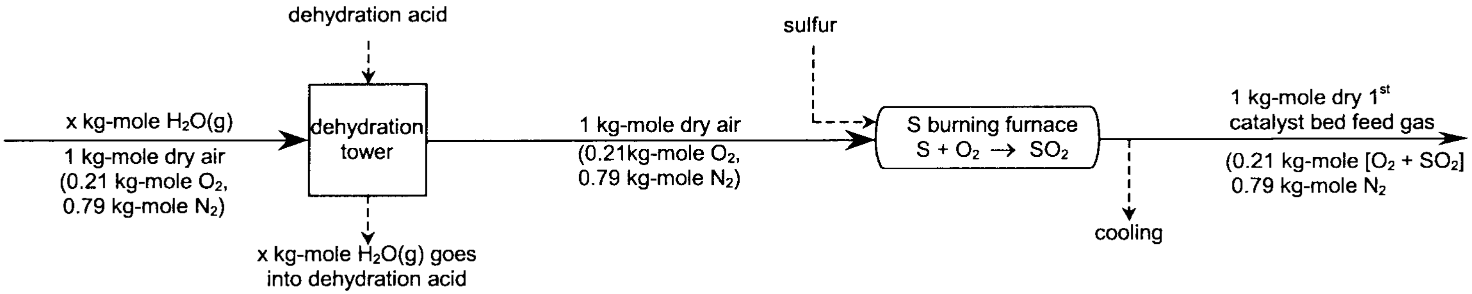

Fig. V.1. Front end of sulfur burning acid plant showing that *kg-mole dry 1st catalyst bed feed gas = kg-mole dry sulfur combustion air.*

It shows that:

(a) kg-mole sulfur burning exit gas (i.e. kg-mole dry 1st catalyst bed feed gas) = kg-mole dry input sulfur combustion air

and therefore that:

(b) kg-mole $H_2O(g)$ entering dehydration tower acid

per kg-mole of dry 1st catalyst bed feed gas

has the same numerical value as kg-mole $H_2O(g)$ entering dehydration tower acid

per kg-mole of dry sulfur combustion air.

This greatly simplifies our sulfur burning $H_2O(g)$ calculations, next section.

V.1 Calculation

This section duplicates Section 23.4.1's calculation of kg-mole $H_2O(g)$ into dehydration tower acid per kg-mole of dry 1st catalyst bed feed gas.

The moist air being fed to the Fig. V.1 sulfur burning dehydration tower is specified to contain:

3 volume% $H_2O(g)$ and 97 volume% dry air.

These are equivalent to 3 and 97 mole% $H_2O(g)$ and dry air respectively.

From Eqns. (23.2) to (23.4):

$$\begin{array}{l}\text{kg-mole } H_2O\text{ (g)}\\ \text{in moist input air}\end{array} = \frac{\begin{array}{c}3\text{ mole\% } H_2O\text{ (g)}\\ \text{in moist input air}\end{array}}{100\%} * \begin{array}{l}\text{kg-mole moist}\\ \text{input air}\end{array} \qquad (V.1)$$

$$\begin{array}{l}\text{kg-mole dry air}\\ \text{in moist input air}\end{array} = \frac{\begin{array}{c}97\text{ mole\% dry air}\\ \text{in moist input air}\end{array}}{100\%} * \begin{array}{l}\text{kg-mole moist}\\ \text{input air}\end{array} \qquad (V.2).$$

Dividing Eqn. (V.1) by Eqn. (V.2):

$$\frac{\text{kg-mole } H_2O\text{(g) in moist input air}}{\text{kg-mole dry air in moist input air}} = \frac{3}{97}$$

$$= 0.031 \text{ kg-mole } H_2O\text{(g) per kg-mole of dry air.}$$

Further, because:

$$\text{kg-mole dry 1}^{\text{st}}\text{ catalyst bed feed gas} = \text{kg-mole dry air}$$

$$\begin{array}{l}\text{kg-mole } H_2O\text{ (g) per kg-mole}\\ \text{of dry 1}^{\text{st}}\text{ catalyst bed feed gas}\end{array} = \begin{array}{l}\text{kg-mole } H_2O\text{ (g) per}\\ \text{kg-mole of dry air}\end{array} = 0.031$$

This value can be used in the remainder of Chapter 23's calculations, starting with Section 23.4.2.

It will be slightly wrong if the sulfur burning exit gas contains a small amount of SO_3.

Appendix W

Calculation of H_2SO_4 Making Tower Mass Flows

The Fig. 24.1 H_2SO_4 making tower's mass flows are calculated by specifying:

input mass $SO_3(g)$ per kg-mole of 1st catalyst bed feed gas
input acid composition, mass% H_2SO_4 and mass% H_2O
output acid composition, mass% H_2SO_4 and mass% H_2O.

These specification plus total and sulfur mass balances permit calculation of the tower's

(a) input SO_3, H_2SO_4 and H_2O flows

(b) H_2SO_4 and H_2O output flows.

W.1 Input and Output Gas Specifications

Fig. 24.1's H_2SO_4 making tower input gas is specified to be Section 16.4's 3rd catalyst bed exit gas. It contains:

0.098	kg-mole	SO_3
0.002	"	SO_2
0.061	"	O_2
0.790	"	N_2

per kg-mole of 10 volume% SO_2, 11 volume% O_2, 79 volume% N_2 1st catalyst bed feed gas.

It is specified that all of the SO_3 in this gas reacts with H_2O (ℓ) in the tower's input acid to form H_2SO_4 (ℓ). The other gases pass unreacted out of the tower.

With this specification, the tower's output gas contains:

0.000	kg-mole	SO_3
0.002	"	SO_2
0.061	"	O_2
0.790	"	N_2

per kg-mole of 1st catalyst bed feed gas, Table 24.1.

W.2 Input $SO_3(g)$ Equation

The mass of input $SO_3(g)$ equivalent to the above 0.098 kg-mole is given by the equation:

$$\text{mass } SO_3 = \text{kg-mole } SO_3 * 80 \text{ kg } SO_3 \text{ per kg-mole } SO_3$$

$$= 0.098 * 80$$

$$= 7.84 \text{ kg per kg-mole of } 1^{st} \text{ catalyst bed feed gas.} \qquad (W.1).$$

(80 is the molecular weight of SO_3.)

W.3 Input and Output Acid Composition Equations

Fig. 24.1's input acid is specified to contain 98.5 mass% H_2SO_4, 1.5 mass% H_2O. As Section 23.6.3 shows, this composition is described by the equation:

$$0 = -1.5 * \text{mass } H_2SO_4 \text{ in input acid} + 98.5 * \text{mass } H_2O \text{ in input acid} \qquad (W.2).$$

The output acid is specified to contain 99.0 mass% H_2SO_4 and 1.0 mass% H_2O. It is described by:

$$0 = -1.0 * \text{mass } H_2SO_4 \text{ in input acid} + 99.0 * \text{mass } H_2O \text{ in input acid} \qquad (W.3).$$

W.4 Total Mass Balance Equation

Excluding SO_2, O_2 and N_2 (which pass unreacted through the tower), Fig. 24.1's total mass balance is:

$$\text{mass } SO_3 \text{ in} + \text{mass } H_2SO_4 \text{ in input acid} + \text{mass } H_2O \text{ in input acid}$$

$$= \text{mass } H_2SO_4 \text{ in output acid} + \text{mass } H_2O \text{ in output acid}$$

or:

$$0 = - \text{mass } SO_3 \text{ in} - \text{mass } H_2SO_4 \text{ in input acid} - \text{mass } H_2O \text{ in input acid}$$

$$+ \text{mass } H_2SO_4 \text{ in output acid} + \text{mass } H_2O \text{ in output acid} \qquad (W.4).$$

W.5 Sulfur Balance Equation

Excluding SO_2 (which passes unreacted through the H_2SO_4 making tower), Fig. 24.1's S mass balance is:

$$\text{mass S in input } SO_3 + \text{mass S in input } H_2SO_4 = \text{mass S in output } H_2SO_4$$

or, because SO_3 and H_2SO_4 contain 40 and 32.7 mass% S respectively:

$$\frac{40}{100}\text{*mass input SO}_3 + \frac{32.7}{100}\text{*mass input H}_2\text{SO}_4 = \frac{32.7}{100}\text{*mass output H}_2\text{SO}_4$$

or

$$0 = -0.4 * \text{mass input SO}_3 - 0.327 * \text{mass input H}_2\text{SO}_4 + 0.327 * \text{mass output H}_2\text{SO}_4 \quad (W.5).$$

W.6 Solving for Flows

The Fig. 24.1 H_2SO_4 making tower has five flows:

mass SO_3 (g) in
mass H_2SO_4 (ℓ) in
mass H_2O (ℓ) in
mass H_2SO_4 (ℓ) out
mass H_2O (ℓ) out.

They are described by five equations, (W.1) to (W.5).

The numerical values of the above five flows are obtained by solving matrix Table W.1, as described in Appendix H.

The results are listed in Tables W.1 and 24.1.

Table W.1. Matrix for determining Fig. 24.1 mass flows using Eqns. (W.1) to (W.5).

	A	B	C	D	E	F	G	H
1	Description	equation	numerical term	mass SO_3 in	mass H_2SO_4 in	mass H_2O in	mass H_2SO_4 out	mass H_2O out
2	mass SO_3 in, per kg-mole of 1st catalyst bed feed gas	W1	7.84	1	0	0	0	0
3	total mass balance	W4	0	-1	-1	-1	1	1
4	S mass balance	W5	0	-0.4	-0.327	0	0.327	0
5	input acid composition specification	W2	0	0	-1.5	98.5	0	0
6	output acid composition specification	W3	0	0	0	0	-1	99
7								
8	Solution (All masses are per kg-mole of 1st catalyst bed feed gas.)							
9	mass SO_3 in	7.840						
10	mass H_2SO_4 in	360.237						
11	mass H_2O in	5.486						
12	mass H_2SO_4 out	369.827						
13	mass H_2O out	3.736						

W.7 Effect of Output Acid Mass% H_2SO_4 on Input and Output Acid Flows

Fig. W.1 shows the effect of specified output acid composition on input and output acid masses, per kg-mole of 1st catalyst bed feed gas. Both <u>decrease</u> markedly with increasing mass% H_2SO_4 in output acid.

This is because each kg of specified composition input acid can accept more SO_3 when it goes (for example) from:

98.5 mass% H_2SO_4 in to 99.2 mass% H_2SO_4 out

than when it goes from:

98.5 mass% H_2SO_4 in to 98.8 mass% H_2SO_4 out

so less acid has to be circulated when 99.2 mass% H_2SO_4 is being produced.

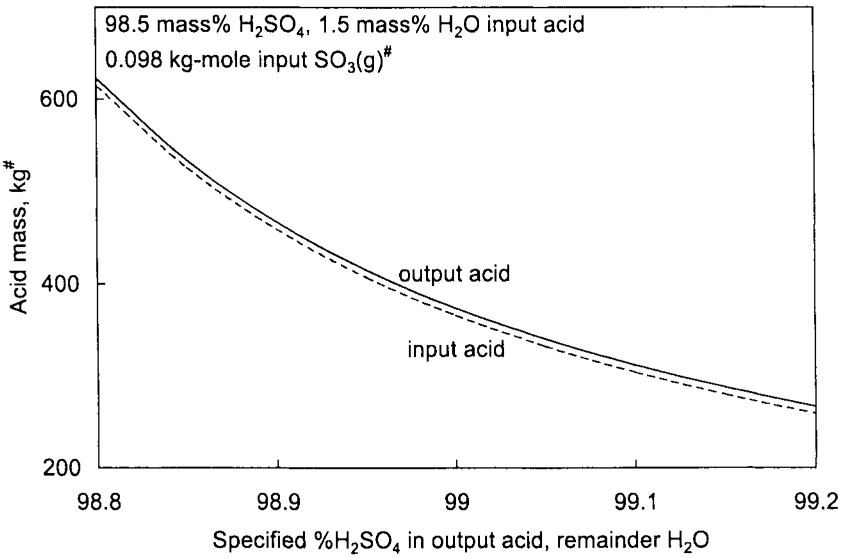

Fig. W.1. Effect of specified output acid mass% H_2SO_4 on H_2SO_4 making tower input and output acid requirements. Input acid composition is constant at 98.5 mass% H_2SO_4, 1.5 mass% H_2O. #per kg-mole of 1st catalyst bed feed gas.

Answers to Numerical Problems

Answers within ± 1% of those listed here indicate correct methods of calculation.

Chapter 10

10.1 854 K
10.2 854 K
10.3 *83.3% SO_2 oxidized*
10.4

	A	B
12	Answer to Problem 10.4	
13	Equilibrium % SO_2 oxidized	Equilibrium temperature, K
14	40	998.2
15	50	963.2
16	60	930.4
17	70	897.2
18	80	860.0
19	90	810.3
20	95	769.9
21	97.5	735.1
22	99	694.7
23	99.5	667.3
24	99.9	611.6
25	99.95	590.4

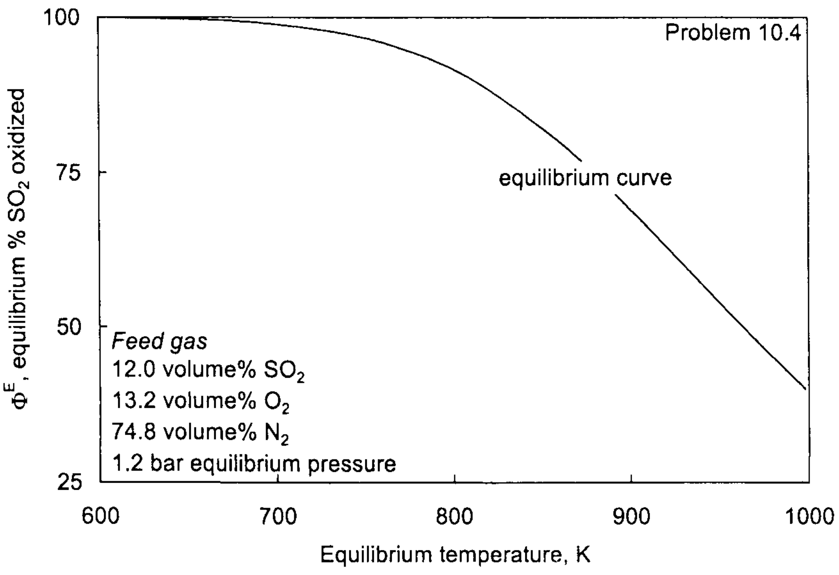

Chapter 11

11.1 37.4% *SO_2 oxidized*

11.2 46.0% *SO_2 oxidized*

11.3 50.3% *SO_2 oxidized*

11.4

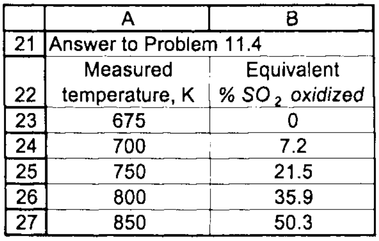

	A	B
21	Answer to Problem 11.4	
22	Measured temperature, K	Equivalent % *SO_2 oxidized*
23	675	0
24	700	7.2
25	750	21.5
26	800	35.9
27	850	50.3

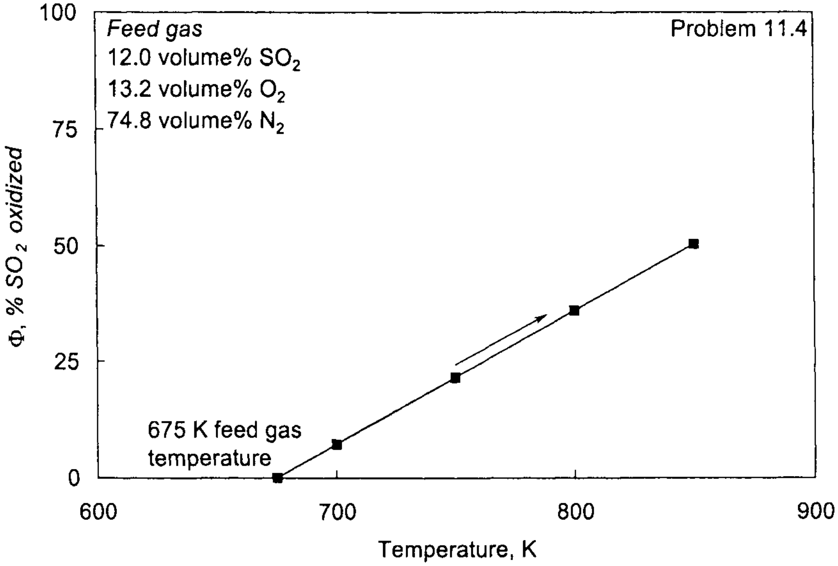

Chapter 12

12.1 and 12.2

	A	B	C
22	Equilibrium temperature	Heatup path *% SO_2 oxidized*	Equilibrium *% SO_2 oxidized*
23	904	65.9	68.0
24	905	66.2	67.7
25	906	66.5	67.4
26	907	66.8	67.1
27	908	67.1	66.8
28	909	67.4	66.5
29	910	67.6	66.2
30	911	67.9	65.9

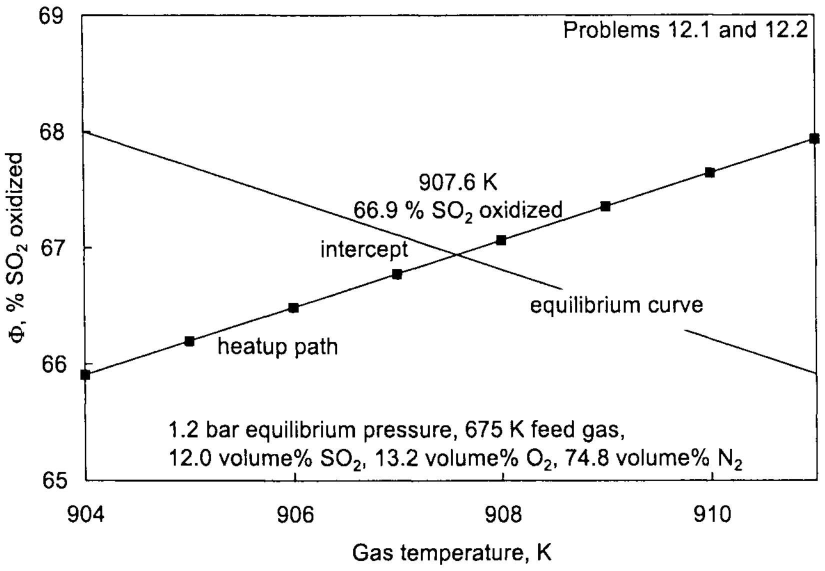

12.3 (a) 1st catalyst bed intercept point: 907.6 K, 66.9% *SO_2 oxidized*

(b) intercept (exit gas) quantities (per kg-mole of 1st catalyst bed feed gas)

	A	B
38	kg-mole SO_3 **out**	0.0803
39	kg-mole SO_2 **out**	0.0397
40	kg-mole O_2 **out**	0.0918
41	kg-mole N_2 **out**	0.7480

Chapter 13

13.1 Chapter 11 heatup path plus Chapter 12 intercept point.

	A	B	C
21	Problem 13.1 heatup path with intercept point		
22	Measured temperature, K	Equivalent *% SO_2 oxidized*	
23	675	0	
24	700	7.2	
25	750	21.5	
26	800	35.9	
27	850	50.3	
28	907.6	66.9	

Problem 13.1 graph

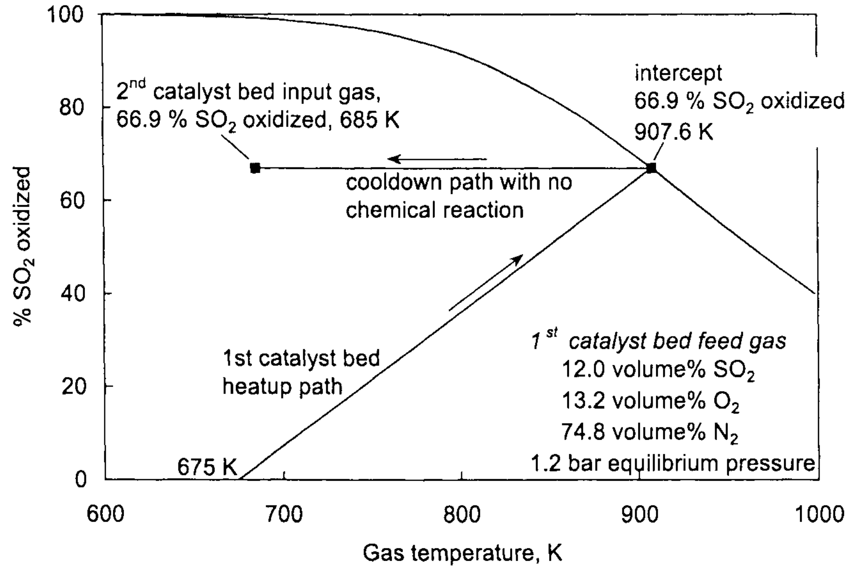

Chapter 14

14.1

	A	B
30	Problem 14.1 heatup path data table	
31	2nd catalyst bed level L	% SO_2 oxidized at level L
32	685	66.9
33	710	74.1
34	730	79.9
35	750	85.7
36	770	91.5

Problem 14.1 graph

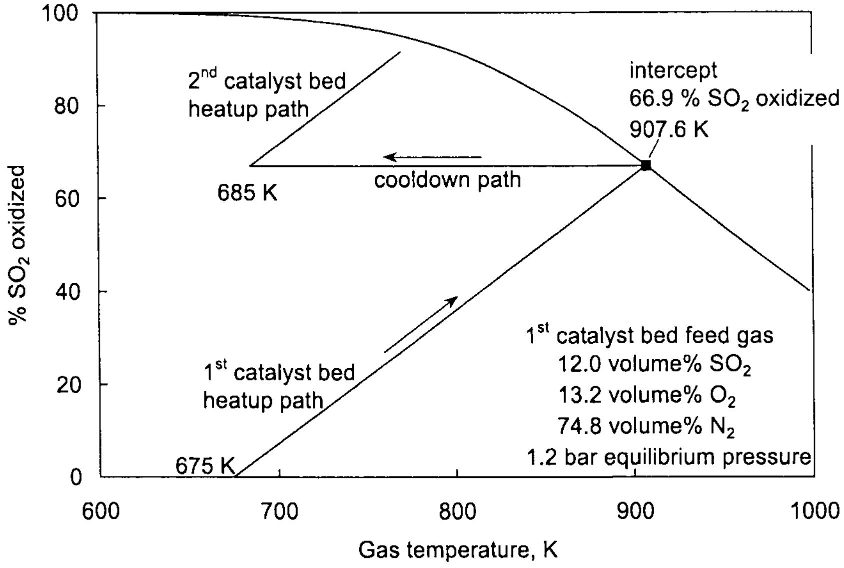

Chapter 15

15.1

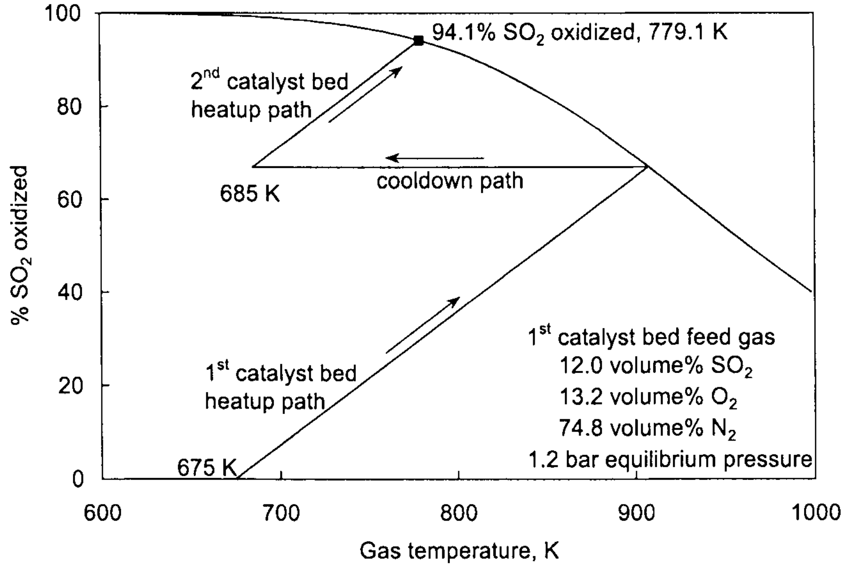

15.2 2nd catalyst bed intercept (exit gas) quantities (per kg-mole of 1st catalyst bed feed gas

	B	C
37	kg-mole SO_3 **out**	0.1129
38	kg-mole SO_2 **out**	0.0071
39	kg-mole O_2 **out**	0.0755
40	kg-mole N_2 **out**	0.7480

Chapter 16

16.1

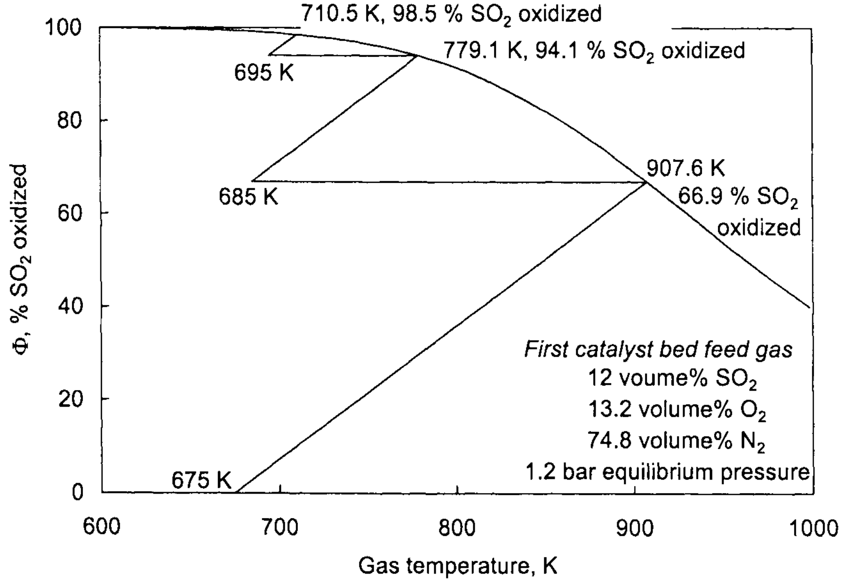

16.2 3rd catalyst bed intercept (exit gas) quantities (per kg-mole of 1st catalyst bed feed gas)

	B	C
37	kg-mole SO_3 **out**	0.1183
38	kg-mole SO_2 **out**	0.0017
39	kg-mole O_2 **out**	0.0728
40	kg-mole N_2 **out**	0.7480

Chapter 17

17.1

(a) 1st catalyst bed intercept: 64.9% SO_2 oxidized at 899.3 K

(b) 1st catalyst bed intercept (exit gas) quantities (per kg-mole of 1st catalyst bed feed gas. They show that the intercept (exit) gas contains a total of 0.07205 kg-mole of SO_3 per kg-mole of 1st catalyst bed feed gas.

	A	B
38	kg-mole SO_3 **out**	0.07205
39	kg-mole SO_2 **out**	0.0379
40	kg-mole O_2 **out**	0.0640
41	kg-mole N_2 **out**	0.7910

17.2 With 10.5, 10.5, 9.0, and 70.0 volume% SO_2, O_2, CO_2 and N_2 the 1st catalyst bed intercept *% SO_2 oxidized* is 66.5% at 899.4 K.

With 10.5, 10.5, 0, and 79.0 volume% SO_2, O_2, CO_2, and N_2 the 1st catalyst bed intercept *% SO_2 oxidized* is 64.9% at 904.6 K.

Chapter 19

19.1 99.98*% SO_2 oxidized* after all 4 beds (with intermediate H_2SO_4 making after the 3rd catalyst bed).

19.2 99.0*% SO_2 oxidized* after all 4 beds (no intermediate H_2SO_4 making).

Chapter 21

21.1

Gas	Temp. K	Enthalpy[#]	
1st catalyst bed feed gas	675	-23.62	
1st catalyst bed exit (intercept) gas	907.6	-23.62	
		heat transfer to 1-2 boiler water→	7.59[#]
2nd catalyst bed input gas	685	-31.21	
2nd catalyst bed exit (intercept) gas	779.1	-31.21	
		heat transfer to superheater steam→	2.87[#]
3rd catalyst bed input gas	695	-34.08	
3rd catalyst bed exit (intercept) gas	710.5	-34.08	
		heat transfer to economizer water→	8.23[#]
H_2SO_4-making input gas	470	-42.31	

[#] per kg-mole of 1st catalyst bed feed gas

21.2 36740 MJ per hour. This is the design capacity of this problem's economizer.

Chapter 22

In all Chapter 22 problems, the 1st catalyst bed feed gas flowrate is 100 000 Nm^3 per hour.

22.1

3rd catalyst bed exit gas enthalpies

Temperature, K	Enthalpy, MJ per kg-mole of 1st catalyst bed feed gas
710.5 (Problem 21.1)	-34.08
480	-41.97
470 (Problem 21.1)	-42.31
460	-42.66

Economizer enthalpy transfers

Cooling temperatures, K	Enthalpy transfer, MJ per kg-mole of 1st catalyst bed feed gas
710.5 to 480	7.89
710.5 to 470 (Problem 21.1)	8.23
710.5 to 460	8.58

(a) 8.23 MJ heat transfer requires 100% of Problem 21.1's economizer capacity

7.89 MJ heat transfer (cooling from 710.5 to 480 K) requires:

$$\frac{7.89}{8.23} * 100\% = 95.9\%$$

of Problem 21.1's economizer capacity.

This is equivalent to a theoretical bypass of:

$$100\% - 95.9\% = 4.1\%$$

(b) Industrial bypass $= (4.1\%)^{1.1} = 4.7\%$

(c) 38 300 MJ per hour, Eqn. (21.6)

22.2

3rd catalyst bed exit gas enthalpies

Temperature K	Enthalpy, MJ per kg-mole of 1st catalyst bed feed gas
715	-33.93
710.5 (Problem 21.1)	-34.08
705	-34.27
470 (Problem 21.1)	-42.31

Economizer enthalpy transfers

Cooling temperatures, K	Enthalpy transfer, MJ per kg-mole of 1st catalyst bed feed gas
715 to 470	8.38
710.5 to 470 (Problem 21.1)	8.23
705 to 470	8.04

Problem 22.1 (b)'s economizer has the heat transfer capacity of:

8.58 MJ per kg-mole of 1st catalyst bed feed gas (@ 100 000 Nm^3 of 1st catalyst bed feed gas per hour)

(a) Cooling of 715 K 3rd catalyst bed exit gas to 470 K requires 8.38 MJ per kg-mole of 1st catalyst bed feed gas. This is:

$$\frac{8.38}{8.58} * 100\% = 97.7\%$$

of the Problem 22.1(b)'s economizer's capacity. It is equivalent to:

2.3% bypass

of gas around the economizer.

(b) Cooling of 710.5 K 3rd catalyst bed exit gas to 470 K requires 8.23 MJ per kg-mole of 1st catalyst bed feed gas. This is:

$$\frac{8.23}{8.58} * 100\% = 95.9\%$$

of the Problem 22.1(b)'s economizer's capacity. It is equivalent to:

4.1% bypass

of gas around the economizer.

(c) Cooling of 705 K 3rd catalyst bed exit gas to 470 K requires 8.04 MJ per kg-mole of 1st catalyst bed feed gas. This is:

$$\frac{8.04}{8.58} * 100\% = 93.7\%$$

of the Problem 22.1(b)'s economizer's capacity. It is equivalent to:

6.3% bypass

of gas around the economizer.

22.3

Prob. 22.2's (a), (b) and (c) bypasses are equivalent to:

	Theoretical bypass, %	Industrial bypass
(a)	2.3	$= 2.3^{1.1} = 2.5\%$
(b)	4.1	$= 4.1^{1.1} = 4.7\%$
(c)	6.3	$= 6.3^{1.1} = 7.6\%$

Chapter 23

23.1 Mass SO_3 entering H_2SO_4 making tower =

$$= 0.1183 \begin{array}{l}\text{kg-mole } SO_3 \text{ per kg-mole of} \\ \text{dry 1st catalyst bed feed gas}\end{array} * 80 \text{ kg } SO_3 \text{ per kg-mole of } SO_3$$

$$= 9.464 \begin{array}{l}\text{kg } SO_3 \text{ per kg-mole of dry} \\ \text{1st catalyst bed feed gas}\end{array}$$

From Eqn. (23.4):

$$\begin{array}{l}\text{kg-mole } H_2O(g) \text{ in moist input gas} \\ \text{per kg-mole of dry 1st catalyst bed} \\ \text{feed gas in moist input gas}\end{array} = \frac{6\%}{94\%} = 0.0638$$

$$\text{Mass input } H_2O(g) = 0.638 \begin{array}{l}\text{kg-mole } SO_3 \text{ per kg-mole of} \\ \text{dry 1st catalyst bed feed gas}\end{array} * 18 \text{ kg } H_2O \text{ per kg-mole of } H_2O$$

$$= 1.149 \text{ kg } H_2O(g) \text{ per kg-mole of dry 1st catalyst bed feed gas}$$

From Table 23.1 (for 98.5 mass% H_2SO_4, 1.5 mass% H_2O output acid):

	A	B	C	D	E	F	G	H
1	Description	equation	numerical term	mass SO_3 into H_2SO_4 making tower	mass H_2O in moist input gas	mass H_2O in input water	mass H_2SO_4 in output acid	mass H_2O in output acid
2	mass SO_3 into H_2SO_4 making tower	23.1	9.464	1	0	0	0	0
3	mass H_2O in moist feed gas	23.5	1.149	0	1	0	0	0
4	S balance	23.6	0	-0.4	0	0	0.327	0
5	total mass balance	23.7	0	-1	-1	-1	1	1
6	output acid composition specification	23.8	0	0	0	0	-1.5	98.5
7								
8								
9	**Matrix solution**	mass*		Kg per 100 000 Nm^3 (4464 kg-mole) dry 1st catalyst bed feed gas per hour				
10	mass SO_3 **in**	9.464				42247	=B10*4464	
11	mass H_2O(g) **in**	1.149				5129		
12	mass water **in**	1.140				5089	(all kg per hour)	
13	mass H_2SO_4 **out**	11.577				51679		
14	mass H_2O **out**	0.176				787		
15	(mass acid **out**)	11.753	=B13+B14			52466		
16	*kg per kg-mole of dry 1st catalyst bed feed gas							

Chapter 24

24.1 The H_2SO_4 making tower matrix with:

(a) 9.464 kg SO_3 per kg-mole of dry 1st catalyst bed feed gas (Problem 23.1)

(b) 98.6 mass% H_2SO_4, 1.4 mass% H_2O input sulfuric acid

(c) 99.2 mass% H_2SO_4, 0.8 mass% H_2O output sulfuric acid

is:

	A	B	C	D	E	F	G	H
1	Description	equation	numerical term	mass SO_3 **in**	mass H_2SO_4 **in**	mass H_2O **in**	mass H_2SO_4 **out**	mass H_2O **out**
2	mass SO_3 in, per kg-mole of 1st catalyst bed feed gas	W1	9.464	1	0	0	0	0
3	total mass balance	W4	0	-1	-1	-1	1	1
4	S mass balance	W5	0	-0.4	-0.327	0	0.327	0
5	input acid composition specification	W2	0	0	-1.4	98.6	0	0
6	output acid composition specification	W3	0	0	0	0	-0.8	99.2
7								
8	Solution (All masses are per kg-mole of dry 1st catalyst bed feed gas.)							
9	mass SO_3 in	9.464						
10	mass H_2SO_4 in	359.639						
11	mass H_2O in	5.106						
12	mass H_2SO_4 out	371.215						
13	mass H_2O out	2.994						

The acid temperature calculation table with:

(a) the appropriate input and output gas compositions

(b) the H_2SO_4 and H_2O input and output masses from the above table

(c) the mass% H_2SO_4 and H_2O in acid values from the above table

is:

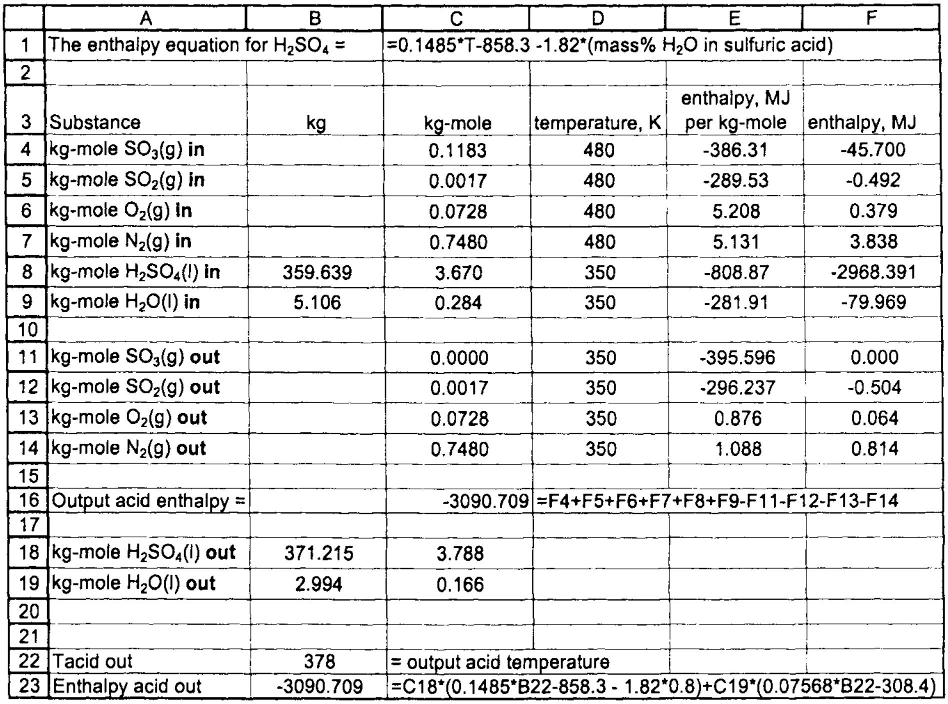

	A	B	C	D	E	F
1	The enthalpy equation for H_2SO_4 =		=0.1485*T-858.3 -1.82*(mass% H_2O in sulfuric acid)			
2						
3	Substance	kg	kg-mole	temperature, K	enthalpy, MJ per kg-mole	enthalpy, MJ
4	kg-mole SO_3(g) **in**		0.1183	480	-386.31	-45.700
5	kg-mole SO_2(g) **in**		0.0017	480	-289.53	-0.492
6	kg-mole O_2(g) **in**		0.0728	480	5.208	0.379
7	kg-mole N_2(g) **in**		0.7480	480	5.131	3.838
8	kg-mole H_2SO_4(l) **in**	359.639	3.670	350	-808.87	-2968.391
9	kg-mole H_2O(l) **in**	5.106	0.284	350	-281.91	-79.969
10						
11	kg-mole SO_3(g) **out**		0.0000	350	-395.596	0.000
12	kg-mole SO_2(g) **out**		0.0017	350	-296.237	-0.504
13	kg-mole O_2(g) **out**		0.0728	350	0.876	0.064
14	kg-mole N_2(g) **out**		0.7480	350	1.088	0.814
15						
16	Output acid enthalpy =		-3090.709	=F4+F5+F6+F7+F8+F9-F11-F12-F13-F14		
17						
18	kg-mole H_2SO_4(l) **out**	371.215	3.788			
19	kg-mole H_2O(l) **out**	2.994	0.166			
20						
21						
22	Tacid out	378	= output acid temperature			
23	Enthalpy acid out	-3090.709	=C18*(0.1485*B22-858.3 - 1.82*0.8)+C19*(0.07568*B22-308.4)			

which shows the output acid temperature to be 378 K.

Author Index

Index